

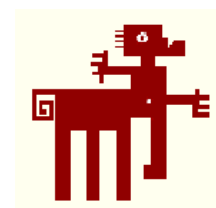
Doctoral Thesis

**Study of the biological
functions of the non-
essential regulatory
subunits of the protein
phosphatase Glc7 in the
yeast *Saccharomyces
cerevisiae***

Jofre Ferrer-Dalmau Falgueras

Dept. Bioquímica i Biologia Molecular
Universitat Autònoma de Barcelona

November 2013



Study of the biological functions of the non-essential regulatory subunits of the protein phosphatase Glc7 in the yeast *Saccharomyces cerevisiae*

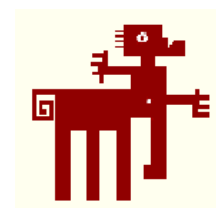
Thesis dissertation for the degree of Doctor in Biochemistry, Molecular Biology and Biomedicine, presented by **Jofre Ferrer-Dalmau Falgueras**. This work was performed at the Veterinary Unit of the Department of Biochemistry and Molecular Biology of the 'Universitat Autònoma de Barcelona' under the direction of **Dr. Antonio Casamayor Gracia**.

Jofre Ferrer-Dalmau Falgueras

Antonio Casamayor Gracia

November 2013

Universitat Autònoma de Barcelona
Departament de Bioquímica i Biologia Molecular
Facultat de Veterinària



Amb aquestes línies vull agrair a totes les persones, sense les quals, aquest treball no s'hagués pogut realitzar. També, vull anticipar-me a les queixes disculpant-me per si en l'anhel d'en recordar-me de tothom, m'he deixat alguna persona sense nombrar.

Primer de tot, agrair molt especialment al Dr. Antonio Casamayor Gracia no només per acollir-me en el seu laboratori i donar-me l'oportunitat d'aprendre sobre la ciència del llevat sinó també per transmetrem part dels seus coneixements i passió per la ciència. També, als membres del grup que han anat passant com en Martí Boleda, el Dr. Daniel Pastor (demostrant-me que amb tofu es pot sobreviure !) i la Dra. Anna Bahí (sort que hi era per mantenir-me a ratlla i l'ordre en el caos que organitzava a la seva poiata quan la intentava envair!).

Agrair molt cordialment al Dr. Joaquín Ariño pel suport logístic del seu laboratori i poder-me beneficiar dels avantatges del seu grup. Avantatges no només d'equipament i material, sinó també dels membres veterans del grup sempre ajudant-me en tot moment. El Dr. Asier González per ser el meu "jefe" durant una setmana fent tot l'estudi fenotípic (mai oblidaré aquells dots!). La Dra. Maria Platara que em va ensenyar la tècnica més nostrada del laboratori: el β -gal !. El Dr. Carlos Casado per creure en l'aneuploidia des d'un principi. La Dra. Amparo Ruiz per ensenyar-me que és possible fer β -gals de més de 300 tubs i pels plàsmidis Snf1 enviats des de NYC. I, la Dra. Raquel Serrano per ensenyar-me a manejar l'Antonio. També, a la Dra. Lina Barreto i en David Canadell pels creixements en baix potassi. No em vull oblidar dels altres membres del grup com l'Albert, la Laura, la Sylvia, en Boris i la Cristina.

Tota aquesta tesis no hagués estat possible sense el treball en la preparació de medis, plaques, comandes, o sigui el dia a dia en el laboratori de l'Anna Vilalta i la Montserrat Robledo. A més, de la Rosa i la Lourdes per tots els tràmits burocràtics que m'han fet. També al laboratori de la Dra. Anna Bassols, la Laia, l'Anna, en Dani, la Maria José i la Laura per fer que bioquímica de veterinària estigués plena de vida. En Nèstor pel seu material gràfic i en Gerard.

També, els consells en els microarrays i la seqüenciació de mostres de la Dr. Anna Barceló, en Xavi i en Roger Lahoz del Servei de Seqüenciació de la UAB.

En anglès, I thank H. Sychrovà and G. Wiesenberger for help in developing and testing the YNB-based, K-free medium. We also thank C. Moore, B. Dichtl, K. Tatchell, A. Amon, K. Kimata and M. Marquina for provision of strains and plasmids provided for cation homeostasis, cell cycle and unfolded protein response experiments.

Agradecer a Clara Navarrete i José L. Martínez del laboratorio del Dr. José Ramos de la Universidad de Córdoba por los experimentos de determinación del contenido y flujos de litio.

A los Dra. M. Francisca Randez Gil i Dr. José Antonio Prieto Alamán I (IATA, València) no sólo por los experimentos que nos han hecho sobre UPR, sino también por toda la asistencia en el diseño, planificación y conocimientos sobre la UPR. Gracias a ellos, hemos indagado en un tema totalmente desconocido en nuestro laboratorio que nosotros solos no nos hubiésemos atrevido a investigar.

A la Dra. Bàrbara Baro del laboratorì de la Dra. Ethel Queralt (IDIBELL) per ajudar-nos en els experiments de FACS en els mutants *ref2*.

No em vull oblidar dels membres de la meva comissió de seguiment: el Dr. David Garcia Quintana i el Dr. Josep Biosca, que va ser la primera persona que em va introduir en el món dels llevats aguantant-me durant tot un any.

Agrair a la família Alonso per les reunions familiars que em permetien desconnectar dels llevats.

Els meus pares per sempre transmetre'm tot el suport per fer la tesi i sempre està al meu costat quan se'ls necessitava.

I, finalment, a la Carol.....en mots no puc explicar tot el que significa per mi. Per sort, sempre a estat i estarà al meu costat....

Table of contents

ABBREVIATIONS	5
SUMMARY	7
INTRODUCTION.....	9
1. <i>Saccharomyces cerevisiae</i> as a model for the investigation.....	9
2. The regulation by protein phosphorylation	9
2.1 General description of phosphorylation properties	9
2.2 Properties of Ser / Thr phosphatase	10
2.2.1 PhosphoProtein Phosphatases (PPPs).....	11
2.2.2 Metal-dependent Protein Phosphatase (PPMs)	11
2.2.3 Aspartate-based phosphatases: FCP/SCP	12
2.3 Protein Phosphatase-1 (PP1).....	12
2.3.1 Mechanisms of interaction for the PP1c regulatory subunit. Binding motifs.....	14
2.3.2 Glc7, the catalytic subunit of yeast PP1	16
2.3.3 The Glc7 regulatory subunit Ref2.....	20
2.3.4 The Glc7 regulatory subunit Reg1	22
3. The stress response in <i>S. cerevisiae</i>.....	24
3.1 Ionic homeostasis.....	25
3.1.1 The ATPases Ena.....	26
3.2 Calcium homeostasis.....	28
3.3 The Cell Wall Integrity signaling pathway	31
3.4 Efflux pump-mediated drug resistance as a stress response.....	35
3.5 Unfolded protein response	38
4. Aneuploidy	43
OBJECTIVES	46
EXPERIMENTAL PROCEDURES	47
1. Growth of <i>Escherichia coli</i> and yeast strains	47
2. DNA recombinant techniques	47
3. Deletion cassettes, gene disruptions	47
4. Diploid generation and obtaining of haploid cells.....	55
5. Plasmids construction	56
6. Growth test.....	60

7. Total RNA Extraction	61
8. cDNA synthesis and DNA microarrays	61
9. Yeast DNA genomic extraction.....	62
10. Comparative Genomic Hybridization.....	62
11. Quantitative Real-Time PCR (qRT-PCR).....	63
12. Semi-quantitative RT-PCR.....	65
13. Northern Blot Analysis	65
14. Preparation of cell lysates, Immunoprecipitation, and Western blotting	65
15. Glucose measurements	66
16. Vacuolar morphology staining	67
17. β -Galactosidase assay.....	67
18. Fluorescence Flow Cytometry Analysis (FACS)	68
19. Lithium content and lithium efflux measurements	68
20. Intracellular calcium determination	69
RESULTS AND DISCUSSION	70
1. Global analysis of the non-essential regulatory subunits of Glc7.....	70
1.1 Phenotypical analysis of Glc7-regulatory subunits	70
1.2 Vacuolar morphological analysis of cells lacking regulatory subunits of Glc7	73
1.3 Transcriptional analysis of cells lacking non-essential Glc7-regulatory subunits	75
1.4 Conclusions	81
2. Study of cation homeostasis in mutants in the non-essential Glc7-regulatory subunits.	82
2.1 Lack of Ref2 causes defects in cation tolerance.....	82
2.2 The Glc7-binding motif of Ref2 is required for cation tolerance	85
2.3 Mutation of Ref2 affects expression of the <i>ENA1</i> ATPase gene under saline and alkaline pH stresses.....	87
2.4 <i>ref2</i> mutant cells display a hyperactivated calcium/calcineurin pathway in the absence of stress and show altered vacuole morphology	91
2.5 The Glc7-binding motif of Ref2 is required for calcium tolerance and calcineurin pathway activation.....	93
2.6 Mutants in components of the APT complex do not share the cation-related phenotypes of the <i>ref2</i> strain	95
2.7 Analysis of the calcium homeostasis in <i>ref2</i> mutant	99
2.8 Sensitivity to cell wall stressors of mutants in components of calcium homeostasis	101
2.9 Analysis of the sensitivities to cell wall stressors of Glc7-regulatory subunits.....	103

2.10	Ref2 is not involved in the activation of the CWI pathway	105
2.11	The hypersensitivity to CWI stressors is shared by other components of the holo-CPF 106	
2.12	The Glc7-binding motif of Ref2 is required for CWI tolerance.....	109
2.13	Analysis of the CWI pathway in <i>ref2</i> mutant cells.....	111
2.14	Conclusions	114
3.	Study of aneuploidy in <i>ref2</i> mutant cells	115
3.1	CML476 tetO ₇ : <i>REF2</i> does not show any aneuploidy.....	116
3.2	New <i>ref2</i> mutant cells show <i>REF2</i> duplication itself.....	121
3.3	New <i>ref2</i> mutant cells display an aneuploidy on chromosome XII.....	122
3.4	Mutants in components of the APT-complex do not share the aneuploid-related phenotypes of the <i>ref2</i> strain.....	124
3.5	Mutants in components of the APT-complex share a decreased biomass production tan wild-type cells	126
3.6	<i>ref2</i> mutant cells in different background show similar phenotypes	127
3.7	<i>ref2</i> mutant cells apparently does not show any delay in cell cycle.....	128
3.8	The Ref2 ^{F4374A} cells have an aneuploidy in chromosome XII	130
3.9	Homozygous diploid <i>ref2</i> cannot sporulate	131
3.10	Conclusions	135
4.	Study of Unfolded Protein response in mutants on non-essential Glc7-regulatory subunits 136	
4.1	Phenotypical analysis of mutants on non-essential Glc7-regulatory subunits	136
4.2	UPRE transcriptional analysis of mutants on non-essential Glc7-regulatory subunits 137	
4.3	<i>glc7-109</i> allele shows a hypersensitive phenotype to UPR inducers.....	138
4.4	Ref2, a possible UPR regulator	141
4.4.1	Tunicamycin tolerance Ire1-independent.....	141
4.4.2	<i>ref2</i> cells phenotype is independent of holo-CPF	143
4.4.3	<i>ref2</i> cells tolerant phenotype is genetic background specific.....	144
4.4.4	Evolutionary response to tunicamycin.....	146
4.4.5	Tunicamycin tolerance implies a chromosome II duplication.....	147
4.4.6	Long-term adaptation to tunicamycin growth.....	152
4.4.7	Defects either in CWI or calcium homeostasis suppresses tunicamycin tolerance phenotype in <i>ref2</i> mutant cells	155
4.5	Reg1, a possible UPR regulator	158

4.5.1	Deletion of <i>SNF1</i> alleviates <i>reg1</i> mutant cells phenotype to tunicamycin	158
4.5.2	<i>PTC2</i> do not rescue <i>reg1</i> mutant cells tunicamycin hypersensitivity	159
4.5.3	<i>reg1</i> mutant cells are unable to deactivate UPR.....	160
4.5.4	UPR does not activate Snf1 pathway	163
4.5.5	Snf1 inactive alleles rescue <i>reg1</i> cells phenotype.....	166
4.5.6	Analysis of Snf1's repressors	167
4.6	Conclusions	171
CONCLUSIONS		172
TABLE OF CONTENTS (Figures and Tables)		175
REFERENCES.....		187
PUBLICATION.....		210

Abbreviations

ABBREVIATIONS

AMP	adenosine 5' monophosphate
AMPK	AMP-dependent kinase
APT	associated to Pta1
ARR1	alkaline responsive region 1
ARR2	alkaline responsive region 2
BSA	bovine serum albumine
CDRE	calcineurin dependent response element
CF	cleavage factor
CPF	cleavage and polyadenylation factor
CRE	c-AMP response element
CTD	C-terminal domain
CWI	cell wall integrity
DMSO	dimethyl sulfoxide
DNA	deoxyribonucleic acid
Dol-P	dolichol phosphate
DTT	dithiothreitol
<i>E. coli</i>	<i>Escherichia coli</i>
Glc-Nac	N-acetylglucosamine
Glc-Nac-P	N-acetylglucosamine phosphate
h	hour
kDa	kilo dalton
MAPK	mitogen activated protein kinase
min	minute
mRNA	messenger ribonucleic acid
ONPG	o-nitrophenyl- β -D-galactopyranoside
PCR	polymerase chain reaction
PF	polyadenylation factor
PK	protein kinase
PP	protein phosphatase
PP1c	catalytic subunit of protein phosphatase 1
PPM	metal-dependent protein phosphatase
PPP	phosphoprotein phosphatases

PTP	protein tyrosine phosphatases
RNA	ribonucleic acid
<i>S. cerevisiae</i>	<i>Saccharomyces cerevisiae</i>
SBF	SCB-binding factor
SCB	Swi4/Swi6 cell cycle box
SDS	sodium dodecyl sulphate
snRNA	small nuclear ribonucleic acid
SSC	saline sodium chloride
TAPS	N-[tris(hydroxymethyl)methyl]-3-aminopropanesulfonic acid
TBST	Tris buffered saline-with Tween-20
TMA	trimethoxyamphetamine
UPR	unfolded protein response
UPRE	unfolded protein response element
5-FOA	5-Fluoroorotic acid

Summary

SUMMARY

The only catalytic subunit of PP1 in *S. cerevisiae*, Glc7, interacts with at least 31 regulatory subunits that regulate the myriad of Glc7 functions. Among those subunits we performed in this thesis both transcriptional and phenotypic analysis of 21 yeast strains lacking one of the non-essential regulatory subunit of Glc7. With these high-throughput technologies we have determined their transcriptional profiles and new phenotypes which allowed us to focus on two regulatory subunits: Ref2 and Reg1.

We demonstrate in this thesis that Ref2, a regulatory subunit necessary for the processing and maturation of mRNA and/or snoRNAs is also required for the proper functioning of ionic homeostasis under conditions of cation stress. Cells lacking *REF2* display hypersensitivity to cation stress which is dependent on the binding to Glc7 involving a new function of the complex Glc7-Ref2. Ref2 is integrated in the holo-CPF (Cleavage Poly(A)denylation factor), where most components are essential for cell survival. For this reason, the study of cells carrying thermo-sensitive alleles of the holo-CPF components in semi-restrictive temperatures allowed us to conclude that this complex is not involved in ionic homeostasis. Despite this unrelated function between holo-CPF and Ref2, the holo-CPF mutants display sensitivity to cell wall stressors agents, as *ref2* cells do. Deletions of *REF2* and mutants in components of the cell wall integrity pathway have synergistic effects under cell wall stressors.

Cells lacking *REF2* display an aneuploidy, implying duplication of chromosomes, being the chromosome XII duplicated in all analysed cases of the BY4741 genetic background. This aneuploidy is due to the inability of Glc7 to bind to the holo-CPF. Furthermore, homozygous diploids lacking the *REF2* genes are unable to sporulate, possibly due to a chromosome missegregation in meiosis, since cells are not defective in the early events of meiosis.

Another phenotype studied in *ref2* cells was the unfolded protein response (UPR). *ref2* cells are hypertolerant to tunicamycin, possible due to its aneuploidy. The evolutionary study of a wild-type strain grown in tunicamycin for 120 generations showed, as an early adaptive step, duplication of chromosome II. Long-term adaptive step involves the loss of the chromosome duplication and the specific induction of certain genes, including those involved in the pleiotropic drug resistance phenomenon.

Reg1, the Glc7 subunit involved in the negative regulation of glucose-repressible genes by dephosphorylating Snf1 kinase, displays hypersensitivity to agents that trigger the accumulation of unfolded proteins, such as tunicamycin. This phenotype is shared by the *glc7-109*, which prevents the binding of the regulatory subunits to Glc7, linking the UPR to a possible regulation of the Ire1 kinase. Our results indicate that hyperactivation of Snf1 or overexpression of constitutively activated Snf1 in *reg1* mutant cells even increases the sensitivity to tunicamycin. Finally, the analysis of mutants of the components of the Snf1 pathway allowed us to conclude that the lack of *RIM101* causes sensitivity to tunicamycin, possibly due to the impossibility of expressing *PMR1*, a high affinity $\text{Ca}^{2+}/\text{Mn}^{2+}$ P-type ATPase required for Ca^{2+} and Mn^{2+} transport into Golgi and essential for UPR.

In summary, results of this thesis allow us to describe new functions for Ref2, including the ionic homeostasis and regulation of the cell wall integrity. On the other hand, we have uncovered that Reg1 is required for the correct response to unfolded proteins.

Introduction

INTRODUCTION

1. *Saccharomyces cerevisiae* as a model for the investigation

Since Sumerian, the yeast *Saccharomyces cerevisiae* is known for its applications in the food industry (bread, wine, beer ...) and now it is an organism widely used in the field of biotechnology as a producer of different compounds with commercial interests. In the context of scientific research, it is an organism well suited to be used as a model of molecular mechanisms which occur in eukaryotic cells, because it is relatively easy to grow and manipulate, moreover, its genetics are also more accessible than other eukaryotic organisms and it has lots of information about its molecular biology.

From the achievement of the *S. cerevisiae*'s genome sequence in 1996 published by (Goffeau et al., 1996), it has been possible to identify all the genes encoding the various protein kinases and phosphatases of this microorganism. This organism is now an excellent model in order to study the role of the protein phosphorylation and its implications in yeast regulation or adaptation to the environment. Moreover, the vast majority of regulatory processes can also be found in other eukaryotes making the yeast a basic tool of reference for understanding and compare molecular biology of a huge variety of organisms.

2. The regulation by protein phosphorylation

2.1 General description of phosphorylation properties

Reversible protein phosphorylation is one of the most important and widespread mechanisms of regulation of many biological process such as metabolism, gene transcription, cell cycle and in response to a plethora of either internal or external stimuli. The phosphorylation state of any protein depends on the specific opposite action of protein kinases (PK) and protein phosphatases (PP), which changes the net charge of the protein leading to an alteration of the functional properties of the protein such as: **i)** the increase or the decrease of its biological activity; **ii)** the induction of stabilization markers responsible for its destruction, activation or inhibition of its mobilization through subcellular compartments and **iii)** either initiation or elimination of interactions with other proteins (P. T. Cohen, 2002). Nowadays, the reversible phosphorylation of proteins is defined as the most common post-

translational modification that plays an important role in all signal transduction pathways known.

The importance of this regulatory mechanism is evident if one considers that affects approximately 30% of the proteome of *S. cerevisiae* (Ptacek et al., 2005) and that the number of genes which encode phosphatases and kinases represents 2-4% of the total number of genes in a typical eukaryotic genome (Manning, Plowman, Hunter, & Sudarsanam, 2002). Moreover, one would think that the number of PPs and PKs encoded by the genome of eukaryotic organisms is similar, which means that each PK has a specific PP. Far beyond reality, the number of PKs is greater than the number of PPs. For example, the fully sequenced human genome is thought to encode 518 potential protein kinases (S. A. Johnson & Hunter, 2005), where 428 are Ser/Thr kinases, but only contains approximately 150 genes encoding PPs, where approximately 30 proteins are Ser/Thr phosphatases (Shi, 2009). Another example is that the connection between Ser/Thr-specific kinases and Ser/Thr-specific phosphatases in *Drosophila melanogaster* is higher than 6:1 (Morrison, Murakami, & Cleghon, 2000).

Proteins can be phosphorylated on nine amino acids residues: tyrosine, serine, threonine, cysteine, arginine, lysine, aspartate, glutamate and histidine; with serine, threonine and tyrosine phosphorylation being predominant in eukaryotic cells and playing key regulatory roles (Moorhead, De Wever, Templeton, & Kerk, 2009). Specifically, a recent study of human proteome shows that the phosphorylation of serine, threonine and tyrosine represents approximately 86.4, 11.8 and 1.8%, respectively, of the total number of amino acids phosphorylated (Olsen et al., 2006).

According to the dephosphorylated residue, protein phosphatases have historically been grouped into three main families: the group of Ser / Thr phosphatases, the superfamily of protein tyrosine phosphatases (PTP, protein Tyr phosphatases) and the set of dual phosphatases which are capable to dephosphorylate both Ser / Thr as well as Tyr residues.

2.2 Properties of Ser / Thr phosphatase

The Ser / Thr phosphatases constitute the most abundant group of phosphatases, which, in turn and based on their sequence, structure and enzymatic properties, is divided into three major families (P. T. Cohen, 1997) (*Figure 1*).

2.2.1 PhosphoProtein Phosphatases (PPPs)

These family members are PP1, PP2A, PP2B, PP4, PP5, PP6 and PP7. Biochemical characterization of the first purified members indicated that type 1 protein phosphatase (PP1) preferably dephosphorylates the β -subunit of the phosphorylated kinase, whereas type 2 (PP2) acts on the α -subunit of the specific PK. In addition, PP1 activity is sensitive to the polypeptides inhibitors 1 and 2 and depends on the presence of Mn^{2+} to catalyze the dephosphorylating reaction *in vitro*, whereas PP2 is not responding to any of those inhibitors. The different needs for divalent cations allows differentiating between type 2A protein phosphatase (PP2A), which does not require these ions, and type 2B protein phosphatase (PP2B), also called calcineurin, which depends on Ca^{2+} to carry out its function. Structurally, all PPPs share a high degree of similarity, especially in an area of 150 amino acids, which is considered the catalytic core of the enzyme (P. Cohen, 1991). Moreover, within the family of PPP phosphatases includes a set of structurally linked but functionally different from those of type 1 and 2A. Most of these protein phosphatases groups (with the exception of PP7) are widely represented in the yeast *S. cerevisiae* (Arino, 2002). As shown in *Figure 1*, Pph3 is the *S. cerevisiae* type 4 protein phosphatase closely linked, showing overlapping functions with the *S. cerevisiae* homologs PP2B, Pph21 and Pph22. Type 5 protein phosphatase, Ppt1 in *S. cerevisiae*, possesses a fused N-terminal domain that contains four tetratricopeptide (TPR) motifs which are essential for substrate targeting. Sit4 encodes for the type 6 protein phosphatase in *S. cerevisiae* and largely studied due to its myriad of functions (Stark, 1996). Molecular cloning technologies allowed the identification of several genes encoding different PPP.

2.2.2 Metal-dependent Protein Phosphatase (PPMs)

These family members are PP2C and pyruvate dehydrogenases phosphatase. PP2C shares the typical PP2 common characteristics such as **a)** acting on the α -subunit of the phosphorylated kinase and **b)** not responding to inhibitors 1 and 2, but this family is structurally more distant from the PPP family (*Figure 1*) and is characterized by its dependency on manganese/magnesium ions (Mn^{2+}/Mg^{2+}). Catalytic subunits of PP2C are implicated in a widespread of pathway such as High Osmolarity Glycerol (*HOG1*), Cell Wall Integrity (CWI) and Pheromone response, among others, , by dephosphorylating several MAPK (reviewed in (Arino, Casamayor, & Gonzalez, 2011)). In contrast to PPPs, members of the PPM family do not have regulatory subunits but they contain instead additional domains and conserved sequence motif that may help determine substrate specificity.

2.2.3 Aspartate-based phosphatases: FCP/SCP

TFIIF-associating component of RNA polymerase II CTD phosphatase/small CTD phosphatase has only one substrate described for this family is the C-terminal domain (CTD) of RNA polymerase II, which contains some tandem repeats of a serine-rich heptapeptide (Shi, 2009). This family is also magnesium dependent.

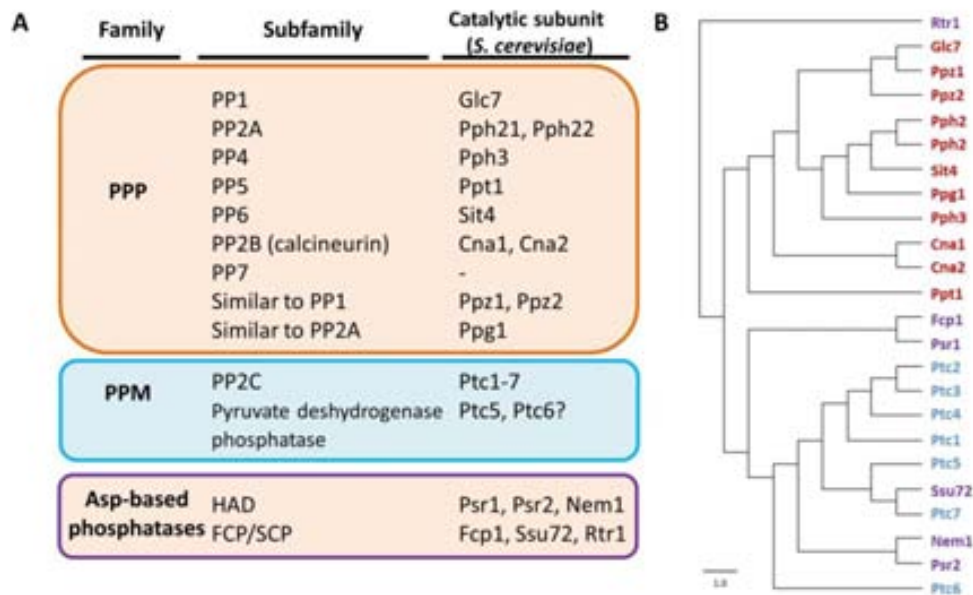


Figure 1. Classification of Ser / Thr phosphatases. **A)** The three main families and the corresponding subfamilies of catalytic subunits of protein phosphatases are shown. The *S. cerevisiae* catalytic subunits of each subfamily are shown in the right column. The symbol (-) indicates that there is not a counterpart of PP7 in *S. cerevisiae*. **B)** Tree alignment of PP sequences of *S. cerevisiae*. Protein sequences were analyzed with ClustalW 2.0 from EMBL-EBI (Larkin et al., 2007). Hierarchical cluster was performed using array correlation parameter plus complete linkage clustering and data was represented by Treeview tool v1.6 from Eisen's lab software (Eisen, Spellman, Brown, & Botstein, 1998). Each PP family is marked with its own color such as PPP (red), PPM (blue) and Asp-based phosphatase (purple).

2.3 Protein Phosphatase-1 (PP1)

Among PPPs family, protein phosphatase-1 was one of the first members discovered and strongly studied (Ingebritsen & Cohen, 1983). Not only is it widely distributed throughout the eukaryotic realm but also is one of the most conserved proteins.

In eukaryotes, the protein phosphatase type 1 is involved in many cellular functions, from the regulation of glycogen metabolism, muscle physiology, RNA processing, protein synthesis, transmission of nerve signals, induction of apoptosis and control of multiple checkpoints and to events that occur throughout the cell cycle (J. F. Cannon, 2010; Hugo

Ceulemans & Bollen, 2004; P. T. Cohen, 2002). To perform these functions, each functional PP1 enzyme consists of a catalytic subunit (PP1c) which binds to different proteins called regulatory subunits. These regulators are needed either to target the PP1 catalytic subunit to specific subcellular localization, modulate substrate specificity or serve as substrates themselves. In this work, we will focus on the study of the yeast regulatory subunits which, as in mammals, allow the catalytic subunit of PP1 (PP1c) to have a myriad of cellular functions.

The catalytic subunit of PP1 (PP1c) is highly conserved among all eukaryotes, with approximately 70% or greater protein sequence identity in a pairwise alignment. Moreover, this is nicely illustrated by the number of genes encoding the PP1 varying from 1 gene in the flagellated protozoan parasite *Giardia lamblia* to 9 isoforms in the plant *Arabidopsis thaliana*. In mammals, for example, PP1c is encoded by three genes (PP1 $_{\alpha}$, PP1 $_{\beta/\delta}$ and PP1 $_{\gamma}$), with two isoforms more (PP1 $_{\gamma_1}$ and PP1 $_{\gamma_2}$) which can be generated by alternative splicing. All isoforms are ubiquitously expressed, except the PP1 $_{\gamma_2}$ isoform that is enriched in the testicles. In yeast, however, this enzyme is the product of a single gene, termed *GLC7/DIS2S1* (Feng et al., 1991a; Ohkura, Kinoshita, Miyatani, Toda, & Yanagida, 1989).

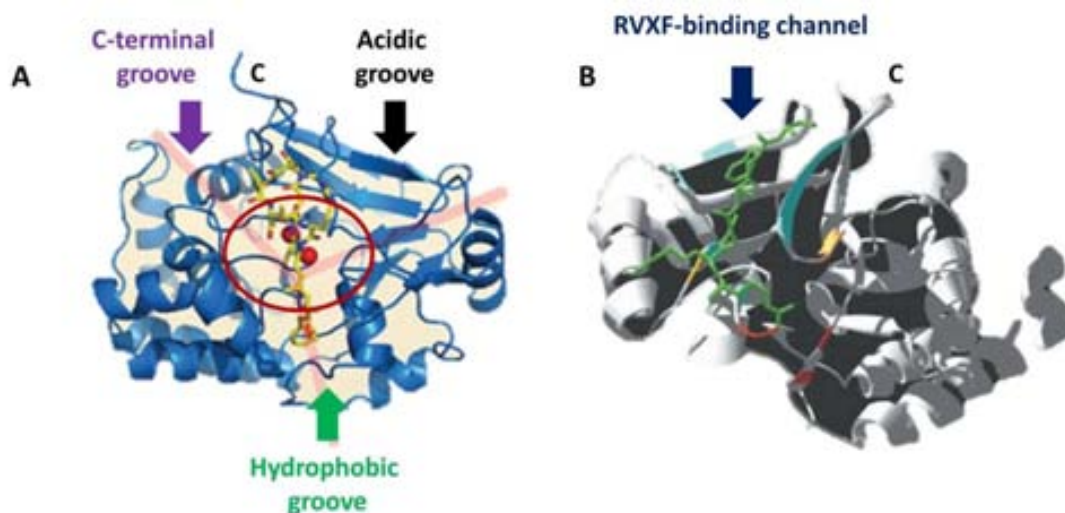


Figure 2. The crystal structure of the catalytic PP1. **A)** Structure of the catalytic subunit (blue) of protein phosphatase 1 (PP1) bound to okadaic acid (OA, yellow ball and stick). A Y-shaped surface groove (pink) is defined by the three domains of PP1. The two metal ions (red spheres) are Mn²⁺ (manganese) and Fe²⁺ (iron). This frontal view of PP1 with the catalytic site (encircled) and the three grooves that emanate from the catalytic site modified from (Shi, 2009). **B)** The dorsal view of the same structure. The RVXF-containing peptide is rendered as a green sticks representation. The accommodating RVXF-binding channel is lined by residues of the last strand and by adjacent residues (cyan). The protein surface near the entrance of the channel, which is thought to bind the basic residues preceding the V-position of the RVXF motif, is negatively charged due to the presence of conserved acidic residues (red and orange) modified from (Hugo Ceulemans & Bollen, 2004).

At least, nine X-ray crystallography and 10 PDB structures of mammalian PP1 catalytic subunit are available. This variety comes from the interest on using the structural information in order to design new inhibitors of PP1. The structure of these PP1 proteins is nearly identical despite the difference in PP1 isoforms, crystallization conditions and crystals packing contact. The catalytic subunit PP1 adopts a compact α/β fold, with a β sandwich wedged between two α -helical domains, which are the COOH terminus, and the extreme N-terminus (Egloff, Cohen, Reinemer, & Barford, 1995; Goldberg et al., 1995). The β sandwich and the two helical domains form a “Y”-shaped cleft where the active site is located (*Figure 2A*). There, an invariant number of residues (three histidines, two aspartic acids and one asparagine) coordinate two metal ions, manganese and iron, which are needed to contribute to catalysis by enhancing the nucleophilicity of metal-bound water and the electrophilicity of the phosphorous atom. These residues are highly conserved in all members of the PPP family suggesting a common mechanism of metal-catalyzed reaction in the protein family (Shi, 2009). Through that cleft, there are three grooves called hydrophobic, acidic and C-terminal (*Figure 2B*).

2.3.1 Mechanisms of interaction for the PP1c regulatory subunit. Binding motifs

We must notice that the catalytic subunit of PP1 is a relatively small protein which does not exist freely in the cell that can interact with a large variety of regulatory subunits non-structurally connected, with distinct effects on the activity, localization and substrate specificity of the phosphatase. In mammals, for example, it has already been described more than 100 putative PP1 regulatory subunits (Moorhead, Trinkle-Mulcahy, & Ulke-Lemée, 2007). and around 31 regulatory subunits of Glc7 (J. F. Cannon, 2010), most of which appear in this thesis.

Work by many groups has determined that the regulatory subunits of PP1 may interact with PP1c using different ways: **1)** a short degenerate sequence motif; **2)** multiple points of interaction with PP1, for most of the cases; and **3)** by sharing PP1 interactions sites with different regulatory subunits. Altogether, it allows us to propose that PP1 is subjected to a combinatorial control that relies on the competition of its different regulatory subunits (Hugo Ceulemans & Bollen, 2004).

Early studies evidenced a short and conserved binding motif in the majority of the regulatory subunits to join PP1 catalytic subunit. These studies were based on the glycogen-

targeting subunits, G_M and G_L , and the myosin-targeting subunit M_{110} . Although they only share an identity of 23%, there is a highly conserved 32 residue region of G_M peptide, that, was able, *in vitro*, to dissociate the M_{110} -PP1c complex (D. F. Johnson et al., 1996). A new crystallization study demonstrated that a shorter version of this peptide (13 residues) also formed a complex with PP1c allowing the identification of the RVXF motif. This motif mediates the interaction with a hydrophobic groove on the surface of PP1c, which is distant from the active site (Egloff et al., 1997). An independent strategy using a screening of a peptide library with PP1c also identified peptides containing VXF and VXW sequences, often preceded by basic residues, as a PP1c binding motif (S. Zhao & Lee, 1997a). Several works on, both mammalian and yeast PP1, have helped to define this important consensus sequence binding motif, which is often degenerated, but appears in most PP1's known regulatory subunits (Bollen, 2001). Thus, it has been demonstrated that most of the regulatory subunits contained a surface motif of 4 - 5 amino acids **[RK][X]₀₋₁[VI]X[F/W]** where the first X may be absent or be any residue, and the second X may be any residue except proline (Wakula, Beullens, Ceulemans, Stalmans, & Bollen, 2003).

More recently, the consensus sequence has been redefined to five amino acids **[H/K/R][A/C/H/K/M/N/Q/R/S/T/V][V][C/H/K/N/Q/R/S/T][F/W]** which allowed the accurate prediction and experimental demonstration of new PP1-binding proteins (Meiselbach, Sticht, & Enz, 2006). Positions 1, 2, and 4 are preferably formed by positively charged amino acids and/or polar, while position 3 is specifically favored by the hydrophobic amino acid valine and the position 5 only tolerates the non-polar and bulky aromatic side chains of phenylalanine or tryptophan. It is also shown that the position 1 is the key anchor point of interaction with PP1 due to the salt bridges and hydrogen bounds which provide dynamic stability of the protein.

Although the RVXF motif is very common among predicted peptide sequences, existing in more than 10% of known proteins (Egloff et al., 1997), its importance in binding PP1c has been confirmed for many targeting subunits (P. T. Cohen, 2002). The RVXF motifs selected to interact with the catalytic subunits must be on the surface and accessible. With regard to this, it has been described that the single mutation of the hydrophobic residues (V,I) and/or aromatic (F,W) of the motif is sufficient to reduce or completely inhibit the interaction with the enzyme (X. Wu & Tatchell, 2001).

The binding of the regulatory subunits through the RVXF motif is not associated with a major conformational change of the catalytic subunit and it does not cause significant effects on its activity (Egloff et al., 1995). Despite the importance of the RVXF motif for the interaction

of targeting subunits of PP1c, additional interactions might not only stabilize the binding but also provide crucial contacts for modulating the activity and/or specificity of PP1c. Another point is likely that many, if not all PP1 regulatory subunits, will have more than one site of interaction with PP1c (X. Wu & Tatchell, 2001).

For example, the RVXF motif of in M_{110} is positioned close to the akryn motif which enables to form a kind of hand with fingers and creates a region involved in suppressing phosphorylase phosphatase activity (D. F. Johnson et al., 1996).

Moreover, some authors suggest that another interaction motif with PP1c is **FX[X][RK]X[RK]**, involved in the recognition and binding of the anti-apoptotic molecules Bcl- x_L and Bcl-w, that targets the protein phosphatase 1 α to Bad (Ayllón, Cayla, García, Fleischer, & Rebollo, 2002). The β_{12} - β_{13} loop, essential for inhibition of PP1 by the toxins mycrocystin, okadaic acid and by the protein inhibitors inhibitor-1, inhibitor-2, DARP-32 and NIPP1, represents another interaction motif (Connor, Kleeman, Barik, Honkanen, & Shenolikar, 1999). Another interaction site in the regulatory subunits is the triangular region delineated by the α_4 -, α_5 - and α_6 -helices of PP1 near the amino-terminal region, which has been identified as a major interaction site for the yeast essential regulatory subunit Sds22 (H Ceulemans et al., 2002). Finally, an interaction site for the conserved N-terminal **K[GS]ILK** motif of inhibitor-2 has been mapped near the entrance of the RVXF-binding channel (H. B. Huang et al., 1999). Despite little is studied about these additional interactions the regulatory subunits may not only bring PP1c in close proximity to its substrates by anchoring the phosphatase in specific cellular compartments, but also induce conformational changes that block the activity of PP1 by acting as a pseudo substrates (Bollen, 2001; P. T. Cohen, 2002).

2.3.2 Glc7, the catalytic subunit of yeast PP1

Unlike what occurs in mammals, yeast genome contains one only gene coding for the catalytic subunit of PP1, called *GLC7* (Clotet, Posas, Casamayor, Schaaff-Gerstenschlager, & Arino, 1991; Feng et al., 1991b). This essential gene, also known under the name *CID1* or *DIS2S1*, encodes a protein of 312 amino acids with a predicted molecular mass of 36 kDa that, has a high degree of similarity (around 86%) with mammalian isoforms (PP1 γ_1 - PP1 γ_2) and, analogously to what happens in those, develops multiple functions in yeast. As its mammals counterpart, the functions of *GLC7* are regulated by the interaction with different regulatory subunits affecting their substrate specificity and/or subcellular localization (*Table 1*) (J. F. Cannon, 2010; P. T. Cohen, 2002).

GLC7 was initially identified as a gene involved in the metabolism of carbohydrates, given the role it plays in the accumulation of intracellular glycogen (Clotet et al., 1991; Feng et al., 1991b; Hardy & Roach, 1993; Ohkura et al., 1989). As in mammals, the yeast PP1c is responsible for the dephosphorylation, and the activation, of glycogen synthase, whose major isoform in *S. cerevisiae* is encoded by *GSY2*. This process appears to be regulated by the binding to Gac1, a regulatory subunit which contains a glycogen synthase binding region and the RVXF motif needed to interact with *GLC7* (X. Wu & Tatchell, 2001).

Name	Functions	Glc7 interface	Homo sapiens homology	References
<u>Afr1</u>	Mating, septin architecture	<u>KDYRE</u>	-	(Bharucha, Larson, Konopka, & Tatchell, 2008)
<u>Bni4</u>	Mitosis, bud formation and chitin synthase localization	<u>QGYRE</u>	-	(Kocubowski et al., 2003; Larson et al., 2008; Zou et al., 2009)
<u>Bud14</u>	Mitosis, pheromone response, filamentous and polarized growth	<u>KSYSE</u>	-	(Cullen & Sprague, 2002; Pinsky, Kotwalliwale, Tatsutanl, Breed, & Biggins, 2006)
<u>Fin1</u>	Mitosis and microtubules binding	<u>KLTE, RARE, KDAPE, KASE, KEK</u>	-	(Mayordomo & Sanz, 2002; Woodbury & Morgan, 2007)
<u>Fpr3</u>	Global regulator	Unknown	FKBP1A	(Hochwagen, Tham, Brar, & Amon, 2005)
<u>Fpr4</u>	Global regulator	Unknown	FKBP54	(Ho et al., 2002; Ho et al., 2002)
<u>Gac1</u>	Glycogen metabolism, binding to glycogen synthase (Gsy2)	<u>KNYRE</u>	Ppp1r3c/R5	(François et al., 1992; X. Wu & Tatchell, 2001)
<u>Gip1</u>	Meiosis and sporulation, septin organization and bud's cell wall formation	Unknown	-	(Tachikawa, Bloecher, Tatchell, & Neiman, 2001; Tu, Song, & Carlson, 1996)
<u>Gip2</u>	Glycogen metabolism	Unknown	Ppp1r3c/R5	(Tu et al., 1996)
<u>Gip3</u>	Unknown	Unknown	-	(Pinsky et al., 2006)
<u>Gip4</u>	Unknown	Unknown	-	(Pinsky et al., 2006)
<u>Glc8</u>	Glycogen metabolism and chromosomes segregation	Unknown	inhibidor-2/Ppp1r2	(Nigavekar, Tan, & Cannon, 2002; Y. S. H. Tan, 2002; Tung, Wang, & Chan, 1995)
<u>Mhp1</u>	Organization/biogenesis of cytoskeleton	Unknown	UGR4	(Irminger-Finger & Mathis, 1998; Walsh, Lamont, Beattie, & Stark, 2002)
<u>Pan1</u>	Actin cytoskeleton	Unknown	-	(Zeng, Huang, Neo, Wang, & Cai, 2007)
<u>Pex31</u>	Peroxisome size regulation	-	-	(Pinsky et al., 2006)
<u>Pig1</u>	Glycogen metabolism	Unknown	Ppp1r3c-d/R5	(C. Cheng, Huang, & Roach, 1997)
<u>Pig2</u>	Glycogen metabolism	Unknown	Ppp1r3c/R5	(C. Cheng et al., 1997)
<u>Pta1</u>	RNA processing	Unknown	Symplekin	(He & Moore, 2005)
<u>Pti1</u>	RNA processing	Not VixF	Cfs2	(He & Moore, 2005)
<u>Red1</u>	Meiosis and sporulation	-	-	(Ballis & Roeder, 2000; Tu et al., 1996)
<u>Ref2</u>	RNA processing, transcription and ionic homeostasis	<u>RVK</u>	-	(Jofre Ferrer-Dalmau et al., 2010; Nedeau et al., 2003, 2008)
<u>Reg1</u>	Glycogen metabolism	<u>RHHE</u>	-	(K. M. Dombek, Voronkova, Raney, & Young, 1999; Sanz, Alms, Haystead, & Carlson, 2000; Sanz, Ludin, & Carlson, 2000)
<u>Reg2</u>	Glycogen metabolism, growth regulation and RNA processing	<u>RHXF</u>	-	(Frederick & Tatchell, 1990)
<u>Scd5</u>	Vesicular secretory pathway, cortical actin organization	<u>KDVF, KQVRF</u>	-	(Chang, Henry, Wolf, Gell, & Lemmon, 2002; Zeng et al., 2007)
<u>Sds22</u>	Nuclear targeting	<u>LLLR</u>	Ppp1r7	(Hong, Trumbly, Reimann, & Schlendler, 2000; Pedelini et al., 2007; Peggie et al., 2002; Ramaswamy, U. Khalil, & Cannon, 1998)
<u>Sof1</u>	tRNA nuclear export	Unknown	6-phosphogluconolactonase	(Pinsky et al., 2006)
<u>Shp1</u>	Mitosis, differentiation in meiosis, glycogen metabolism and ubiquitination	Unknown	p47	(Schuberth, Richly, Rumpf, & Buchberger, 2004)
<u>Sip5</u>	Starvation response	Unknown	-	(Sanz, Ludin, et al., 2000)
<u>Sla1</u>	Cytoskeleton formation and endocytosis	<u>KNE</u>	-	(Gardiner, Costa, & Ayscough, 2007; Howard, Hutton, Olson, & Payne, 2002)
<u>Ypi1</u>	Nuclear activity regulator	<u>YRW</u>	Pppr11	(Bharucha, Larson, Gao, Daves, & Tatchell, 2008; Garcia-Gimeno, Munoz, Arino, & Sanz, 2003; Pedelini et al., 2007)
<u>Ysw1</u>	Pro-spore membrane formation	Unknown	-	(Ishihara et al., 2009)

Table 1. **Known Glc7-regulatory subunits.** The underlined residues were mutated and found to be important for Glc7 binding. The Glc7 regulatory subunits analysed on this thesis are marked in blue

As it happens in mammals and as we have already described above, we can divide the PP1 interacting proteins in: **regulatory subunits**, which make a distinct PP1 holoenzyme; **regulators**, which modulate the global PP1 activity; and **substrates**, which interact with PP1 transiently (J. F. Cannon, 2010). Moreover, not all regulatory subunits interact to Glc7 in the same way. We may find three possibilities: **1)** many PP1 regulatory subunits have, at least, a consensus RVXF primary sequence (Moorhead et al., 2007; S. Zhao & Lee, 1997b), such as Ref2, Afr1, Reg1, Reg2, Sla1, Bud14, Bni4 and Gac1; or more than one binding motif such as Scd5 and Fin1; **2)** there are regulatory subunits which do not bind to the Glc7's hydrophobic groove using an RVXF domain, specifically Sds22 and Pti1 (Hugo Ceulemans et al., 2002; He & Moore, 2005); finally, **3)** formation of larger complexes: it has been reported that, and in order to translocate to the nucleus, Glc7 forms a trimeric complex with Sds22 and Ypi1 (Pedelini et al., 2007) additionally, Glc7 has also found bound to poly(A) binding protein (Nab2) and to the nucleolar RNA helicase Hca4 (Batisse, Batisse, Budd, Böttcher, & Hurt, 2009; Gavin et al., 2002).

Glc7 is involved in a myriad of functions and cellular localizations in yeast cells (J. F. Cannon, 2010). For instance, the phosphatase activity of Glc7 is important in the phenomenon of repression by glucose. Reg1 and Reg2, also assisted by Sip5, regulate the dephosphorylation of Snf1 in presence of high glucose concentrations (Sanz, Alms, et al., 2000; Sanz, Ludin, et al., 2000). Moreover, the tandem Glc7-Reg1 may also be important for inactivation of genes unnecessary for growth in high glucose such as *HXK2*, *PDA1* and *HSP60* (Alms, Sanz, Carlson, & Haystead, 1999; Juana M Gancedo, 2008). The glucose-unrelated subunits Bni4, Afr1 and Gip1 mediate different septin localization activities. Specifically, the Glc7-Bni4 holoenzyme regulates the targeting of chitin synthase III (Chs3) to the incipient bud sites when Bni4 is phosphorylated by Pho85-Pcl1,2 (Kozubowski et al., 2003). The Glc7 regulatory subunit Afr1 targets the phosphatase activity toward the mating projection to coordinate the polarized mating projection growth (Bharucha, Larson, Konopka, et al., 2008). The Glc7-Gip1 is required for septin ring organization and spore wall formation during spore maturation (Tachikawa et al., 2001). Glc7 also controls the bud-site selection pattern using the regulatory subunit Bud14, because the lack of *BUD14* leads to defects in secretory vesicle movement (Chesarone, Gould, Moseley, & Goode, 2009; Cullen & Sprague, 2002). Another cytoplasmic function of Glc7 is based on the Glc7-Scd5 holoenzyme which regulates endocytosis and actin organization (Chang et al., 2002).

Most of Glc7 protein is found in the nucleus, in particular, in the nucleolus (Bloecher & Tatchell, 2000). There Glc7 may interact with Sds22 and Ypi1 the two essential regulatory subunits that directly regulate the nuclear localization and function of Glc7 (Pedelini et al., 2007). Moreover, Sds22 is important for yeast alkaline cation homeostasis (Marquina et al., 2012). Bud14, Ref2 and Gac1 have an important role in transcriptional regulation (Nedea et al., 2003; X. Wu, Hart, Cheng, Roach, & Tatchell, 2001). The interaction of Fin1 and Red1 with Glc7 can promote the microtubule attachment to kinetochores during the chromosome segregation process and may reverse some of the cell cycle checkpoints (Bailis & Roeder, 2000; Mayordomo & Sanz, 2002). Other regulatory subunits have the ability to modulate up (Glc8 and Shp1) or down (Fpr3) the global activity of Glc7 (J. F. Cannon, 2010).

Phenotypic analyses of different *GLC7* mutant alleles have been shown that this protein may also be involved in the maintenance of cell integrity (Andrews & Stark, 2000) and in the regulation of ion homeostasis yeast (T Williams-Hart, Wu, & Tatchell, 2002) but, in at beginning of this thesis, the regulatory subunits which control the function were not discovered yet.

2.3.3 The Glc7 regulatory subunit Ref2

The protein encoded by *REF2* was initially described as a factor required for termination of mRNA (RNA-End Formation-2) because its deletion causes a shortening of the poly(A) tails of nuclear mRNA (Rusnak, Nehrke, & Platt, 1995). Ref2 has 533 amino acids (expected molecular weight of 59 kDa) and a high content of lysine and serine residues. Its importance in the Glc7 accurate regulation has already been described in (Nedea et al., 2008).

Ref2 has recently been identified as a protein that forms part of the new complex holo-CPF (Cleavage and Poly-adenylation Factor). This complex couples the transcription and mRNA termination/maturation in *S. cerevisiae* and is formed by: the core-CPF (PFI, Pap1 and CFII), the APT-complex (Associated to Pta1) and the COMPASS/Set1C complexes (Nedea et al., 2003; Proudfoot, Furger, & Dye, 2002) (*Figure 3A*).

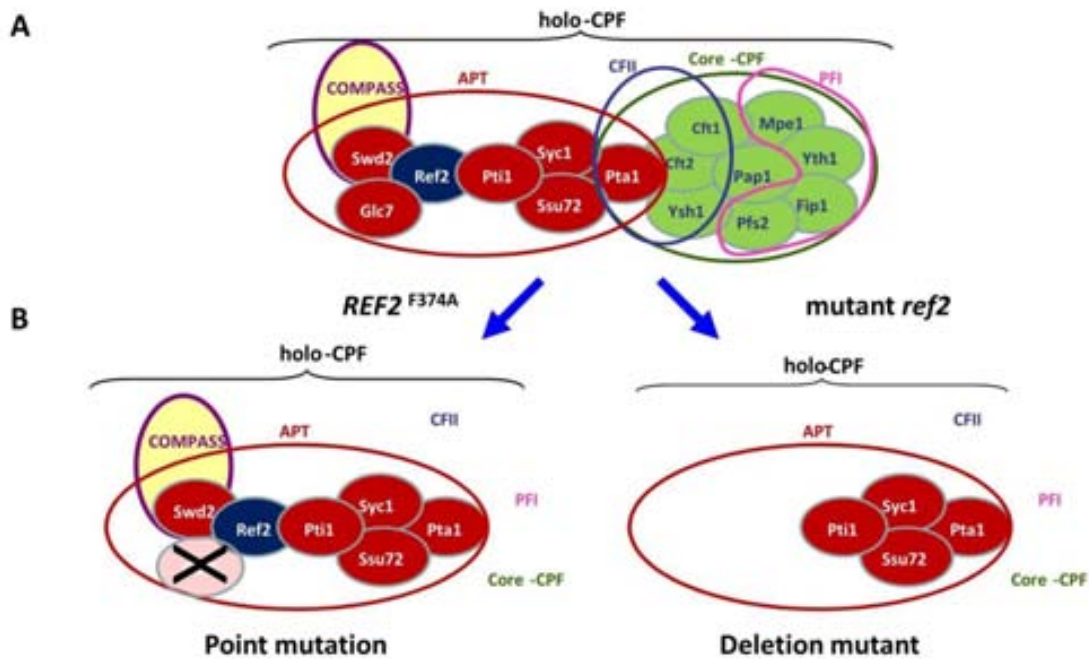


Figure 3. Ref2 is a key component in holo-CPF integrity. **A)** Scheme of the components of the holo-CPF and the proteins that compose each complex. **B)** Illustration of the different effects caused by deletion or the F374A point mutation of *REF2*.

It is assumed that the holo-CPF is a dynamic complex which fits perfectly the dynamism required for the genomic DNA's transcription (Nedeia et al., 2003). Complete deletion of *REF2* partially disaggregates the APT-complex, however, the point mutation of phenylalanine (F) 374 to alanine (A) residues only decouples Glc7 from the APT-complex (Nedeia et al., 2008) (Figure 3B). On the other hand, the APT complex allows us to observe three new features of Ref2:

1. Its binding to Glc7 is needed for the correct transcription of the 92 yeast small nucleolar RNAs (snRNAs). snRNAs are components of enzymes that cleave, methylate, or pseudouridylate ribosomal RNAs and are also transcribed by the RNA polymerase II (Kiss, 2002).
2. The interaction Glc7-Ref2 allows the dephosphorylation of Pap1, the poly-A polymerase. *PAP1* gene encodes for a protein of 64 kDa whose main role is to add ribonucleotides of adenosines to the poly(A) mRNA tail. It is also involved in the phase S to G₂ transition of the cell cycle (Mizrahi & Moore, 2000), which appears to be regulated by phosphorylation and ubiquitination. In this second control mechanism Pap1 activity is partially disabled, leaving a minimum of activity in order to transcribe genes which are required for S phase such as histones and telomerase. Ref2 seems to help locating Glc7 to Pap1, allowing regulation of Pap1 by dephosphorylation.

3. Ref2 is also involved in the mechanism of telomere antisilencing and histone methylation in yeast. Ref2 is bound to the complex Set1 complex or COMPASS (Complex Proteins Associated with Set1) which is directly involved in the transcription of genes by covalent modification of histones (Dehé et al., 2006). Specifically, it is important in the methylase activity of Set1 on lysine 4 of histone 3 (H3K4). This complex interacts with the RNA polymerase II through Paf1 (RNA Polymerase II Associated Factor 1), depending on the level of methylation of the H3K4 which describes the phase of transcription: H3K4-trimethylated (initial), H3K4-dimethylated (elongation) and H3K4-monomethylated (termination) (J.-S. Lee et al., 2007). Furthermore, Ref2 may also be linked to the signals necessary to protect the coding regions from telomeres of chromosome silencing (Venkatasubrahmanyam, Hwang, Meneghini, Tong, & Madhani, 2007).

2.3.4 The Glc7 regulatory subunit Reg1

The main glucose repression or catabolite repression pathway controls the adaptation of yeast carbon metabolism to the availability of glucose in the medium (see (Smets et al., 2010) for a recent review). In the presence of glucose the Ser/Thr protein kinase Snf1, the central component of this pathway, is inactivated resulting in the transcriptional repression of genes that are not needed during fermentative growth on glucose such as, genes encoding for enzymes involved in gluconeogenesis, the Krebs cycle, respiration and the uptake and metabolism of alternative carbon sources (J M Gancedo, 1998; Hedbacker & Carlson, 2008; Ronne, 1995).

Reg1 was initially characterized as a regulatory subunit directly involved in restoring the glucose repression phenotype of the *glc7-T152K* allele, unable to dephosphorylate Snf1, when overexpressed (Tu & Carlson, 1995a). *REG1* encodes a protein of 1014 residues, with a RHIHF motif between amino acids 464 and 468 amino acids, which matches the Glc7-regulatory subunits general binding consensus sequence. Reg1 interacting proteins, such as Bmh1, Bmh2, Ssb1 and Ssb2, may also have roles in glucose repression (Alms et al., 1999; K M Dombek et al., 1999; Kenneth M Dombek, Kacherovsky, & Young, 2004).

Briefly, Snf1 belongs to the cAMP activated protein kinase (AMPK) family (Hardie, 2007; Woods et al., 1994) and is a heterotrimeric protein: a catalytic α subunit (Snf1), a regulatory γ subunit (Snf4) and three different scaffold-regulatory β subunits. The specific binding to the β subunits localizes Snf1 in the nucleus (Gal83), cytoplasm (Sip2) or vacuole

(Sip1) where it will trigger a specialized response to stresses (*Figure 4*) (Hedbacker & Carlson, 2006; Hedbacker, Townley, & Carlson, 2004; Vincent, Townley, Kuchin, & Carlson, 2001). When glucose levels drop the Snf1 kinase complex is controlled through two mechanisms: **1)** by an increased interaction Snf4-Snf1, avoiding the auto-inhibitory intramolecular interaction between the N-terminal catalytic domain and the C-terminal regulatory domain of Snf1 and; **2)** to achieve a full activation, Snf1 is phosphorylated in a conserved threonine residue in its activation loop (Thr210) by three protein upstream kinases, Elm1, Sak1 and Tos3 (Jiang & Carlson, 1996; Sutherland et al., 2003). In order to activate Snf1, the glucose signal may be transduced to the protein kinase. There are two hypotheses to explain the transduction between the low glucose signal and the activation of Snf1: **i)** low levels of the AMP; or **ii)** the hexokinase 2 (Hxk2), which acts in the first step of glycolysis phosphorylating glucose on C6, may act either stimulating Glc7-Reg1 phosphatase complex or interacting with the transcription factor Mig1 avoiding its phosphorylation (Momcilovic, Iram, Liu, & Carlson, 2008; Sanz, Alms, et al., 2000; Wilson, Hawley, & Hardie, 1996). In order to accurately regulate the Snf1 phosphorylation, a competitive model has been described by (Tabba, Mangat, McCartney, & Schmidt, 2010). This model assumes that Reg1 possesses a surface to which Glc7 and Snf1 compete each other for the binding. When bound to Glc7, Reg1 directs the phosphatase to the Snf1 activation loop, thereby promoting the inactivation of Snf1 kinase activity. On the other way, when bound to Snf1, Reg1 protects the Snf1 activation loop from dephosphorylation, thereby stabilizing the active site of the Snf1 kinase.

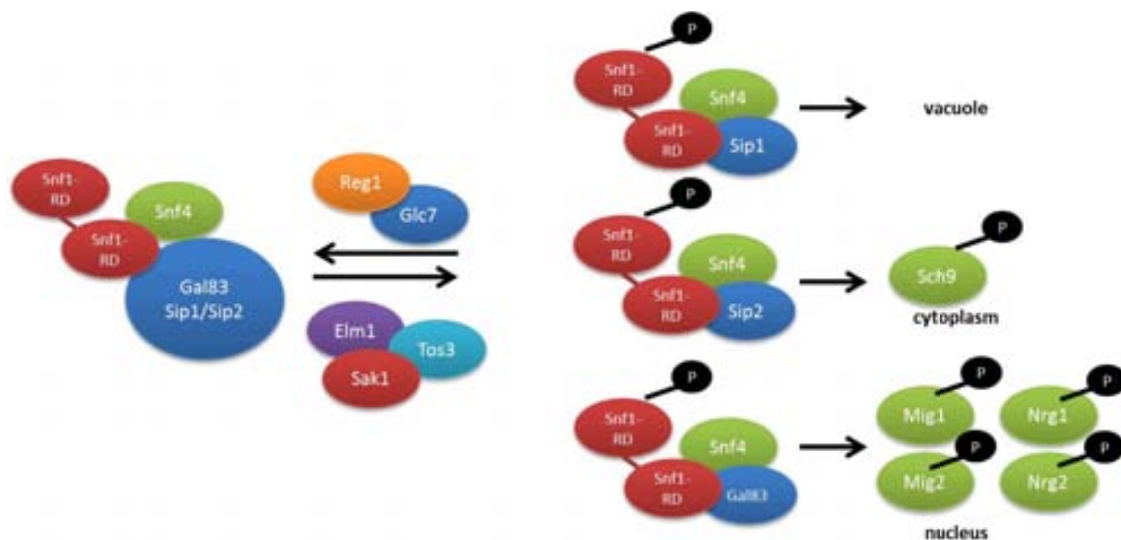


Figure 4. Reg1 is the phosphatase of Snf1. Summary of the three different localizations through which Snf1 can respond in front of different stresses, associating to each β subunit, localizing differently Snf1. It also shows the key role of Reg1 being, so far, the only phosphatase of Snf1.

The main target of Snf1 in the absence of glucose is the transcriptional repressor Mig1, which upon phosphorylation is released from the nucleus through the importin Msn5 (DeVit & Johnston, 1999) allowing the transcription of genes linked to gluconeogenesis, the Krebs cycle, respiration and the uptake and metabolism of alternative carbon sources (Papamichos-Chronakis, Gligoris, & Tzamarias, 2004). The transcriptional activators Cat8, Sip4, Nrg1 and Mig2 are additional effectors of Snf1 that control the expression of gluconeogenic genes in response to glucose exhaustion (Hedges et al., 1995; Lesage et al., 1996; Randez-Gil et al., 1997; Zhou and Winston, 2001). Interestingly, the response elicited by Snf1 to the alkalization of the medium is similar to that of low glucose (M Platara et al., 2006). There are also another functions of Snf1 pathway apart from those directly linked to the carbon metabolism (Smets et al., 2010): **i)** controls the subcellular localization of transcription factors Msn2/4 and increases the activity of Hsf1, a transcription factor involved in general stress responses; **ii)** promotes the translocation to the nucleus of the transcription factor Gln3 by a TOR-independent phosphorylation; and **iii)** phosphorylates the Ser10 of histone H3, thereby stimulating chromatin remodeling. This H3-Ser10 phosphorylation, in concert with the Gcn5 acetyltransferase, recruits co-activators and the TATA binding protein to the promoter of genes like *INO1*, encoding inositol 1-phosphate synthase, and *HXT4*, which encodes one of the high-affinity glucose transporters (Bertram et al., 2002; J.-S. Hahn & Thiele, 2004; Lo et al., 2001; Mayordomo, Estruch, & Sanz, 2002; van Oevelen, van Teeffelen, van Werven, & Timmers, 2006).

Until now, it has always been linking Reg1 to Snf1 and glucose repression. In this thesis we will show some data that may explain a new role for the Reg1-Glc7 tandem.

3. The stress response in *S. cerevisiae*

The yeast's optimal growth conditions are not only depending on the growth medium composition (including fermentable sugars such as glucose or fructose) but also on physical parameters such temperature (around 25°C), agitation, oxygen supply, osmotic conditions, pH (around 5), absence of toxic effects among others factors. Conditions deviated from optimal can be defined as stressful, which invoke particular stress responses in order to avoid cell damage (Bond, 2006). At this point it is important to comment the yeast cells ability to adapt to changing conditions determines their usefulness and applicability to industry processes (Francisca Randez-Gil, Córcoles-Sáez, & Prieto, 2013). Stress responses, which may eventually lead to stress tolerance as a long-term defense mechanism towards damaging agents, are

evolutionarily conserved in all living organism, obviously with the own characteristics for uni- or pluricellulars organisms.

Thus, yeast cells need to sense the stress conditions and consequently will activate the specific pathways for each stress in order to response, adapt and survive. Stress response pathways end up with the regulation of transcriptional, post-transcriptional and post-translational mechanisms. Some of these signal transduction pathways will be explained in this work.

3.1 Ionic homeostasis

The ionic homeostasis, which is an essential property of yeast cells, allows them to keep an adequate intracellular concentration of cations. This process enables cell survival in different environments which usually differs from cytoplasmic conditions. In *S. cerevisiae*, the ionic homeostasis affects several processes such as membrane potential, ionic contents or intracellular pH. Importantly, among the cellular functions attributed to the Glc7 phosphatase, a role in ion homeostasis was postulated some years ago as a result of the characterization of the *glc7-109* allele (Tara Williams-Hart, Wu, & Tatchell, 2002), which carries a mutation at Arg-260, responsible for the mutant phenotypes. *glc7-109* mutants displayed, among other phenotypes, a marked sensitivity to sodium, cesium, magnesium cations, hygromycin B and alkaline pH. Ypi1, an essential Glc7-regulatory subunit has been involved in the regulation of cation homeostasis, largely mediated by calcineurin but independent of its key function as regulator of Glc7 in mitosis (Marquina et al., 2012).

Yeasts, as well as other single-cell eukaryotic organisms, have developed mechanisms to maintain a safe cytosolic concentration of the otherwise toxic cations such as sodium, potassium, lithium, calcium and magnesium even when the external concentration of those ions in their natural environments is high. To this end, these organisms employ three distinct strategies: **i)** discrimination among different alkali metal cations at the level of uptake (favoring transport of potassium over that of sodium); **ii)** triggering the efficient efflux of toxic cations; and **iii)** sequestering the excess of cations in organelles, such as the vacuole. An elevated intracellular concentration of sodium ions, for example, is harmful for most eukaryotic cells, probably because they interfere with the correct functioning of certain cellular targets (R Serrano, 1996). To maintain the intracellular concentration of ions, yeast cells have developed several transporters either in the plasma membrane or in organellar membranes. These

transporters have substrate specificity and may use different mechanism of transport such as primary active ATPases, secondary active symporters and antiporters, and passive channels. As described in *Figure 5*, there are at least six characterized plasma membrane transport systems: the potassium uptake systems Trk1 and Trk2, the potassium channel Tok1, the P_i - Na^+ symporter Pho89, the efflux system Ena Na^+ -ATPases and the Nha1 Na^+/H^+ antiporter. Moreover, there also exists several intracellular transporters such as the alkali metal cation/ H^+ antiporters of vacuolar (Vnx1), endosomal (Nhx1) and Golgi apparatus (Kha1) (Ariño, Ramos, & Sychrová, 2010).

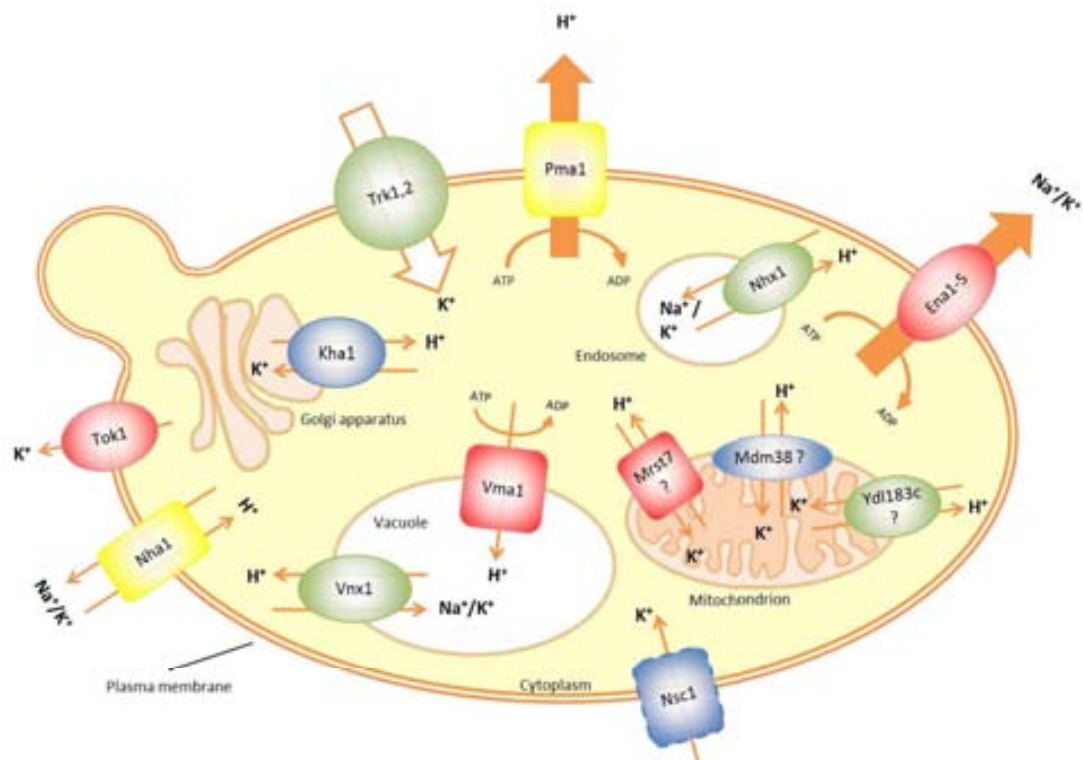


Figure 5. The major plasma membrane and intracellular cation transporters in the yeast S. cerevisiae. The main transporters located either in the plasma membrane or in the organelles are shown. The questions marks on the mitochondria indicate that it is not known if these proteins are transporters or they participate in their regulation (adapted from (Ariño et al., 2010)).

3.1.1 The ATPases Ena

In order to understand this work, we may explain deeply the Ena ATPase. The genes *ENA1* to *ENA5* encode P-type ATPases, coupling the hydrolysis of ATP to the transport of cations against electrochemical gradient by forming a typical phosphoenzyme intermediate (Haro, Garcíadeblas, & Rodríguez-Navarro, 1991). They belong to a protein subfamily of ATPases which are able to extrude sodium, lithium and potassium with different affinities

(Benito, Garcíadeblás, & Rodríguez-Navarro, 2002). In *S. cerevisiae* the *ENA* genes, which encode nearly identical proteins, are disposed in tandem repeats, from *ENA1* to *ENA5*, with a variable number of copies depending on the strain (Wieland, Nitsche, Strayle, Steiner, & Rudolph, 1995). Deletion of the entire *ENA* cluster in *S. cerevisiae* results in a phenotype of dramatic sensitivities to sodium and lithium cations as well as to alkaline pH (Posas et al., 2000).

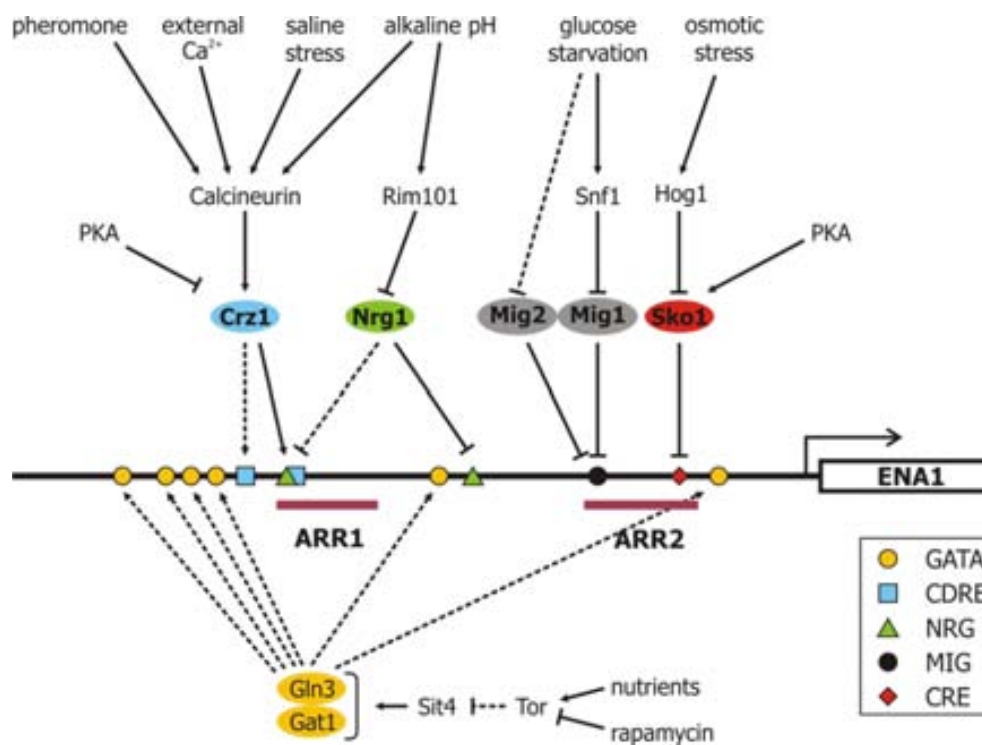


Figure 6. Schematic outline of the regulation of the *ENA1* promoter in *S. cerevisiae*. Only the major components of the signal transduction pathways and the corresponding stimuli that activate them are denoted. Discontinuous lines represent inputs to the promoter that were not documented when the work started or that still remain obscure. The regulatory DNA-motifs are represented to their relative position on the promoter (which is not drawn at to scale) with basic shapes and indicated in the inset (figure based on (Amparo Ruiz & Ariño, 2007)).

It is widely accepted that *ENA1* is the functionally relevant component of the cluster on the basis that **i)** cation sensitivity is largely restored by expression of *ENA1* and **ii)** whereas under standard growth conditions expression of the *ENA* genes is almost undetectable, *ENA1* expression dramatically increases in response to osmotic, saline or alkaline pH stresses (Ariño et al., 2010; Garcíadeblás et al., 1993; Mendoza, Rubio, Rodríguez-Navarro, & Pardo, 1994). As shown in *Figure 6*, expression of *ENA1* is also activated by other stimuli such glucose starvation (Alepuz, Cunningham, & Estruch, 1997), limited nitrogen conditions (Crespo, Daicho, Ushimaru, & Hall, 2001) or high concentrations of extracellular calcium (Withee, Sen, & Cyert, 1998).

The transcriptional regulation of *ENA1* by diverse stimuli mentioned above requires the intervention of multiple pathways that transmits the signal to its promoter. According to the *Figure 6*; diverse regulatory elements have been identified on the *ENA1* promoter that is recognized by specific transcription factors which activate or inhibit its transcription, depending on the signal.

3.2 Calcium homeostasis

An increase in the concentration of cytosolic calcium cations implies the activation of the PP2B or calcineurin. Although it is well-known that several stresses cause a raise in the intracellular calcium concentration in yeast, the details of the response mechanisms are not yet fully understood. The regulation of intracellular calcium concentration in the cell cytoplasm and other cell compartments is completely accurate by using a net of calcium transporters (M Bonilla & Cunningham, 2002).

Calcineurin is an heterodimer that consists of two subunits: **a)** a regulatory subunit encoded by *CNB1* and **b)** a catalytic subunit encoded by two genes *CNA1* and *CNA2* (reviewed in (Cyert, 2003). Its phosphatase activity may be blocked by adding to the medium the inhibitors, commonly used as immunosuppressive drugs, FK506 (tacrolimus) and cyclosporin A (Foor et al., 1992). Calcineurin, the Ca^{2+} /calmodulin-regulated protein phosphatase, is highly conserved through eukaryotes and it is a critical component of Ca^{2+} -regulated signaling in a wide range of unicellular and multicellular eukaryotes. In *S. cerevisiae*, calcineurin is activated due to the direct binding of calcium to calmodulin (Cyert, Kunisawa, Kaim, & Thorner, 1991).

Several stresses lead to an increase in the intracellular calcium concentration, such as: high temperature (C. Zhao et al., 1998), addition of glucose to starving cells (Nakajima-Shimada, Iida, Tsuji, & Anraku, 1991), sphingosine (Birchwood, Saba, Dickson, & Cunningham, 2001), prolonged exposure to mating pheromone α -factor (Iida, Yagawa, & Anraku, 1990), elevated extracellular concentrations of ions such as Mn^{2+} , Ca^{2+} or Li^+/Na^+ (V Denis & Cyert, 2002; Farcasanu, Hirata, Tsuchiya, Nishiyama, & Miyakawa, 1995; Matsumoto et al., 2002), alkaline pH (R Serrano, Ruiz, Bernal, Chambers, & Arino, 2002; L Viladevall et al., 2004), hypotonic shock (Batiza, Schulz, & Masson, 1996) or the response to an unfolded protein stressor such as tunicamycin (M Bonilla, Nastase, & Cunningham, 2002).

The raise of intracellular calcium in each of these stimuli may be possible due to either influx of calcium cations from the extracellular environment or the release from the main intracellular stores, such as the vacuole and the endoplasmatic reticulum (

) (Halachmi & Eilam, 1989; Strayle, Pozzan, & Rudolph, 1999). For example, exposure to pheromones and endoplasmatic reticulum stress leads to the entry of extracellular calcium through the plasma membrane Mid1-Cch1 calcium channel (Iida, Nakamura, Ono, Okumura, & Anraku, 1994; Paidhungat & Garrett, 1997). On the other hand, in case of hypotonic stress, calcium comes out of the vacuole through the Yvc1, a calcium-channel involved in the transient receptor potential (TRP) family of ion channels (Batiza et al., 1996). Finally, it has been described that under hyperosmolarity conditions the calcium is released from the vacuole through the Yvc1 channel (Valerie Denis & Cyert, 2002), but another study also demonstrated that its origin is extracellular, through the Mid1-Cch1 channel (Matsumoto et al., 2002). This exemplifies the complexity of the calcineurin pathway (

).

Active calcineurin can dephosphorylate its main target, Crz1, which is a zinc finger transcription factor (Matheos, Kingsbury, Ahsan, & Cunningham, 1997; Stathopoulos & Cyert, 1997a). Its dephosphorylation may change its tridimensional structure exposing the nuclear localization sequence (NLS) that is recognized by the Nmd5 importin, through which Crz1 is translocated to the nucleus (Polizotto & Cyert, 2001). Once in the nucleus, this transcription factor binds to the promoters containing a specific consensus DNA motif (5'-GNGGC(G/T)CA-3') denominated Calcineurin Dependent Response Element (CDRE) (Stathopoulos & Cyert, 1997a). Large scale transcriptional studies performed in yeast using DNA microarrays revealed that calcineurin activation induces the expression of more than 160 genes, most of which contain one or more CDREs on their promoters (Yoshimoto et al., 2002).

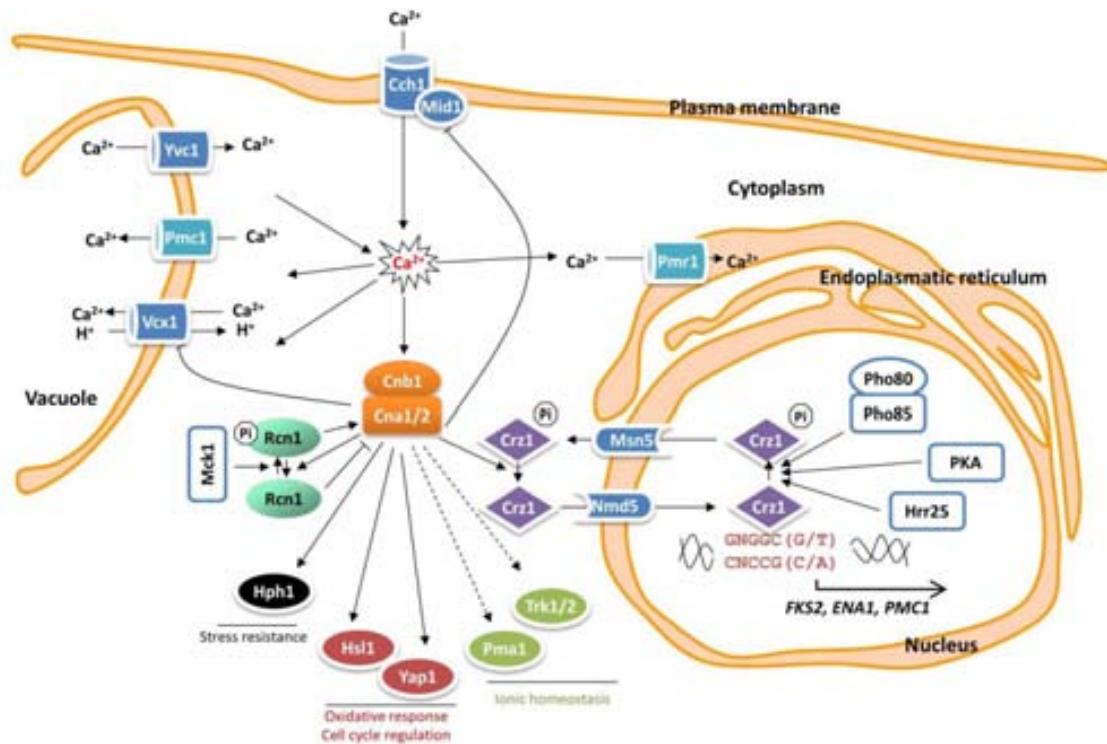


Figure 7. Scheme of the calcineurin pathway. The main transporters involved in calcium homeostasis are depicted: Mid1-Cch1 and Yvc1 which contribute to intracellular Ca^{2+} raises and Pmc1, Vcx1 and Pmr1 which eliminate calcium from the cytoplasm. Specific environmental conditions provoke increases of intracellular Ca^{2+} and the phosphatase calcineurin is activated dephosphorylating Crz1 which then enters the nucleus to activate CDRE-containing genes. Deactivation of Crz1 occurs upon phosphorylation by PKA, Hrr25 and the Pho85-Pho80 CDK complex. Calcineurin activation depends on the phosphorylation state of the calci-repressin Rcn1. Adapted from Raquel Serrano's thesis.

As expected, exit of Crz1 from the nucleus is regulated by its phosphorylation state. The karyopherin Msn5 is needed for the translocation of Crz1 from the nucleus to the cytoplasm (Boustany & Cyert, 2002). It has been demonstrated that Crz1 is a substrate of three different kinases: the casein kinase I isoform, Hrr25, the cyclic AMP-dependent protein kinase (PKA) and the cyclin dependent kinase Pho85 (under Pho80 regulation) (Kafadar & Cyert, 2004; Kafadar, Zhu, Snyder, & Cyert, 2003; Sopko et al., 2006).

Although Crz1 is the main target of calcineurin, other targets involved in diverse functions have also been described such as: Vcx1, Cch1-Mid1, Rcn1, Hsl1, Yap1, Hph1 and the ion transporters Pma1 and Trk1/2 (

).

Very few is known about the role of Glc7 in the calcineurin pathway: a phenotypical analysis of *glc7-109 cnb1* double mutant strain demonstrated that the ions-related phenotypes conferred by the double mutant are additive or synergistic, because this strain is more sensitive to Mn^{2+} , Li^+ , and Cs^+ than either of the single mutants. These data may indicate that the substrates of Glc7 responsible of the sensitivities to ions are different to those of calcineurin (Tara Williams-Hart et al., 2002).

3.3 The Cell Wall Integrity signaling pathway

The yeast cell wall has four principal functions: **i)** provide protection from osmotic shocks; **ii)** protect cells from mechanical stress; **iii)** regulate cellular shape and size and **iv)** serve as a scaffold for cell-surface proteins (Klis, Boorsma, & De Groot, 2006; David E Levin, 2011).

This cellular structure may comprise between 10 to 25% of cellular dry weight depending on growth conditions. Structurally yeast cell wall is formed by two layers: the electron-transparent inner layer and an electron-dense outer layer (Cappellaro, Baldermann, Rachel, & Tanner, 1994). The inner layer is basically constructed by β -1,3-glucan chains branched through β -1,6 linkages and chitin chains, whose main role is to provide mechanical strength and elasticity of the cell wall. On the other hand, the outer layer is made up by highly glycosylated proteins. There are two major classes of cell wall glycoproteins: **1)** glycosylphosphatidylinositol (GPI) proteins, which are bound to the layer through β -1,6-glucans, and **2)** Pir proteins (Protein with internal repeats) which are directly bound through β -1,3-glucans (Free, 2013; Klis et al., 2006; Klis, Mol, Hellingwerf, & Brul, 2002). Some of the functions of those cell wall glycoproteins are linked to cellular adhesion, processing of the own cell wall, growth and metabolism (reviewed by (Klis et al., 2002; G. Lesage & Bussey, 2006)).

The cell wall integrity pathway (CWI) allows yeast cells to respond and modulate the morphological changes needed to adapt to potential damaging environmental challenges. This pathway is formed by a family of membrane sensors, signal transducers and effectors which specifically regulate either the transcription of certain genes or the function of some proteins depending on the stimuli (*Figure 7*).

The CWI signaling is activated by multiple stresses such as: **i)** growth at elevated temperatures (which implies an increase in the internal pressure due to trehalose accumulation); **ii)** hypo-osmotic shock; **iii)** pheromone-induced morphogenesis, which induces

cell arrest in G₁ phase; **iv**) agents that interfere with the cell wall assembly stress such as the chitin antagonist Calcofluor white and Congo red (Ketela, Green, & Bussey, 1999), caffeine (Kuranda, Leberre, Sokol, Palamarczyk, & Francois, 2006) or the cell wall lytic activities Zymoliasse; **v**) mutation of genes involved in the cell wall biogenesis; **vi**) endoplasmatic stressor agents (tunicamycin, dithiothreitol) and finally, **vii**) oxidative, mechanical or pH stresses (all reviewed in (David E Levin, 2011)).

All those stimuli are detected on the cell surface by several sensors such as Wsc1/2/3, Mtl1 and Mid2 (which is also a calcium sensor) that recruit Rom1/2 to the plasma membrane. Rom1/2, together with Tus2, are considered GEF proteins (Guanoside nucleotide Exchange Factors), which exchange GDP for GTP, activating Rho1. On the other hand, there also exists Bem2, Sac7, Bag7 and Lrg1 which act as GAP proteins (GTPase Activating Proteins) inactivating Rho1. Rho1 is considered the master regulator of CWI signaling not only because it receives the major inputs from the cell surface but also because it regulates a variety of outputs involved in: activating protein kinase C (PKC), upregulating β -1,3-glucan synthase activity (Fks1 and Fks2), actin organization (Bni1 and Bnr1) and polarized secretion (Sec3) (D E Levin, 2005). It is important to remark that phosphoinositides play an important role in both, the proper localization and activation of Rom1/ (*Figure 8*) (David E Levin, 2011).

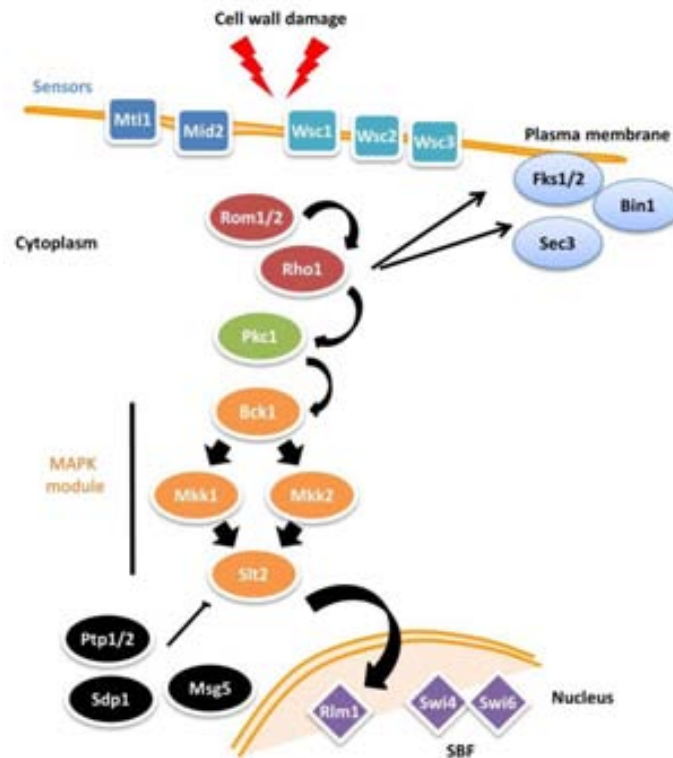


Figure 8. Cell Wall Integrity pathway. Cell wall stress is perceived from the cell surface sensors Wsc1-3, Mid2 and Mtl2 and the signal is transmitted through the G-protein Rho1 to the Pkc1 protein kinase. When activated, Pkc1 in turn activates the members of the MAP kinase cascade, Bck1, Mkk1/2 and Slt2. Two transcription factors, Rlm1 and the SBF complex (Swi4/Swi6) are targets of Slt2 MAP kinase.

Among the effectors of Rho1, the most studied pathway is Pkc1/Slt2, which is one of the five MAPKs pathways (Mitogen Activated Protein Kinase) found in *S. cerevisiae*. This is a linear signal transduction pathway based on phosphorylation. Activation of the Slt2 MAPK pathway is initiated with the activation of the G-protein Rho1 that associates with Pkc1. This complex activates the MAPKKK Bck1 by phosphorylation in the residues Ser939, Thr1119 and Ser1134, which phosphorylates the redundant Mkk1/Mkk2 MAPKKs which, in turn, recognize and phosphorylate the residues Thr190 and Tyr192 located on the typical "T-X-Y" MAPK motif (reviewed extensively in (D E Levin, 2005; David E Levin, 2011)). These four kinases differ in their location in non-stress conditions: Bck1 and Mkk1/2 are located in the cytoplasm while Slt2 resides predominantly in the nucleus. However, in case of cell wall stress Slt2 is relocated quickly in the cytoplasm. A small fraction of both Slt2 and Mkk1/2 is positioned to the polarisome in a dependent manner of Spa2, a protein that functions in the organization of the actin cytoskeleton (Kamada, Jung, Piotrowski, & Levin, 1995; van Drogen & Peter, 2002). It has been shown that Slt2 is able to phosphorylate *in vitro* both Mkk1 and Mkk2 revealing the

possible existence of a complex feedback mechanism whose functional implications remain to be determined (Jimenez-Sanchez, Cid, & Molina, 2007).

The inactivation of Slt2 is due to dephosphorylation and it is catalyzed by at least four phosphatases. Msg5 is a dual specificity phosphatase that also has the ability to inactivate Fus3, the MAPK of the pheromone response and invasive growth-filamentous pathway (Doi et al., 1994; Flandez, Cosano, Nombela, Martin, & Molina, 2004). It has also been described a positive feedback through which Slt2 phosphorylates Msg5 phosphatase interfering in the association of both proteins and avoiding the dephosphorylation of Slt2 (Flandez et al., 2004). The tyrosine phosphatases Ptp2 and Ptp3, which also dephosphorylate the Hog1 and Fus3 MAPKs, also dephosphorylate *in vitro* and *in vivo* Slt2 (Mattison, Spencer, Kresge, Lee, & Ota, 1999). Unlike Msg5, Slt2 has a negative feedback with Ptp2 facilitating the inactivation of Slt2. It is postulated that Ptp2 and Ptp3 probably exert their function by restoring the basal levels of phosphorylation of Slt2 upon activation by stress, although it appears that Ptp2 is more effective than Ptp3 (D E Levin, 2005). Finally Sdp1, a dual specificity phosphatase, appears to act specifically on Slt2 (Collister et al., 2002; J. S. Hahn & Thiele, 2002).

Known substrates of Slt2 are located in the nucleus. The best characterized is the transcription factor Rlm1 constitutively located in the nucleus, which is activated by phosphorylation in Ser427 and Thr439 by Slt2, stimulating its function. Rlm1 is responsible for most of the transcriptional response generated via CWI, affecting the expression of genes involved in cell wall biogenesis having the motif 5'-CTA(A/T)4TAG-3' in their promoters (K. S. Lee, Hines, & Levin, 1993). An interesting target of Rlm1 is the gene coding for the pseudokinase Mlp1, very similar to Slt2, that is strongly regulated by Rlm1 (Torre-Ruiz, Torres, Arino, & Herrero, 2002; J. Torres, Di Como, Herrero, & De la Torre, 2002).

A second transcription factor implicated in CWI signaling is the SBF complex, a regulator of G₁-specific transcription composed by Swi4 and Swi6 (Breedon, 2003; Madden, Sheu, Baetz, Andrews, & Snyder, 1997), specifically activated during bud emergence and mating projection formation, the periods of the cell cycle during which cell growth is highly polarized. Swi4 is the sequence-specific DNA-binding subunit that recognizes a seven-nucleotide sequence called an SCB (CA/GCGAAA) and, Swi6 is required for the binding to promoters (Taylor et al., 2000). It has been described that SBF drives gene expression in response to cell wall stress in a manner that is independent of its role in G₁-specific transcription. Basically, when Slt2 and Mlp1 are activated, they recruit the RNA polymerase II and Paf1 in a Swi6-dependent manner, allowing the elongation process of genes linked to the

CWI response (K. Y. Kim, Truman, & Levin, 2008; K.-Y. Kim & Levin, 2010; K.-Y. Kim, Truman, Caesar, Schlenstedt, & Levin, 2010; Truman, Kim, & Levin, 2009).

Besides the Ser/Thr phosphatases, other PPs are also playing an important role in the maintenance of cellular integrity. For example, Ppz1/2 also control Pkc1 activity (K. S. Lee et al., 1993; Lynne Yenush, Mulet, Ariño, & Serrano, 2002), Sit4 exercises control over the membrane sensors and regulates the pathway of cell integrity together with the TOR kinase, another important component in this pathway, which activates Rom1/2 proteins in response to nutrient availability (Torre-Ruiz et al., 2002; J. Torres et al., 2002). The study of *glc7-10* a thermo-sensitive allele of the Glc7 has helped to establish a functional link between this phosphatase and the CWI response (Andrews & Stark, 2000). At the restrictive temperature, *glc7-10* strains accumulated a high proportion of budded cells with an unmigrated nucleus, duplicated spindle pole bodies, short spindles, delocalized cortical actin patches and 2C DNA content, indicating a cell cycle block prior to the metaphase to anaphase transition. The phenotype of *glc7-10* allele was suppressed either by growth on high osmolarity medium or by extra copies of *PKC1*, *ROM2*, *RHO2*, *WSC1* or *MID2*. Neither a high dosage of Bck1 hyperactive version (*BCK1-20*) nor Mkk1 nor nonfunctional versions of Pkc1 were able to restore the wild-type phenotypes of the *glc7-10* strain. Thus, it appears that the dephosphorylation, by Glc7, is also able to promote the maintenance of cell integrity in a manner that depends on the signal transduction pathway controlled by Pkc1 kinase (Andrews & Stark, 2000).

3.4 Efflux pump-mediated drug resistance as a stress response

While the response of microorganism to stresses such as pH, temperature, ionic homeostasis, osmolarity changes have been well studied, it is important to claim that the administration of antifungal drugs also represents a stress to which fungi must respond to (R. D. Cannon et al., 2009; Cowen & Steinbach, 2008). The nature of the fungal response to antifungal drugs depends on the fungus, the dose, its duration, and the mechanism of drug action.

There are five main antifungal drug classes: fluorinated pyrimidine analogues, polyenes, allylamines, imidazoles and echinocandins. Besides fluorinated analogs and echinocandins which primary target are the DNA/RNA and the cell wall synthesis, respectively, the other antifungals act on the ergosterol biosynthetic pathway (R. D. Cannon et al., 2009). Antifungal drugs initially stimulate classic intermediate stress response such as metabolic

alterations that minimize the toxicity of the drug, as well as the activation of chaperones and signal transduction cascades dedicated to sensing and responding to various stresses (Cowen, 2008). This short-term phenotypic stress responses, which are reversible and do not involve mutations or chromosomal rearrangements, lead to drug tolerance which are needed to develop long-term genetically stable resistance mechanisms that could also confer a fitness gain (R. D. Cannon et al., 2009). Later responses may include mechanisms to bypass the effects of the antimicrobial drugs involving genetic mutations, usually point mutations in drug targets, enzymes or in transcription factors, leading to either the block of drug binding or to overexpression of multidrug transporters which remove the drug from the cell. To achieve this long-term tolerance response to any drug, yeast cells may trigger genetic rearrangements or even aneuploidy as a transient evolutionary solution to the stress, before a more specific and accurate adaptation to the new environmental growth conditions (Yona et al., 2012). Whole-genome sequencing, physical mapping, chromosomal-genome hybridization and haplotype analysis shown that chromosome deletions, translocations, and gain or loss of chromosomes generating aneuploidy strains, are common mechanism of long-term adaptation to either drugs or stresses (Hughes et al., 2000; Ma & Liu, 2010; Perepnikhatka et al., 1999; Yona et al., 2012).

Two are the families of multidrug transporters or efflux-pumps: the ATP-binding cassette (ABC) and the Major facilitator superfamily (MFS) (*Figure 9*). Both transporters have common characteristics: **i)** are widespread among plants, animals, bacteria and fungi; **ii)** are membrane proteins that actively translocate compounds across cell membrane using different energy sources; and **iii)** have transmembrane domains (TMD) which determine the substrates specificity (R. D. Cannon et al., 2009).

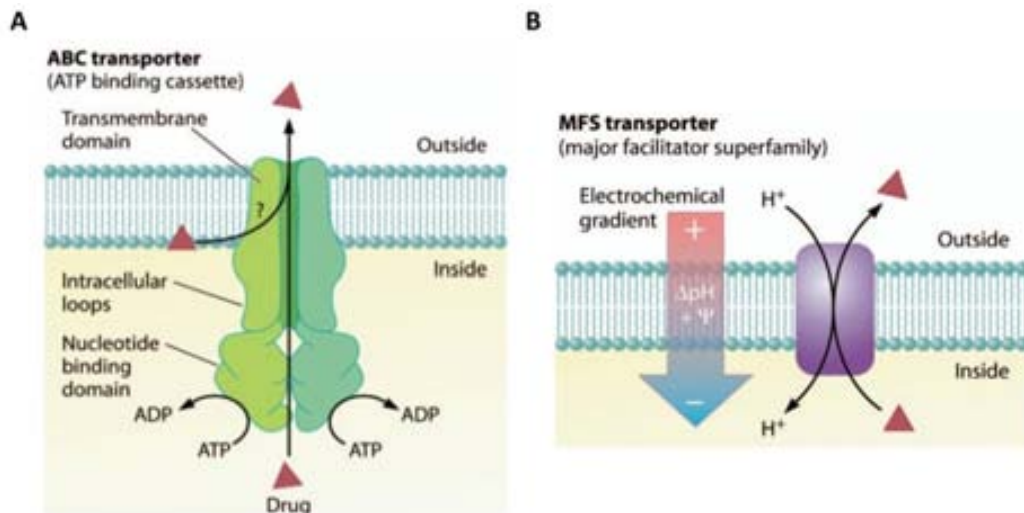


Figure 9. Domain arrangements of ABC (A) and MFS transporters (B) (R. D. Cannon et al., 2009).

- a) ATP-binding cassette (ABC) transporters are primary transporters which use the hydrolysis of ATP. The basic structure of ABC transporters consist of two cytoplasmatic nucleotide binding domains (NBDs) (involved in binding and hydrolysis of ATP) and two TMDs which usually span the membrane six times via putative α -helices. *S. cerevisiae* has three subfamilies of ABC proteins encoded by 28 genes: pleiotropic drug resistance (PDR), multidrug resistance (MDR) and multidrug resistance-associated proteins (MRP). They differ in the arrangement of the NBDs and TMDs within the pump polypeptide. Pdr5 is the archetype and one of the best characterized of PDR proteins in *S. cerevisiae* (Balzi, Wang, Leterme, Van Dyck, & Goffeau, 1994; Bissinger & Kuchler, 1994; Hirata, Yano, Miyahara, & Miyakawa, 1994). This PDR subfamily has three unique features: **i)** the diversity of individual members of the family mainly resides in TMDs and external loops; **ii)** a PDR signature motif which suggests either topological motifs or a role in drug efflux and, finally, **iii)** an asymmetry in NBD motifs (Lamping et al., 2010). Deletion of PDR genes in *S. cerevisiae* confers a hypersensitivity to certain ions and xenobiotics, including the azole compounds (Decottignies, Owsianik, & Ghislain, 1999). Moreover, the overexpression of these ABC transporters may indirectly cause antifungal resistance through the effects of membrane composition, function or protein activity, since particular ABC proteins are involved in phospholipid transport across the lipid bilayer that may help maintain an asymmetry in the compositions of the two leaflets (Smriti et al., 2002).
- b) Major facilitator superfamily (MFS) transporters are secondary transporters which employ the proton-motive force across the plasma membrane. Those transporters

have lower range of substrate specificity than ABC pumps. MFS can be divided in two subfamilies based on the number of transmembrane spans (TMS): DHA1 (drug:H⁺ antiporter 1; 12 TMS) and DHA2 (14 TMS). *MDR1* was the first characterized gene of this, by its ability to confer benomyl and methotrexate resistance on *S. cerevisiae* (Fling et al., 1991).

At the beginning of this thesis was not evident the connections between antidrug resistance/sensitivity and the role of Glc7.

3.5 Unfolded protein response

Protein folding is an important aspect of cellular function in eukaryotic cells. The endoplasmatic reticulum (ER) is a membrane-enclosed interconnected organelle responsible for synthesis, folding, modification and quality control of numerous secreted and membrane proteins as well as most lipids biosynthesis, calcium storage and release (Wickner & Schekman, 2005). In order to efficient folding, the ER provides an oxidizing environment with chaperones, glycosylation and oxidoreductase activities (Gething & Sambrook, 1992). Improper protein maturation, changes in the environment or in cellular protein load may trigger the unfolded protein response (UPR). This response mediate by an intracellular signaling pathway, that is initiated in the ER and affecting the transcriptional machinery in the nucleus, aims to increase the ER's protein folding capacity when needed (Back, Schröder, Lee, Zhang, & Kaufman, 2005; Kawaguchi & Ng, 2011). In metazoans, three parallel pathways collectively comprise the UPR. The sensors are an ER-resident integral membrane protein, Ire1 (Inositol Requiring Enzyme I), PERK (Protein kinase RNA (PKR)-like ER Kinase) and ATF6 (Activating Transcription Factor 6) which transmits the information from the ER across the membrane into the cytosol where a series of transcription factors will carry this information to the nucleus (*Figure 10* and *Figure 11A*) (Walter & Ron, 2011). In mammals, UPR is also activated in cancer, viral infections, protein-folding diseases and other cellular anomalies (Korennykh et al., 2009).

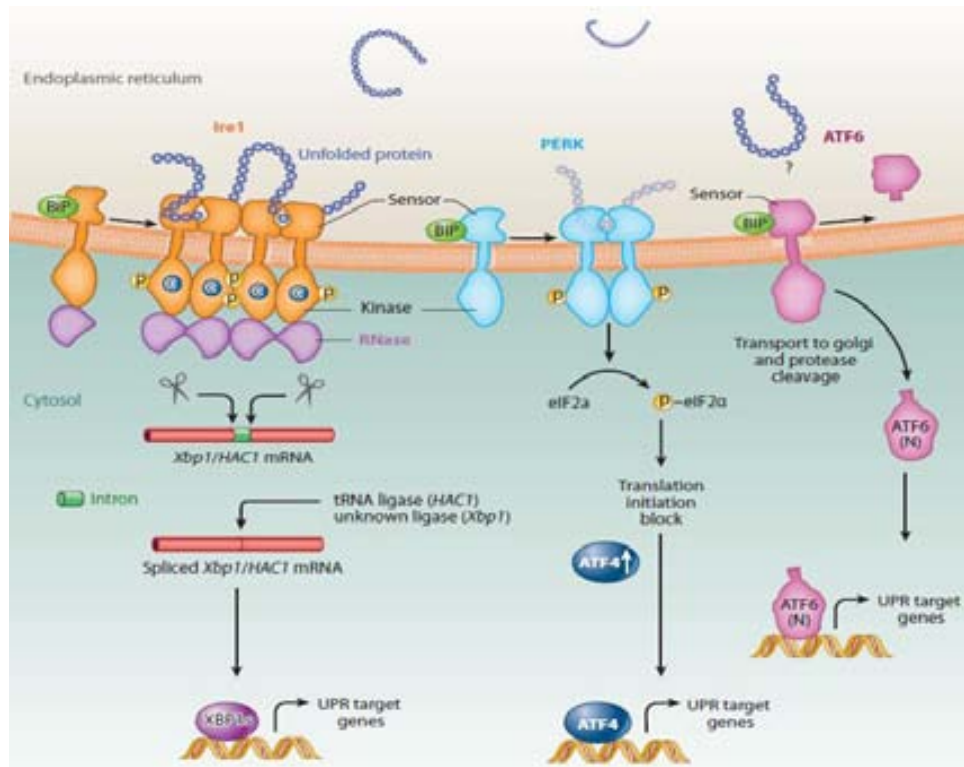


Figure 10. The three unfolded protein response (UPR) branches in higher eukaryotes (Korennykh & Walter, 2012).

In eukaryotes, approximately one third of the proteins enter the ER for processing and folding. The quality of protein folding in yeast cells is only monitored by the ER-membrane-resident kinase/RNase Ire1 through three different biochemical activities: **a)** sensing misfolded proteins in the ER lumen, that trigger the oligomerization of Ire1; **b)** oligomerized Ire1 undergoes autophosphorylation through its protein kinase domain; and **c)** activation of the Ire1 endoribonuclease activity causes the atypical splicing reaction that results in the cleavage of the mRNA encoding the transcription factor Hac1, allowing its translation, Hac1 is translocated to the nucleus where will activate the transcriptional response to the unfolded protein stress (Figure 11).

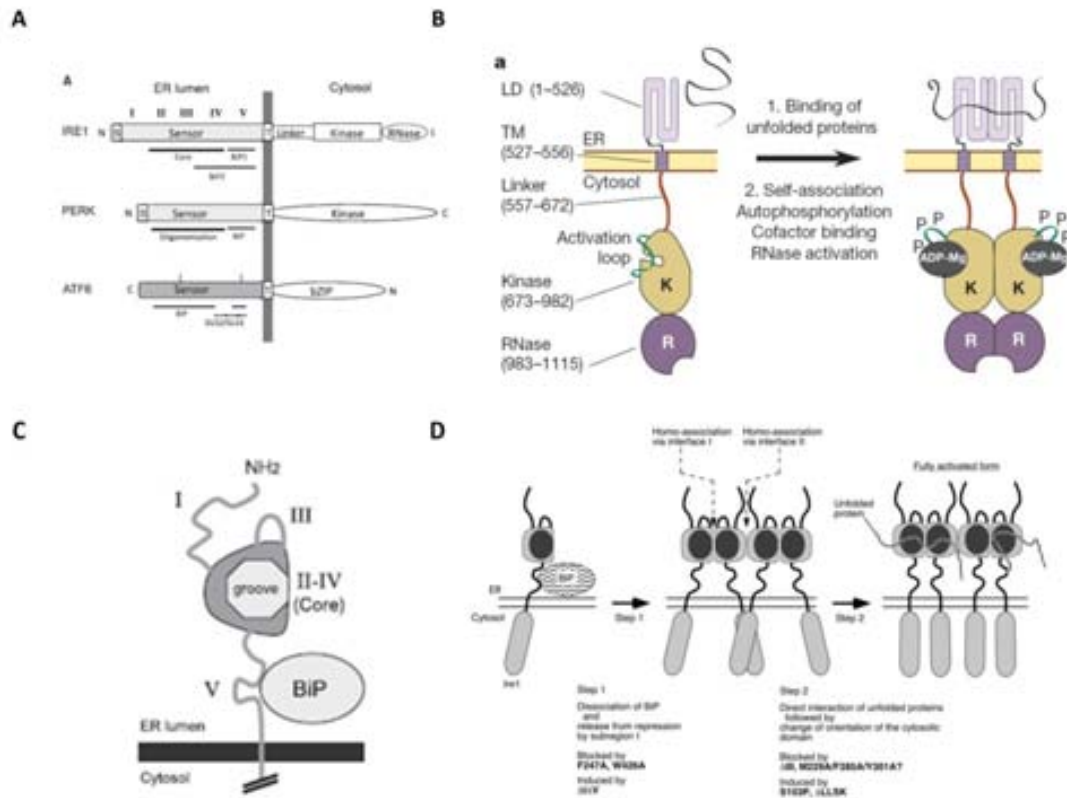


Figure 11. The structure of Ire1 and its role in the activation of the UPR pathway. **A)** Schematic representation of three transmembrane ER mammalian stress sensors: Ire1, PERK and ATF6. Thin lines indicate BiP binding regions (BiP1, assigned by yeast Ire1; BiP2, a potential binding region of human IRE1a). Bold lines represent regions that are indispensable for sensing stress (core). The broken line represents a region necessary for Golgi translocation (GLS: Golgi localization signal). Vertical bars indicate conserved cysteine residues in the ER luminal region of ATF6. S, signal sequence; T, transmembrane region; bZIP, transcription factor containing basic leucine zipper; N, amino terminus; C, carboxyl terminus; IV, yeast Ire1 subregion (Kohno, 2010). **B)** A general scheme of Ire1 activation during the UPR summarizing the key events. The kinase domain of Ire1 (K) is colored brown and the RNase domain (R) is colored purple (Korennikh et al., 2009). **C)** A diagram of yeast Ire1 luminal region where is represented the core stress-sensing region (CSSR) (Kohno, 2010). **D)** Chaperone protein Kar2 (similar to mammalian BiP) binds to Ire1 and dissociates in response to endoplasmic reticulum stress (Kimata et al., 2007).

Ire1 was originally identified as a gene encoding a protein of 127 kDa required for inositol auxotrophy (Inositol Requiring Element 1) (Nikawa & Yamashita, 1992) due to its genetic complementation of a myoinositol auxotrophic mutant. It was found to be essential for cell viability during tunicamycin-induced ER stress and induction of the *KAR2* gene (Cox, Shamu, & Walter, 1993; Mori, Ma, Gething, & Sambrook, 1993). Structurally, Ire1 is an atypical type I transmembrane protein, which contains an N-terminal ER luminal domain and, both a kinase and an RNase domains, at the C-terminal domain (Figure 11C). The ER luminal domain has been exhaustively analyzed by deletion mutagenesis which resulted in the identification of five subregions (I to V) (Figure 11C) (Kimata, Oikawa, Shimizu, Ishiwata-Kimata, & Kohno, 2004). Regions II-IV form a tightly folded domain that is responsible for the dimer/oligodimer formation and includes the core sensing-stress response (CSSR) which is needed to activate the

UPR. In the subregion V is located the ER-resident chaperone-binding immunoglobulin protein Kar2/(BiP)-binding site. To activate Ire1, the sensor domain detects the unfolded proteins by: **a)** a competition between the sensor domain of Ire1 and unfolded proteins which bind to BiP causing its dissociation from the sensor domain (Bertolotti, Zhang, Hendershot, Harding, & Ron, 2000); **b)** a direct binding of unfolded proteins to the sensor domain of Ire1 suggesting that BiP maintains the concentration of free Ire1 monomers at an appropriate level for sensing unfolded proteins (Credle, Finer-Moore, Papa, Stroud, & Walter, 2005; Pincus et al., 2010).

Activating the UPR implies the oligomerization of Ire1, a mechanism that is independent of its kinase domain. This domain acts as an allosterically regulated scaffold that enables oligomerization of the RNase domains (Chawla, Chakrabarti, Ghosh, & Niwa, 2011; Korennykh et al., 2009; Papa, Zhang, Shokat, & Walter, 2003). The activation of Ire1 endo-RNase activity depends on the trans-autophosphorylation (up to 20 phosphates) and binding of ADP helps to fully activate Ire1. It is important to note that, however oligomerization driven trans-autophosphorylation is a common stereotype of cell signaling, Ire1 does not signal downstream via phosphorylation. Rather, a conformational change that occurs upon nucleotide binding acts as a molecular switch to activate Ire1's RNase (Gardner, Pincus, Gotthardt, Gallagher, & Walter, 2013).

The next step is the splicing of the RNA of the transcription factor Hac1 (**H**omologous to **A**tf/**C**reb1) in yeast (homologue to the mammalian XBP1), which is the only substrate for the Ire1 endoribonuclease activity. Interestingly, the SAGA complex, responsible for histone acetylation during transcriptional activation (Daniel & Grant, 2007; Timmers & Tora, 2005), is required for the Ire1-mediated cleavage of *HAC1* mRNA in yeast through Ada5, one of its multiple subunits (Welihinda, Tirasophon, & Kaufman, n.d.). Hac1 is a basic leucine zipper (bZIP) transcription factor which can translocate to the nucleus and activates the UPR genes due to the binding to UPRE (Nojima et al., 1994). Under non-stress conditions, the mRNA encoding for Hac1 uninduced form (*HAC1^u*) resides in the cytoplasm and cannot be translated because of base pairing between the intron and the 5' untranslated region (UTR) that causes ribosomes to stall (Rüeggsegger, Leber, & Walter, 2001). The activated Ire1 RNase domain cleaves the *HAC1* mRNA removing a 252-ribonucleotides intron by a two-step cleavage reaction to produce the mature (induced) form of its mRNA, *HAC1ⁱ*, after ligation of the exons by the tRNA ligase Trl1. It is important to remark that this is a non-conventional splicing event, independent of the spliceosome (T. N. Gonzalez, Sidrauski, Dörfler, & Walter, 1999; Kawahara, Yanagi, Yura, & Mori, 1998; Sidrauski, Cox, & Walter, 1996). Once *HAC1* has been translated, it

enters in the nucleus where acts as a UPR-specific transcription factor, inducing the expression of the UPR target genes expression which contain the unfolded protein response element (UPRE) in their promoters (Travers et al., 2000). The UPRE was originally defined as a 22-bp sequence element of the *KAR2* promoter and subsequently was refined as the seven-nucleotides consensus, CAGNGTG (Mori et al., 1992; Mori, Ogawa, Kawahara, Yanagi, & Yura, 1998). Microarrays experiments have shown that approximately 5% of the yeast genome (381 genes) gets upregulated by Hac1 during the UPR (Travers et al., 2000). These transcriptional changes implies the up-regulation of genes induced in several functional categories such as: translocation (*SEC61*, *SEC62*, *SPC2*), glycosylation (*DPM1*, *OST2*, *ALG6*), ER-resident chaperones (*KAR2*, *PDI1*, *FKB2*), protein degradation (*DER1*, *HRD1*, *DOA4*), vesicle trafficking (*ERV25*, *SEC12*, *SEC13*), lipid metabolism (*EPT1*, *INP51*, *LPP1*), vacuolar protein sorting (*LUV1*, *VPS17*, *VPS35*), cell wall biogenesis (*GAS5*, *CHS7*, *PKC1*) and, the ER-associated protein degradation (ERAD) which do not have a recognizable UPRE in their promoter.

Finally, down regulation of the UPR is an important aspect due to the fact that a constitutively active Ire1 pathway is not compatible with the proper function of the ER and has been shown to have significant impact on cell survival, triggering apoptosis (Lin et al., 2007). Since Ire1 is a multi-domain protein, it is plausible to think that its deactivation will most likely involve changes that affect both its luminal and cytosolic domains, although the mechanism involved in the inactivation remain to be discovered. Based on the activation mechanism, disassociation of the unfolded peptides and the reassociation of Kar2 will probably trigger the transition of Ire1 from its oligomeric to its monomeric form.

Currently, two are the hypotheses have been proposed for the yeast UPR deactivation process:

- a) It is supposed that a phosphatase activity will return Ire1 to its basal state, reversing its autophosphorylation. So far, two Ire1 phosphatases have been identified, Ptc2 and Dcr2 (Guo & Polymenis, 2006; Welihinda, Tirasophon, Green, & Kaufman, 1998). Ptc2 is one of the a PP2C phosphatases (Ariño, Casamayor, & González, 2011) that interacts with the cytosolic domain of Ire1 in a yeast two-hybrid assay. Dcr2 has a genetic interaction with Ire1 in a suppressor screen. Both phosphatases physically interacted with Ire1, could dephosphorylate Ire1 *in vitro*, and when over-expressed, they caused a decrease in the levels of spliced form of *HAC1*, thus indirectly, implying an effect on Ire1 (Guo & Polymenis, 2006; Welihinda et al., 1998). There is, however, a lack of any direct evidence for the involvement of either of

these phosphatases in turning off UPR signaling or even in their role of dephosphorylating Ire1's activation loop in vivo. Thus, it is plausible that either another one of the forty non-essential phosphatases or any regulatory subunit of the essential phosphatase in yeast might regulate the turning off on the UPR.

b) Recently, it has been postulated that phosphorylation of Ire1 is dispensable for its activation but it contributes significantly to its deactivation (Rubio et al., 2011). A sequence stretch located in a 28-amino acid surface loop of Ire1 contains seven residues of serine and two of threonine which can be phosphorylated and the phosphorylation of this hyper-phosphorylated loop (HPL) is important for the efficient shut down of Ire1 signaling. It has been speculate that the hyperphosphorylation of the HPL leads to the destabilization of the Ire1 oligomers by charge repulsion. Nonetheless, the authors also hypothesize that some other unknown UPR-modulating proteins might bind the phosphorylated HPL to control the shutdown of Ire1.

When we began this work, there was no evidence associating PP1 with the UPR neither in mammals nor in yeast. We will try to explain, in this thesis, a possible relationship between Glc7-regulatory subunits and the UPR.

4. Aneuploidy

Aneuploidy is the leading cause of miscarriages and mental retardation in humans and is found in 90% of human cancers (Hassold & Jacobs, 1984; Holland & Cleveland, 2009). It has already been more than a century when aneuploidy was first linked to tumors (reviewed in (Thompson, Bakhoun, & Compton, 2010)). Therefore, determining how aneuploidy affects cell physiology is critical for understanding the principles underlying many human diseases (E M Torres, Williams, Tang, & Amon, 2010).

Aneuploidy is a change in chromosome number that is not an exact multiple of the haploid karyotype meaning an unbalanced genomic state. By contrast, polyploidy refers to a state in which a cell contains an exact multiple of the entire genome, triggering a balanced genomic state (Pfau & Amon, 2012). Two types of model are being used to analyze the effects of aneuploidy on cell physiology: **1)** “chronic defined aneuploidies”, when the identity of the aneuploid chromosome is known, created by through single-chromosome transfers or spontaneous meiotic non-disjunction or; **2)** “acute random aneuploidies” when cells with high ratio of chromosome instability are used, given rise to spontaneous missegregation of

chromosomes (Geigl, Obenauf, Schwarzbraun, & Speicher, 2008). Consequences of aneuploidy in yeast cells, at the protein level are: **a)** a decreased in protein activities due to the reduction in gene dosage (haploinsufficiency) in cases of monosomy; or **b)** an imbalance in the protein stoichiometry deriving from chromosome gain.

Basically, polysomic yeast cells display decreased fitness, relative to wild-type cells. Other than the specific phenotypes characteristics for any given polysomy, there are a set of common traits which are shared among the different aneuploid yeast strains (E M Torres et al., 2010; Eduardo M Torres, Williams, & Amon, 2008). Some of common phenotypes are:

1. Impaired at elevated temperature (37°C)
2. The imbalance in protein stoichiometry due to the extra chromosome causes a proteotoxic stress (Oromendia, Dodgson, & Amon, 2012). Analyses of the transcripts and protein levels in yeast cells having an extra copy of one particular chromosome revealed that most genes of the extra chromosome are transcribed at twice the rate as the rest of the genome, meaning that the aneuploid chromosomes are active in yeast. (Tang & Amon, 2013; Eduardo M Torres et al., 2007). Maintaining the exact number of each protein is regulated by protein quality-control pathways, such as protein degradation or chaperone-mediated sequestration or feedback control which regulates the gene expression to maintain the balance of multiprotein complexes. For that, aneuploid strains may show hypersensitivity to conditions or compounds that interfere with protein synthesis, folding and degradation, such as cycloheximide, hygromycin, thiolutin, rapamycin and proteasome inhibitor MG132 (Cetin & Cleveland, 2010). Deletion of the *UBP6* gene, coding for an ubiquitin-specific protease (Park et al., 1997), increase the growth rate of certain aneuploid strains by attenuating the changes in intracellular protein composition leading to suppress the adverse effects of aneuploidy (Eduardo M Torres et al., 2010).
3. An increase in glucose uptake, partially due to the proteotoxic stress, meaning that the cells are spending more energy producing and degrading unneeded proteins than generating biomass which is the main goal of yeast cells (*Figure 13*) (Eduardo M Torres et al., 2007).

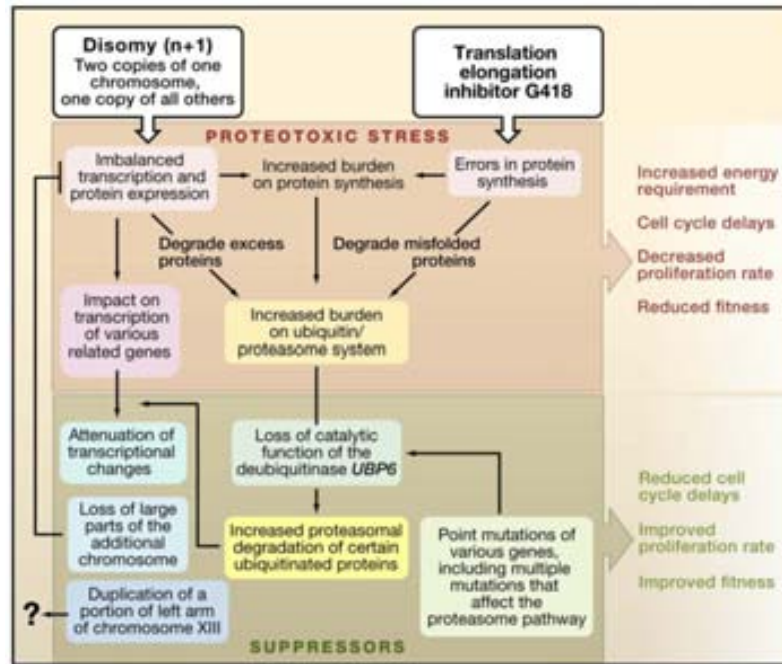


Figure 12. Aneuploidy induces proteotoxic stress. (Top) An extra copy of an individual yeast chromosome, or disomy in haploid cells, causes imbalanced expression of the proteins encoded on that chromosome. Adding an inhibitor of protein synthesis, such as G418 (Geneticin), increases the errors in translation and enhances the proteotoxic stress. This stress reduces fitness and inhibits cell growth primarily during the G₁ phase. (Bottom) Suppressors of proteotoxic stress, including mutations in components of ubiquitin/proteasome pathway, can ameliorate the proteomic imbalance and restore fitness (Eduardo M Torres et al., 2010). For example, disrupting the deubiquitinase *UBP6* can increase the growth rate of aneuploid cells by triggering more rapid protein degradation by the proteasome (Cetin & Cleveland, 2010).

4. A cell-cycle delay in G₁-phase. The doubling time and cell size are slightly increased in aneuploid cells grown in complete medium due to the fact that the gain of an extra chromosome interferes with cell proliferation. Basically, this phenotype may be caused by either the amount of additional yeast DNA or by affecting the Cln3-CDK function (Thorburn et al., 2013; Eduardo M Torres et al., 2007). In summary, aneuploidy causes a proliferative defect in yeast cells, which is the opposite effect the advantage in cellular proliferation typical of cancer cells.

In our study, we show that the lack of Ref2 in yeast cells causes aneuploidy which is dependent on the binding to Glc7 but independent of its functions in the holo-CPF.

Objectives

OBJECTIVES

The long-term goal of this work is functional characterization, by a combination of phenotypic, genetic and transcriptomic analyses of non-essential regulatory subunits of type 1 protein phosphatase in the yeast *S. cerevisiae*.

After the high-throughput analyses, and having had interesting experimental results, we focused our work the detailed analysis of two of these regulatory subunits: Ref2 and Reg1.

For Ref2, a subunit involved in mRNA/snoRNA maturation and processing, we analyzed its role in ionic homeostasis, cell wall integrity and unfolded protein response pathways as well as in the chromosome disorders, demonstrating new functions that are dependent on its binding to Glc7.

For Reg1, a subunit involved in the regulation of glucose-repressible genes, we focused our attention in its possible new function involved in the unfolded protein response, since it is important for the proper regulation, by phosphorylation, of Ire1.

Experimental procedures

EXPERIMENTAL PROCEDURES

1. Growth of *Escherichia coli* and yeast strains

E. coli DH5 α cells were used as plasmid DNA hosts and were grown at 37°C in LB (Luria–Bertani) medium, supplemented with 50 μ g/ml ampicillin when plasmid selection was required. Yeast cells were cultivated at 28°C, otherwise it will be specified, in YPD medium [1% (w/v) yeast extract/2% (w/v) peptone/2% (w/v) glucose] or in appropriate synthetic complete drop-out medium (Adams, Gottschling, Kaiser, & Stearns, 1997) for plasmid selection. Yeast strains used in this work are listed *Table 2-8*.

2. DNA recombinant techniques

E. coli were transformed with calcium chloride using the standard protocol from (Sambrook, E.F., & Maniatis, 1989). *S. cerevisiae* cells were transformed by a modified method of lithium acetate (Ito, Fukuda, Murata, & Kimura, 1983).

Treatment with restriction enzymes, DNA ligations and other recombinant DNA techniques were performed using standard methods from (Sambrook et al., 1989).

The resolution of the DNA fragments presents in complex reactions such as enzyme restrictions and PCR were performed by electrophoresis in agarose gels. The DNA fragments recovered from agarose gels were purified by solid resin affinity columns (GeneClean kit, QiaGen).

The plasmid preparations from *E. coli* cells were performed using the Eppendorf FastPlasmid MiniPreps extraction kit based on the lysozyme digestion of bacterial cells (now: QuickLyse Miniprep kit, Qiagen). Purified DNA was quantified by measuring the absorbance at 260 nm and its integrity/size verified by electrophoresis in agarose gels.

3. Deletion cassettes, gene disruptions

The gene disruptions were carried out with the one-step disruption methodology from (Rothstein, 1983). Yeast cells were transformed with the disruption cassettes, obtained by PCR, containing a selectable marker amplified from pAG25 or pFA6-kanMX4 (Ahmed et al., 1999),

and tails for homologous recombination. Disruptions by the proper insertion of the cassette were confirmed by PCR using specific oligonucleotides described in the *Table 9*.

ref2::nat1. Wild-type BY4741 (*Table 2*) was transformed with a 1.7 kbp *ref2::nat1* cassette amplified with the primers OJFD021 and OJFD22 (*Table 9*). Homologous recombination was verified by colony PCR using the primers OJFD020 and nat1-3' (*Table 9*) to amplify a 700 bp fragment in the cases of correct insertion or a 220 bp fragment, with the primers OJFD020 and OJFD023 (*Table 9*), when the gen *REF2* was not altered. This cassette was used to generate **YJFD1**, **YJFD2**, **YJFD3** and **YJFD4** strains (*Table 4*) that all gave the expected PCR fragment expected for the *REF2* gene disruption. Strains **YJFD49** and **YJFD50** (*Table 4*), however, simultaneously produced both PCR fragments, what could be explained by a chromosome (or a section harboring the *REF2* gene) duplication. The **YJFD5** strain (*Table 5*) was obtained when the wild-type DBY746 (*Table 5*) was transformed with the *ref2::nat1* cassette and only carries the deleted version of the *ref2* gene. The **YJFD9** (*Table 5*) strain was obtained when wild-type BY4742 cells (*Table 5*) were transformed with the *ref2::nat1* cassette. The **YJFD89** strain (*Table 5*) was obtained when the wild-type FY61 (*Table 5*) was transformed with the *ref2::nat1* cassette and only carries the deleted version of the *ref2* gene. The **YJFD90** (*Table 5*) strain was obtained when wild-type TM141 cells (*Table 5*) were transformed with the same cassette. The **YJFD92** and **YJFD94** strains (*Table 5*) were obtained when wild-type 1700 and CML476 cells (*Table 5*) were transformed with this cassette. The isogenic derivatives of BY4741 genetic background (*Table 2*) from EUROFAN collection were transformed with the *ref2::nat1* cassette to yield the double mutants collection listed in *Table 4*.

glc7::nat1. Wild-type BY4741 and its isogenic derivative BY4741 *ref2* (*Table 2*) were co-transformed with the centromeric *URA3*-marked pJFD10 plasmid (containing the *glc7-109* allele, see *Plasmid construction section*) and a 1.7 kbp *glc7::nat1* disruption cassette amplified with the primers OJFD81 and OJFD82 (*Table 9*). Diverse tests were carried out to ensure that the only *GLC7* gene copy corresponded to the plasmid-borne *glc7-109* allele (colony PCR with primers nat1-3' and OJFD80 (*Table 9*) and growth in 5'FOA plates). The **YJFD17** and **YJFD18** (*Table 5*) strains were obtained when wild-type BY4741 and its derivative *ref2* were transformed (*Table 2*) that all gave the expected PCR fragment expected for the *GLC7* gene disruption. The **YJFD17** and **YJFD18** (*Table 5*) strains were transformed with the centromeric *LEU2*-marked pJFD11 plasmid (containing the *glc7-109* allele, see *Plasmid construction section*) and selected in a drop-out leucine medium plates yielding **YJFD36** and **YJFD39** (*Table 5*) strains, respectively.

KanMX4-(tetO₇):REF2. Wild-type CML476 (*Table 5*) was transformed with a 2.2 kbp *KanMX4-(tetO₇)* cassette amplified with the primers OJFD067 and OJFD68 (*Table 9*) from the pCM325 plasmid (Yen, Gitsham, Wishart, Oliver, & Zhang, 2003). Homologous recombination was verified by colony PCR using the primers OJFD013 and K2 (*Table 9*) to amplify a 1 kbp fragment in the cases of correct insertion. This cassette was used to generate **YJFD16** strain (*Table 5*) which gave the expected PCR fragment expected for the *KanMX4-(tetO₇)* insertion in *REF2* promoter.

Strains	Genotype	Reference
BY4741 wt	MAT a <i>his3Δ1 leu2Δ met15Δ ura3Δ</i>	(Winzeler et al., 1999)
BY4741 <i>bck1</i>	<i>bck1::KanMX4</i>	(Winzeler et al., 1999)
BY4741 <i>bni4</i>	<i>bni4::kanMX4</i> ¹	(Winzeler et al., 1999)
BY4741 <i>bud14</i>	<i>bud14::kanMX4</i> ¹	(Winzeler et al., 1999)
BY4741 <i>cch1</i>	<i>cch1::KanMX4</i>	(Winzeler et al., 1999)
BY4741 <i>cnb1</i>	<i>cnb1::KanMX4</i>	(Winzeler et al., 1999)
BY4741 <i>dcr2</i>	<i>dcr2::kanMX4</i>	(Winzeler et al., 1999)
BY4741 <i>fin1</i>	<i>fin1::kanMX4</i> ¹	(Winzeler et al., 1999)
BY4741 <i>gac1</i>	<i>gac1::kanMX4</i> ¹	(Winzeler et al., 1999)
BY4741 <i>gip1</i>	<i>gip1::kanMX4</i> ^{1,4}	(Winzeler et al., 1999)
BY4741 <i>gip2</i>	<i>gip2::kanMX4</i> ¹	(Winzeler et al., 1999)
BY4741 <i>gip3</i>	<i>gip3::kanMX4</i> ¹	(Winzeler et al., 1999)
BY4741 <i>gip4</i>	<i>gip4::kanMX4</i> ¹	(Winzeler et al., 1999)
BY4741 <i>glc8</i>	<i>glc8::kanMX4</i> ¹	(Winzeler et al., 1999)
BY4741 <i>hac1</i>	<i>hac1::kanMX4</i>	(Winzeler et al., 1999)
BY4741 <i>i re1</i>	<i>ire1::kanMX4</i>	(Winzeler et al., 1999)
BY4741 <i>mhp1</i>	<i>mhp1::kanMX4</i> ¹	(Winzeler et al., 1999)
BY4741 <i>mid1</i>	<i>mid1::KanMX4</i>	(Winzeler et al., 1999)
BY4741 <i>mkk1</i>	<i>mkk1::KanMX4</i>	(Winzeler et al., 1999)
BY4741 <i>mkk2</i>	<i>mkk2::KanMX4</i>	(Winzeler et al., 1999)
BY4741 <i>mlp1</i>	<i>mlp1::KanMX4</i>	(Winzeler et al., 1999)
BY4741 <i>mpk1</i>	<i>mpk1::KanMX4</i>	(Winzeler et al., 1999)
BY4741 <i>msg5</i>	<i>msg5::KanMX4</i>	(Winzeler et al., 1999)
BY4741 <i>pig1</i>	<i>pig1::kanMX4</i> ¹	(Winzeler et al., 1999)
BY4741 <i>pig2</i>	<i>pig2::kanMX4</i> ¹	(Winzeler et al., 1999)
BY4741 <i>pmc1</i>	<i>pmc1::KanMX4</i>	(Winzeler et al., 1999)
BY4741 <i>pmr1</i>	<i>pmr1::KanMX4</i>	(Winzeler et al., 1999)
BY4741 <i>ppz1</i>	<i>ppz1::kanMX4</i>	(Winzeler et al., 1999)
BY4741 <i>ptc2</i>	<i>ptc2::kanMX4</i>	(Winzeler et al., 1999)
BY4741 <i>ptp2</i>	<i>ptp2::KanMX4</i>	(Winzeler et al., 1999)
BY4741 <i>ptp3</i>	<i>ptp3::KanMX4</i>	(Winzeler et al., 1999)
BY4741 <i>red1</i>	<i>red1::kanMX4</i> ¹	(Winzeler et al., 1999)
BY4741 <i>ref2</i>	<i>ref2::kanMX4</i> ¹	(Winzeler et al., 1999)
BY4741 <i>reg1</i>	<i>reg1::kanMX4</i> ¹	(Winzeler et al., 1999)
BY4741 <i>reg2</i>	<i>reg2::kanMX4</i> ¹	(Winzeler et al., 1999)
BY4741 <i>rlm1</i>	<i>rlm1::KanMX4</i>	(Winzeler et al., 1999)
BY4741 <i>sdp1</i>	<i>sdp1::KanMX4</i>	(Winzeler et al., 1999)
BY4741 <i>shp1</i>	<i>shp1::kanMX4</i> ¹	(Winzeler et al., 1999)
BY4741 <i>sip5</i>	<i>sip5::kanMX4</i> ¹	(Winzeler et al., 1999)
BY4741 <i>sla1</i>	<i>sla1::kanMX4</i> ¹	(Winzeler et al., 1999)
BY4741 <i>snf1</i>	<i>snf1::kanMX4</i>	(Winzeler et al., 1999)
BY4741 <i>swi6</i>	<i>swi6::KanMX4</i>	(Winzeler et al., 1999)
BY4741 <i>syc1</i>	<i>syc1::kanMX4</i>	(Winzeler et al., 1999)

Table 2. *S. cerevisiae* strains derived from BY4741 (MAT a *his3Δ1 leu2Δ met15Δ ura3Δ*) genetic background from EUROFAN (continue Table 3) ¹ Strains checked for correct gene deletion.

Strains	Genotype	Reference
BY4741 <i>vcx1</i>	<i>vcx1::KanMX4</i>	(Winzeler et al., 1999)
BY4741 <i>wsc2</i>	<i>wsc2::KanMX4</i>	(Winzeler et al., 1999)
BY4741 <i>ysw1</i>	<i>ysw1::kanMX4</i>	(Winzeler et al., 1999)
BY4741 <i>yvc1</i>	<i>yvc1::KanMX4</i>	(Winzeler et al., 1999)

Table 3. *S. cerevisiae* strains derived from BY4741 (MAT a *his3Δ1 leu2Δ met15Δ ura3Δ*) genetic background.

Strains	Genotype	Reference
BY4741 wt	MAT a <i>his3Δ1 leu2Δ met15Δ ura3Δ</i>	(Winzeler et al., 1999)
YJFD1	BY4741 <i>ref2::nat1 N4</i>	This work
YJFD2	BY4741 <i>ref2::nat1 N5</i>	This work
YJFD3	BY4741 <i>ref2::nat1 N6</i>	This work
YJFD4	BY4741 <i>ref2::nat1 N8</i>	This work
YJFD49	BY4741 <i>REF2 ref2::nat1 N1</i>	This work
YJFD50	BY4741 <i>REF2 ref2::nat1 N2</i>	This work
YJFD7	BY4741 <i>cnb1::KanMX4 ref2::nat1</i>	(Jofre Ferrer-Dalmau et al., 2010)
YJFD10	BY4741 <i>pmc1::KanMX4 ref2::nat1</i>	This work
YJFD36	BY4741 <i>glc7::nat1 pJFD10</i>	(Jofre Ferrer-Dalmau et al., 2010)
YJFD39	BY4741 <i>ref2::KanMX4 glc7::nat1 pJFD10</i>	(Jofre Ferrer-Dalmau et al., 2010)
YJFD23	BY4741 <i>cch1::KanMX4 ref2::nat1</i>	This work
YJFD24	BY4741 <i>pmr1::KanMX4 ref2::nat1</i>	This work
YJFD25	BY4741 <i>yvc1::KanMX4 ref2::nat1</i>	This work
YJFD26	BY4741 <i>vcx1::KanMX4 ref2::nat1</i>	This work
YJFD27	BY4741 <i>reg1::KanMX4 ref2::nat1</i>	This work
YJFD28	BY4741 <i>slt2::KanMX4 ref2::nat1</i>	This work
YJFD29	BY4741 <i>mid1::KanMX4 ref2::nat1</i>	This work
YJFD72	BY4741 <i>mkk2::KanMX4 ref2::nat1</i>	This work
YJFD35	BY4741 pJFD11	This work
YJFD36	BY4741 <i>glc7::nat1 pJFD11</i>	This work
YJFD38	BY4741 <i>ref2::KanMX4 pJFD11</i>	This work
YJFD39	BY4741 <i>ref2::KanMX4 glc7::nat1 pJFD11</i>	This work
YJFD73	BY4741 <i>wsc2::KanMX4 ref2::nat1</i>	This work
YJFD74	BY4741 <i>mlp1::KanMX4 ref2::nat1</i>	This work
YJFD75	BY4741 <i>sdp1::KanMX4 ref2::nat1</i>	This work
YJFD76	BY4741 <i>rlm1::KanMX4 ref2::nat1</i>	This work
YJFD77	BY4741 <i>msg5::KanMX4 ref2::nat1</i>	This work
YJFD78	BY4741 <i>ptp2::KanMX4 ref2::nat1</i>	This work
YJFD79	BY4741 <i>ptp3::KanMX4 ref2::nat1</i>	This work
YJFD80	BY4741 <i>swi6::KanMX4 ref2::nat1</i>	This work
YJFD81	BY4741 <i>mkk1::KanMX4 ref2::nat1</i>	This work
YJFD88	BY4741 <i>ire1::KanMX4 ref2::nat1</i>	This work
YJFD101	BY4741 <i>bck1::KanMX4 ref2::nat1</i>	This work

Table 4. *S. cerevisiae* strains derived from BY4741 (MAT a *his3Δ1 leu2Δ met15Δ ura3Δ*) genetic background generated from the disruption cassettes.

Strains	Genotype	Reference
DBY746 wt	<i>MATα leu 2-3, 112 his3Δ1 trp1-289 ura 3-52</i>	D. Bolstein
YJFD5	<i>DBY746 ref2::nat1</i>	This work
BY4742 wt	<i>Mat α his3Δ leu2Δ lys2Δ ura3Δ</i>	(Winzeler et al., 1999)
YJFD9	<i>BY4742 ref2::nat1</i>	This work
FY61	<i>Mat a his4-917δ leu2-Δ1 ura3-52</i>	(Nishimura, Yasumura, Igarashi, Harashima, & Kakinuma, 1999)
YJFD89	<i>FY61 ref2::nat1 N1</i>	This work
YJFD89	<i>FY61 ref2::nat1 N2</i>	This work
YJFD89	<i>FY61 ref2::nat1 N3</i>	This work
YJFD89	<i>FY61 ref2::nat1 N4</i>	This work
TM141	<i>Mat a ura3 leu2 trp1 his3</i>	Francesc Posas
YJFD90	<i>TM141 ref2::nat1 N1</i>	This work
YJFD90	<i>TM141 ref2::nat1 N2</i>	This work
YJFD90	<i>TM141 ref2::nat1 N3</i>	This work
YJFD90	<i>TM141 ref2::nat1 N4</i>	This work
1700	<i>Mat a ura3-52 leu2-3,112 trp1-1 his4 can-1r</i>	Unknown
YJFD92	<i>1700 ref2::nat1 N1</i>	This work
YJFD92	<i>1700 ref2::nat1 N2</i>	This work
YJFD92	<i>1700 ref2::nat1 N3</i>	This work
YJFD92	<i>1700 ref2::nat1 N4</i>	This work
CML476	<i>MATα ura3-52 leuΔ1 his3Δ200 GAL2 CMVp(tetR⁻-SSN6)::LEU2 trp1::tTA</i>	(Yen et al., 2003)
YJFD16	<i>CML476 KanMX4-(tetO₇):REF2</i>	This work
YJFD94	<i>CML476 ref2::nat1 N1</i>	This work
YJFD94	<i>CML476 ref2::nat1 N2</i>	This work
YJFD94	<i>CML476 ref2::nat1 N3</i>	This work
YJFD94	<i>CML476 ref2::nat1 N4</i>	This work
BY4743	<i>MATα/MATα his3Δ0/his3Δ0; leu2Δ/leu2Δ0; met15Δ0/MET15; LYS2/lys2Δ0;u ra3Δ0/ura3Δ0</i>	(Winzeler et al., 1999)
YJFD69	<i>BY4743 (BY4741/BY4742 ref2::nat1)</i>	This work
YJFD70	<i>BY4743 (BY4741 ref2::KanMX4/BY4742)</i>	This work
YJFD71	<i>BY4743 (BY4741 ref2::KanMX4/BY4742 ref2::nat1)</i>	This work

Table 5. *S. cerevisiae* strains generated from the deletion cassette *ref2::nat1* in several genetic backgrounds. Diploid strains derived from BY4743 (*MAT α /MAT α his3 Δ /his3 Δ ; leu2 Δ /leu2 Δ ; met15 Δ 0/MET15; LYS2/lys2 Δ ; ura3 Δ /ura3 Δ) genetic backgrounds.*

Strains	Genotype	Reference
DBY746 wt	<i>MATα leu2-3, 112 his3-Δ1 trp1-Δ289 ura3-52</i>	D. Bolstein
CCV180	DBY746 <i>snf1::LEU2</i>	Carlos Casado
CCV181	DBY746 <i>reg1::KanMX4 snf1::LEU2</i>	Carlos Casado
MAR197	DBY746 <i>nrg1::nat1</i>	Amparo ruiz
MAR198	DBY746 <i>mig1::LEU2 mig2::TRP1 nrg1::nat1</i>	(Maria Platara et al., 2006)
MAR199	DBY746 <i>mig1::LEU2 mig2::TRP1 nrg2::KanMX4 nrg1::nat1</i>	(Maria Platara et al., 2006)
MAR200	DBY746 <i>nrg2::TRP1 rim101::KanMX4 nrg1::nat1</i>	(Maria Platara et al., 2006)
MAR201	DBY746 <i>mig1::LEU2 nrg1::nat1</i>	Amparo ruiz
MAR202	DBY746 <i>mig2::TRP1 nrg1::nat1</i>	Amparo ruiz
MAR203	DBY746 <i>mig1::LEU2 nrg2::KanMX4 nrg1::nat1</i>	Amparo ruiz
MAR204	DBY746 <i>mig2::TRP1 nrg2::KanMX4 nrg1::nat1</i>	Amparo ruiz
MAR205	DBY746 <i>nrg2::TRP1 nrg1::nat1</i>	Amparo ruiz
MAR206	DBY746 <i>rim101:kanMX4 nrg1::nat1</i>	(Maria Platara et al., 2006)
MAR31	DBY746 <i>mig2::TRP1</i>	Raquel Serrano
MAR32	DBY746 <i>mig1::LEU2 mig2::TRP1</i>	Raquel Serrano
MAR33	DBY746 <i>rim101::KanMX4 mig1::LEU2</i>	Amparo ruiz
MAR34	DBY746 <i>rim101::KanMX4 mig2::TRP1</i>	Amparo ruiz
MAR35	DBY746 <i>rim101::KanMX4 mig1::LEU2 mig2::TRP1</i>	Amparo ruiz
MP014	DBY746 <i>snf1::LEU2 mig1::kanMX4</i>	(Maria Platara et al., 2006)
MP015	DBY746 <i>snf1::LEU2 mig2::TRP1</i>	(Maria Platara et al., 2006)
MP016	DBY746 <i>snf1::LEU2 mig2::TRP1 mig1::kanMX4</i>	(Maria Platara et al., 2006)
MP018	DBY746 <i>nrg2::TRP1</i>	(Maria Platara et al., 2006)
MP020	DBY746 <i>snf1::LEU2 nrg1::kanMX4</i>	(Maria Platara et al., 2006)
MP021	DBY746 <i>snf1::LEU2 nrg2::kanMX4</i>	(Maria Platara et al., 2006)
MP022	DBY746 <i>nrg1::kanMX4 nrg2::TRP1 snf1::LEU2</i>	(Maria Platara et al., 2006)
MP030	DBY746 <i>reg1::KanMX4</i>	Maria Platara
MP052	DBY746 <i>rim101::KanMX4 snf1::LEU2</i>	Maria Platara
RSC13	DBY746 <i>mig1::LEU2</i>	(Maria Platara et al., 2006)
RSC21	DBY746 <i>rim101::KanMX4</i>	(R Serrano et al., 2002)

Table 6. *S. cerevisiae* strains derived from DBY746 (*MAT α leu2-3, 112 his3- Δ 1 trp1- Δ 289 ura3-52*) genetic background from our laboratory's database.

Strains	Genotype	Reference
BYT12-30-2	BY4741 <i>TRK1::loxP TRK2::loxP</i>	Hanna Sychrova
KT1112	MAT a <i>leu2 ura3-52 his3</i>	(Stuart, Frederick, Varner, & Tatchell, 1994)
KT1935	KT1112 <i>glc7-109</i>	(T Williams-Hart et al., 2002)
KT2210	KT1112 <i>glc7-F256A</i>	(T Williams-Hart et al., 2002)
XH5	MAT a <i>ura3-52 leu2Δ1 trp1Δ63 his3Δ200 pta1::TRP1 YCpLEU-PTA1</i>	(Ghazy, He, Singh, Hampsey, & Moore, 2009)
<i>pta1 Δ1-75</i>	<i>XH5 pta1::TRP1 pta1-Δ75</i>	(Ghazy et al., 2009)
SB6	<i>Mat a ade2, leu2, ura3, trp1Δ, his3 yth1::TRP1 pFA-YTH1 (CEN4 ADE2 YTH1)</i>	(Barabino, Hübner, Jenny, Minvielle-Sebastia, & Keller, 1997)
SB7	<i>SB6 yth1::TRP1 pFA-yth1-1 (CEN4 ADE2 yth1-1)</i>	(Barabino et al., 1997)
YWK168	Mata <i>his3Δ, ura3Δ, leu2Δ swd2::KanMX4 (SWD2-LEU2-CEN)</i>	(Dichtl, Aasland, & Keller, 2004)
YWK172	YWK168 <i>swd2::KanMX4 (swd2-3-LEU2-CEN)</i>	(Dichtl et al., 2004)
W303-1A	<i>Mat a ade2-1 ca1-100 his3-112 leu2-3 trp1-1 ura3-1</i>	(Thomas & Rothstein, 1989)
YWK186	W303-1A <i>ssu72-2</i>	(Dichtl et al., 2002)

Table 7. *S. cerevisiae* strains from different genetic backgrounds kindly provided by international laboratories.

Strains	Genotype	Reference
BY4741 wt	MAT a <i>his3Δ1 leu2Δ met15Δ ura3Δ</i>	(Winzeler et al., 1999)
BY4741 <i>ref2</i>	<i>ref2::kanMX4</i>	(Winzeler et al., 1999)
BY4742 wt	Mat α <i>his3Δ leu2Δ lys2Δ ura3Δ</i>	(Winzeler et al., 1999)
YJFD9	BY4742 <i>ref2::nat1</i>	This work
BY4743	MATa/MATα <i>his3Δ0/his3Δ0; leu2Δ/leu2Δ0; met15Δ0/MET15; LYS2/lys2Δ0;u ra3Δ0/ura3Δ0</i>	Winzeler et al., 1999)
YJFD69	BY4743 (BY4741/BY4742 <i>ref2::nat1</i>)	This work
YJFD70	BY4743 (BY4741 <i>ref2::KanMX4</i> /BY4742)	This work
YJFD71	BY4743 (BY4741 <i>ref2::KanMX4</i> /BY4742 <i>ref2::nat1</i>)	This work

Table 8. *S. cerevisiae* diploid strains generated in this thesis.

Name	Sequence (from 5' to 3')
5'-<i>snf1</i>_comp	CTCTTACTGCGCATTCTGTGTC
K2	CACGTCAAGACTGTCAAGGA
nat1-3'	GTGAAGGACCCATCCAGTGC
OJFD013	CTTTGAGGTTGCTAATTTGC
OJFD020	CTGTATCACGTCCGGCACACC
OJFD021	AACGATACGATAAGTAAAGACACTGTGGAAGAATTGAACACGTACGCTGCAGGTCGAC
OJFD022	TGTATATATACTACATGTTTATGTATCAGCATGTCATAGCTCGATGAATTCGAGCTCG
OJFD023	AATTGAGGAACAGGTGCTG
OJFD067	GAAACGATACGATAAGTAAAGACACTGTGGAAGAATTGAACACAGCTGAAGCTTCGTACGC
OJFD068	GGCATGAGAAATATTTACTAATTGAGGAACAGGTGCTGACATATAGGCCACTAGTGGATCTG
OJFD080	CATTGCTTATTCGCTCTTCC
OJFD081	TATACATTCAAATTAAGAAATGGACTCACAACCAGTTGACGTACGCTGCAGGTCGAC
OJFD082	GTATTTTGGTTTTTAAACTTTGATTTAGGACGTGAATCTATCGATGAATTCGAGCTCG
SNF1_nat1_F	TTTGTAAACAAGTTTTGCTACACTCCCTTAATAAAGTCAACCGTACGCTGCAGGTCGAC
SNF1_nat1_R	TACATAAAAAAAGGGAACCTCCATATCATTCTTTTACGTTCCACCACGAGCTCGAATTCATCGA

Table 9. Oligonucleotides used in this work for generation and verification of genes disruptions.

4. Diploid generation and obtaining of haploid cells

Yeast cells of opposed mating type BY4741 MAT **a** and BY4742 MAT **α** wild-type and its derivative BY4741 *ref2* and YJFD9, respectively, were crossed by incubation at 25°C during 24 h (Table 8). The indicated diploid cell strains were transformed with the plasmids pRS415, pJFD1 and pJFD2 and grown selected in minimum media supplemented with the appropriate amino acids for plasmid selection. Saturated cultures of selected plasmid-bearing cells were washed and transferred to sporulation media, consisting in 1% (v/w) potassium acetate supplemented with uracil, histidine and adenine, and incubated at 25°C for 1 week or until enough number of sporulating cells were visible. One ml of the sporulated culture was transferred to 5 ml of water and 0.5 ml Zymoliase 1 mg/ml (Sigma) plus 10 μ l 2-mercaptoethanol were added and incubated overnight at 30°C. Cell pellet was resuspended in 1 ml water and about 100 μ l of 0.5 mm diameter Zirconia/Silica beads (BioSpec) were added and then vortexed for 3 minutes. Finally, serial dilutions of each sample were plated on YPD plates and growth was monitored after 2-3 days of incubation at 28°C to evaluate the growth of haploid cells.

5. Plasmids construction

YEp195-VPS70: contains a fragment of 3946 bp comprising from -676 upstream the initial ATG codon to 834 downstream the stop codon of the *VPS70* gene cloned in the *URA3*-marked episomal yeast plasmid YEp195 (González, Ruiz, Serrano, Ariño, & Casamayor, 2006).

YEp195-VPS73: contains a fragment of 2808 bp comprising from -1048 upstream the initial ATG codon to 359 downstream the stop codon of the *VPS70* gene cloned in the *URA3*-marked episomal yeast plasmid YEp195 (González et al., 2006).

pPHO84-LacZ: the PCR-amplified promoter of *PHO84* (-603/+19 respect the ATG of the ORF) was cloned into the YEp357 plasmid to drive the expression of the *E. coli lacZ* reporter gene (Raquel Serrano, Ruiz, Bernal, Chambers, & Ariño, 2002).

pJFD1 (pRS415-REF2): for low-copy, centromeric expression of *REF2*, a 2.28 kbp fragment containing the entire *REF2* ORF, flanked by 500 bp and 200 bp from its promoter and terminator regions respectively, was amplified using the pair of oligonucleotides OJFD027 and OJFD026 (Table 10) as a upstream and downstream primers, containing the artificially added BamHI and SacI restriction sites, respectively. The resulting DNA fragment was digested with BamHI and SacI and cloned in the same restriction sites of the centromeric *LEU2*-marked pRS415 plasmid (Sikorski & Hieter, 1989) to yield pRS415-*REF2* (pJFD1). The generated plasmid was sequenced (with primers OJFD030 and OJFD031 (Table 10)) to ensure the absence of unexpected mutations (Jofre Ferrer-Dalmau et al., 2010). Yeast cells carrying the pRS415-*REF2* construct were selected in a drop-out leucine medium.

pJFD2 (pRS415-REF2^{F374A}): the pRS415-*REF2* construct was used as a PCR template to change the TTT codon, encoding a phenylalanine residue at position 374, to a GCT codon, encoding an alanine residue. Two overlapping DNA fragments (**a** and **b**) were generated. The 1.75 kb fragment (**a**), spanning from -501 to +1140 (relative to the initiating methionine residue), was obtained using oligonucleotides OJFD029 and M13-20 reverse. The 0.7 kb length fragment (**b**) comprises from +1101 to +1785 and was amplified with oligonucleotides OJFD063 and M13-20 (Table 10). To allow *in vivo* DNA-recombination, these two fragments were co-transformed in yeast cells together with the linearized pRS415 plasmid digested with BamHI and SacI. Yeast cells carrying the pRS415-*REF2*^{F374A} construct were selected in a drop-out leucine medium and the plasmid was recovered and sequenced (OJFD030 and OJFD031 (Table 10)) to ensure the absence of unexpected mutations (J Ferrer-Dalmau et al., 2010).

pRDN-wt-U (plasmid 2 μ expressing rDNA): Plasmid pRDN-wt-U (also called pAV163) contains the 9 kb rDNA fragment from YEpT7RI.OXho, inserted into the BamHI site of the *URA3*-containing episomal plasmid YEplacI95 (Gietz & Sugino, 1988). Plasmid pRDN-wt-U (also called pAV164) contains the 1 kb *TRP1* SmaI-SalI fragment of pJJ281 (Jones & Prakash, 1990) inserted into NruI and SalI sites of YEpT7RI.OXho.

pJFD10 (YCplac33-*glc-109*): The coding region of the *glc7-109* allele, flanked by 2068 bp upstream and 148 bp downstream, was amplified by PCR using genomic DNA from strain KT1935 and the oligonucleotides Glc7-BamHI.Up and Glc7-PstI.Do (Table 10) as primers, which contain artificial BamHI and PstI restriction sites respectively. The amplified DNA fragment was digested by BamHI and PstI and cloned in the same restriction sites of the centromeric *URA3*-marked YCplac33 to yield plasmid pJFD10 (YCplac33-*glc7-109*). The plasmid was sequenced (with primers Glc7-1673 and Glc7-1256 (Table 10)) to ensure the absence of unexpected mutations (J Ferrer-Dalmau et al., 2010).

pJFD11 (YCplac111-*glc-109*): The *glc7-109* fragment was obtained from pJFD10 by digestion with BamHI and PstI and then cloned into the same restriction sites of the centromeric *LEU2*-marked YCplac111 to yield plasmid pJFD11 (YCplac111-*glc7-109*). The plasmid was sequenced (primers Glc7-1673 and Glc7-1256 (Table 10)) to ensure the absence of unexpected mutations.

p1335 (YIp335-*Ime1*): Two kb corresponding to the promoter of *IME1* is cloned in the plasmid YIp335 to drive the expression of the *lacZ* reporter gene. This plasmid was generously gift of Angelika Amon Ph.D., MIT (van Werven et al., 2012).

pMCZ-Y: The UPRE element from the *KAR2* promoter is cloned into the in the 2-microns plasmid *URA3*-marked pMCZ-Y plasmid the expression of the *lacZ* reporter gene. Kindly provided by José Antonio Prieto Ph.D. (IATA, CSIC) (Mori et al., 1996; Torres-Quiroz et al., 2010).

pJR65 (pLexA-Reg1): The entire *REG1* coding region fused with the LexA DNA-binding of the two-hybrid pLexA plasmid (Tu & Carlson, 1995b).

pLexA-Reg1^{F468R}: The pJR65 plasmid was site-directed mutagenized to introduce the F468R point mutation into Reg1 (Alms et al., 1999; Tu & Carlson, 1995b).

pLexA-Reg1^{F468D}: The pJR65 plasmid was site-directed mutagenized to introduce the F468D point mutation into Reg1 (Alms et al., 1999; Tu & Carlson, 1995b).

Yep195-*PTC2*: an EcoRI/HindIII 5.1 kb fragment derived from amplifying the *PTC2* gene was inserted into the same restriction sites of the YEp195 plasmid (Munoz, Simon, Casals, Clotet, & Arino, 2003).

Yep195-PTC3: a *SacI*/*HindIII* 2.7 kb fragment derived from amplifying the entire *PTC3* gene was cloned into the same sites of the YEp195 plasmid (Munoz et al., 2003).

Yep195-HEX2 (Yep195-REG1): The *REG1* coding sequence was cloned into the YEp195 plasmid under control of the *ADH1* promoter. Kindly provided by José Antonio Prieto Ph.D. (IATA, CSIC).

pRS315-IRE1-HA: This plasmid was generated by insertion of the C-terminal HA-tagged *IRE1* gene into centromeric LEU2-marked yeast vector pRS315 (Sikorski & Hieter, 1989). A kindly gift of Yukio Kimata Ph.D., Nara Institute of Science and Technology (Kimata et al., 2007).

pRS426-IRE1-Flag: This plasmid was generated by insertion of the Flag-tagged *IRE1* gene into the two-micron *URA3*-marked yeast vector pRS426 (Christianson, Sikorski, Dante, Shero, & Hieter, 1992). A kindly gift of Yukio Kimata Ph.D., Nara Institute of Science and Technology (Kimata et al., 2007).

p1365 (SLT2-lacZ): The promoter region from *SLT2* (nucleotides -949 to 1) was cloned into the *SmaI* and *BamHI* sites of the pLGΔ-312 to drive the expression of the *lacZ* gene (Guarente & Mason, 1983). A kindly gift of David D. Levin Ph.D., Boston University School of Medicine (Un Sung Jung, Sobering, Romeo, & Levin, 2002).

p2056 (FKS2-lacZ): A fragment of the *FKS2* promoter (residues from -540 to -375 bp) fused to the *CYC1* minimal promoter was cloned into the two-micron *URA3*-marked pLGΔ-312 plasmid (Guarente & Mason, 1983) to yield a *FKS2-CYC1-lacZ* fusion construct. Plasmid kindly gift of David D. Levin Ph.D., Boston University School of Medicine (K. Y. Kim et al., 2008).

pAMS366 (CDRE-lacZ): This plasmid contains four tandem repeats of the CDRE from *FKS2* gene (Stathopoulos & Cyert, 1997b) cloned into the two-micron *URA3*-marked pLGΔ178 plasmid (Guarente & Mason, 1983).

YEp357-SUC2 (SUC2-lacZ): The *SUC2* promoter (from -745 to +125 bp respect to the start codon) cloned between the *EcoRI* and *PstI* restriction sites of the two-micron *URA3*-marked YEp357.

pSK119 (pWS93-3xHA-Snf1): The *SNF1* gene is cloned into the two-micron pWS93 plasmid (derived from pSH2-1 with *LexA* replaced by 3xHA sequence and *HIS3* replaced by *URA3*) and expressed under *ADH1* gene promoter (Song & Carlson, 1998).

pSK119A (pWS93-3xHA-Snf1^{T210A}): *SNF1* gene containing the mutation that replaces the Thr210 by Ala is cloned into pWS93 plasmid (Hedbacker, Hong, & Carlson, 2004).

pSK120 (pWS93-3xHA-Snf1^{K84R}): *SNF1* gene containing the mutation that replaces the Lys 210 by Arg is cloned into pWS93 plasmid (Hedbacker, Hong, et al., 2004).

pCE108 (YEp50-Snf1): The *SNF1* gene is cloned into the plasmid centromeric *URA3*-marked YEp50 (Celenza & Carlson, 1989).

pCE108-Y106A (YCp50-Snf1^{Y106A}): The *SNF1* gene containing the mutation that replaces the Tyr210 by Ala is cloned into the YCp50 plasmid (Momcilovic & Carlson, 2011).

pCE108-G53R (YCp50-Snf1^{G35A}): The *SNF1* gene containing the mutation that replaces the Gly35 by Ala is cloned into the YCp50 plasmid (Momcilovic & Carlson, 2011).

YEp195-GLC7: A PCR-amplified 3.7 kbp fragment of *GLC7* gene, comprising from – 2068 bp upstream the initial ATG codon to +1632 bp downstream the stop codon, is cloned into the YEp195 (J Ferrer-Dalmau et al., 2010).

pKC201 (ENA1-lacZ): The promoter of *ENA1* gene (between- 1385 to + 35 bp respect to the initial ATG codon) is cloned into the pLGD178 (Guarente & Mason, 1983) to drive the expression of the *lacZ* gene (Cunningham & Fink, 1996).

pMRK212 (ENA1-lacZ): A fragment of the *ENA1* promoter containing the ARR1 region fuse to a *CYC1* minimal promoter is cloned into the two-micron *URA3*-marked pSLFA-178K plasmid (Idrissi, Fernández-Larrea, & Piña, 1998) to drive the expression of the *lacZ* gene (R Serrano et al., 2002).

pMRK213 (ENA1-lacZ): A fragment of the *ENA1* promoter containing the ARR2 region fuse to a *CYC1* minimal promoter is cloned into the two-micron *URA3*-marked pSLFA-178K plasmid (Idrissi et al., 1998) to drive the expression of the *lacZ* gene (R Serrano et al., 2002).

pEV11/AEQ: The apoaequorin gene is cloned into the two-micron *URA3*-marked pEV11 plasmid (Russell & Nurse, 1986), under the control of the *ADH1* promoter (Batiza et al., 1996).

pLT12 (CRH1-lacZ): a 1.1 kbp (EcoRI/BamHI) and a 0.5 kbp (XbaI/HindIII) fragment upstream and downstream from the *CRH1* coding region were cloned into the two-micron *URA3*-marked YEp352. The *lacZ* coding region, from the YEp356R plasmid, was inserted between the fragments described above to drive its expression under the control of the *CRH1* promoter (Bermejo et al., 2008).

pMLP1-lacZ: The *lacZ* gene the 1.1 kbp EcoRI/BamHI fragment containing the promoter of *CRH1* was replaced from the pLT12 plasmid by the PCR-amplified promoter region (from -1186 to -1 bp respect the start codon) of *MLP1* (García, Rodríguez-Peña, Bermejo, Nombela, & Arroyo, 2009).

Name	Sequence (from 5' to 3')
Glc7-1256	GCAGGGCCCATCAAGTTGTGG
Glc7-1673	CGCGGTTTGTTCACATAAAGGG
Glc7-BamHI.Up	CGGGATCCGATGGTGGTTGTAATACGGTC
Glc7-PstI.Do	AAAACGACGACGAGTGATGATTGCATCTTCC
M13-20	GTAAAACGACGGCCAGTG
M13-20 reverse	GGAAACAGCTATGACCATG
OJFD026	CGGCCAGTGAATTGTAATACGACTCACTATAGGGCGAATTGGAGCTCCATAAGTAAAGACACTTTGAG
OJFD027	GTATCGATAAGCTTGATATCGAATTCCTGCAGCCCGGGGATCCTGGAGTATTTCCACCTTTTG
OJFD028	ACGCATAAGTAGCATCAAAGCTTTGGATGATTCCCAACTATAAAAAG
OJFD030	CGATTCTTTGCAAGCGGC
OJFD030	CGATTCTTTGCAAGCGGC
OJFD031	GTCTACAGAATCTCTACC
OJFD063	ACGCATAAGTAGCATCAAAGCTTTGGATGATTCCCAACTAATAAAAAG

Table 10. Oligonucleotides used for plasmid constructions.

6. Growth test

The sensitivity of different yeast strains to several stresses were assayed by drop test on either YPD plates (YP + 2% glucose) or YP plates with different carbon energy source, which will be detailed in each particular experiment. Yeast saturated cultures were diluted to an OD₆₆₀ of 0.05 and 3 µl were spotted on the plate. In some cases the indicated dilutions of the cultures to an OD₆₆₀ of 0.01, 0.005 and 0.002 were also dotted. Plates were then incubated at 28°C, except when otherwise specified, for the indicated periods of time.

Phenotypic analyses were also evaluated by growth test in liquid media which was performed in 96-well plates. Yeast cultures (250 µl) at an initial A₆₆₀ of 0.01 or 0.02 were grown without shaking for 16-24 hours at 28°C in the conditions detailed for each experiment. Growth was monitored by measuring the OD₆₅₀ in a Multiskan Ascent (ThermoFisher).

In experiments using doxycycline, saturated cultures in 5 ml YPD at 28°C, were used to prepare fresh cultures at 0.05 OD₆₆₀ in the presence of 100 µg/ml doxycycline (Sigma) which comes from a fresh stock (<10 days-old) of 5 mg/ml in 50% ethanol. After 8 h of growth at 28°C, new cultures were prepared, by inoculation at 0.01 OD₆₆₀ plus 100 µg/ml doxycycline. After growing for 16 h, fresh doxycycline (100 µg/ml) was added and this procedure was repeated as long as indicated in the experiment. Samples were recollected by filtration and washed with cold water. Finally, dried cells samples were frozen at -80°C until needed.

Growth under limiting potassium concentration was carried out using an YNB (yeast nitrogen base)-based medium (Translucent K-free medium; Formedium) formulated so that potassium content in the final medium is negligible (15 μM approx.). Then yeast growth was evaluated by growth test in liquid media in 96-well plates. Yeast cultures (250 μl) at an initial A_{660} of 0.01 or 0.02 were grown without shaking for 16-24 hours at 28°C in different conditions detailed for each experiment. Growth was monitored by measuring the OD_{650} in a Multiskan Ascent (ThermoFisher).

7. Total RNA Extraction

For RNA purification, yeast cultures were grown at 28 °C in YPD medium at pH 5.5 until the OD_{660} reached 18 approximately. Then, yeast cells were collected by sedimentation and treated according to specific conditions of each experiment. Yeast cells were sedimented by centrifugation (4°C) or by filtration, washed both with cold water and the cell pellet was kept dry at -80°C until the RNA purification. The total RNA was extracted using the RiboPure-Yeast kit (Ambion) following the manufacturer's instructions, using the final treatment with DNase. The quality of RNA was checked by denatured 1.2% agarose gel electrophoresis in the FlahGel RNA Cassette system from Lonza and the RNA was quantified by measuring the OD_{260} in a spectrophotometer BioPhotometer A_{260} (Eppendorf).

8. cDNA synthesis and DNA microarrays

The transcriptional analyzes were performed using DNA microarrays containing 6014 ORFs amplified PCR fragments of *S. cerevisiae*'s genomic DNA (Alberola et al., 2004; L Viladevall et al., 2004). The amplified DNA was resuspended in 50% DMSO and spotted in a glass surface of aminosilane (UltraGAPSTM; Corning Gaps) using a Microgrid II robot spotter (BioRobotics). The cDNA marked with the Cy3 or the Cy5 fluorochrome dyes was prepared from 8 μg of total purified RNA using the method of indirect dUTP labeling with the CyScribe post-labeling kit (Amersham, GE Healthcare). Pre-hybridization, hybridization and microarray washes were performed according to the recommendations of The Institute for Genomic Research with minimal modifications.

Briefly, the pre-hybridization of DNA microarrays was performed at 42°C for 1 h in a solution of 5xSSC, 0.1% SDS, 1% BSA. For hybridization, the Cy3 and Cy5 marked cDNA were dried and then were resuspended in 48 μl of hybridization solution (50% formamide, 5xSSC, 0.1% SDS) and mixed. Then, 5 μg of ssDNA were added and the mix was denatured 3 min at

95°C. Hybridization of the DNA microarrays were performed in an ArrayBooster hybridization station (Sunergia Group) at 42°C for 16 h, at least. Each experimental condition studied (mutant versus wild-type strain) was analyzed using the dye-swapping technique. The scanner ScanArray 4000 (Packard Instrument Co.) was used for obtention of the Cy3 and Cy5 images with a resolution of 10 microns. The fluorescence intensity was measured and processed with GenePix Pro 6.0 software (Molecular Devices). Points either with a diameter less than 120 microns and/or fluorescence intensity of Cy3 or Cy5 below 150 units were not considered in subsequent analysis. A gene was considered induced or repressed when the \log_2 ratio of the mutant strain versus wild-type strain was greater than 0.85 or less than -0.85, respectively. GEPAS v3.1 and 4.0, software now integrated in the or Babelomics 4.2 were used for pre-processing and processing data (Medina et al., 2010; Montaner et al., 2006). The genes were also sorted by functional categories using the MIPS interactive function classifier (Ruepp et al., 2004). Processed microarray data is in the supplementary CD-ROM.

9. Yeast DNA genomic extraction

Yeast strains were grown until saturated (overnight) in 40 ml of YPD. Then DNA genomic was extracted as explained in (Sambrook et al., 1989) section Yeast DNA Isolations A. Briefly, yeast cells were resuspended in 3 ml of 0.9 M sorbitol plus 0.1 N Na₂EDTA pH 7.5 and treated with 2.5 mg/ml solution of Zymoliasse 100T (Sigma) incubating for 1 hour at 37°C. Cells were slowly centrifuged and cell pellet was resuspended in 5 ml 50 mM Tris-HCl (pH 7.4) plus Na₂EDTA + 0.5 ml 10% SDS and then samples were incubated at 65°C for 30 minutes. Then, 1.5 ml of 5 M potassium acetate were added and stored for 1 hour on ice. The supernatant was transferred and added one volume of 100% isopropanol. After centrifugation for 10 minutes, supernatant was discarded; cell pellet was dried and then resuspended in 3 ml TE (pH 7.4). Then, cells were treated with 15 µl of 1 mg/ml RNase A incubating for 1 h at 37°C and then 30 µl of 3 M potassium acetate was added to the samples plus 200 µl of 100% isopropanol. Finally, the precipitate, which should look like a loose “cocoon” of fibers, was removed, air-dried and suspended in 300 µl of TE (pH 7.4).

10. Comparative Genomic Hybridization

Approximately 4 µg of DpnII-digested yeast genomic DNA were used to realize the Comparative Genomic Hybridization (CGH) following the protocol described in BioPrime® Plus Array CGH Indirect Genomic Labelling System for generating fluorescently labeled genomic

DNA using amino-modified nucleotides and Alexa Fluor® dyes. Pre-hybridization, hybridization and microarray washes were performed according to the recommendations of The Institute for Genomic Research with minimal modifications and we have already described in the *cDNA synthesis and DNA microarrays section*.

11. Quantitative Real-Time PCR (qRT-PCR)

Fifteen ng of total RNA were used for the quantitative real-time PCR by using the QuantiTect SYBR Green protocol reverse transcriptase-PCR kit (Qiagen). The reverse transcription reaction was performed at 50°C for 30 min, followed by incubation at 95°C for 15 min to inactivate reverse transcriptase and activate the polymerase. The reactions were performed in two instruments, the SmartCycle (Cepheid) or CFX96 Real-Time PCR (BioRad) on a final volume of 25 µl or 10 µl, respectively. Fifty cycles of PCR (15" at 94°C, 30" at 50°C, and 30" at 72°C) were performed. The amplification primers used are described in *Table 11* Primers to amplify a fragment of the *ACT1* gene was used as a loading control of total RNA concentration.

Name	Sequence	Gene amplified (from 5' to 3')
pho84_f_rtPCR	TGCTAGAGACGGTAAGCCGCCAA	<i>PHO84</i>
pho84_r_rtPCR	ATGGGCTGGAAGATTCAATG	<i>PHO84</i>
HAC1-F	TGAACTAACTAGTAATTCGC	<i>HAC1</i>
HAC1-R	ATTACGCCAATTGTCAAG	<i>HAC1</i>
KAR2-F	ACTGTTATCGGTATTGAC	<i>KAR2</i>
KAR2-R	ATAGACAATAGAGAGACATC	<i>KAR2</i>
OJFD030	CGATTCTTTGCAAGCGGC	<i>REF2</i>
OJFD032	ATGGGCGAAGGAAGACTACTAAG	<i>ENA1</i>
OJFD033	CTGTGGACGAACCTCATCTGG	<i>ENA1</i>
OJFD034	GCTGGTTTAAACATTCCAGTT	<i>HTA2</i>
OJFD035	CTTTGGCAACAAGTTTTGG	<i>HTA2</i>
OJFD036	AAGAGATAACATCCAAGGTATT	<i>HHF1</i>
OJFD037	CTAAATTAACCACCGAAACCG	<i>HHF1</i>
OJFD040	GGTGTTAAGAAGCCTCAC	<i>HHT1</i>
OJFD041	ATAGTGACACGCTTGCGC	<i>HHT1</i>
OJFD042	AAGACTTTGTGTCATCCAGAA	<i>GAT3</i>
OJFD043	TACCGTTTTGCCAGATCC	<i>GAT3</i>
OJFD044	GATCCGCCCTTGATTGG	<i>SRO77</i>
OJFD045	ACCGCCCGGAGCATAACGG	<i>SRO77</i>
OJFD046	TCCGTTGACGGAGAAGAC	<i>PTC4</i>
OJFD047	ACTGCCGTTACCATCGCG	<i>PTC4</i>
OJFD048	ACAGTGTCGGCTCAGGAG	<i>CHS3</i>
OJFD049	CCGCAACACCTTCATCAC	<i>CHS3</i>
OJFD050	CTCTGACCTATGGAAGCC	<i>COS111</i>
OJFD051	ATTTGCCCAAGCATGG	<i>COS111</i>
OJFD052	CTTAACGCGATCACCTGG	<i>YBR063C</i>
OJFD053	GTTTCGTACCAAATTGGC	<i>YBR063C</i>
OJFD058	CAGGTCAGTGTGGTAACC	<i>TUB2</i>
OJFD059	TTGGCCACACGTTGCC	<i>TUB2</i>
OJFD072	CAGGGAGACATCATTAGC	<i>REF2</i>
OJFD110	ACTGTTATCGGTATTGAC	<i>KAR2</i>
OJFD111	ATAGACAATAGAGAGACATC	<i>KAR2</i>
RT_ACT1_do2	ATTGAGCTTCATCACCAAC	<i>ACT1</i>
RT_ACT1_up2	TGCTGTCTTCCATCTATCG	<i>ACT1</i>
RT-CHR1_DO	TGGTTTCACCACCAGCCC	<i>CHR1</i>
RT-CRH1_UP	ACTGCTTCGTGTAACCCG	<i>CHR1</i>
SNR19-F	CTAAGGCGACGAGTTTTTC	<i>U1</i>
SNR19-R	GATCCACCCGTTCTACTC	<i>U1</i>

Table 11. Oligonucleotides used in qRT-PCR, RT-PCR and Northern blot experiments. Orange indicates 5'-primers.

12. Semi-quantitative RT-PCR

Ready-to-Go RT-PCR Beads kit (Amersham, GE Healthcare) was used in order to compare the differential expression of several genes between strains by obtaining DNA fragments of approximately 300 bp for each gene. The oligonucleotides use as primers for each gene are listed in *Table 11*. The reactions were carried out in a final volume of 50 μ l and starting with 50 to 150 ng total RNA, depending on the level of expression of each gene. The initial reverse transcriptase reaction was carried out for 30 min at 42°C, followed by incubation for 5 min at 95°C (inactivation of reverse transcriptase and Taq polymerase activation). The PCR amplification was performed in the same tube for 25-35 cycles (1 min at 95°C, 1 min at 50°C and 1 min 72°C). Finally, equal volumes of each amplified DNA sample were resolved and quantified by electrophoresis in a 2% agarose gel.

13. Northern Blot Analysis

Northern Blot analysis was performed by M. Francisca Rande Gil and José Antonio Prieto Alamán lab's (IATA, València). Total RNA was extracted, purified, and separated as described previously (Panadero, Pallotti, Rodríguez-Vargas, Rande-Gil, & Prieto, 2006). Then, samples were transferred to a nylon membrane and hybridized with nonradioactive digoxigenin-labeled probes containing sequences of *KAR2* (primers *KAR2-F* and *KAR2-R*), *HAC1* (*HAC1-F* and *HAC1-R*), or *U1* (primers *SNR19-F* and *SNR19-R*) (*Table 11*). DNA sequences were obtained from the MIPS (Munich information center for protein sequences) database. PCR labeling of DNA probes, membrane pre-hybridizations and hybridizations were performed with the PCR digoxigenin probe synthesis kit and Digoxigenin Easy Hyb solution of Roche (Roche Diagnostics GmbH, Mannheim, Germany). After stringency washes, the blots were subjected to immunological detection using anti-digoxigenin antibody conjugated to alkaline phosphatase (Roche Diagnostics), followed by CDP-Star detection (Roche Diagnostics). Images were captured with the Las-1000 Plus imaging system (Fuji, Kyoto, Japan). Spot intensities were quantified with Image Gauge software (version 3.12; Fuji).

14. Preparation of cell lysates, Immunoprecipitation, and Western blotting

Ten OD₆₆₀ equivalent of yeast cells carrying both pRS426-*IRE1*-Flag and pRS315-*IRE1*-HA were harvested after treatment, washed with PBS, and suspended in 200 μ l of buffer A (50

mM Tris-Cl, pH 7.9, 5 mM EDTA, and 1% Triton X-100) supplemented by protease inhibitors (2 mM phenylmethanesulfonyl fluoride, 10 µg/ml each of pepstatin, leupeptin, and aprotinin). Glass beads 0.5 mm diameter Zirconia/Silica beads (BioSpec) were added up to the meniscus. Cells were broken by vigorous vortexing six times for 30 s each at maximum speed. After removal of the glass beads, the cell lysates were clarified by centrifugation (15,000 x g for 10 min).

Cell lysates were then diluted with 800 µl buffer B (the same composition as buffer A except containing 180 mM NaCl and 6% skim milk) and incubated for 1 h at 4°C with 0.5 µg of the anti-HA mAb 12CA5 (Roche Diagnostics, Basel, Switzerland), followed by the addition of 15 µl of protein A-conjugated Sepharose beads (Protein A Sepharose 4 FF; Amersham Biosciences), as described in (Kimata et al., 2003). After further incubation at 4°C for 1 h, the Sepharose beads were collected by centrifugation, washed five times with buffer C (the same composition as buffer B except for containing no skim milk), and used as immunoprecipitates. Proteins were resolved by electrophoresis in 6% polyacrylamide gel and transferred, using a semi-dry transfer, to a polyvinylidene fluoride (PVDF) microporous Immobilon F Transfer membrane (Millipore). Membranes were blocked with 5% skim milk in TBST (10 mM Tris-HCl, pH 7.5, 100 mM NaCl and 0.1% Tween-20) and then incubated with the indicated antibodies for 1h. The anti-Flag (Sigma) and the anti-HA (Roche Diagnostics) were used at 1/2000 dilution in TBST 5% skim milk buffer. A 1/25000 dilution ECL Mouse IgG, HRP-linked whole Ab from sheep (GE Healthcare) was used as secondary reactant. The complex was detected by the ECL detection system Prime (GE Healthcare). Images were captured with the VersaDoc 4000 MP Image System (Bio-Rad) and images were analyzed with Quantity One 1-D (Bio-Rad).

15. Glucose measurements

Yeast cells from saturated cultures in YPD were inoculated at 0.05 OD₆₆₀ in fresh YPD (pH5.5). Cells of each time point sample were sedimented by centrifuged and the supernatant was collected and kept at -20°C until glucose determination. The optical density of cultures was measured at OD₆₆₀. The glucose determination experiments were based on the Trinder reaction (Barham & Trinder, 1972; Trinder, 1969) using the GLUCOSE MR *Enzymatic colorimetric method ENDPOINT* (Linear Chemicals) using a standard provided by the kit of 100 mg/dl glucose. In this system glucose of the sample is oxidized to D-gluconate by the glucose oxidase (GOD) with the formation of hydrogen peroxide. In the presence of peroxidase (POD),

a mixture of phenol and 4-aminoantipyrine (4-AA) is oxidized by hydrogen peroxide, to form a red quinoneimine dye proportional to the concentration of glucose in the sample.

16. Vacuolar morphology staining

Vacuolar morphology was studied through the distribution of soluble dye FM4-64 following the protocol described in (Vida & Emr, 1995). Briefly, yeast cells were grown in 5 ml of culture to OD₆₆₀ 1.0, and were resuspended in 100 µL in fresh YPD. The fluorescent marker FM4-64 (Molecular Probes) was added to a final concentration of 20 µM and cells incubated at dark for 15 min at 30°C. The fluorescent dye excess was eliminated by washing yeast cells with fresh YPD, and then yeast cells were incubated for 45 min at dark with 1.5 ml of fresh YPD to allow the complete dye internalization by endocytosis and its accumulation by the vacuole. 200 µl of each mutant were extracted, washed with PBS and then observed under fluorescent microscope Nikon Eclipse E800 x 1000 with FITC filter. Digital images were taken with ORCA-ER 4742-80 camera (Hamamatsu) using Wasabi software.

17. β-Galactosidase assay

Yeast cells were grown to saturation in the appropriate drop-out media overnight and then inoculated in YPD (pH 5.5) at an OD₆₆₀ 0.2. Growth was resumed until an OD₆₆₀ of 0.5 to 0.8 was reached and cultures were distributed to 1.0 ml aliquots. Yeast cells were sedimented by centrifuged for 5 min at 1620 x g. and resuspended in fresh media with or without the appropriate stressors as described in each experiment.

Yeast cells were centrifuged and resuspended in 300 µl f buffer Z (60 mM Na₂HPO₄, 40 mM NaH₂PO₄, 10 mM KCl, 1 mM MgSO₄, 35 mM 2-mercaptoethanol). One hundred µl of the cell suspension were diluted in 900 µl of buffer Z in assays tubes and cells were permeabilized by addition of 40 µl of chloroform and 20 µl of 10% SDS and then vortexed for fifteen seconds. The assay mixture was equilibrated by placing the assay tubes at 30°C in a water bath, where after 15 minutes, 0.2 ml of the reaction substrate ONPG (o-nitrophenyl-β-D-galactopyranoside) were added to the assay mixture in order to start the enzymatic reaction (Reynolds, Lundblad, Dorris, & Keaveney, 1997). After sufficient yellow color was developed, the enzymatic reaction was stopped by adding 0.5 ml of 1 M Na₂CO₃, which shifts pH of the reaction solution to 11. The product formation was evaluated spectrophotometrically at OD₄₀₅ in 96-well plates using a Multiskan Ascent (ThermoFisher). Cell density was also spectrophotometrically determined at OD₆₅₀. β-galactosidase activity was calculated in Miller Units using the formula [(1000 x

$OD_{405}/(\text{time}_{\text{reaction}} \times OD_{660})$], where the time parameter are the minutes between the addition of the substrate and the end of the reaction.

18. Fluorescence Flow Cytometry Analysis (FACS)

FACS experiments were performed by Bàrbara Baró Ph.D. in Ethel Queralt's Lab (IDIBELL, Barcelona). Yeast strains were cultured overnight at 25°C and then inoculated in YPD medium. For the determination of the DNA content cells from unsynchronic exponential-phase cultures were collected in absolute ethanol and resuspended in cold 50 mM sodium citrate buffer pH 7.4. Cells were first treated with RNase 0.2 mg/ml during 1 h at 50°C and treated with proteinase K 1mg/ml during 1 h at 50°C. Finally, 50 mM sodium citrate buffer pH 7.4 containing 16 µg/ml propidium iodide was added to each sample. Flow citometer used was Gallios Beckman Coulter, with Gallios software. Excitation was carried out with laser at 488 nm. Signal was collected with the FL3 detector and analyzed with Kaluza Flow Cytometry software.

19. Lithium content and lithium efflux measurements

Lithium content and efflux were performed in laboratory of José Ramos (Universidad de Córdoba) and were measured as reported previously, with minor modifications (A Ruiz, Gonzalez, Garcia-Salcedo, Ramos, & Arino, 2006). For determination of the intracellular lithium cation concentration, cells were grown overnight in liquid YPD medium. When cultures reached an OD_{600} 0.5–0.6, cells were collected by sedimentation (centrifugation at 1620 x g for 5 min) and diluted, to an OD_{600} of 0.2–0.3, in fresh YPD medium containing the indicated concentration of LiCl. Cells were loaded with lithium for 8 h and then samples were filtered, washed with 20 mM $MgCl_2$, and treated with acid (0.2 M HCl and 10 mM $MgCl_2$) overnight. Lithium was analyzed by atomic absorption spectrophotometry as described previously (Gomez, Luyten, & Ramos, 1996). Lithium efflux was studied in cells grown overnight as described above. Cells were suspended in fresh medium and loaded with 75 mM LiCl for 2 h. Yeast cells were separated from the culture medium by centrifugation at 1620 x g for 5 min, washed, and suspended in fresh lithium-free medium. At various time intervals, samples were taken and treated as above for lithium determination.

20. Intracellular calcium determination

The determination of intracellular calcium was based on the use of pEV11/AEQ (Batiza et al., 1996) which carries the apoaequorin gene under the control of the *ADH1* promoter. Evaluation of cytoplasmic calcium was carried out essentially as described previously (Batiza et al., 1996; Laia Viladevall et al., 2004). Briefly, DBY746 wild-type and *ref2* mutant cells (YJFD5) were transformed with plasmid pEVP11/AEQ and grown to an OD₆₆₀ of 1.0. Aliquots of 30 μ l were incubated in luminometer tubes for 20 min at room temperature (22°C), a one-tenth volume of 592 μ M coelenterazine (Sigma–Aldrich) in methanol was then added to each sample and the mixture was incubated further at room temperature for 20 min. Basal luminescence was recorded every 0.1 s for 5 s using a Berthold LB9507 luminometer. The RLUs (relative luminescence units) were normalized to the number of cells in each sample.

Results and Discussion

RESULTS AND DISCUSSION

1. Global analysis of the non-essential regulatory subunits of Glc7

A hallmark of PP1 enzymes is that the catalytic subunit always works in a complex. For this thesis, we analyzed the non-essential regulatory subunits of Glc7, meaning that the complete disruption of the specific gene does not cause lethality to the yeast cell strain and, consequently, the corresponding mutants are available at the yeast mutant collection generated by the Genome Deletion Project consortium. We did not analyze strains disrupted in *SDS22* or *YPI1* genes since they are essential genes. The yeast strains analyzed are listed in the *Table 1* (Introduction, section 2.3.2) and were re-checked for carrying the correct gene disruption.

It is important to remark that we began our study analyzing 19 mutant strains (*Table 1*), but then we introduced two new regulatory subunits, *Afr1* and *Ysw1*, which were subsequently described as regulatory subunits (Bharucha, Larson, Konopka, et al., 2008; Ishihara et al., 2009).

1.1 Phenotypical analysis of Glc7-regulatory subunits

Initially, the study was conducted using the phenotypic drop-test to explore the behavior of each mutant on non-essential Glc7-regulatory subunits compared to that of BY4741 wild-type strain. We summarize our phenotypic studies in *Figure 13* and *Table 12*.

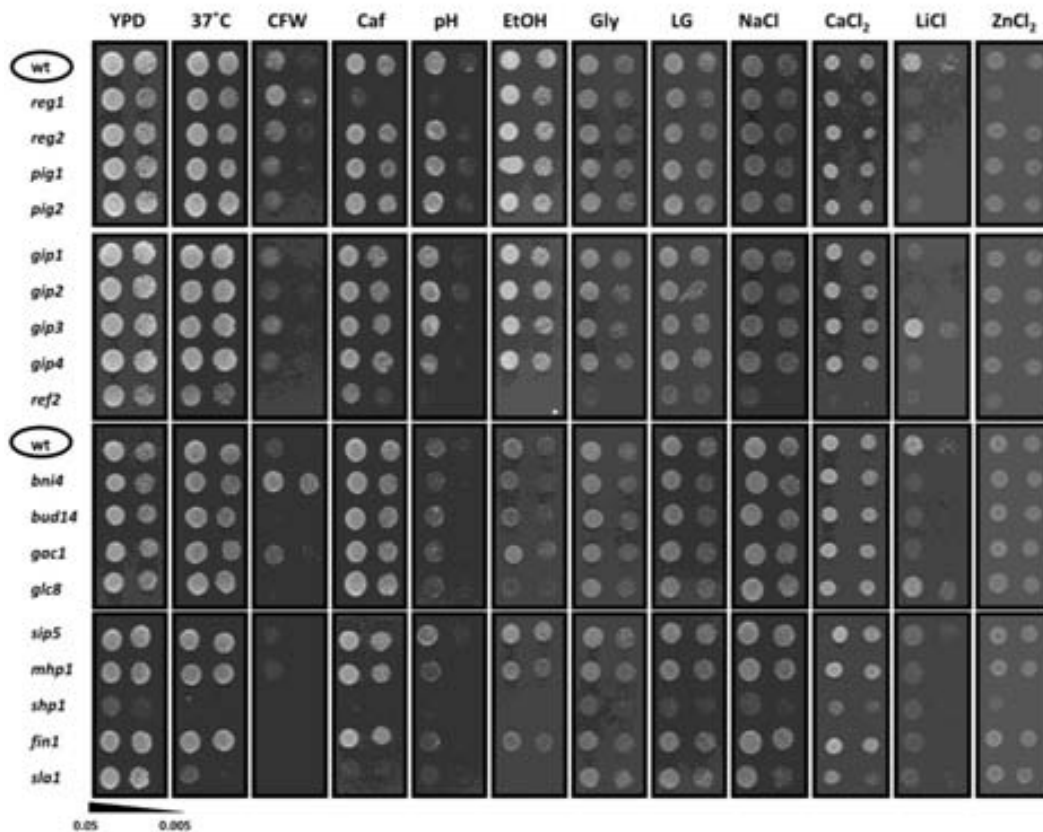


Figure 13. Effect of the mutation of Glc7-interacting proteins on different stressors or conditions. Two dilutions from cultures of wild-type strain BY4741 (**wt**) and the indicated isogenic derivatives were grown on either YPD plates in the presence of **CFW** (Calcofluor white 50 ug/ml), **Caf** (caffeine 7 mM), **pH** (alkaline pH with TAPS 8.2), **NaCl** (0.6 M), **LiCl** (150 mM), **CaCl₂** (0.2 M), **ZnCl₂** (4 mM); or YP plates in the presence of **EtOH** (ethanol 2%), **Gly** (glycerol 2%) and **LG** (low glucose 0.05%) for 2-3 days.

As expected, the mutant strains studied show different sensitivities and tolerances relative to the wild-type strain. It is important to remark that cells lacking *SHP1* have already a severe growth defect phenotype even in YPD. It has already been described that *shp1* strain mutations markedly reduce Glc7 catalytic activity without noticeably affecting the level or distribution of the protein, and producing strong phenotypes referable to the involvement of Glc7 in a subset of its dependent pathways, such as sporulation (absolute defect), glycogen biosynthesis, and whatever process(es) is lethally deranged by overproduction of the wild-type protein, without abolishing or seriously perturbing the essential Glc7-G₂/M function (Zhang, Guha, & Volkert, 1995). Those phenotypes of *shp1* cells are coincident with those described in a *glc7^{cs}* allele at its restrictive temperature (Hisamoto, Sugimoto, & Matsumoto, 1994).

Strains	Phenotype															
	YPD											YP				
	LiCl	NaCl	CaCl ₂	37°C	CFW	Caf	ZnCl ₂	high pH	Tn	β-merp	Hyg	Sper	TMA	EtOH	Gly	LG
<i>ofr1</i>																
<i>bni4</i>					HT				MS	HT						
<i>bud14</i>										MS			MS			
<i>fin1</i>												HT				
<i>gac1</i>					HT				HT							
<i>gip1</i>																
<i>gip2</i>																
<i>gip3</i>	HT	HT	HT										HT			
<i>gip4</i>																
<i>glc8</i>	HT	HT	HT						HT							
<i>mhp1</i>																
<i>pig1</i>																
<i>pig2</i>																
<i>red1</i>																
<i>ref2</i>	MS	MS	MS		MS	MS	MS	MS	HT	MS	MS	MS	MS	MS	MS	MS
<i>reg1</i>	MS				HT	MS	MS	MS	MS	MS	MS	MS	MS	MS	MS	MS
<i>reg2</i>																
<i>sip5</i>																
<i>shp1</i>				MS		MS	MS	MS	MS	MS	MS	MS	MS	MS	MS	MS
<i>sla1</i>	MS											HT				
<i>ysw1</i>																

Table 12. Phenotypic array comparing multiple wild-type phenotypes with those of the non-essential regulatory subunits of Glc7 mutant strains. Growth of each mutant was compared with that of the corresponding wild-type strain grown under the same set of conditions. Black squares denote strong sensitivity (SS), grey squares indicate mild phenotype (MS), white squares correspond with wild-type behavior (WT) and red square indicates an hypertolerance phenotype (HT). Conditions tested to construct the array were: **LiCl**, 50–300 mM LiCl; **NaCl**, 0.4–1.2 M NaCl; **high pH**, pH 8.0–8.3; **CaCl₂**, 100–300 mM CaCl₂; **ZnCl₂**, 1–6 mM ZnCl₂; **CFW**, 1–300 µg/ml Calcofluor white; **Caf**, 1–20 mM caffeine; **Tn**, 0.1–1–4 µg/ml tunicamycin; **β-merp**, 5–40 mM β-mercapthenol; **Hyg B**, 20–60 µg/ml hygromycin B; **TMA**, 0.2–0.6 M TMA; **Sper**, 0.1–0.7 mM spermine; **YPGly**, YP plus 2% glycerol; **YP-EtOH**, YP plus 2% ethanol; **YP-LowGlu**, YP plus 0.05% glucose.

We also identified several phenotypes which have already been designated to different *GLC7* mutant alleles described in the *Introduction*. For instance, the *glc7-10* allele shows a phenotype of hypersensitivity to cell wall integrity stressors basically due to the incapacity of dephosphorylating Pkc1-Slt2-mediated signaling (Andrews & Stark, 2000). Our results illustrate that cells lacking *REF2* has a severe hypersensitive to cell wall integrity phenotypes compared to wild-type strain; but *bni4*, *gac1* and *reg1* strains display a tolerant phenotype. Another interesting phenotype is linked to ionic homeostasis stressors. Our results show that, for example, cells lacking *GLC8* or *GIP3* have a tolerant phenotype, when compared to wild-type strain, in high concentrations of extracellular salts (lithium, sodium and calcium), while the mutant strains for *REG1*, *REF2*, *SHP1* and *SLA1* genes show a phenotype of hypersensitivity which could be linked to the *GLC7* mutant alleles (*glc7-R260P* and *glc7-109*) described in (Tara Williams-Hart et al., 2002).

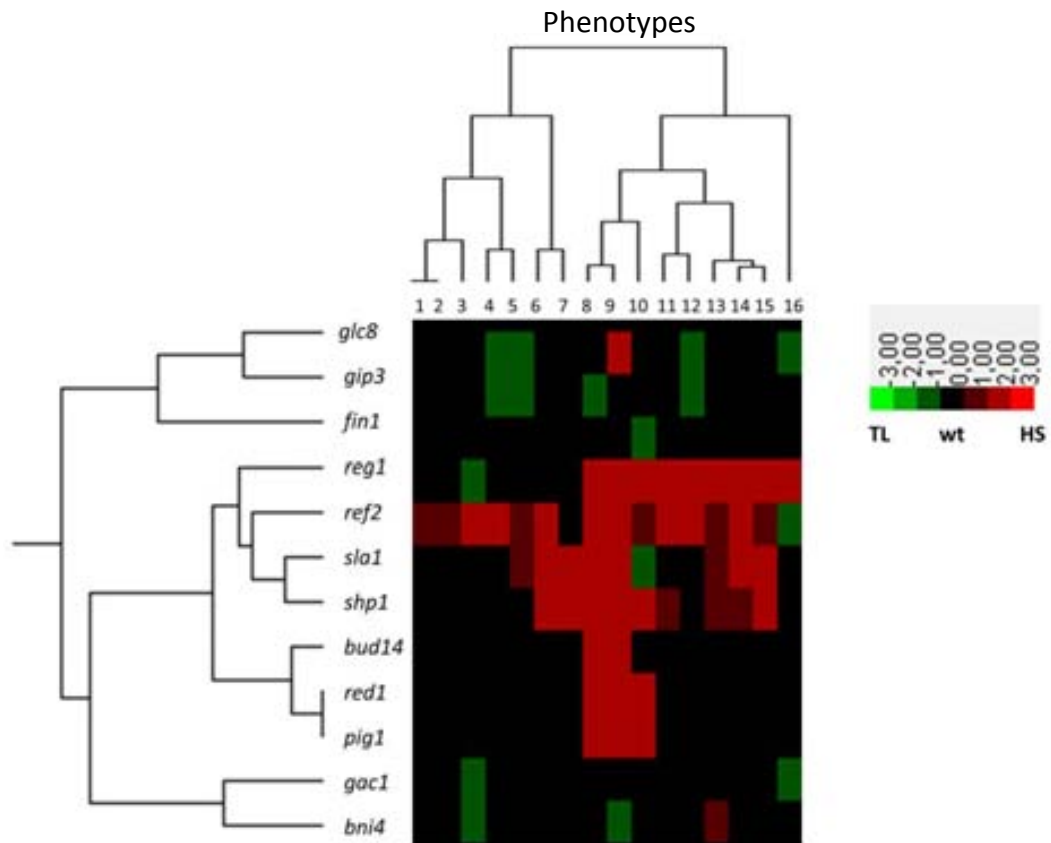


Figure 14. Phenotypic array comparing multiple wild-type phenotypes with those of the non-essential regulatory subunits of Glc7 mutant strains. Tree alignment of phenotypes of mutants of the non-essential Glc7-regulatory subunits analyzed with ClustalW 2.0 from EMBL-EBI (Larkin et al., 2007). Hierarchical cluster was performed using array correlation parameter plus complete linkage clustering and data was represented by Treeview tool v1.6 from Eisen's lab software (Eisen et al., 1998). Conditions tested to construct the array were: YP plus 0.05% glucose (1), YP plus 2% glycerol (2), 1-300 $\mu\text{g/ml}$ Calcofluor white (3), 100–300 mM CaCl_2 (4), 0.4–1.2 M NaCl (5), YP plus 2% ethanol (6), 37 °C (7), 0.2–0.6 M TMA (8), 20–60 $\mu\text{g/ml}$ hygromycin B (9), 0.1–0.7 mM spermine (10), 1–6 mM ZnCl_2 (11), 50–300 mM LiCl (12), 5–40 mM 2-mercapthenol (13), pH 8.0–8.3 (14), 1–20 mM caffeine (15) and 0.1–1.4 $\mu\text{g/ml}$ tunicamycin (16). Red color denote strong sensitivity (**HS**), black color correspond with wild-type behavior (**wt**) and green color indicates an hypertolerance phenotype (**TL**).

To summarize, in this thesis, we eventually decided to focus on the study of *REF2* because it is one of the less studied non-essential regulatory subunit of Glc7 and, because, *ref2* cells show hypersensitivity to nearly every examined condition.

1.2 Vacuolar morphological analysis of cells lacking regulatory subunits of Glc7

Yeast cells possess lysome-like vacuoles that perform the main functions of the vacuole (adjustment of proteins, biosynthetic and endocytosis pathways, proteolytic activation of zymogen precursors, among others) as well as the control of calcium homeostasis, osmotic control, detoxification of cations and storage of metabolites in building blocks. These functions

are sensitive to acidification of the organelle, so there is the vacuolar ATPase (V-ATPase) which regulates ion afflux from the vacuole and is encoded by *VMA*s genes (P M Kane, 2006).

Cells lacking *REF2* show a hypersensitivity phenotype to both alkaline pH and high concentrations of extracellular calcium (*Figure 13*). This situation is the trademark of a phenotype *vma* (P M Kane, 2006) which may indicate a defect in the function of the V-ATPase in the *ref2* mutant.

To test this hypothesis, and since the *vma* mutants are characterized by either defects in the vacuolar morphology or number of vacuoles per cell, we decided to analyze the number of vacuoles in the *ref2* mutant, as well as other mutants on non-essential Glc7-regulatory subunits (*Figure 15A*) by using the lipophilic styryl dye FM4-64 to stain vacuole membranes..

As shown in *Figure 15A*, the majority of mutants on non-essential Glc7-regulatory subunits display either a vacuole distribution and morphology equivalent to these of the wild-type cells. Cells lacking *REF2* (as well as *red1* and *reg1* mutant cells) show severe morphological defects in vacuoles which can be classified as class C (*Figure 15B*). Class C represents mutant cells that do not really have an organelle definable as a vacuole, which possibly indicates a dysfunction, at least partially, of the V-ATPase (Raymond, Howald-Stevenson, Vater, & Stevens, 1992). It has been described that Glc7 activity seems to be essential not only for vacuolar fusion, but also for ER-to-Golgi trafficking. Thus, the *glc7-13* allele has impaired in the internalization of FM4-64 fluorescent dye implying a block in endocytic pathway similar to the *ref2* cells (data not shown) (Peters et al., 1999). Glc7 has also been involved in the membrane fusion event since it is required for the vacuolar import and degradation (Vid) vesicle to vacuole trafficking (Cui, Brown, & Chiang, 2004; P. H. Huang & Chiang, 1997). Cells lacking *REG1* or carrying the *glc7-T152K* allele (Tu & Carlson, 1995b) are defective in the glucose-induced targeting of the key gluconeogenic enzyme fructose-1,6-biphosphatase to the vacuole for degradation, displaying a defective Vid vesicles trafficking to the vacuole. Therefore, our results indicate that Ref2 regulate the Glc7 function in the vacuolar trafficking.

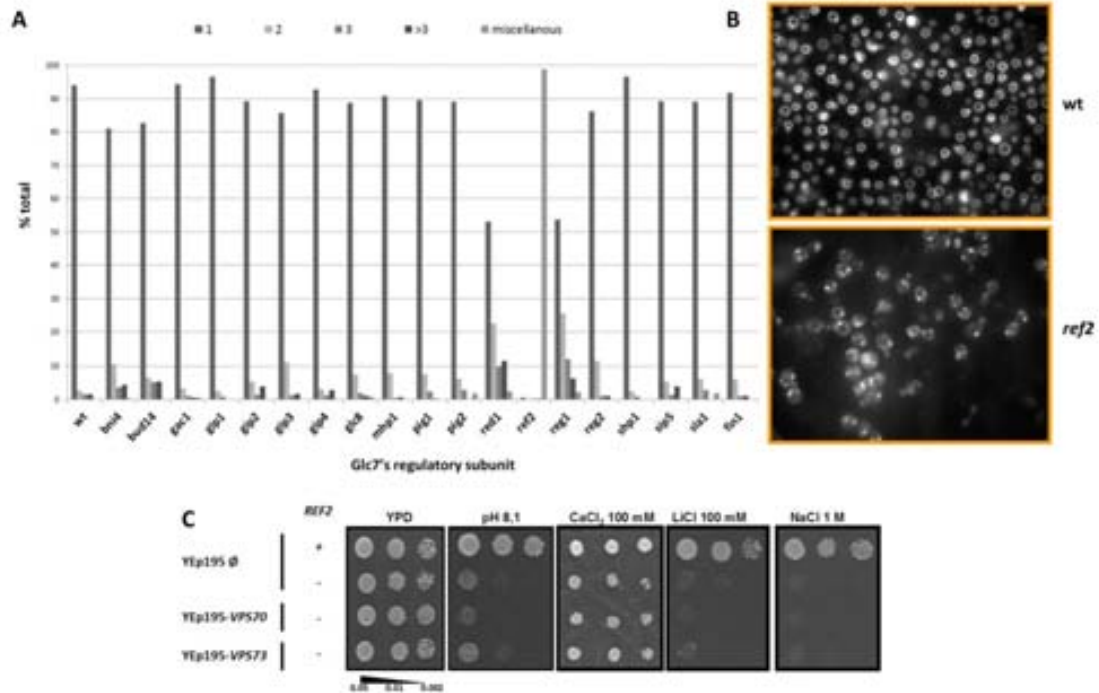


Figure 15. Vacuolar analysis of Glc7 subunits. A) Distribution of the number of vacuoles in different mutant cells on the non-essential regulatory subunits of Glc7 by using the internalization of FM4-64 fluorescent dye. The categories used for the number of vacuoles are 1, 2, 3 > 3 and miscellaneous which represents no functional vacuole observed. **B)** Comparative picture of stained vacuoles in wild-type cells (**wt**) and in cells of its derivative *ref2* mutant strain (**ref2**). **C)** Three dilutions from cell cultures of the wild-type strain BY4741 (**wt**) and the indicated isogenic derivatives (**ref2**) transformed with multicopy plasmid carrying *VPS70* and *VPS73* were spotted on YEP plates in the presence of the indicated conditions. Growth at 28°C was monitored for 2-3 days.

It had been characterized that the overexpression of *VPS70* or *VPS73* genes can not only rescue the phenotypes of different sensibilities (such as alkaline pH, high extracellular concentrations of calcium, lithium and sodium) but also serious morphological flaws characteristic of the vacuoles class B vacuole defects characterized in the laboratory for the *ptc1* mutant (A. Gonzalez, Ruiz, Serrano, Arino, & Casamayor, 2006). *VPS70* and *VPS73* encode two proteins with unknown function, which are involved in the setting of proteins in the vacuole, but its mechanism of action has not been determined yet. As shown in *Figure 15C*, overexpression of these genes does not rescue the described phenotypes for *ref2* cells. Thus, the observed vacuolar defects of *ptc1* and *ref2* cells are of different origin.

1.3 Transcriptional analysis of cells lacking non-essential Glc7-regulatory subunits

The transcriptional analysis of mutants on non-essential Glc7-regulatory subunits was performed comparing the expression patterns of each mutant to that of the wild-type strain in

exponential growth (OD_{660} 0.6-0.8) in YPD (pH 5.5). The dye-swapping strategy allows us not only to have two DNA microarrays experiment for each pair comparison but also to prevent the dye bias effect (Lyne et al., 2003).

We have analyzed the transcriptomic profiles of *bni4*, *bud14*, *gac1*, *gip2*, *glc8*, *pig2*, *reg1*, *ref2* and *sip5* strains. The first part of the analysis of the DNA microarrays, once duplications were eliminated by pre-processing with GEPAS, consisted on sending induced and repressed genes to perform a functional classification analysis, which would allow us to determine the functional categories to help us explain these sensitivities observed in the drop-test (*Figure 13*). We initially thought to only consider functional categories with a P-value (reference value) lower than 10^{-4} , but we had hardly obtained results. For that we decreased our restrictive conditions and accepted P-value lower than 10^{-3} . The *Table 13* shows a summary of the results indicating the functional categories to which the sets of up- and down-regulated genes in each mutant belong. Globally, we only found out that the functional category of metabolism of arginine was repressed in *reg1*, *reg2*, *bni4*, *glc8*, *gip2* and *pig2* strains. However, we were not able to determine a common functional category in the mutant strains for the induced genes.

Strain	Induced Categories	P-value	Genes % Ind
	Homeostasis of phosphate	2.83E-04	
	Valcine biosynthesis	3.43E-04	
	Amino transport	4.23E-04	
	Homeostasis of nitrite	3.43E-03	
	Phosphate metabolism	3.76E-03	
bni4	Cell, stress, defense and virulence	1.83E-03	101 2.09
	Ion transport	2.06E-03	
	Drug/toxin transport	2.34E-03	
	Transported compounds (substrates)	3.44E-03	
	Metabolism of urea (urea cycle)	3.43E-03	
	Modification by phosphorylation, dephosphorylation, adenylation	2.90E-03	
	Glycolytic cycle	2.93E-03	
gac1	Sugar transport	1.25E-04	189 3.78
	C-compound and carbohydrate transport	3.26E-04	
gip2	Homeostasis of phosphate	3.04E-03	59 1.34
	Valcine biosynthesis	3.26E-03	
glt8	Siderophore-iron transport	1.11E-03	27 0.48
	Heavy metal ion transport (Zn, Fe, Ni, etc.)	1.83E-03	
	Drug processing	1.83E-04	
gip2	Ion transport	3.38E-03	69 1.34
	ATP processing	3.43E-04	
	Phosphate transport	3.76E-04	
reg2	Homeostasis of nitrite	3.76E-03	45 0.93
	Homeostasis of phosphate	3.11E-03	
sip5	NO		75 1.43
bud24	NO		49 0.99
	electron transport and membrane-associated energy conservation	1.33E-08	
	Energy	3.19E-27	
	Respiration	1.83E-24	
	aerobic respiration	3.21E-16	
	energy generation (e.g. ATP synthesis)	1.83E-13	
	electron transport	1.84E-13	
	Transported compounds (substrates)	2.80E-10	
	tricarballic acid pathway (tricaric cycle, Krebs cycle, TCA cycle)	3.81E-09	
	C-compound and carbohydrate metabolism	6.64E-09	
	energy conversion and regeneration	3.71E-08	
	ion transport	2.75E-07	
	C-compound and carbohydrate transport	1.87E-06	
	sugar, glucose, glycerol and carbohydrate catabolism	4.50E-06	
	sugar, glucose, glycerol and carbohydrate metabolism	6.21E-06	
	intracellular transport	6.38E-06	275 5.20
	sugar transport	1.86E-05	
	homeostasis of protons	2.87E-05	
	cation transport (Na, K, Ca, Cd, etc.)	1.83E-04	
	biosynthesis of glutamate	2.79E-04	
	metabolism of glutamate	3.01E-04	
	transport ATPases	3.84E-04	
	cellular transport, transport facilities and routes	4.73E-04	
	metabolism of energy reserves (e.g. glycogen, trehalose)	5.08E-04	
	transport facilities	5.96E-04	
	complex cellular/molecular/cytoskeletal binding	6.44E-04	
	Fe/Zn binding	7.08E-04	
	Metabolism	1.84E-03	
	cellular transport	4.73E-03	
ref2	nitric metabolism	3.53E-03	186 3.61
	nitric metabolism	3.53E-03	

Strain	Repressed Genes	P-value	Genes % Rep
bni4	ribosome proteins	3.76E-11	
	ribosome biogenesis	1.75E-08	319 6.6
	Metabolism of arginine	1.12E-02	
gac1	Homeostasis of nitrite	3.63E-03	
	Autophagy/lysosome processing	3.76E-03	79 1.58
	Metabolism of arginine	3.73E-03	
	biosynthesis of arginine	1.29E-03	
gip2	Metabolism of urea (urea cycle)	2.77E-04	29 0.66
	Metabolism of aspartate	4.02E-04	
	Metabolism of urea cycle, creatine and polyamines	1.89E-03	
	sugar transport	3.73E-03	
	C-compound and carbohydrate transport	5.10E-03	
	metabolism of arginine	1.86E-03	
	sugar, glucose, glycerol and carbohydrate catabolism	1.89E-03	
	biosynthesis of arginine	2.17E-04	
	sugar, glucose, glycerol and carbohydrate metabolism	3.69E-04	
	metabolism of urea (urea cycle)	3.94E-04	
	transported compounds (substrates)	4.17E-04	
	development of amino acids or arginine	4.92E-04	193 3.44
	metabolism of secondary monoamines	2.83E-04	
	transport facilities	1.01E-03	
	nitrogen, sulfur and selenium metabolism	1.89E-03	
	sugar, glucose, glycerol and carbohydrate catabolism	1.83E-03	
	accumulation of ammonia, metabolism of the glutamate group	3.74E-03	
	metabolism of primary metabolic sugar derivatives	2.73E-03	
	cell adhesion	4.88E-03	
	metabolism of arginine	4.10E-04	
	metabolism of urea (urea cycle)	1.83E-04	
	metabolism of the aspartate family	4.73E-03	
gip2	sugar, glucose, glycerol and carbohydrate metabolism	4.08E-03	203 3.94
	sugar, glucose, glycerol and carbohydrate catabolism	3.94E-03	
	metabolism of energy reserves (e.g. glycogen, trehalose)	1.84E-04	
	C-compound and carbohydrate transport	2.49E-03	
	nitrogen transport	3.93E-03	
	C-compound and carbohydrate transport	2.84E-05	
	sugar transport	2.31E-05	
	sugar, glucose, glycerol and carbohydrate catabolism	3.94E-05	
	sugar, glucose, glycerol and carbohydrate metabolism	1.84E-04	
	metabolism of arginine	4.14E-04	
reg2	Metabolism of urea (urea cycle)	5.10E-04	58 1.22
	sugar, glucose, glycerol and carbohydrate metabolism	4.08E-03	
	metabolism of the aspartate family	4.73E-03	
	cellular transport	5.10E-03	
gip2	Metabolism of arginine	2.73E-03	186 3.54
	metabolism of urea cycle, creatine and polyamines	1.89E-04	
	metabolism of urea (urea cycle)	4.10E-04	
bud24	C-compound and carbohydrate transport	1.29E-03	49 0.99
	sugar transport	1.29E-03	
	metabolism of aspartate	1.93E-03	
	Drug/toxin transport	2.79E-03	
	metabolism of arginine	2.73E-03	
	biosynthesis of arginine	1.79E-04	
	metabolism of urea (urea cycle)	1.62E-04	
reg1	accumulation of ammonia, metabolism of the glutamate group	4.83E-04	171 3.23
	metabolism of inorganic amino acids	1.86E-03	
	C-compound and carbohydrate transport	3.63E-03	
	metabolism of the aspartate family	4.98E-03	
	Cell, stress, defense and virulence	1.09E-03	
	degradation of lactate	1.23E-03	135 2.84
	stress response	2.53E-03	
ref2	amino acid metabolism	4.98E-03	

Table 13. Functional characterization of induced and repressed genes in the mutants of the Glc7-regulatory subunits analyzed. Analysis of induced genes (relative expression > 1.80 folds) or repressed genes (relative expression < 0.55 folds) of each strain were obtained by the functional categories classifier (Funcat) tool of MIPS (Ruepp et al., 2004). Only functional categories with P-value < 10⁻³ are shown and either the percentage of induced genes (% Ind) or repressed genes (% Rep) were calculated respect the total of genes with existing data.

So, in order to check the accuracy and veracity of our DNA microarray experiment, we decided to analyze one specific gene using a plasmid reporter for β -galactosidase assay. The expression of *PHO84*, a high-affinity inorganic phosphate (Pi) transporter, was found induced in seven strains (*bni4*, *gip2*, *gip2*, *reg1*, *reg2*, *sip5*, *glt8*) and repressed in *ref2* cells. Surprisingly, we were not able to repeat the DNA microarray results for most of mutant strains (*Figure 16A*). Specifically, *ref2* strain also displayed a repression of *PHO84* in both experiments, but other strains do not exhibited any induction of this gene (*Figure 16A*).

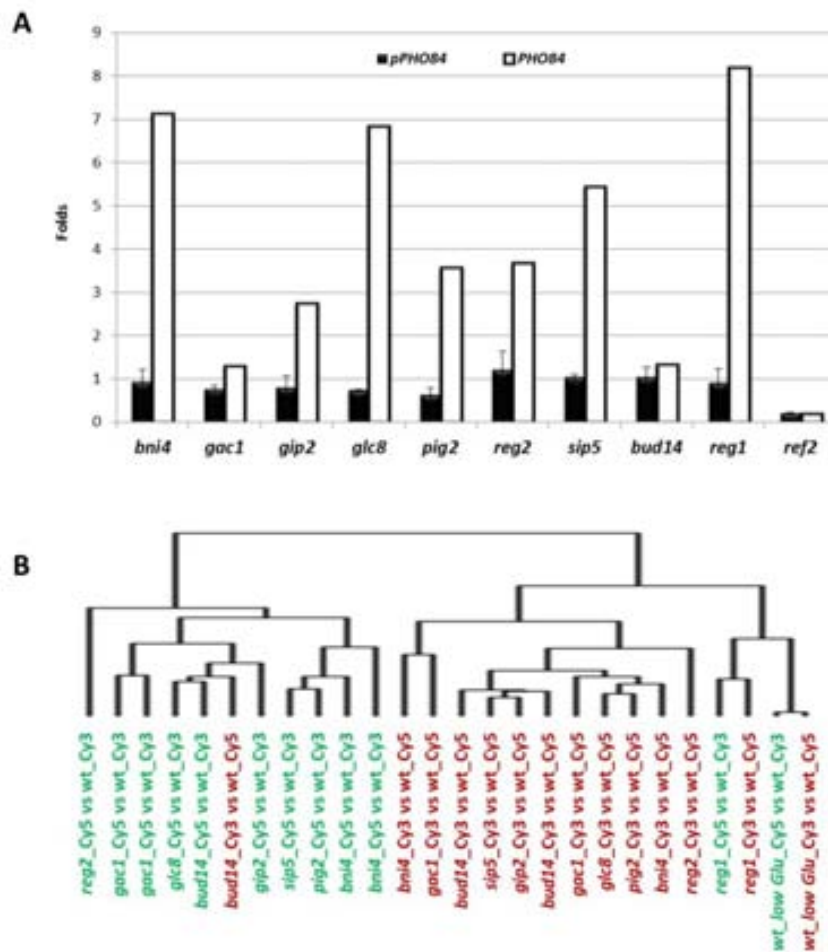


Figure 16. Glc7-regulatory subunits do not show a specific expression profile. A) Wild-type and its derivative strains were transformed with the construct pPHO84-lacZ and cultures were grown in YPD (pH 5.5) until 0.8 OD₆₆₀ was reached. Cells were collected and β -galactosidase activity measured as described in *Experimental procedures*. Data are mean \pm SEM from at least six independent clones. The β -galactosidase activity results are represented in folds increased respect that of wild-type cells (black bars). The expression data, also in fold increase respect wild-type cells, for the PHO84 gene obtained from DNA microarray experiments is also shown (white bars). **B)** Expression changes found in each DNA microarray experiment data from indicated strains were analyzed with Cluster tool v2.11 from Eisen's lab software (Eisen et al., 1998). Hierarchical cluster was performed using array correlation parameter plus complete linkage clustering and data was represented by TreeView toll v1.6 from Eisen's lab software.

In *Figure 16B*, we represented the correlation of the results obtained for each particular analyzed microarray, where the dye-swapping experiments are represented by different colors. As a control for verifying hierarchical cluster through correlation, we used our lab's experiment where wild-type strain was shifted from medium containing 2% of glucose to medium containing low glucose concentration (0.05% glucose) and growth was resumed for 1 h (wt_low_Glu). This analysis showed that the expression of 1040 and 1090 genes was found up- (expression ratio > 1.80 fold) and down-regulated (expression ratio < 0.55 folds) representing 18.5% and 19.4% of the total number of genes, respectively. Genes included in

the functional categories correlated to the response to stress conditions were found among the induced genes. In fact, data from these experiments (wt_low_Glu in *Figure 16*) correlated well with that obtained from the *reg1* mutant microarrays. In fact these dye-swapping microchips of the *reg1* experiment are the only that are clustered together, since the correlation of the expression patterns found for most of the subunit mutants (except for *bud14*) were principally based on the dye-preference labeling.

To summarize, the transcriptional changes between some mutants on non-essential Glc7-regulatory subunits are dye-specific and not correlate between the same strain experiments. That means that in standard growth conditions some of strains do not show significant transcription changes or, in any case, those are less important than the dye bias.

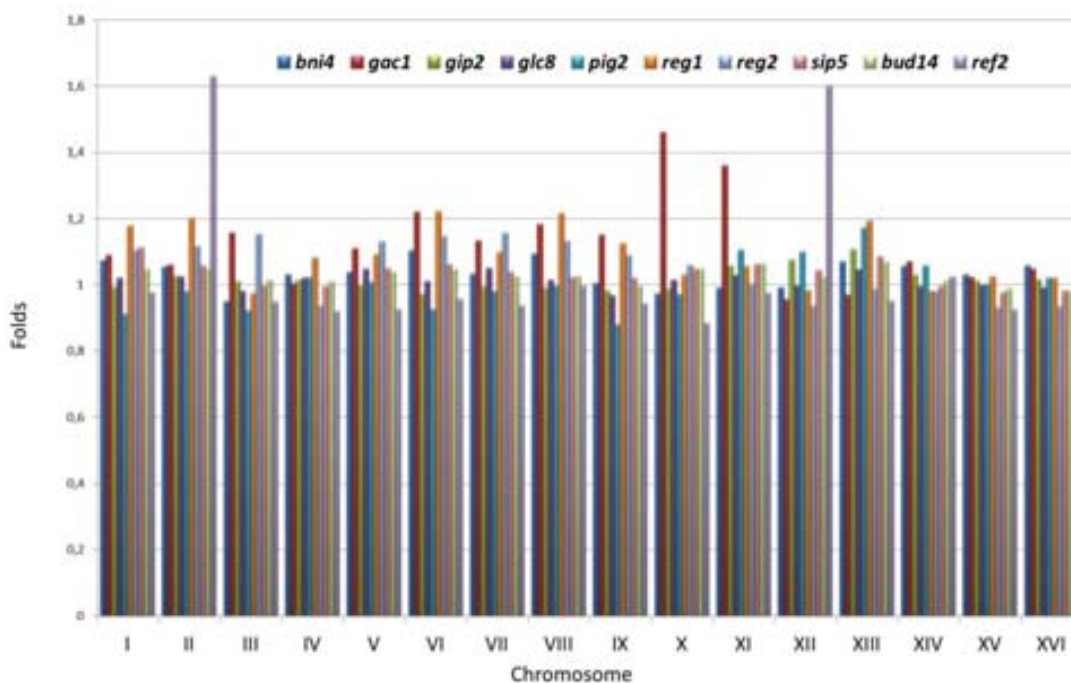


Figure 17. Cells lacking *REF2* show a possible aneuploidy in chromosome II and XII. Once analyzed the DNA microarray experiments as explained in *Experimental procedures*. The mean of the expression values (in \log_2) for the genes of each chromosome was calculated and represented for some of the analyzed mutants as fold change.

Another performed analysis with the data from the DNA microarrays experiments was the calculation of average expression values of the genes of each chromosome for the mutants on non-essential Glc7-regulatory subunits. As shown in the *Figure 17*, cells lacking *REF2* display an important change of the expression levels of the genes contained in chromosome II and XII, which could be indicative of a possible aneuploidy affecting these chromosomes which will be deeply studied in this work. Cells lacking *GAC1* also display an increased average of gene expression in chromosome X and XI. For that, we analyzed the gene distribution in these

chromosomes in *gac1* mutant strain showing that are represented 6.5% and 9.6% of induced genes, respectively; whereas cells lacking *REF2* have the 90% of total induced genes (266 genes) which are distributed between chromosome II (105 genes, 39%) to chromosome XII (136 genes, 51%). Therefore, *gac1* cells do not display aneuploidy as *ref2* cells.

Some large-scale studies already used the DNA microarrays as a useful tool to find aneuploid strains (Hughes et al., 2000) due to the fact that duplicated chromosomes are transcriptionally active in budding yeast, which means that these changes in the amounts of chromosomal DNA can be detected at the RNA content by increasing the expression of the involved genes between 1.8 to 2 folds for the whole chromosome (Tang & Amon, 2013; Eduardo M Torres et al., 2010).

Since we will focus our on the study of the Ref2 regulatory subunit, we decided to perform a phylogenetic analysis of this protein using two different databases: Fungal Orthogroups Repository (Wapinski, Pfeffer, Friedman, & Regev, 2007) and PhylomeDB (Huerta-Cepas et al., 2011; Huerta-Cepas, Bueno, Dopazo, & Gabaldón, 2008). Both databases display around 13 putative protein Ref2 orthologs. *Figure 18* shows the orthologs of Ref2 are only located in some species of the *Saccharomycetaceae* family. BLAST analysis based on the REF2 nucleotide coding sequence shows that similar sequences are only present in the genus *Saccharomyces*, except for a fragment of 402 nucleotides of a supposed clon corresponding to telomeric human DNA (accession number AF270643) that perfectly match with REF2 sequence excluding two single nucleotide gaps and another gap of 76 nucleotides.

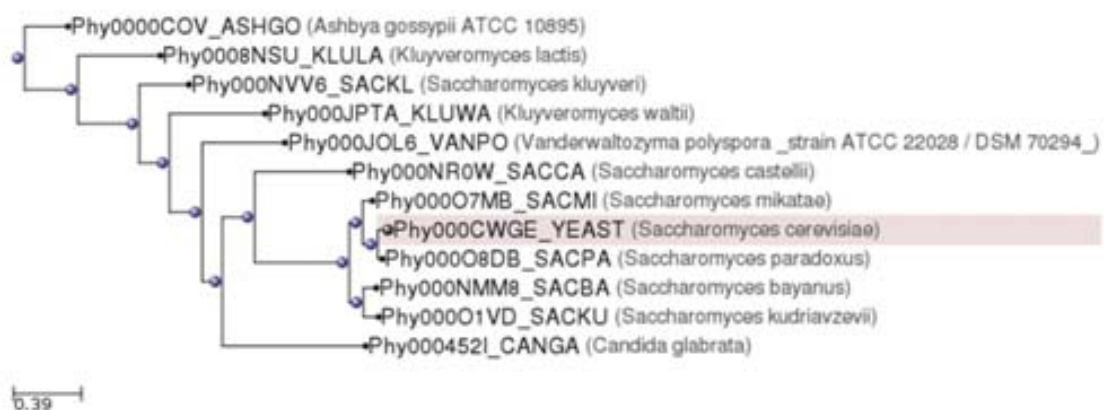


Figure 18. Phylome of S.cerevisiae Ref2. Protein Ref2 is compared to Yeast Phylome 60 database (Marcet-Houben & Gabaldón, 2009) to find protein orthologs using PhylomeDB (Huerta-Cepas et al., 2011, 2008) with the Blosum62 comparative method.

1.4 Conclusions

1. The phenotypic analysis revealed that mutants on non-essential Glc7-regulatory subunits display a high variety of sensitive/tolerant phenotypes under stress conditions. These myriad of phenotypes also correspond to the incredible number of functions where Glc7 has been involved. Moreover, some of these phenotypes have already been described for some of the *GLC7* alleles.
2. The vacuolar analysis of those mutants showed that two new subunits, Ref2 and Red1, are involved in the proper function of vacuole, through regulating Glc7. The abnormal vacuole density in *reg1* mutant cells was already described and its role in vacuole regulation has already been demonstrated. Importantly, Ref2 seems to be involved in the endocytic pathway regulation.
3. The transcriptomical analysis demonstrated that some of the mutants in non-essential Glc7-regulatory subunits have no sufficient defects in our standard conditions (YPD pH 5.5) compared to wild-type strain, meaning that they could not be evaluated using DNA microarray experiments and growth in optimal conditions. Further analyses for some mutants in non-optimal conditions have been carried out (such as *reg1* mutant cells growing in low glucose concentration or in alkaline pH). Specifically, *ref2* mutant cells showed an aneuploidy in chromosome II and XII.

2. Study of cation homeostasis in mutants in the non-essential Glc7-regulatory subunits

2.1 Lack of Ref2 causes defects in cation tolerance

The observation that point mutations in Glc7 that cause alterations in ion homeostasis lay in the vicinity of residues relevant for binding diverse regulatory subunits (T Williams-Hart et al., 2002) may indicate that alterations in ion homeostasis observed in some alleles of *GLC7* could be due to its regulation by regulatory subunits. This reasoning prompted us to examine tolerance to NaCl, LiCl, alkaline pH and CaCl₂ in 21 strains carrying a deletion of functionally well-documented regulatory subunits of Glc7. *Figure 19* shows a panel of drop-test growth selected conditions for 18 mutant strains; additionally, *red1*, *afr1* and *ysw1* mutant strains have their phenotypes summarized in *Table 12*.

As shown, mutation of most regulatory subunits did not result in significantly altered sensitivity or tolerance to the indicated treatments, with the exception of the *ref2* and *shp1* mutant cells. However, deletion of *SHP1* caused a rather severe growth defect even in the absence of stress, as previously described (Zhang et al., 1995), making it difficult to assess the actual effect of the mutation under the conditions tested. In contrast, lack of Ref2, which only caused a slight growth defect under standard culture conditions, prevented growth in the presence of lithium, sodium and calcium cations, as well as under alkaline conditions. *ref2* cells were also markedly sensitive to cesium ions (results not shown).

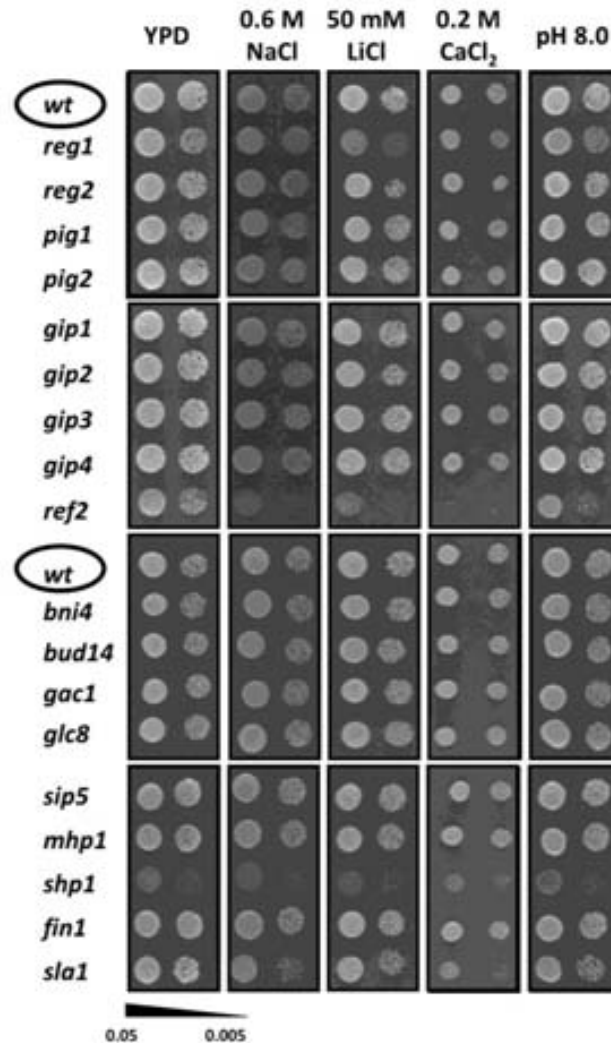


Figure 19. Effect of the mutation of several Glc7-interacting proteins on cation-related phenotypes. Two dilutions from cultures of wild-type strain BY4741 (**wt**) and the indicated isogenic derivatives were grown on YPD plates in the presence of 0.6 M NaCl, 50 mM LiCl, 0.2 M CaCl₂ or at alkaline pH (**pH 8.0**) for 2 days.

The intensity of the phenotype for sodium and lithium stress was comparable with that of a *trk1 trk2* strain, which has defective potassium uptake (*Figure 20A*). The phenotype was not caused by the inability to adapt to hyperosmotic stress, as (i) growth was not affected by inclusion of 1 M sorbitol or KCl in the medium and (ii) an obvious growth defect was already observed at a lithium concentration as low as 30 mM, which does not represent an osmotic stress condition (*Figure 20*). Increased sensitivity to sodium and lithium cations is often observed in strains with defective potassium uptake (i.e. in *trk1* mutants) (Gómez, Luyten, & Ramos, 1996).

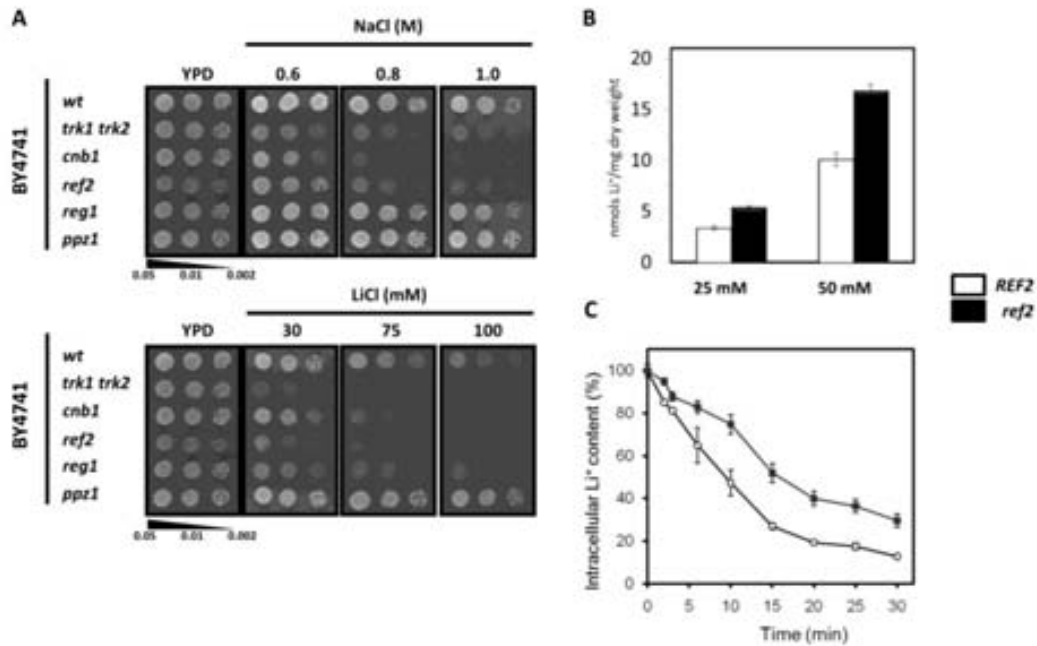


Figure 20. *ref2* mutant cells show phenotypes of hypersensitivity to Na⁺ and Li⁺ and also defective cations efflux. A) Three dilutions from the indicated cultures were spotted on YPD plus the indicated concentrations either of NaCl or LiCl. Growth at 28°C was monitored for 2-3 days. **B)** Wild-type BY4741 cells (white bars) and the *ref2* derivative (black bars) were incubated with 25 or 50 mM LiCl as described in the *Experimental procedures section 19* and the intracellular content of lithium ions measured. Results are means ± SEM for at least six independent determinations. **C)** Strains BY4741 and its isogenic derivative *ref2* were loaded with 75 mM LiCl, samples taken at different times and the efflux of the cation determined as described in the *Experimental procedures section 19*. Results are expressed as a percentage of the intracellular lithium content for each strain at the start of the experiment and are means ± SEM for at least six independent assays.

Moreover, increased sensitivity to sodium and lithium cations can be the result of the increased uptake, decreased efflux, or inability to sequester these toxic cations into intracellular compartments, such as the vacuole. To get an insight into a possible cause for sensitivity in the *ref2* mutant, the intracellular concentration of lithium in cells grown in the presence of 25 or 50 mM LiCl was tested. As shown in *Figure 20B*, *ref2* mutants accumulate 60–70% more lithium than the wild-type strain. This suggested that lack of Ref2 might favor lithium entry or make detoxification of the cation more difficult by interfering with the efflux systems. To this end, we tested the ability of *ref2* cells to extrude lithium. As shown in *Figure 20C*, lithium efflux was markedly impaired in cells lacking Ref2, suggesting that the absence of this Glc7-regulatory subunit interferes with the normal efflux mechanisms.

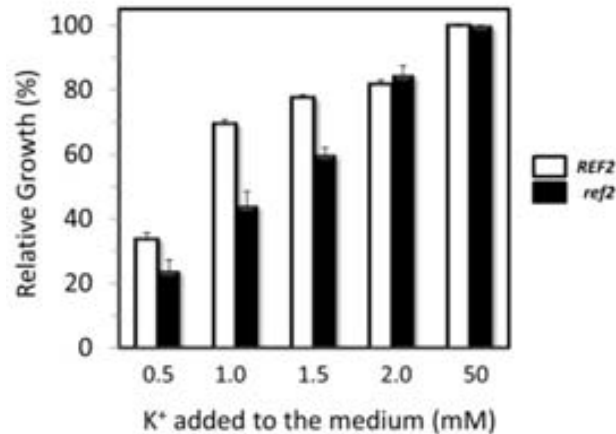


Figure 21. Mutation of REF2 increases potassium requirements for growth. Cultures of wild-type strain BY4741 (white bars) and its *ref2* derivative (black bars) were inoculated at an OD₆₆₀ of 0.004 in Translucent K-free medium, supplemented with the indicated amounts of KCl, and grown for 16 h. Results are represented as a percentage of growth compared with cells incubated with 50 mM KCl and are means \pm S.E.M. for three independent cultures.

Results from *Figure 20* prompted us to test the requirements for potassium in the *ref2* mutant, by using a recently developed YNB-based potassium-free medium. As shown in *Figure 21*, *ref2* cells display a slow-growth phenotype at limiting potassium concentrations (0.5–1.5 mM) that was alleviated by increasing the amount of potassium in the medium. This suggests that *ref2* cells might have a decreased high-affinity potassium uptake, although direct measurement of rubidium influx (an analogue commonly used to assess for potassium uptake capacity (Rodriguez-Navarro, 2000) failed to reveal a significant decrease in rubidium ion uptake (results not shown). In any case, the *ref2* strain showed increased sensitivity to several organic toxic cations, such as hygromycin B, spermine and TMA (tetramethylammonium) (*Figure 22A*), a phenotype which is commonly observed in strains with altered cation homeostasis (L Yenush, Mulet, Arino, & Serrano, 2002).

2.2 The Glc7-binding motif of Ref2 is required for cation tolerance

As extensively explained in *Introduction section 2.3.3*, Ref2 contains a RISSIKFLD sequence (residues 368–376) that closely matches the **(R/K)(V/I)X(F/W)** Glc7-binding consensus sequence. We considered it necessary to test whether or not the salt-related phenotypes, derived from the absence of Ref2, could be explained by its role as a non-essential Glc7-regulatory subunit.

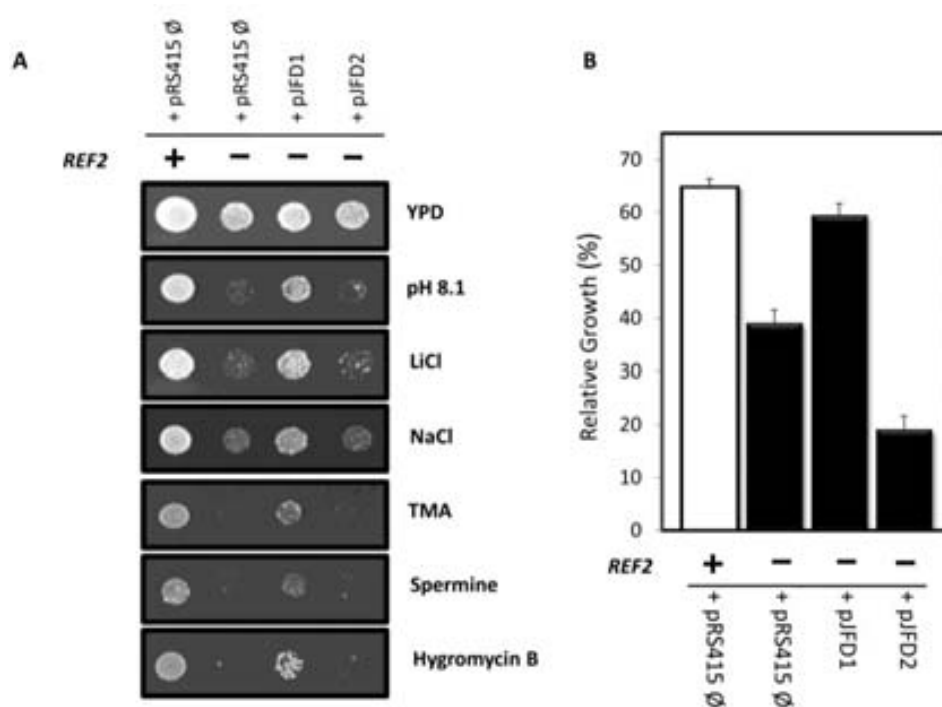


Figure 22. Mutation of Phe-374 within the Glc7-binding consensus sequence abolishes the function of Ref2 in cation tolerance. **A**) Wild-type BY4741 (+) and *ref2* strains (-) were transformed with the empty plasmid pRS415 or the same plasmid expressing the wild-type Ref2 protein (pJFD1) or the Ref2^{F374A}-mutated version (pJFD2). Transformants were spotted on to YPD plates, which were adjusted to pH 8.1 or contained LiCl (150 mM), NaCl (1 M), TMA (0.3 M), Spermine (0.6 mM) or Hygromycin B (20 μ g/ml) as indicated. Growth was monitored after 3 days, except for the LiCl and NaCl conditions when growth was monitored after 6 days. **B**) Wild-type (+) and *ref2* (-) strains were transformed with the indicated plasmids and growth was tested at a limiting concentration of external potassium (1 mM). Experimental conditions were as described in Figure 21.

To this end, the Phe-374 of Ref2 was replaced with an Ala residue and the point-mutated version of the gene (including its own promoter) was cloned into a centromeric plasmid. As shown in Figure 22A, introduction of the wild-type version of *REF2* (pJFD1) in a *ref2* mutant was able to increase tolerance to sodium, lithium and alkaline pH, as well as to diverse toxic organic cations. In contrast, mutation of Phe-374 (pJFD2) resulted in a complete inability to do so. It must be noted that this mutation does not affect Ref2 cellular levels, but it is known to disrupt the interaction with Glc7 (Nedea et al., 2008). Expression of the mutated form of Ref2 from a high-copy number plasmid, which should lead to overexpression of the protein, was also unable to rescue the *ref2* defects (results not shown). These evidences suggest that blocking the interaction between Ref2 and Glc7 results in loss of the Ref2 function in salt tolerance. A similar effect was observed when the growth deficiency at limiting external potassium concentrations of the *ref2* mutant was tested (Figure 22B). In this case, expression of the F374A-mutated version of *REF2* (pJFD2) even aggravated the growth defect of the strain lacking the chromosomal copy of the gene. We then considered the possibility that the cation-

related defects of the *ref2* strain could be attenuated or even suppressed by a surplus of Glc7. However, expression of Glc7 on a multicopy plasmid did not increase the tolerance of a *ref2* strain to LiCl or NaCl (Figure 23A). In contrast, the same plasmid was able to abolish the salt-sensitive phenotype of specific Glc7 mutants (Figure 23B), indicating proper expression of Glc7.

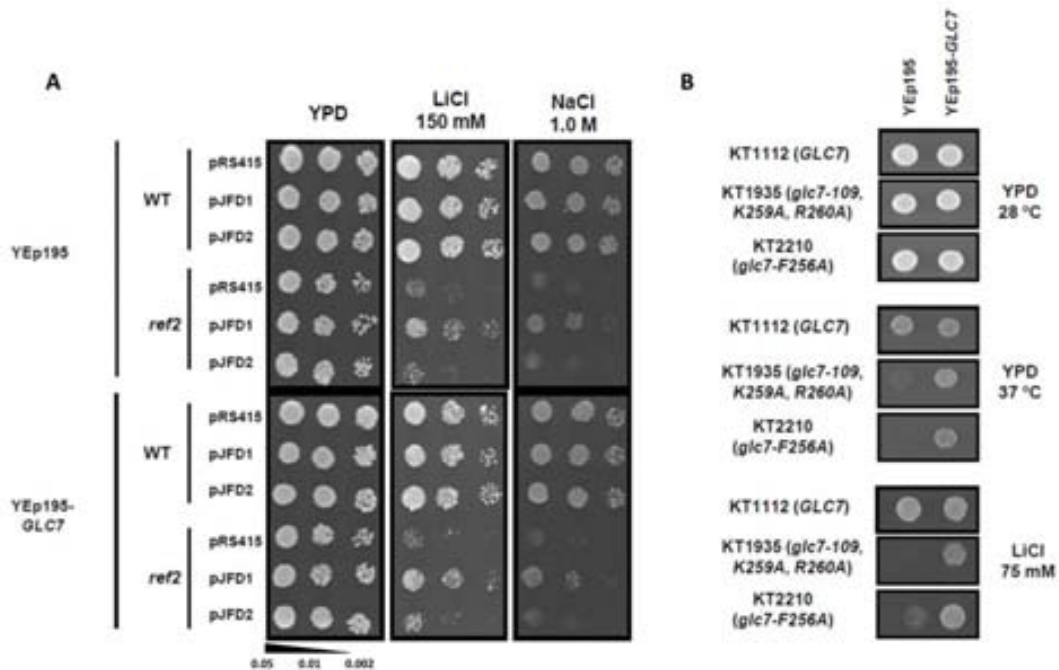


Figure 23. Effects of overexpression of Glc7 on Ref2-deficient *S. cerevisiae* strains. **A)** Wild-type strain BY4741 (WT) and its *ref2* derivative were co-transformed with the indicated plasmids. Three dilutions of the cultures were plated in the conditions indicated. Growth at 28°C was recorded after 4 days. **B)** Strains carrying wild-type (KT1112) and mutated forms of Glc7 (KT1935 or KT2210) were transformed with the indicated plasmid and spotted on YPD plates. Growth at 28° was recorded after 3 days.

2.3 Mutation of Ref2 affects expression of the *ENA1* ATPase gene under saline and alkaline pH stresses

The Na⁺-ATPase Ena1 is a major determinant of sodium and lithium tolerance. The expression of the gene is dramatically increased by exposure to high concentrations of sodium or lithium cations or by alkalization of the medium, and many mutations impairing *ENA1* induction upon stress has been shown to lead to hypersensitivity to these cations. Therefore we considered it necessary to monitor the expression of *ENA1* in *ref2* cells under cation stress conditions. To this end, cells were transformed with plasmid pKC201, which carries the entire *ENA1* promoter fused to the *lacZ* reporter gene. As shown in Figure 24, expression driven from the *ENA1* promoter in cells exposed to sodium or lithium cations, as well as to alkaline pH, is

drastically reduced in *ref2* cells. Therefore the increased sensitivity of the *ref2* mutant to these stresses could be attributable, at least in part, to a defect in *ENA1* induction.

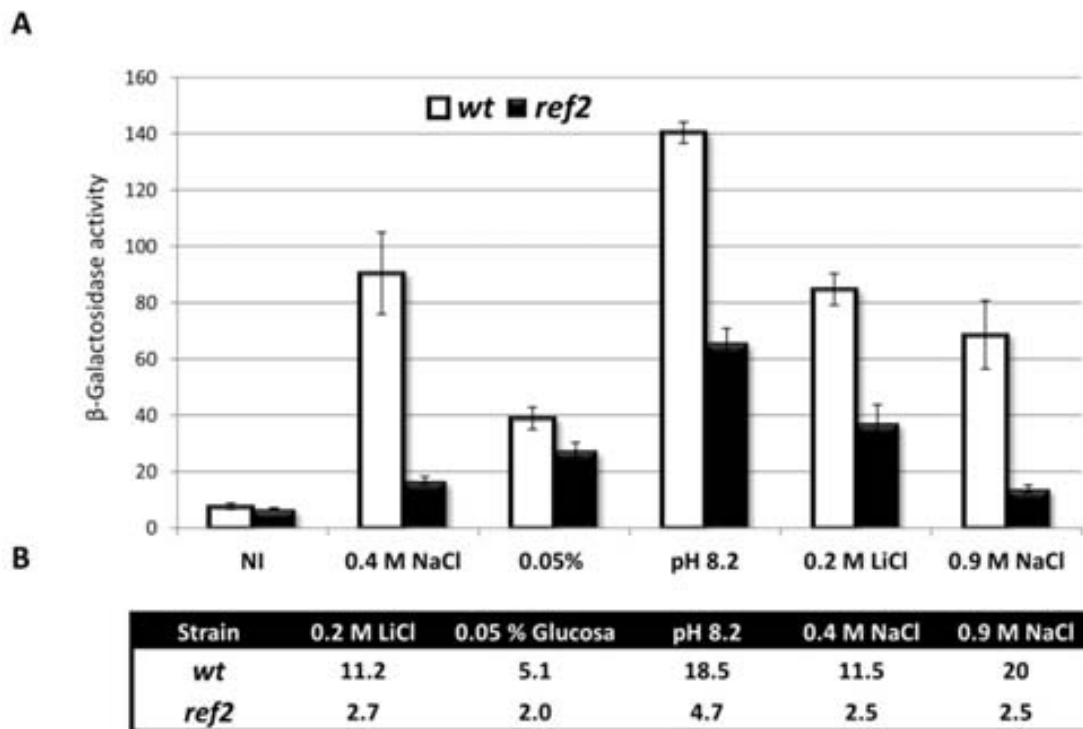


Figure 24. Mutation of Ref2 affects expression of the *ENA1* ATPase gene under saline and alkaline pH stresses. **A)** Wild-type strain BY4741 (*wt*) and its *ref2* derivative (*ref2*) were transformed with pKC201 (*ENA1-lacZ*) and cultures were grown until reached 0.8 OD₆₆₀ in YPD (pH 5.5). Cells were transferred to fresh YPD (non-induced, NI) with 0.4 M NaCl, 0.05% glucose, 0.2 M LiCl and alkaline pH 8.2 for 90 min and, YPD plus 0.9 M NaCl for 4 h at 28°C. β -galactosidase activity was measured as described in *Experimental procedures*. Data are mean \pm SEM from at least twelve independent clones. **B)** Folds were calculated dividing each stress condition to non-induced response activity for each strain.

The expression of *ENA1* under saline or alkaline stress is controlled by a variety of signaling pathways, including activation of calcineurin, which is triggered by a burst of cytosolic calcium. As observed in *Figure 24A*, the effect of the *ref2* mutation on *ENA1* expression can be even more severe than that caused by mutation of *CNB1*, encoding the regulatory subunit of calcineurin. Furthermore, the *cnb1* mutation seems additive to *ref2* both with respect to *ENA1* expression (*Figure 25A*) and to lithium, sodium and alkaline pH tolerances (*Figure 25B*). Therefore *ref2* phenotypes cannot be exclusively explained by a hypothetical impairment of calcineurin signaling under stress. Most regulatory inputs acting on the *ENA1* promoter target two relatively small regions named *ARR1* and *ARR2* (*Figure 6*) and reviewed in (Ariño et al., 2010). To gain insight into the effect of the *ref2* mutation, cells were transformed with plasmids pMRK212 and pMRK213. The former contains a region that mostly integrates calcium/calcineurin inputs, whereas the latter is regulated by calcineurin-independent stimuli. As shown in *Figure 25A*, deletion of *REF2* decreases expression driven from both promoter

regions, suggesting that the mutation has a complex and diverse effect. Analysis of the expression from these constructs further supports an additive effect of the *cnb1* and *ref2* mutations on cation homeostasis *Figure 25B*.

Our results suggest that the decreased tolerance to alkaline cations in the *ref2* mutant could be due, at least in part, to the inability to fully induce expression of the *ENA1* Na⁺-ATPase gene, which is a major determinant in saline tolerance. As lack of Ref2 blocked the response of *ENA1* to diverse stresses, which are mediated through a variety of signaling pathways (Marquez & Serrano, 1996; M Platara et al., 2006), the effect of Ref2 on *ENA1* expression is possibly pleiotropic and may involve multiple targets.

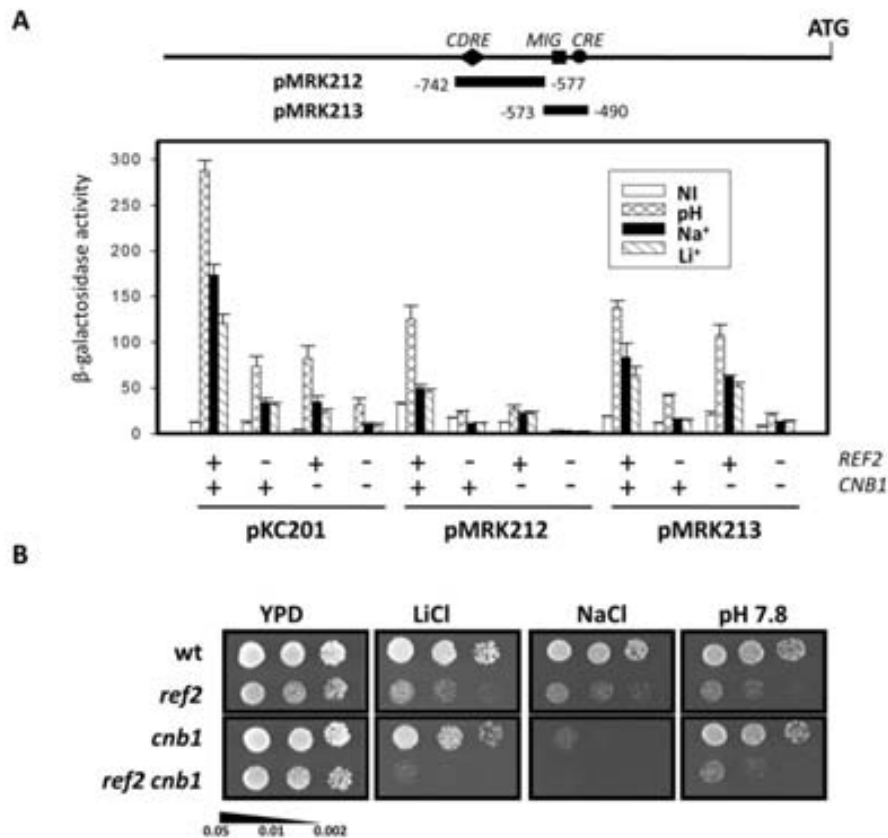


Figure 25. Effects of the *ref2* mutation in wild-type and *cnb1* strains on the *ENA1* promoter activity. A) The indicated strains were transformed with plasmids pKC201, carrying the entire *ENA1* ATPase gene promoter, or plasmids pMRK212 or pMRK213, which contain specific regions of the *ENA1* promoter, as indicated in the diagram at the top of the panel. MIG, Mig1/2 binding sequence; CRE, cAMP regulatory element. Cells received no treatment (NI), were shifted to pH 8.2 (pH) or were exposed to 0.4 M NaCl (Na⁺) or 0.2 M LiCl (Li⁺) for 1 h. β -Galactosidase activity was measured in permeabilized cells as described in the *Experimental procedures*. Results are means \pm SEM for eight or nine independent transformants. **B)** Three dilutions of the indicated cultures were spotted on to plates at the conditions YPD plus 50 mM LiCl (LiCl) and 0.6 M NaCl (NaCl) and growth recorded after 72 h (LiCl and NaCl) or 48 h (alkaline pH).

2.4 *ref2* mutant cells display a hyperactivated calcium/calcineurin pathway in the absence of stress and show altered vacuole morphology

A striking phenotype that can be observed in *Figure 19* is that lack of Ref2 results in a substantial sensitivity to calcium cations. It has been reported that hyperactivation of calcineurin results in a calcium-sensitive phenotype, whereas deletion of calcineurin-encoding genes yields calcium hypertolerance (Cunningham & Fink, 1994; A. Gonzalez et al., 2006). We therefore hypothesized that the calcium-sensitive phenotype of *ref2* mutants could be attributed to an unusually high basal calcineurin activity (i.e. in the absence of saline or alkaline pH stress).

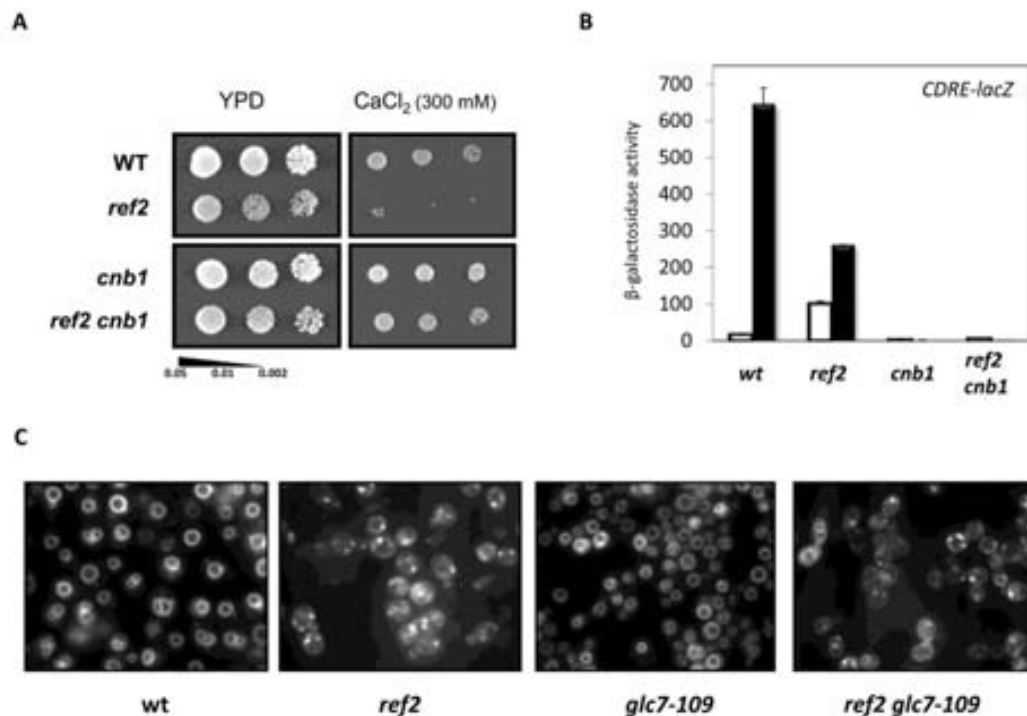


Figure 26. Lack of *REF2* results in altered calcium homeostasis and vacuolar morphology. **A)** The indicated strains were grown in the presence or absence of calcium cations (300 mM $CaCl_2$) and growth was monitored after 72 h. **B)** Yeast strains were transformed with plasmid pAMS366, which contains a tandem-repeat of four CDREs fused to a *lacZ* reporter (CDRE-lacZ), and incubated for 1 h in the absence (white bars) or presence (black bars) of 0.2 M $CaCl_2$. β -Galactosidase activity was measured as described in the *Experimental procedures*. Results are means \pm SEM for six independent transformants. **C)** Vacuolar staining of wild-type BY4741 (*wt*), *ref2::kanMX4* (*ref2*), YJFD17 (*glc7-109*) and YJFD18 (*ref2 glc7-109*) strains with the fluorescent dye FM4-64 was performed as described in the *Experimental procedures* for 30 min and monitored by fluorescence microscopy.

To test this possibility, we evaluated calcium tolerance in cells lacking both Ref2 and Cnb1, and compared them with the single *ref2* and *cnb1* mutants. As shown in *Figure 26A*, the calcium sensitivity conferred by the *ref2* mutation is largely abolished in the absence of Cnb1.

This suggests that the *ref2* growth defect in the presence of calcium is caused by hyperactivation of calcineurin and leads to the possibility that calcium levels might be higher than normal in *ref2* cells. This was directly tested by introducing the calcium-reporter plasmid pEV11/AEQ in wild-type and *ref2*-mutant cells. Our measurements indicated that the luminescence observed in *ref2* cells was 141.9 ± 3.7 RLU per 10^6 cells; whereas this parameter was 64.8 ± 3.5 RLU per 10^6 cells in the wild-type strain, thus confirming the existence of higher free cytosolic calcium levels in the mutant. On the basis of this result, one would expect that expression from a specific calcium/calcineurin-sensitive promoter would be increased in *ref2* cells grown under basal (non-stressing) conditions. To test this conjecture, wild-type and *ref2* strains (as well as their *cnb1* derivatives) were transformed with plasmid pAMS366, which carries a tandem-repeat of four copies of the CDRE from the promoter of the *FKS2* gene. As shown in *Figure 26B*, under basal growth conditions, expression from this synthetic promoter is 4–5-fold higher in *ref2* cells than in the wild-type strain. As expected, this effect is abolished in the absence of calcineurin activity (*ref2 cnb1* strain). Remarkably, whereas in the wild-type strain addition of calcium ions to the medium triggers a dramatic, calcineurin-mediated increase in expression, this effect is much less prominent in cells lacking Ref2. This could be explained if the *ref2* mutation somehow interferes with stress-triggered effects mediated by activation of calcineurin. Increased sensitivity to alkaline pH and calcium is a characteristic phenotype of yeast strains with deficient vacuolar function (P M Kane, 2006). Therefore the possibility that *ref2* mutants may display some alteration in this subcellular compartment was already confirmed in *Figure 15*; where incubation of wild-type and *ref2* cells with the lipophilic fluorescent dye FM4-64, which stains the vacuole membrane, reveals that vacuolar structure is dramatically altered in the *ref2* mutant, with a punctuated fluorescent pattern and lack of discernible vacuolar structure. Because of the similarity between the saline phenotypes of the *ref2* deletion and the *glc7-109* allele, we considered it interesting to evaluate vacuolar morphology in the latter. As shown in *Figure 26C*, FM4-64 staining of strain YJFD17, which carries a centromeric plasmid borne *glc7-109* allele as the only source of *GLC7* function, reveals that this strain has vacuoles with essentially wild-type morphology (in a similar manner to the original cation-sensitive strain KT1935; results not shown). Interestingly, combination of the *ref2* deletion and the *glc7-109* mutation results in cells with a *ref2*-type phenotype i.e. altered vacuoles. The disruption of *REF2* in the KT1935 background was repeatedly attempted without success. This is probably due to the close genetic relationship of this strain with the W303 genetic background (K.Tatchell, personal communication), in which the *REF2* deletion was reported to be lethal (Dheur et al., 2003).

2.5 The Glc7-binding motif of Ref2 is required for calcium tolerance and calcineurin pathway activation

As previously done in section 2.2, we considered it necessary to test whether or not the calcium-related phenotypes, derived from the absence of Ref2, could be explained by its role as a non-essential putative Glc7-regulatory subunit.

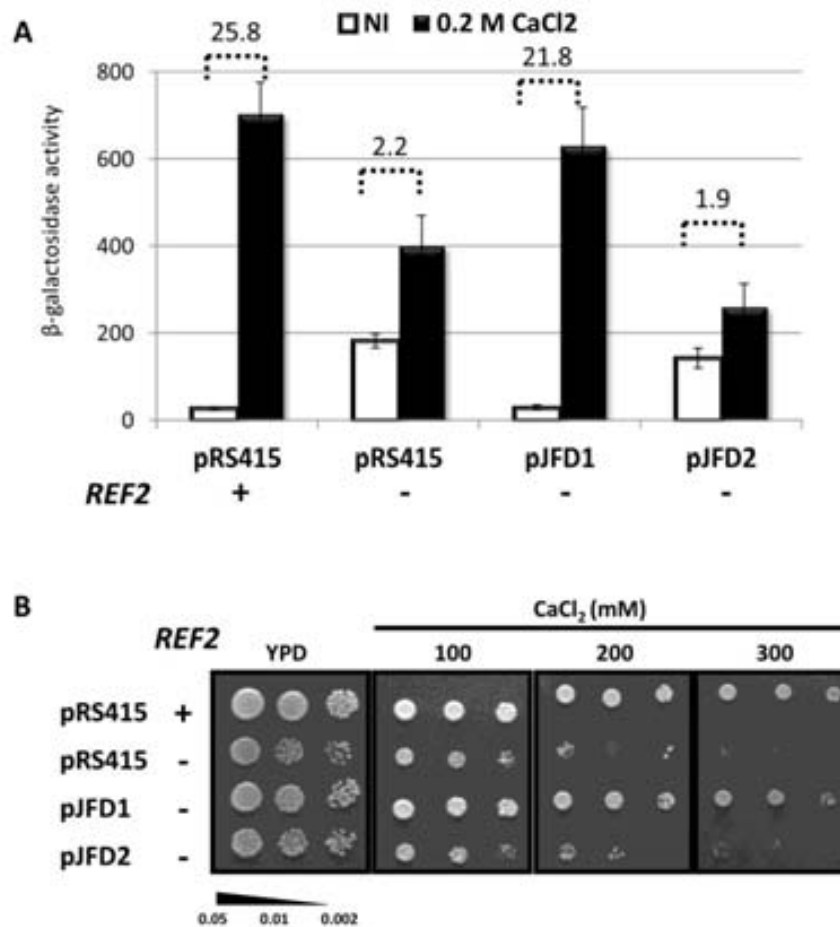


Figure 27. Mutation of Phe-374 within the Glc7-binding motif abolishes the function of Ref2 in calcium tolerance. **A)** BY4741 wild-type and *ref2* strains were transformed with the empty plasmid pRS415 or the same plasmid harboring the wild-type Ref2 protein (pJFD1) or the Phe-374 mutated version (pJFD2). Yeast strains were transformed with plasmid pAMS366, which contains a tandem of four CDREs, and incubated for 1 h in the absence or presence of 0.2 M CaCl₂. β -galactosidase activity was measured as described in *Experimental procedures*. Data are mean \pm SEM from 9 independent transformants. **B)** BY4741 wild-type and *ref2* strains were transformed with the empty plasmid pRS415 or the same plasmid harboring the wild-type Ref2 protein (pJFD1) or the Phe-374 mutated version (pJFD2). Three dilutions of transformants were spotted on plates containing a rank of calcium concentrations and growth was monitored after 3-4 days.

To test our hypothesis, we transformed *ref2* strain with the plasmid harbouring a *REF2* wild-type version (pJFD1) and another plasmid harbouring a *REF2*^{F374A} allele (pJFD2) plus

pAMS366, which contains the CDRE element fused to *lacZ* gene. As shown in *Figure 27A*, the high basal transcription rate of the calcineurin-dependent response elements (CDRE) in *ref2* cells is due to the inability to bind Glc7 because both *ref2* and *REF2^{F374A}* strains have a hyperactivated calcineurin in non-induced conditions. Moreover, it also shows that, meanwhile wild-type strain can induce CDRE around twenty times under calcium stress conditions, *ref2* strains can only induce 2 folds the calcineurin-dependent response element; which may not be enough to adapt to environmental conditions and growth properly. Additionally, as expected *Figure 27B* also shows that *REF2^{F374A}* allele is hypersensitive to calcium.

Although it has been described that *glc7-109* allele in the original background (KT1935) displays no hypersensitivity to calcium cations (T Williams-Hart et al., 2002), we decided to test in our background. As shown in *Figure 28B*, the *glc7-109* strain (YJFD36) shows minor calcium hypersensitivity which aggravates when Ref2 is deleted (YJFD39). This situation may be explained because *ref2* mutant cells carrying the *glc-109* allele (YJFD39) displays a constitutive activation of CDREs (*Figure 28A*) and an altered vacuolar morphology which possibly increases the cytoplasmatic calcium levels (*Figure 27C*). This situation claims that Ref2 might be a Glc7-regulatory subunit implicated in calcium homeostasis, but not the only one. It is important to remark that we used two new strains, which carry a centromeric plasmid borne *glc7-109* allele as the only source of *GLC7* function, the difference between YJFD17 and YJFD18 to YJFD36 and YJFD39 is the plasmid marker which can be *URA3* or *LEU2*, respectively.

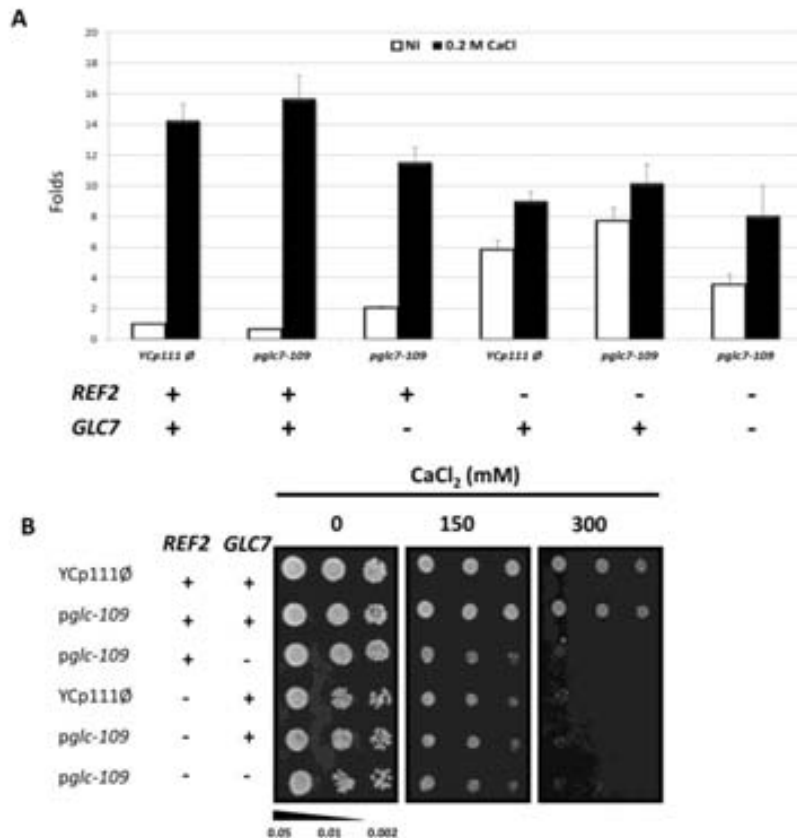


Figure 28. The lack of Ref2 increases the calcium hypersensitivity of a Glc7 allele unable to interact with its regulatory subunits (*glc7-109*). To generate the strains, a deletion cassette for *GLC7* and a plasmid YCp111 harbouring the *glc7-109* allele (pJFD11) were cotransformed in BY4741 wild-type (YJFD36) and *ref2* mutant (YJFD39). **A**) Yeast strains were transformed with plasmid pAMS366, which contains a tandem of four CDREs, and incubated for 1 h in the absence (white bars) or presence of 0.2 M CaCl₂ (black bars). β -galactosidase activity was measured as described in *Experimental procedures*. Data are mean \pm SEM from 9 independent transformants. Folds were calculated dividing each sample to wild-type strain in non-induced conditions. **B**) Three dilutions of transformants were spotted on plates containing a rank of calcium concentrations and growth was monitored after 3-4 days.

2.6 Mutants in components of the APT complex do not share the cation-related phenotypes of the *ref2* strain

Ref2 and Glc7 are components of the APT complex and they are required for efficient 3'-processing of mRNAs and transcription termination of certain snoRNA genes (Dheur et al., 2003; Nedeia et al., 2003, 2008; Russnak et al., 1995). Therefore it would be reasonable to speculate that the cation-related phenotypes of the *ref2* mutant could be caused by malfunction of this complex, which is itself a component of the holo-CPF. We reasoned that, if this was the case, mutations in other components of the complex would yield phenotypes reminiscent of those of the *ref2* strain. As many members of the APT complex are essential (including Pta1), we had to resort in most cases to temperature sensitive mutants cultured at sublethal temperatures. *Figure 29A* shows that deletion of *SYC1*, encoding a non-essential

member of the complex, does not alter cell growth under conditions that clearly affect proliferation of *ref2* mutants. The *yth1-1* mutant displayed a slight sensitivity to LiCl, but was indistinguishable from the wild-type in its sensitivity to NaCl and alkaline pH. The *swd2-3* and *ssu72-2* strains did not show any sensitivity to LiCl or NaCl and only a marginal sensitivity to high pH. None of these strains displayed sensitivity to high calcium levels in the medium. Similarly, a temperature-sensitive strain lacking the N-terminal region of Pta1 (strain *pta1Δ1-75*) exhibited a near wild-type tolerance to cations or alkaline pH even at 37°C. None of the tested APT complex mutants were sensitive to low-glucose or non-fermentable carbon sources (data not shown). We also observed sensitivity to formamide in the *yth1-1* strain when grown at 30°C as reported previously (Barabino et al., 1997). Interestingly, we observed a similar phenotype in the *swd2-3* mutant at 30°C and the *ref2* or *pta1Δ1-75* strains at 37°C, clearly showing that under these conditions the function of the APT complex is compromised. The almost complete lack of overlap between specific *ref2* phenotypes and those of the other mutants in components of the APT complex is exemplified in the phenotypic array shown in Figure 29B.

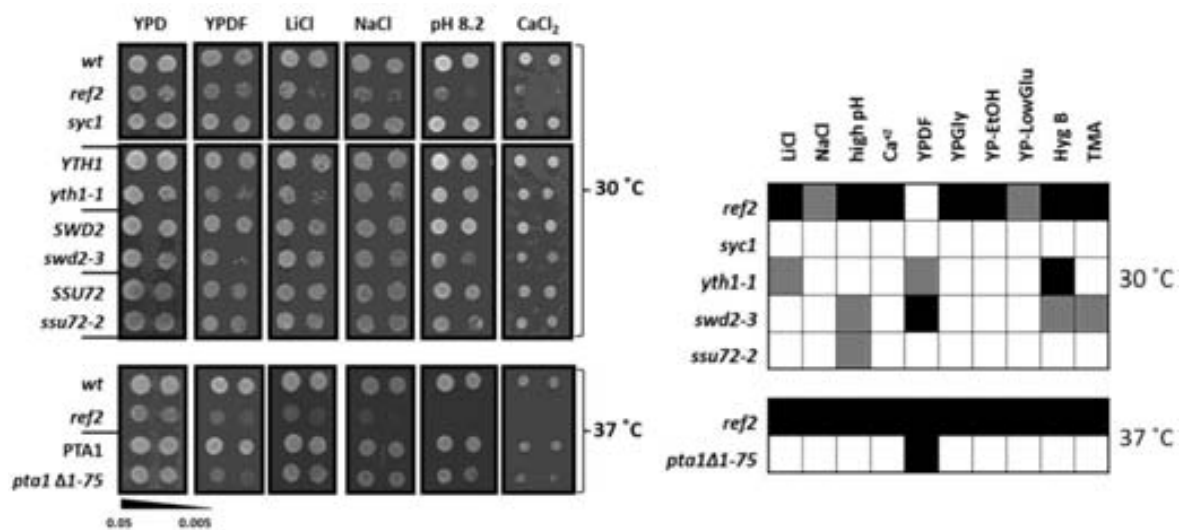


Figure 29. Comparison of *ref2* phenotypes with those of diverse APT-related mutants. **A)** Three dilutions of the strains indicated to the left of the panel were spotted on to plates and grown at the temperatures indicated to the right of the panel for 3 days. Conditions used were: **YPDF**, YPD plus 3% formamide; **LiCl**, 100 mM LiCl (30°C) or 150 LiCl mM (37°C); **NaCl**, 800 mM NaCl; **pH 8.2**; **CaCl₂**, 200 mM CaCl₂. **B)** Phenotypic array comparing multiple *ref2* phenotypes with those of other APT-related mutants. Growth of each mutant was compared with that of the corresponding wild-type strain grown under the same set of conditions. Black squares denote strong sensitivity, grey squares indicate a mild phenotype and white squares correspond with wild-type behaviour. Conditions tested to construct the array were: **LiCl**, 50–200 mM LiCl; **NaCl**, 0.4–1.2 M NaCl; **high pH**, pH 8.0–8.3; **Ca²⁺**, 100–300 mM CaCl₂, **YPDF**, YPD plus 3% formamide; **YPGly**, YP plus 2% glycerol; **YP-EtOH**, YP plus 2% ethanol; **YP-LowGlu**, YP plus 0.05% glucose; **Hyg B**, 20–60 µg/ml hygromycin B; **TMA**, 0.2–0.6 M TMA.

We also examined the basal expression level of *ENA1* in these strains and the ability of the *ENA1* promoter to be activated by salt stress. As shown in *Figure 30*, changes in expression levels induced by exposure to LiCl or NaCl were smaller in the *swd2-3* strain. However, the expression observed in the *syc1*, *ssu72-2* or *pta1 Δ 1-75* derivatives was virtually identical with that of their respective wild-type strains. Taken together, these results demonstrate that the mutation of diverse components of the APT complex does not mimic the cation-related phenotypes of the *ref2* strain.

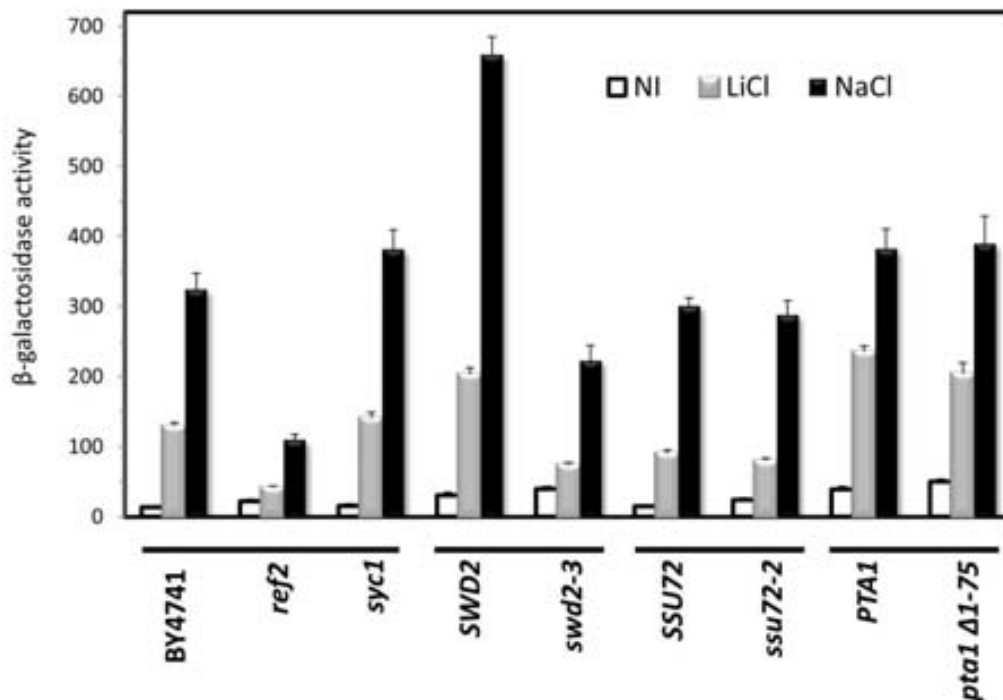


Figure 30. Expression of ENA1 under saline stress in diverse APT-related mutants. The indicated mutants and their corresponding wild-type strains (the bars show isogenic strains) were transformed with plasmid pKC201, carrying the entire *ENA1* ATPase gene promoter. Stress conditions were as in described in *Figure 25*, except that the growth temperature was 30°C for all strains but PTA1 and *pta1 Δ 1-75*, which were grown at 37°C. Results are means \pm SEM for 12 independent transformants.

Although none of the APT-related mutants were hypersensitive to calcium cations, we characterized their calcium response through CDRE. Surprisingly, except for *syc1* strain, APT-related mutant strains display an increased basal induction of CDRE (*Figure 31A*) and, when cells are stressed with high calcium extracellular concentrations, these strains can only respond by activating the CDRE around 2 folds, such as *ref2* strain (data not shown). Moreover, this situation might lead to a calcium hypersensitivity of APT-related mutant strains. For that, we analyzed the vacuole morphology, which is directly linked with cation homeostasis being one of the main cation accumulator organelle (P M Kane, 2006). As shown in *Figure 31B*, either *yth1-1* or *ssu72-2* or *swd2-3* display a class B *vma* phenotype (Raymond et al., 1992). This phenotype indicates a large number of small vacuolar compartments with a functional V-

ATPase onto the membranes of vacuoles; therefore it has been described that in some mutants, V-ATPase may show a partial defect. Despite hyperactivation of CDRE of APT-related mutant strains, these strains do not display a hypersensitive calcium phenotype because they are able to internalize calcium cations into vacuoles; meanwhile *ref2* cells may not decrease the intracellular calcium cations in the cytoplasm due to a dysfunctional vacuole.

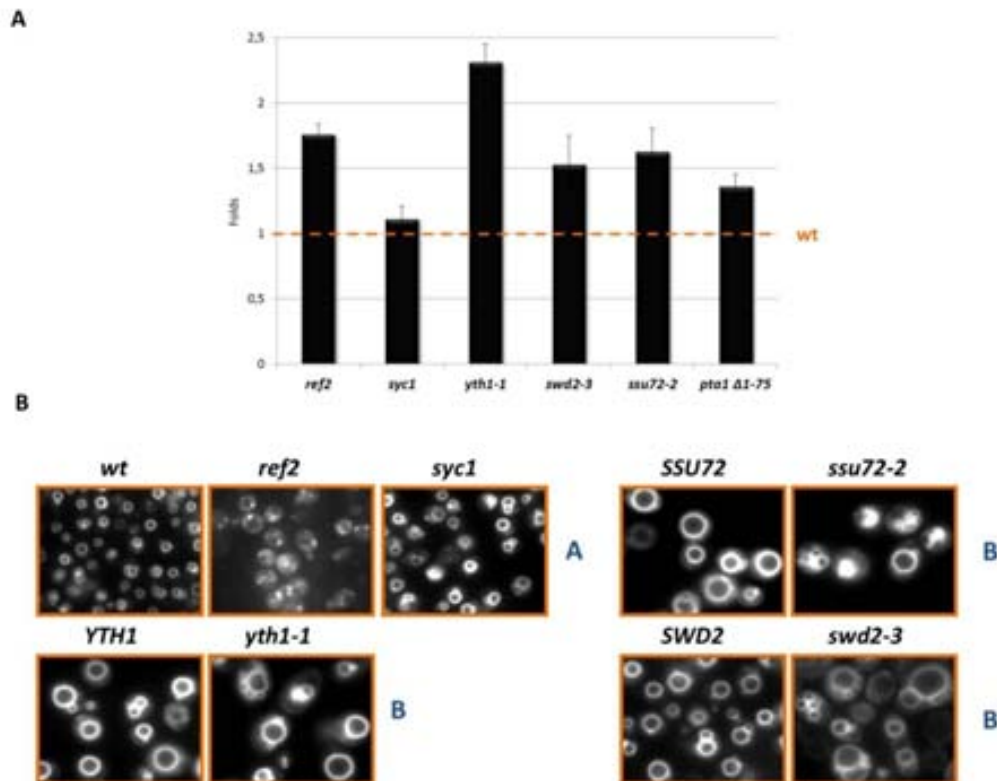


Figure 31. APT-related mutants display a hyperactive calcineurin-dependent response element in basal conditions. A) APT-related mutants were transformed with pAMS366 (*CDRE-lacZ*) and cultures were grown until OD_{660} 0.8 in YPD (pH 5.5) at their semi-permissive temperatures. β -galactosidase activity was measured as described in *Experimental procedures*. Data are mean \pm SEM from twelve independent transformants. Folds were calculated dividing each sample to wild-type strain in non-induced conditions. **B)** Vacuolar staining of APT-related mutant strains with the fluorescent dye FM4-64 was performed as described in the Experimental section for 30 min and monitored by fluorescence microscopy. Color blue indicates the vacuole class (Patricia M Kane, 2006).

However, our results show that deletion or temperature-sensitive mutations of diverse components of the APT complex, tested under conditions that impair their function in the complex (Dichtl et al., 2002, 2004; Ghazy et al., 2009), do not consistently mimic the growth defects or impaired *ENA1* expression of the *ref2* strain (*Figure 29* and *Figure 30*). The same situation is observed for the conditional mutation of *YTH1*, whose product participates in polyadenylation factor I, a different subcomplex of the CPF (Barabino et al., 1997). Furthermore, we also observe that, whereas the *ref2* strain fails to grow on non-fermentable

carbon sources and grows poorly on low-glucose medium, none of the APT-related mutations tested display such phenotypes (*Figure 29*), thus providing an additional example of disparate phenotypes. On the other hand, Ref2 function has been implicated in COMPASS/Set1 complex function via the Swd2 protein (Nedea et al., 2003). The function of Swd2 in this complex has been shown to be independent from its role in the APT complex (Dichtl et al., 2004). The COMPASS/Set1 complex is required for histone H3 methylation at Lys-4, which is a fingerprint of actively transcribed genes (Shilatifard, 2008). Therefore defective COMPASS function could be invoked to explain the effect of the *ref2* mutation on *ENA1* expression. However, this seems to be unlikely as **i)** either (Giaever et al., 2002) or our own results (data not shown) indicate that mutants in the non-essential components of the complex do not display salt-related phenotypes nor are they sensitive to organic toxic cations; **ii)** no evidence for a role of Glc7 on COMPASS function has been reported so far; and **iii)** deletion of *REF2* does not perturb histone H3 methylation at Lys-4 (H. Cheng, He, & Moore, 2004).

2.7 Analysis of the calcium homeostasis in *ref2* mutant

We have already shown that Ref2 mutant cells have higher intracellular calcium content than wild-type cells. Intracellular calcium could be of extracellular, ER or vacuole origin. As shown in *Figure 7*, there are specific calcium channels for the regulation of the calcium homeostasis. In order to know which calcium channel is affected in the *ref2* mutant cells we generate double mutants by combining the *ref2* mutation with mutation of several components of the calcium homeostasis. With these strains we analyze the sensitivities to high extracellular calcium concentration and the transcriptional response of the CDRE after induction by calcium.

Our analysis of calcium homeostasis in the generated mutants (*Figure 32*) shows that the mutation that rescues most of the calcium sensitivity of the *ref2* mutant cells, other than the *cnb1* used as a control, is the lack of Pmr1, an ATPase essential to maintaining the proper cytosolic calcium concentrations by pumping these ions from cytosol to the Golgi/ER. Lack of the Cch1 or Mid1, calcium plasma membrane channels required for Ca²⁺ influx to the cytosol, and lack of Vcx1 or Yvc1, vacuolar cation channels of opposite fluxes, also rescue the growth of *ref2* cells in the presence of extracellular calcium. Only the deletion of *PMR1* on *ref2* strain alleviates the lithium hypersensitivity of single *ref2* mutant cells (*Figure 32*).

The high basal transcriptional response of *ref2* mutant cells is alleviated when the Cch1 or Mid1 channels are absent. The lack of Vcx1 or Yvc1 vacuolar channels, however, does not alter the *ref2* response (Figure 33). It is worth to remark that lack of Pmr1 pump causes a basal transcriptional hyperactivation of the CDRE (that almost duplicate the levels of wild-type cells when stimulated with calcium). Lack of Ref2 in *pmr1* strain decreases this constitutive activity of the calcineurin pathway. Lack of Ref2 when cells were challenged with 200 mM extracellular calcium, decreases until one third the transcriptional response observed in wild-type cells under the same treatment. Similar responses were observed in *ref2 cch1*, *ref2 mid1* and *ref2 vcx1* double mutant cells when compared to channel single mutant cells. Lack of Ref2 in *yvc1* cells does not alter the calcium-induced response. Cells lacking Pmr1 do not respond to extracellular calcium probably due to the maximal level of activation in non-induced conditions. Additional mutation of *REF2* gene also decreases about 3 times this response. Some of those results could be only explained if indirect regulatory processes are considered. For example, high cytosolic calcium levels expected in *pmr1* mutant cells could be involved in the negative regulation of Cch1/Mid1 channels through the calcineurin phosphatase (Myriam Bonilla & Cunningham, 2003). Thus, Ref2 could interfere the function of the Golgi membrane ATPase ion pump Pmr1.

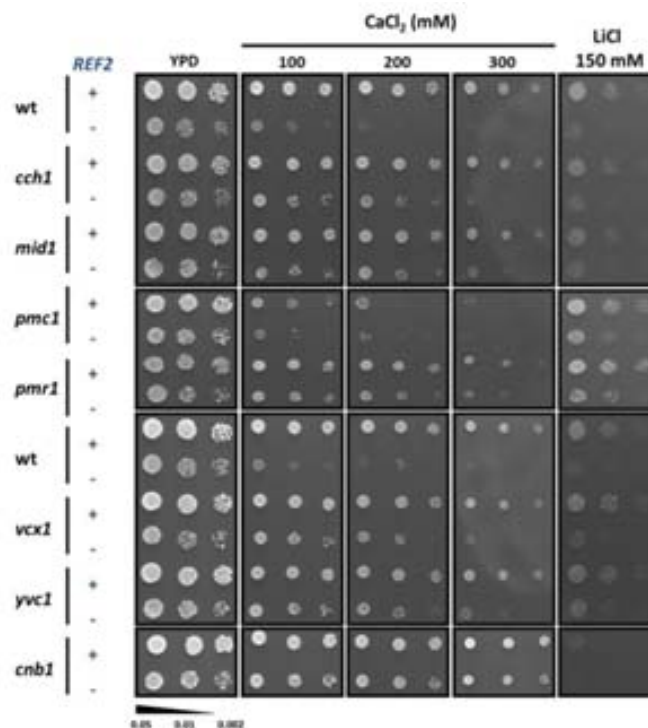


Figure 32. Analysis of the calcium homeostasis in *ref2* mutant. We combined the deletion of *REF2* with several components of the calcium homeostasis machinery. Using the generated strains, three μ l of the indicated dilutions of each strain were inoculated on YPD plates containing different concentrations of calcium (100-300 mM calcium) or 150 mM LiCl and growth was monitored after 2-4 days.

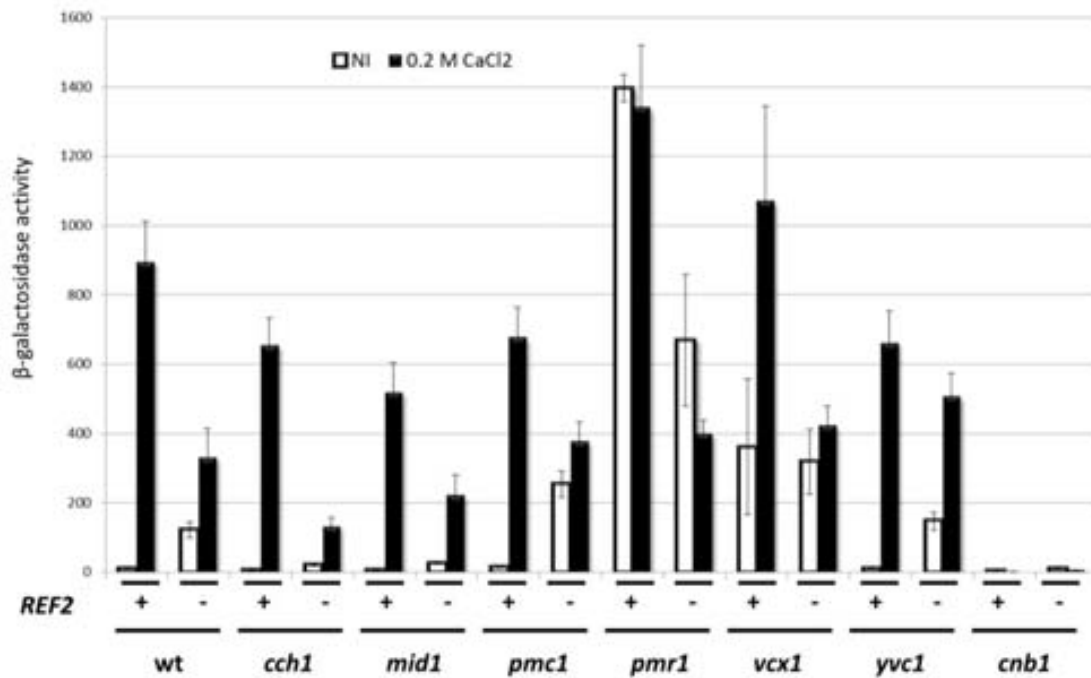


Figure 33. Analysis of the calcium homeostasis in *ref2* mutant. We combined the deletion of *REF2* with several components of the calcium homeostasis machinery. The generated strains were transformed with plasmid pAMS366 (*CDRE-lacZ*) and incubated for 1 h in the absence (white bars) or presence of 0.2 M CaCl₂ (black bars). β -galactosidase activity was measured as described in *Experimental procedures*. Data are mean \pm SEM from twelve independent transformants.

2.8 Sensitivity to cell wall stressors of mutants in components of calcium homeostasis

Our observation that *ref2* cells are calcium-sensitive is consistent with the multiple phenotypes shared with *pmr1* mutant cells, such as hypersensitivity to different cell wall stressors (Yadav, Muend, Zhang, & Rao, 2007). Two possible signals connecting the calcium signaling pathway to the CWI response were described: Slt2 and Rho1 (D E Levin, 2005; David E Levin, 2011). Firstly, the Mid1-Cch1 Ca²⁺ channel is activated by many of the same stresses that activate the Slt2 MAPK signaling pathway such as response to ER stress and hypo-osmotic shock to support cell wall biosynthesis (Myriam Bonilla & Cunningham, 2003; Garrett-Engele, Moilanen, & Cyert, 1995). Secondly, Rho1 may activate the Skn7 transcription factor involved in osmoregulation and oxidative stress (Roemer, Delaney, & Bussey, 1993). Skn7 makes an additional contribution to the maintenance of CWI by binding and stabilizing the Ca²⁺/calcineurin-activated transcription factor Crz1, which will induce, at least, the expression of *FKS2* and other cell wall-related genes (Garcia et al., 2004; Stathopoulos & Cyert, 1997a; C. Zhao et al., 1998b).

To study the possible connection between the high intracellular calcium concentration of the *ref2* mutant cells and the components of the CWI pathway, we have analyzed the sensitivities to cell wall stressors of component of the calcium homeostasis in the presence and in the absence of REF2.

We confirm the sensitivity to CWI stressors of *pmr1* cells. However, none of the mutants in components of the calcium homeostasis are sensitive to Calcofluor white and Congo red. *ref2 pmr1* double mutant cells show stronger CWI defect than *pmr1* cells (Figure 34). As expected *slt2* mutant cells are hypersensitive to those stressors, but cells lacking Ref2 are even more sensitive than *slt2* cells and display similar sensitivity that *slt2 ref2* double mutant cells (Figure 34).

These results prompt us to analyze the sensitivity to cell wall stressors of the mutants in the non-essential regulatory subunits of Glc7.

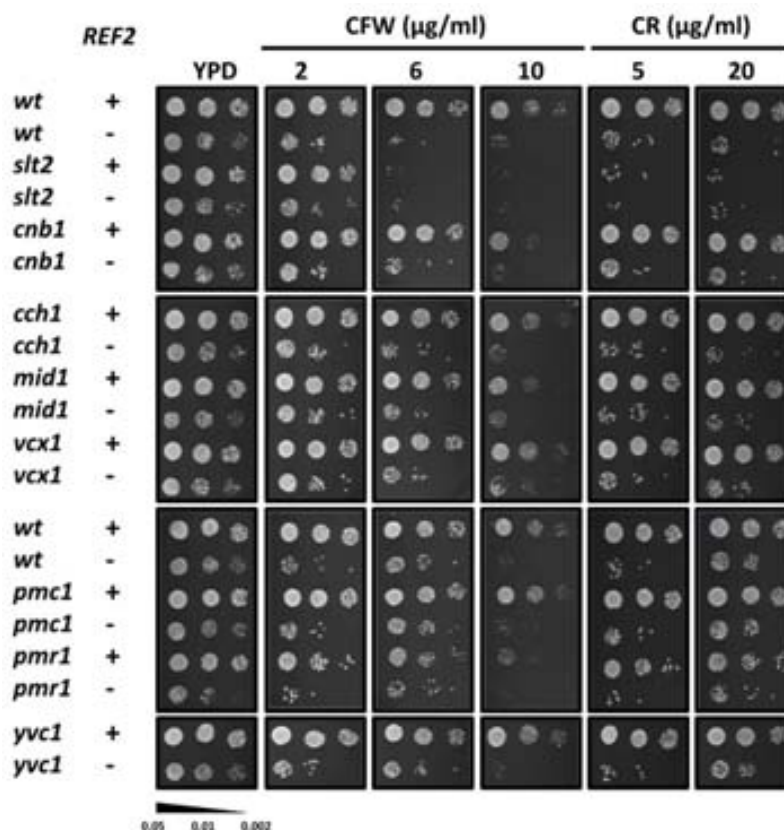


Figure 34. Analysis of the calcium homeostasis in *ref2* mutant under cell wall integrity stressors. We combined the deletion of *REF2* with several components of the calcium homeostasis machinery. Using the generated strains, dilutions of each strain were inoculated on YPD plates containing different concentrations of Calcofluor white (CFW) and Congo red (CR) and growth was monitored after 2-4 days.

2.9 Analysis of the sensitivities to cell wall stressors of Glc7-regulatory subunits

The fact that cells lacking Ref2 are sensitive to Calcofluor white and Congo red could indicate a role of Glc7 in the CWI pathway. Previous evidences established a functional link between Glc7 and the CWI response since the *glc7-10* thermosensitive allele concluding that dephosphorylation by Glc7 therefore functions positively to promote cell integrity, bud morphology and polarization of the actin cytoskeleton (Andrews & Stark, 2000). This possibility prompted us to examine tolerance to cell-wall stressors such as Calcofluor white, Congo red, caffeine and heat shock (37°C) in 21 strains carrying a deletion of functionally well-documented regulatory subunits of Glc7. *Figure 35* shows a selected panel of conditions for 18 strains; additionally, *red1*, *afr1* and *ysw1* strains have their phenotypes summarized in *Table 12*.

As shown in *Figure 35*, mutation of most regulatory subunits did not result in significantly altered phenotype to the indicated treatments, with the exception of the *ref2* and *shp1* mutants. This last mutant already displays a severe growth defect even in the absence of stress (Zhang et al., 1995). In contrast, lack of Ref2, which only caused a slight growth defect under standard culture conditions, prevented growth in the presence of Calcofluor white (CFW) and slightly in caffeine (Caf). *bni4* and *reg1* cells display tolerance to the chitin antagonist Calcofluor white, which was already described for *bni4* mutants in two global screenings (de Groot et al., 2001; Tong et al., 2004). Furthermore, *reg1* cells show hypersensitivity to caffeine (Dudley, Janse, Tanay, Shamir, & Church, 2005) which is an unusual cell wall stress agent. The mechanism by which it induces wall stress is not understood, but genome profiling suggests that the primary target may be the *TORC1* protein kinase complex and prevent Slt2 from associating with Swi4 thus blocking this part of the transcriptional program (Kuranda et al., 2006).

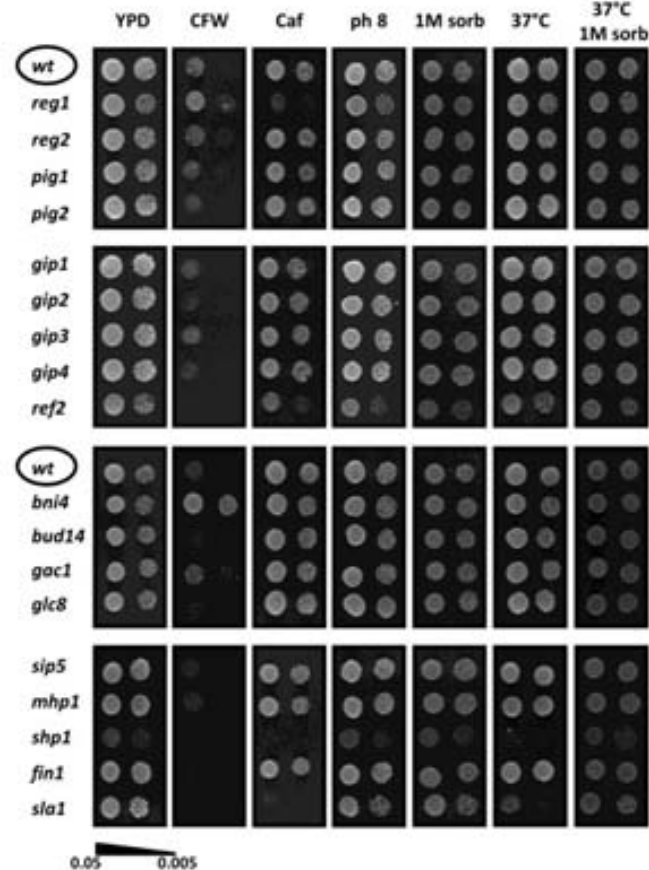


Figure 35. The sensitivity to CWI stressors of *ref2* mutant is only shared by *sla1* mutant. Three μ l of different dilutions of each BY4741 background strain were inoculated on YPD plates containing different cell wall integrity (CWI) stressors: 50 μ g/ml Calcofluor white (**CFW**), 7 mM caffeine (**Caf**), alkaline pH (**pH 8**) and 1 M sorbitol (**1 M Sorb**) and incubated at 30°C or 37°C as indicated for 2 - 3 days.

Moreover, the lack of *SLA1* causes hypersensitivity to cell-wall stressors such as Calcofluor white, caffeine or growth at 37°C (*Figure 35*). *Sla1* is crucial for NPFXD-mediated endocytosis which is required for the function of the CWI pathway sensor *Wsc1*, thus connecting endocytosis and CWI (Ragni et al., 2011). It plays a critical role in proper localization of two proteins, *Sla2* and the small GTP-binding protein *Rho1*, and in the spatial control of cell wall biosynthesis, basically maintaining daughter yeast cell wall polarity or integrity (Ayscough et al., 1999; Piao, Machado, & Payne, 2007). Finally, growth under cell wall stressors of *sla1* mutant may be restored when the osmotic stabilizer sorbitol is added into plates (D E Levin & Bartlett-Heubusch, 1992).

Despite the four non-essential *Glc7*-regulatory subunits which display interesting phenotypes, in this thesis we decided to further study the role of *Ref2* because *ref2* cells have the most aggravated phenotype under cell wall stressors and never has been directly involved in CWI pathway.

2.10 Ref2 is not involved in the activation of the CWI pathway

As *ref2* mutant shows hypersensitivity to several cell wall integrity stressors, we decided to evaluate the response of Slt2 MAP kinase pathway in the absence of Ref2 since this sensitivity could be consequence of a defect on Slt2 activation (as happens in *slt2* mutant cells) or caused by a constitutive activation of the pathway (a long-term cell wall damage response), as described for *ptc1* mutant cells (A. Gonzalez et al., 2006). In order to evaluate this response we transformed *ref2* cells with the two β -galactosidase reporters for the promoters of *SLT2* and *FKS2* genes, two of the well-known targets of the Rlm1 transcription factor.

Expression of *SLT2* is increased through Rlm1-dependent translocation to nucleus (U S Jung & Levin, 1999). Environmental stressors activate the canonical MAP kinase cascade and trigger the Rlm1 translocation to the nucleus and the transcriptional activation of a set of genes including *SLT2* (U S Jung & Levin, 1999; U S Jung, Sobering, Romeo, & Levin, 2002). As shown in *Figure 36A* the transcription of the *SLT2-lacZ* reporter is activated by Calcofluor white and Congo red in wild-type cells. Similar results were obtained for cells lacking Ref2, meaning that Ref2 does not affect transmission of the signal through phosphorylation of the MAP kinase module. As described, the response is hyperactivated *ptc1* mutant cells, even in the absence of stressors.

FKS2 transcription activation is dependent on Swi4/Swi6 (SBF) transcriptional factors but independent of Slt2 phosphorylation. Specifically, its activation is dependent of a non-catalytic mechanism of Slt2 or Mlp1 which drive gene expression in response to cell wall stress in a manner that is independent of the role of SBF in the G₁-specific transcription (K.-Y. Kim, Truman, & Levin, 2008). *Figure 36B* shows that *ref2* cells have similar transcriptional induction of *FKS2* than wild-type cells, which means that the non-catalytic mechanism of activation of CWI pathway is not compromised by the lack of Ref2. Lack of Swi4 or Swi6 causes an attenuated response (about 50% of the observed for wild-type cells).

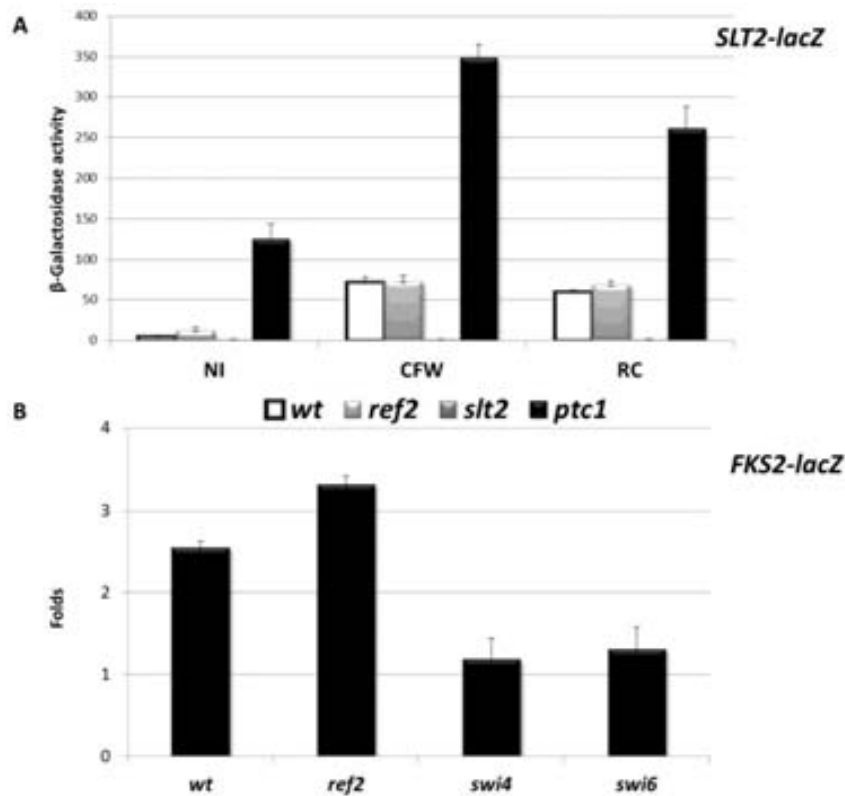


Figure 36. *ref2* cells show a wild-type induction of cell wall integrity pathway. **A)** The indicated yeast strains were transformed with plasmid p1365, which contains the promoter of *SLT2* driving the expression of the *lacZ* gene, and incubated for 2 h in the absence or presence of 40 $\mu\text{g/ml}$ Calcofluor white (**CFW**) and 40 $\mu\text{g/ml}$ Congo red (**CR**). β -galactosidase activity was measured as described in *Experimental procedures*. Data are mean \pm SEM from 9 independent transformants. **B)** Yeast strains were transformed with plasmid p2052, which contains the reporter for the *FKS2* promoter and incubated for 16 h at 39°C. β -galactosidase activity was measured as described in *Experimental procedures*. Folds were calculated as the ratio of 39°C /28°C β -galactosidase activities for each strain. Data are mean \pm SEM from 12 independent transformants.

2.11 The hypersensitivity to CWI stressors is shared by other components of the holo-CPF

Ref2 and Glc7 are components of the APT complex and they are required for efficient 3'-processing of mRNAs and transcription termination of certain snoRNA genes (Dheur et al., 2003; Nedeja et al., 2003, 2008; Rusznak et al., 1995). Therefore it would be reasonable to speculate that the CWI-related phenotypes of the *ref2* mutant could be caused by malfunction of this complex, which is itself a component of the holo-CPF. We reasoned that, if this was the case, mutations in other components of the complex would yield phenotypes reminiscent of those of the *ref2* strain. As many members of the APT complex are essential (including Pta1), we had to resort in most cases to temperature sensitive mutants cultured at sublethal temperatures.

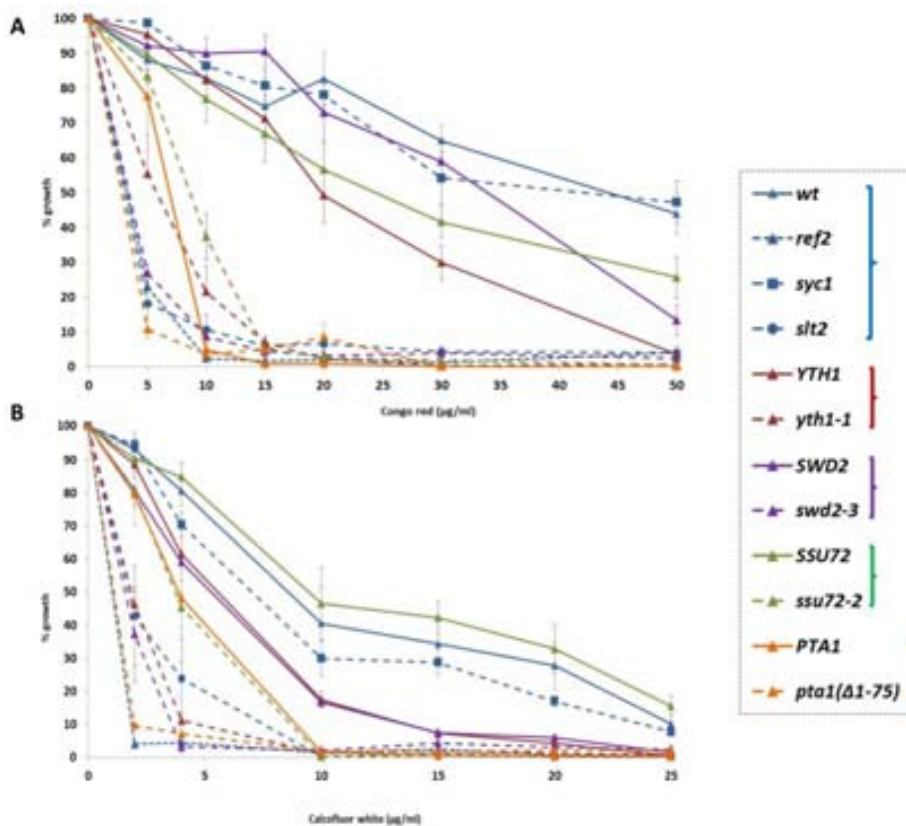


Figure 37. The analysis of different mutants for the subunits of the holo-CPF was performed using a liquid growth test which was initialized at OD_{660} 0.025 and an increasing rank of concentrations of Congo red (A) and Calcofluor white (B). Growth was monitored after 17-24 h. Plates were incubated at 30°C or 37°C, semi-permissive temperatures for the thermo-sensitive mutants used. Brackets have been used to group the wild-type strain (the first in each bracket) with its mutant derivatives, shown as discontinuous lines. Data are mean \pm SEM from 9 independent cultures.

Figure 37 shows that deletion of *SYC1*, encoding a non-essential member of the complex, does not alter cell growth under conditions that clearly affect proliferation of *ref2* (and *slt2*) mutants. It is worth to note that the *syc1* mutant in the BY4741 genetic background used always had a wild-type phenotype in all performed tests. Mutants in other components of the APT complex such as *swd2-3*, *yth1-1*, *ssu72-2* and *pta1(Δ1-75)* do display hypersensitivity to cell wall stressors when compared to its respective wild-type strains. As far as we know, these results indicated that there is an unexplored connection between the function of the APT complex and the sensitivity to cell wall stressors.

In order to know if the mutants in components of the APT complex have a constitutively active CWI pathway even in the absence of stressors, we decide to analyze the mRNA levels of the *CRH1* gene, whose transcriptional activation is controlled by Rlm1. As seen in *Figure 38* the analyzed mutants do not show elevated levels of *CRH1* mRNA in basal conditions, indicating that they do not display long-term cell wall damage. Additionally, APT-

related mutant strains shown a wild-type transcriptional response when the activation of the promoters of *SLT2*, *FKS2*, *MLP1* and *CRH1* was tested by using the *lacZ* reporter gene under cell wall stressors such as Calcofluor white and Congo red (data not show) was tested. Additionally, APT-complex mutants display wild-type activation by phosphorylation of Slt2 in response to cell wall stressors (data not shown). Finally, as shown in *Figure 44A*, the newly generated tetO₇::*REF2* strain, in which the expression of *REF2* is controlled by a doxycycline-regulatable promoter, also displays hypersensitivity to Calcofluor white when the expression of *REF2* is repressed. Thus, our results directly involve the Ref2 function as a component of the APT-complex to cell wall hypersensitivity phenotype.

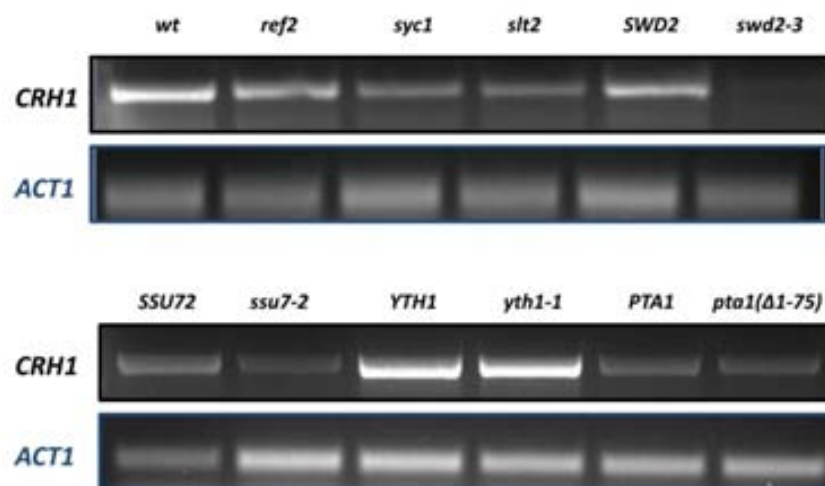


Figure 38. APT-related mutant strains does not show an induction of the transcriptional response driven by Rlm1. Semi-quantitative analysis of the *CRH1* expression levels was performed in yeast strains which were grown in YPD until exponential phase at semi-permissive temperatures, then RNA purification was made using RiboPure-Yeast kit (Ambion). Semi-quantitative RT-PCR was performed with *Ready-to-Go* RT-PCR Beads kit (Amersham) loading 50 ng of total RNA of each sample with 23 cycles of amplification and using specific primers to amplify *CRH1* and *ACT1*, which was used as a loading control.

Ref2 has been implicated in COMPASS/Set1 complex function via the Swd2 protein (Nedea et al., 2003). The COMPASS/Set1 complex is required for histone H3 methylation at Lys-4, which is a fingerprint of actively transcribed genes (Shilatifard, 2008). Therefore defective COMPASS function has been described to be involved in cell wall integrity regulation in the presence of heat shock stress. Specifically, loss of H2B ubiquitination and histone H3 methylation at Lys-4 are required for inhibiting the function of the Sir silencing complex associating with euchromatin genes important for the CWI and the response to heat shock, describing a possible function of Set1C in cell wall organization (Dehé & Géli, 2006; Leung et al., 2011). Although the function of Swd2 in this complex has been shown to be independent from its role in the APT-complex (Dichtl et al., 2004), it may not be in this specific case. So far,

from the eight components of COMPASS/Set1C (Swd1-3, Set1, Bre2, Shg1 and Spp1) only Swd2 has been related to the cell wall, since cells carrying the *swd2-3* allele are hypersensitive to cell wall stressors. Therefore, the APT-complex plays a role in the CWI maintenance, which is independent of the CWI pathway.

2.12 The Glc7-binding motif of Ref2 is required for CWI tolerance

As extensively explained in the *Introduction section 2.3.3*, Ref2 contains a RISSIKFLD sequence (residues 368–376) that closely matches the **(R/K)(V/I)X(F/W)** Glc7-binding consensus sequence. We considered it necessary to test whether the cell wall-related phenotypes, derived from the absence of Ref2, could be explained by its role as a Glc7-regulatory subunit or could be consequence of other Glc7-independent functions as a component of the APT-complex.

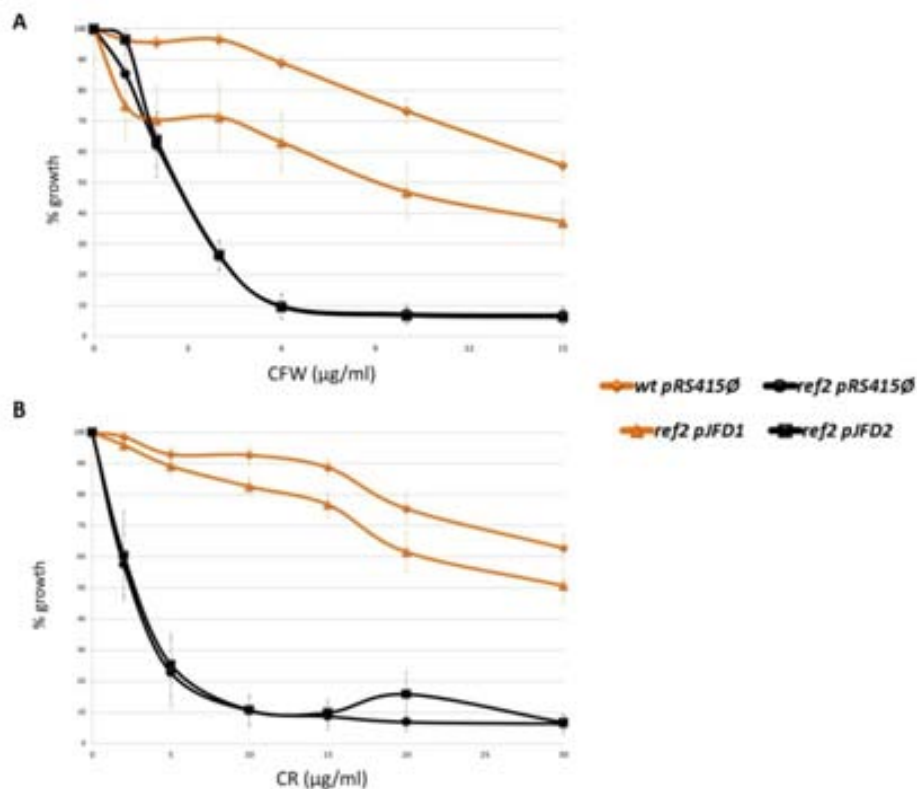


Figure 39. Mutation of Phe-374 within the Glc7-binding motif mimics the phenotypes of cells lacking Ref2. BY4741 wild-type and *ref2* strains were transformed with the empty plasmid pRS415 or the same plasmid harboring the wild-type Ref2 protein (**pJFD1**) or the Phe-374 mutated version (**pJFD2**). Liquid growth test was initialized at OD_{660} 0.01 using an increasing rank of concentrations of Calcofluor white (**A**) and Congo red (**B**). Growth was monitored for 17-24 h. Data are the mean \pm SEM from 12 independent cultures.

As explained in section 2.2, mutation of Phe-374 in Ref2 (pJFD2) avoids the binding of Glc7 to APT-complex (Nedeia et al., 2008). This point mutation causes cell wall hypersensitivity,

meaning that Glc7 has an important role in APT-complex in order to provide a wild-type growth under Calcofluor white or Congo red (Figure 39). Moreover, Figure 40 shows that Rlm1-dependent genes are correctly induced under cell wall stressors. However, lack of interaction between Ref2 and Glc7 does not alter the transcriptional response driven by the Rlm1 transcription factor in response to cell wall stressors (Figure 40).

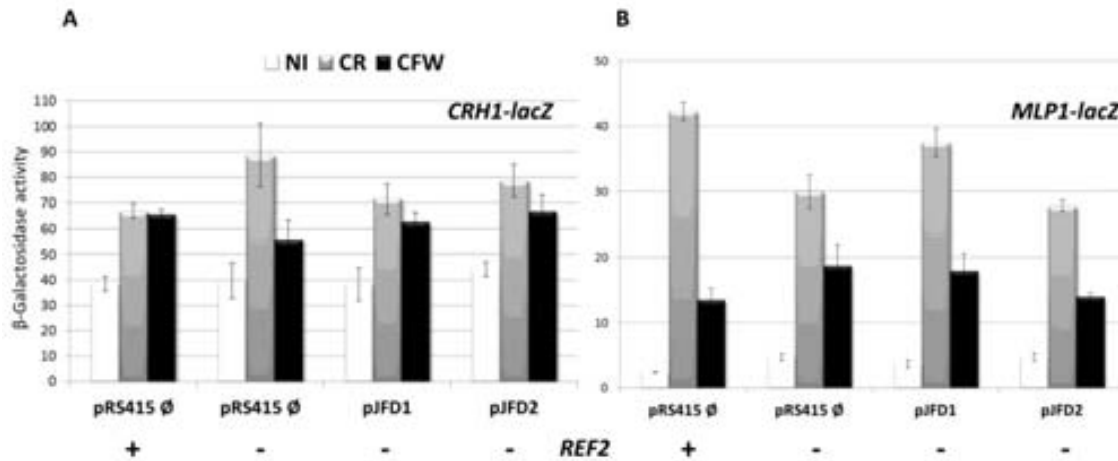


Figure 40. The Phe-374, within the Glc7-binding motif of Ref2, is not important for the transcriptional response driven by Rlm1. BY4741 wild-type and *ref2* strains were transformed with the empty plasmid pRS415 or the same plasmid harbouring the wild-type Ref2 protein (pJFD1) or the Phe-374 mutated version (pJFD2). **A)** Yeast strains were transformed with plasmid pLT12, which contains the promoter of *CRH1*, and incubated for 2 h in the absence or presence of 40 μ g/ml Calcofluor white (CFW) and 40 μ g/ml Congo red (CR). β -galactosidase activity was measured as described in *Experimental procedures*. Data are mean \pm SEM from 9 independent transformants. **B)** Yeast strains were transformed with plasmid p1365, which contains the promoter of *SLT2*, and incubated for 2 h in the absence or presence of 40 μ g/ml Calcofluor white (CFW) and 40 μ g/ml Congo red (CR). β -galactosidase activity was measured as described in *Experimental procedures*. Data are mean \pm SEM from 9 independent transformants.

Although it has not been described that *glc7-109* allele in the original background (KT1935) displays hypersensitivity to cell wall integrity stressors (T Williams-Hart et al., 2002), we decided to test in our background. Additionally, *glc7-10* allele has already been described its hypersensitivity to cell wall stressors (Andrews & Stark, 2000). Moreover, (Casagrande et al., 2009) reported that the cesium-specific response mediated by Yaf9, that counteracts the efficiency of the HOG pathway, involves the cell wall integrity (CWI) pathway, which is activated by low concentration of cesium chloride. *glc7-109* alleles and *ref2* strain are hypersensitive to cesium chloride. Adaptation to cesium requires a reshuffling of the cell wall structure (Bianchi et al., 2004). As shown in Figure 28 and Figure 41, the *glc7-109* strain (YJFD36) shows either Calcofluor white or Congo red hypersensitivity which aggravates when *REF2* is deleted (YJFD39).

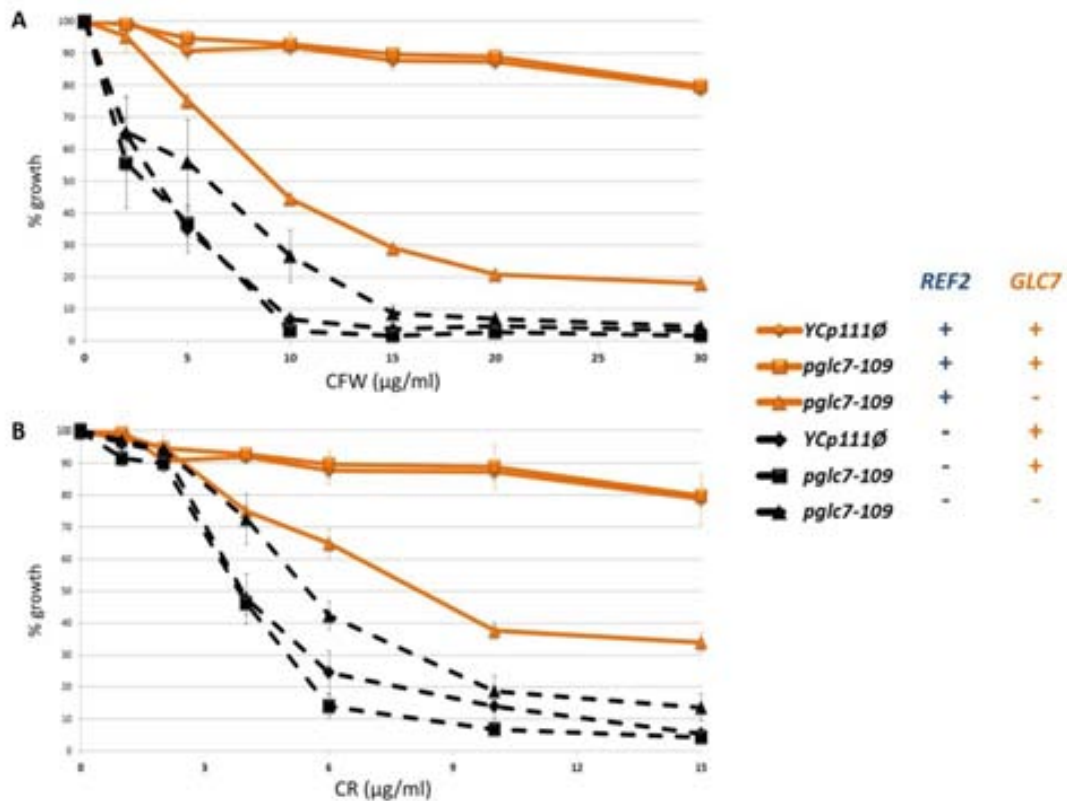


Figure 41. The lack of Ref2 aggravates the CWI stressors hypersensitivity of a Glc7 allele unable to interact with its regulatory subunits (*glc7-109*). To generate the strains, a deletion cassette for *GLC7* and a plasmid YCplac111 harbouring the *glc7-109* allele (*pglc7-109*, pJFD11) were cotransformed in BY4741 wild-type (YJFD36) and *ref2* mutant (YJFD39). Liquid growth test was initialized at OD₆₆₀ 0.01 using an increasing rank of concentrations of Calcofluor white (A) and Congo red (B), respectively. Growth was monitored for 17-24 h. Data is mean ± SEM from 12 independent cultures.

Glc7 has a role in APT-complex through binding Ref2 (Nedeja et al., 2003, 2008). However, no evidence for a role of Glc7 on COMPASS function has been reported so far; and deletion of *REF2* does not perturb histone H3 methylation at Lys-4 (H. Cheng et al., 2004). For that, we hypothesize that APT-complex is necessary for regulating cell wall integrity (CWI). Additionally, Ref2 function basically is kept Glc7 in APT-complex to maintain the functionality either of the mRNA processing or snoRNA maturation. Finally, this additive and synergistic effect between CWI components and APT-complex may indicate that the substrates which cause these sensitivity phenotypes are likely to be different.

2.13 Analysis of the CWI pathway in *ref2* mutant cells

We have already shown that *ref2* mutant cells have hypersensitivity to CWI stressors such as Calcofluor white, Congo red, caffeine and alkaline pH. As shown in *Figure 8*, the CWI is a complex pathway involving the MAPK module, several transcription factors and specific

protein phosphatase. In order to know if there is any defect in CWI pathway in the *ref2* mutant cells we generate double mutants by combining the *ref2* mutation with mutation of several components of the CWI. With these strains we analyze the sensitivities to CWI stressors such as Calcofluor white and Congo red (*Figure 42*). It is important to remark that deletion of *REF2* in *swi4* mutant cells has been impossible, possibly indicating a synthetic lethality between these genes.

Figure 42 confirms that cells lacking of *SLT2*, *SWI4* or *RLM1* display hypersensitivity to cell-wall stressors. As expected, single *mkk1* or *mkk2* mutant cells display a wild-type phenotype due to its redundant function in CWI pathway. The single mutants in the transcriptional factors *RLM1* or *SWI4* also displays hypersensitivity to CWI stressors; whereas the lack of *SWI6* does not display any differential phenotype than wild-type cells at all. Basically, our analysis demonstrates that deletion of *REF2* aggravates all the phenotypes of CWI components. This situation might imply that Ref2 is not involved in directly regulating cell wall integrity response by dephosphorylation. Even so, the lack of *REF2* is deleterious for yeasts cells under cell wall stressors possibly because there is a dysfunction on the APT-complex. However, no relation between either snoRNA processing or mRNA maturation, which are the main roles for APT-complex, and CWI has been described yet.

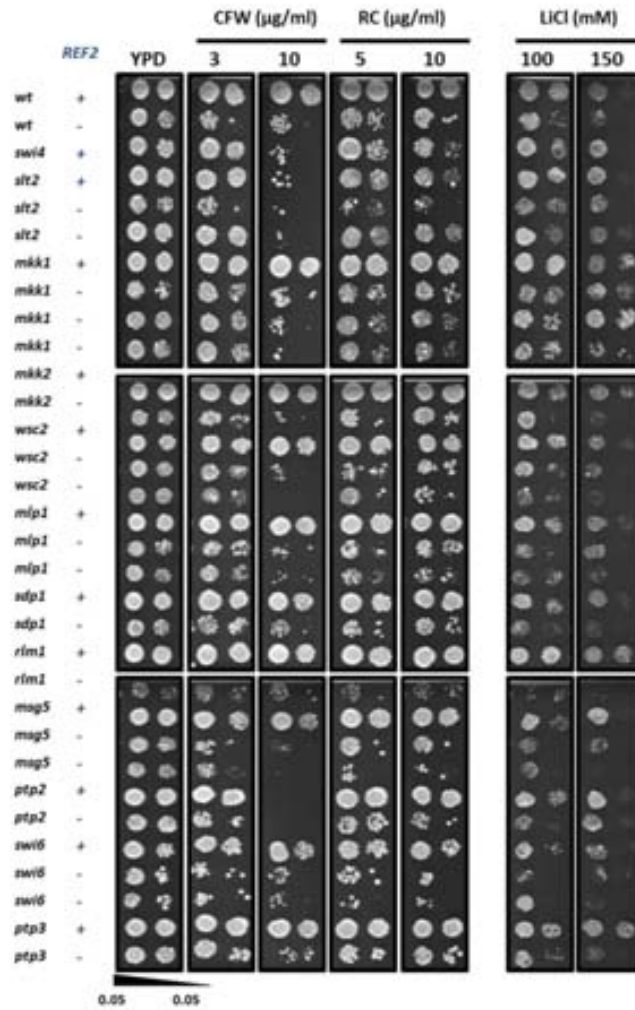


Figure 42. Analysis of the CWI pathway in *ref2* mutant. We combined the deletion of *REF2* with several components of the cell wall integrity response machinery. Using the generated strains, three μl of different dilutions of each strain were inoculated on YPD plates containing different concentrations of Calcofluor white (**CFW**), Congo red (**CR**) and Lithium (**LiCl**) and growth was monitored after 2-4 days.

Finally, in this thesis, the deletion of *SLT2* in *ref2* mutant cells causes sensitivity to UPR stressors, abolishing the tolerant phenotype shown by *ref2* mutant cells (Figure 67). That means that the substrates of CWI and APT-complex are likely different causing an additive phenotype.

2.14 Conclusions

4. The results of the present study demonstrate that the role of Ref2 on cation tolerance is not attributable to its function in regulating Glc7 in the CPF complex but, instead, it suggests that Ref2 must direct Glc7 to alternative target(s); therefore Ref2 would represent a novel example of multifunctional Glc7-regulatory subunits.
5. Our results demonstrate a possible positive relation between Pmr1 and Ref2. The lack of *PMR1* in *ref2* mutant cells alleviates its phenotype in calcium and lithium, so cation homeostasis may be somehow related to the entry of cations in the endoplasmic reticulum.
6. APT-complex is needed to cell wall integrity response. Deletion of *REF2* in mutants of CWI causes an additive and synergistic phenotype to cell wall stressors, therefore these data indicate that the hypersensitivity of APT-complex is due to different substrates than a malfunctioning of CWI components.

3. Study of aneuploidy in *ref2* mutant cells

The transcriptional analysis of mutants on non-essential Glc7-regulatory subunits was performed comparing the wild-type strain to each mutant in exponential growth in YPD (pH 5.5). Therefore, the initial analysis of *ref2* cells displayed 266 induced genes (expression value > 1.80 folds). Imposing an arbitrary criterion such as a P-value of less than 10^{-4} was not able to determine any specific functional group using MIPS. Simply, the function highlighted the chitin anabolism ($p\text{-value} = 3.53 \cdot 10^{-3}$) as the most representative group. On the other hand, the same analysis was performed with 135 repressed genes (expression value < 0.55 folds), three different functional categories were determined such as cell rescue, stress response and amino acid metabolisms ($p\text{-value} = 1.09 \cdot 10^{-3}$; $2.55 \cdot 10^{-3}$ and $4.90 \cdot 10^{-3}$ respectively). The high P-value in both induced and repressed genes can be stated that the analysis of the data do not provide any functional category which stands out above the others which could help on *ref2* cells study.

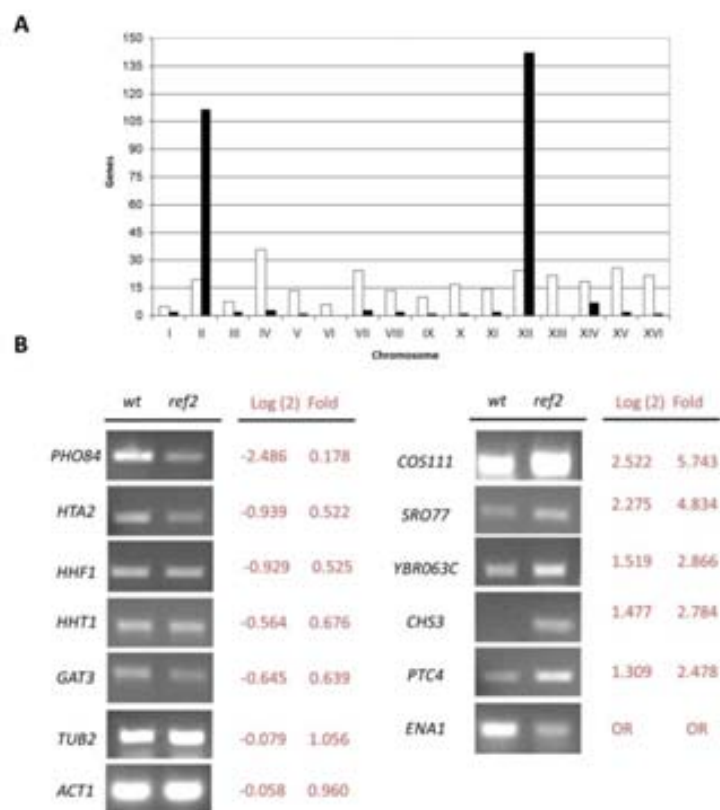


Figure 43. Gene copy-number analysis determines the aneuploidy on chromosome II and XII. A) Distribution of induced genes through chromosomes of *ref2* cells (black bars) and theoretical distribution due to chromosome size of induced genes in *ref2* cells (white bars). **B)** Representative data from semi-quantitative RT-PCR compared with the DNA microarray values, where OR means out of range.

As explained above, *ref2* cells displayed an aneuploidy in chromosome II and XII. In *Figure 43A*, genes were classified into the 16 chromosomes of yeast genome. The 90% of total induced genes (266 genes) are distributed between chromosome II (105 genes, 39%) to chromosome XII (136 genes, 51%). As shown in *Figure 43A*, chromosomes II and XII are 5.72 and 5.76 folds more induced, respectively, than induced genes statically expected. From these data, it can be drawn two possible situations: **1)** genes in chromosomes II and XII are induced in *ref2* mutant or **2)** there is no induction of genes located in chromosomes II and XII in *ref2* mutant, but a general repression of the whole genes compared to wild-type strain, and this effect is due to the normalization of DNA microarray data.

To validate the data from DNA microarrays, we analyzed the expression of groups of genes using semi-quantitative RT-PCRs which are not affected by normalization data from : **a)** genes that are induced in chromosome II and XII; **b)** genes that are repressed in other chromosomes and **c)** genes that maintain levels comparable to wild-type strain (*Figure 43B*). These semi-quantitative RT-PCRs allowed us to determine that the genes of chromosomes II and XII are mainly induced. Furthermore, these data could suggest a chromosomal gene deregulation defects. Considering, however, that such a phenomenon has ever been described so far, we hypothesize the presence of chromosomal duplications.

As described in the *Introduction, section 4*, aneuploid strains have multiple phenotypes which may be common among aneuploid yeast strains. So, we decided to realize an exhaustive characterization of *ref2* cells using different approaches.

3.1 CML476 tetO₇:REF2 does not show any aneuploidy

Our first approach was to generate a strain where *REF2* expression could be switch off using doxycycline. For that, we generated a strain using wild-type CML476 background where *REF2* is under the tetO-*off* expression system (Yen et al., 2003) named YJFD16.

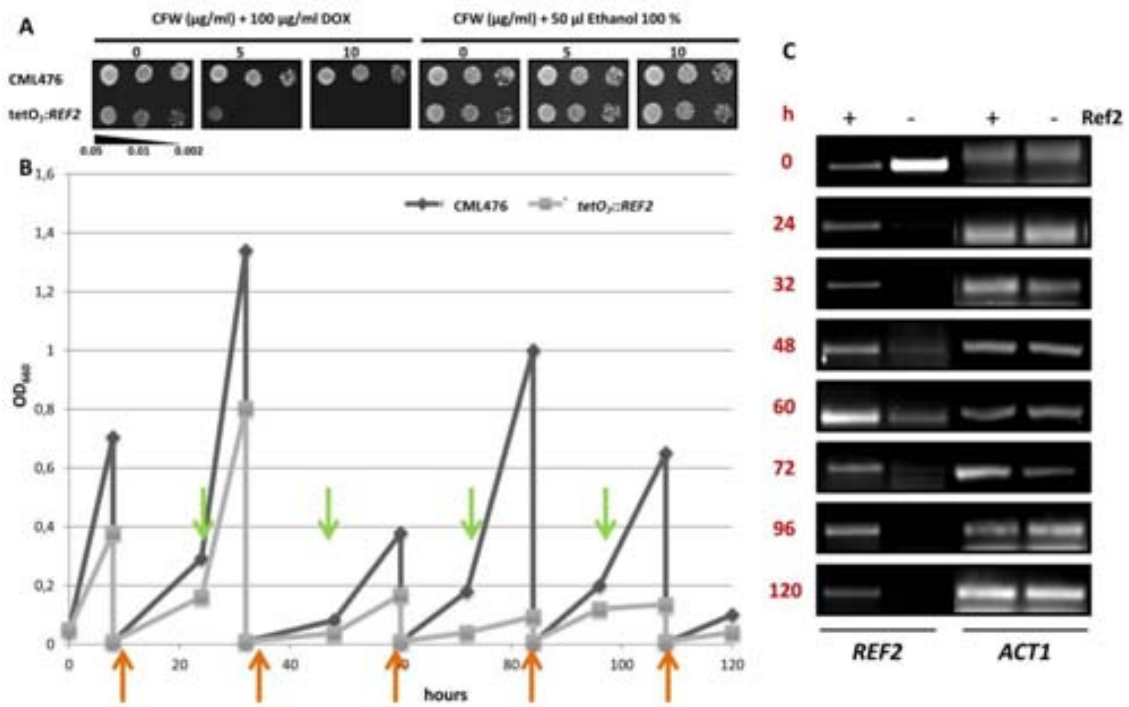


Figure 44. CML476 tetO₇:REF2 works properly inhibiting REF2 when doxycycline is added. A) Three dilutions from cultures of wild-type strain CML476 and its derivative tetO₇:REF2 were spotted on plates containing YPD plus calcofluor-white (CFW) with or without doxycycline as indicated. Growth at 28°C was monitored for 2-3 days. **B)** Monitored liquid growth of CML476 wild-type and its derivative tetO₇:REF2 strain in YPD was followed during 120 h at OD₆₆₀. Orange arrows indicated the addition of 100 $\mu\text{g/ml}$ doxycycline and cells were inoculated at 0.01 OD₆₆₀; green arrows indicated the addition of 100 $\mu\text{g/ml}$ doxycycline. **C)** Semi-quantitative RT-PCR of REF2 and ACT1 (used as a loading control) was performed in each sample treated with doxycycline (-) or untreated with doxycycline (+).

As shown in *Figure 44A-B*, tetO₇:REF2 strain works properly when 100 $\mu\text{g/ml}$ of doxycycline are added in YPD due to the fact that it phenotypically behaves as *ref2* cells either being hypersensitive to cell wall stress (CFW) or growing lesser than wild-type strain in presence of doxycycline. So, we decided to go one step further which consisted on generating a pool of DNA microarray experiments at indicated times (8, 24, 32, 48, 72, 96, 120 h). Firstly, we checked that REF2 transcription is switched off in the new strain generated (YJFD16). As expected, REF2 transcription decreases even at 8h after addition doxycycline (Ref2 -) compared to a wild-type strain (Ref2 +) which is always transcribed, but there is always a residual REF2 transcription (*Figure 44C*). Interestingly, in basal conditions, tetO₇:REF2 strain has already a higher REF2 transcription than wild-type cells meaning that REF2 is hardly expressed in cells. Then, we basically analyzed the microarray data creating a graphic representing the mean of the 16 yeast chromosomes *Figure 45A*. our results do not show an aneuploidy such as found in *ref2* cells.

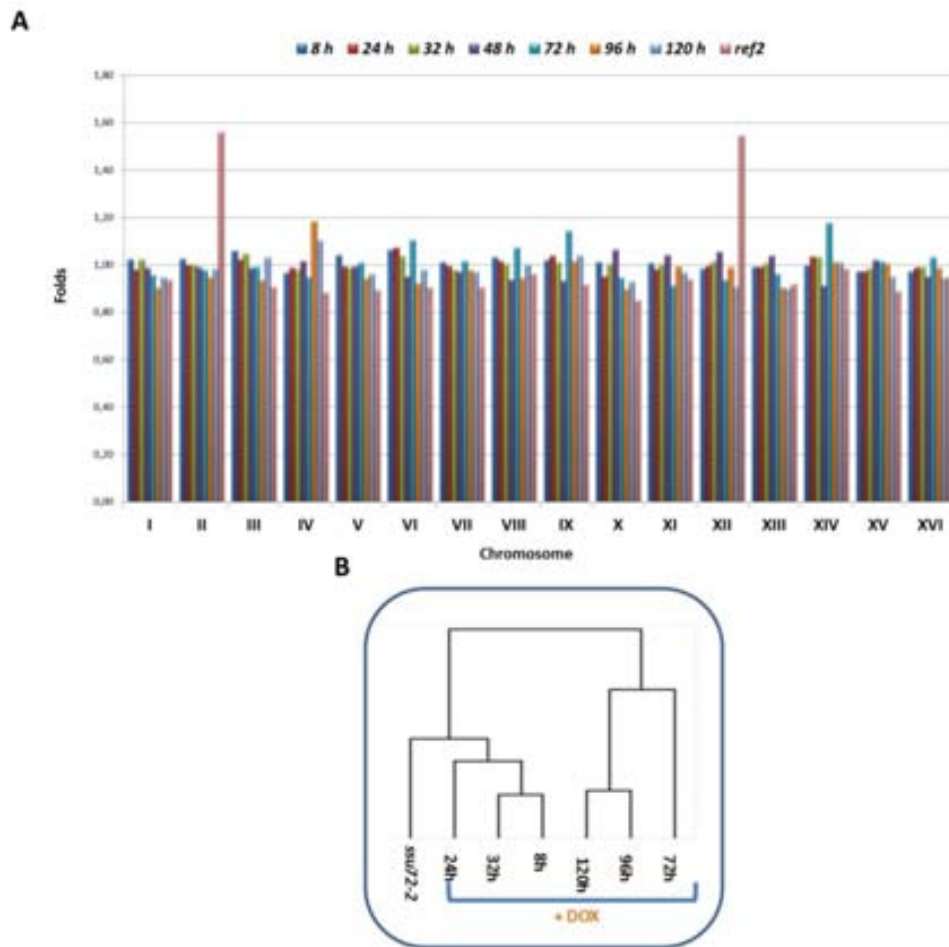
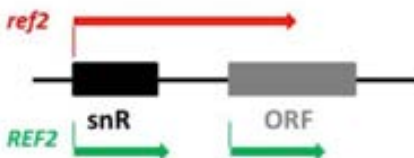


Figure 45. After 120 h, cells treated with doxycycline do not show any aneuploidy. A) Once analyzed the DNA microarray experiments, the mean of each chromosome was calculated in tetO₇:REF2 (8, 24, 32, 48, 72, 96 and 120 h) and *ref2* mutant from EUROSCARF and graphed in folds. **B)** DNA microarray data from indicated strains was analyzed with Cluster tool v2.11 from Eisen's lab software (Eisen et al., 1998). Hierarchical cluster was performed using array correlation parameter plus complete linkage clustering and data was represented by Treeview toll v1.6 from Eisen's lab software.

In *Figure 45B*, the tree-view correlation indicates two different responses from tetO₇:REF2: early and late responses. In the early response (8, 24 and 32 h), there are no characteristic functional category either in induced or repressed genes using a P-value lower than 10⁻⁵. Moreover, this response correlates with DNA microarray experiment of *ssu72-2* strain which has also no representative functional category. Finally, the late response has representative functional categories which are repeated in the three studied times. In induced genes, it is noticed that ion transport, glutamate metabolism plus transport facilities (ABC transporters) are the main characteristic functional categories. On the other hand, C-compound and carbohydrate transport are represented in repressed genes. Surprisingly, none of these functional categories is showed in *ref2* cells.

Over 95% of the nucleic acid in growing yeast cells is noncoding RNA which includes ribosomal RNA (rRNA), tRNA, spliceosomal RNA (snRNA), small nucleolar RNA (snoRNA, which specifically are the targeting components of enzymes that cleave methylate, or pseudouridylate ribosomal RNAs and are transcribed by RNA polymerase II (Pol II) (Kiss, 2002)), telomerase RNA, signal recognition particle RNA, the RNA components of RNase P and RNase MRP (which process tRNA and rRNA, respectively), and mitochondrial rRNA (Peng et al., 2003). Structurally snoRNA are classified in C/D or H/ACA type due to RNA component conserved sequence motif (Henras, Dez, & Henry, 2004). The main problem resides that those snoRNAs, which are mainly located within introns of protein coding or in polycistronic cluster, have their own promoter and termination sequences which implies maturation process for correct processing. Moreover, snoRNAs have a 5' cap, such as mRNAs, but mature transcripts are not polyadenylated (Nedea et al., 2008). It has already described that APT-complex subunits (Ssu72, Pta1, Pti1 and Ref2), Pol II subunits Rpb3 and Rpb11, Pol II-associated proteins such as components of the polymerase associated factor (PAF) complex and proteins that recognize the snoRNA termination signals (Nrd1-Nab3-Sen1) are necessary for forming the 3'-ends termination of many snoRNAs (Dheur et al., 2003; Fatica, Morlando, & Bozzoni, 2000; Morlando et al., 2002; Nedea et al., 2008; Steinmetz, Conrad, Brow, & Corden, 2001). It is important to note that transcriptional readthrough into vital downstream protein coding gene is detrimental for yeast cells (Steinmetz et al., 2001). Finally, snoRNAs are required for endonucleolytic cleavage steps in the processing to convert the primary rRNA transcript into the mature 18S, 5.8S, and 25S rRNA molecules (Piekna-Przybylska, Decatur, & Fournier, 2007; Venema & Tollervey, 1999). Moreover, it is unknown where the effects of APT-complex subunits on the expression of downstream genes were caused by transcriptional read-through or stabilization of the downstream RNA as a consequence of failure to cleave at the upstream cleavage signal.

GENE (snoRNA)	8h	24h	32h	48 h	72h	96 h	120 h	ref2
FLX1 (snR68)								
HEM4 (snR5)								
INO1 (snr128, snR190)	ND							ND
POL4 (snR33)								
POC4 (snR17b)								
SEN2 (snR79)								
SFT1 (snR87)	ND	ND	ND	ND		ND		
SMCS (snR50)								ND
UBX6 (snR60)	ND	ND		ND				
USE1 (snR82)								
YCRO15C (snR33)					ND			
YDRO42C (snR47)	ND						ND	ND
YJL107C (snR37)	ND	ND		ND	ND		ND	ND
YML057C-A (snR54)	ND	ND			ND	ND	ND	ND
YPR089W (snR41, snR50, snR71)		ND						
YPR091C (snR41, snR50, snR71)								
YPR092W (snR41, snR50, snR71)	ND				ND	ND	ND	ND
YPR150W (snR45)	ND	ND			ND	ND	ND	ND



Grey	> 0.8 (>1.75-fold)
Black	> 1.0 (>2.0-fold)
Orange	Induced in <i>ssu72</i> for Nedeia
Yellow	Induced in <i>ssu72-2</i> for us
Red	Induced in <i>ssu72</i> for Nedeia and us

Table 14. Distribution of snoRNA read-throughs due to the lack of REF2 transcription. Array of genes located downstream of snoRNA loci whose expression is increased more than 1.75-fold (grey) or 2.0-fold (black) by tetO₇:REF2 strain (8, 24, 32, 48, 72, 96 and 120 h) and *ref2* cells as a result of read-through. Colors indicate a comparison between different strains: *ssu72-2* data from (Nedeia et al., 2003) (orange); *ssu72-2* data from our experiment (yellow) and data from both strains (red).

As marked in Table 14, the lack of REF2 implies the deregulation of genes downstream snoRNAs due to read-throughs for possibly decoupling APT-complex components. *ref2* cells are unspecific for snoRNA type. That means that maturation and processing of snoRNA is general because gene read-throughs appear in both C/D snoRNA (snR68 and snR128) and H/ACA snoRNA (snR5). This result is not new, but our goal was to mimic *ref2* mutant and try to observe the appearance of the chromosome II and XII aneuploidy.

Finally, it has already been observed a role of Glc7 in the biogenesis of ribosome through snoRNAs maturation and processing needed for ribosomal RNA maturation done by APT-complex components such as Ref2, Pta1, Ssu72 and Pti1 (Nedeia et al., 2008; Peng et al., 2003). Glc7 has also shown to be required for release of Rna15 from poly(A) RNA together with displacing Nrd1 and Nab3 from snoRNAs by regulation Sen1's helicase activity (Gilbert & Guthrie, 2004; Nedeia et al., 2008).

3.2 New *ref2* mutant cells show *REF2* duplication itself.

As explained in the *Experimental procedures*, BY4741 wild-type strain was transformed with the disruption cassette *ref2::nat1* in order to generate new *ref2* strains. Surprisingly, those new mutants display a double band pattern in checking DNA agarose gel. As shown in *Figure 46A (right panel)*, colony PCR experiment with primers OJFD20, OJFD23 and *nat1-3'* should only describe two possible patterns: *REF2* deletion (700 bp) and *REF2* wild-type (220 bp). Using wild-type as a control where the only present DNA band is *REF2* (700 bp). We analyzed a set of possible mutants, where *ref2* cells showed a 220 bp, a vast majority of those mutants displayed a pattern of double DNA band (220 bp and 700 bp), meaning that these strains may have not only a wild-type copy of *REF2* but also the *ref2::nat1* cassette integrated in the same locus.

Moreover, to continue checking the new strains, we performed a liquid growth experiment in stress conditions where *ref2* cells are sensitive (*Figure 13*). Both wild-type and double DNA band strains (*Ref2/ref2*) have similar phenotypes at LiCl, NaCl and CaCl₂; meanwhile *ref2* strains display a hypersensitive phenotype to three cations as expected (*Figure 46B*).

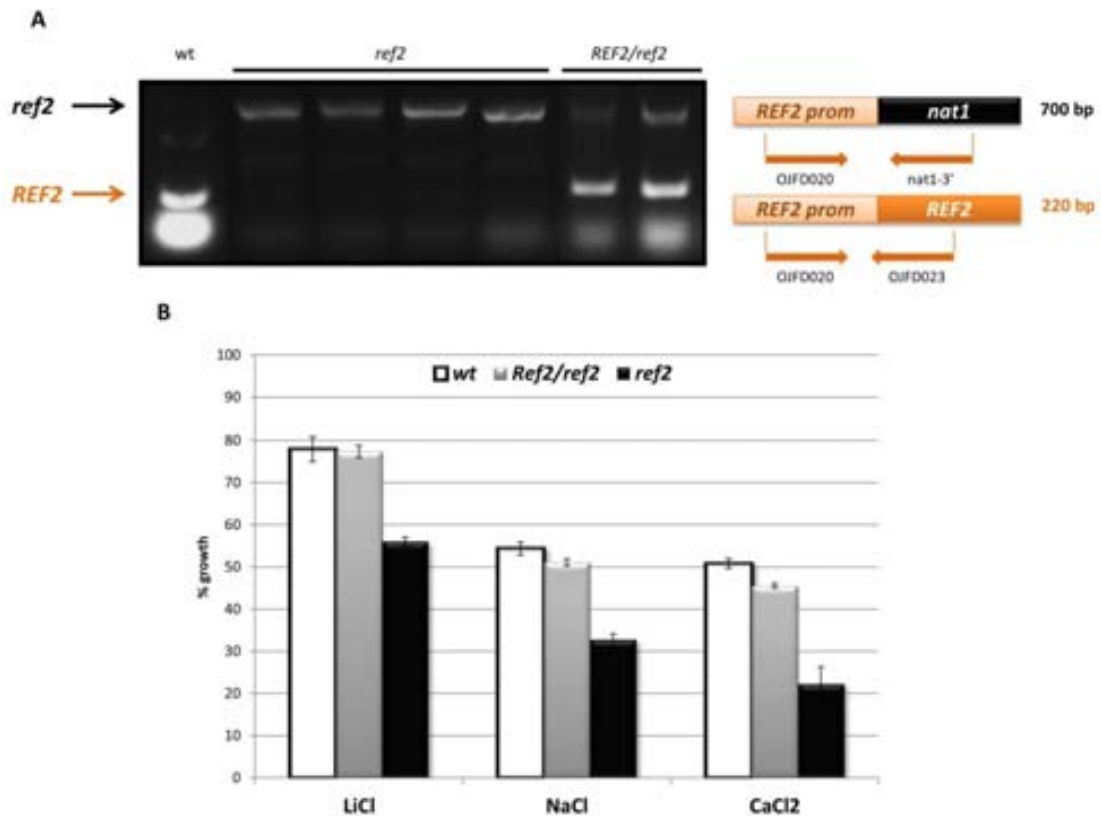


Figure 46. The generation of new *ref2* strains is difficult due to genomic duplication of *REF2* itself. A) Test colony PCR amplifying the *REF2* ORF with primers OJFD20 and OJFD23 (220 bp) and *REF2* deletion with primers OJFD20 and nat1-3' (700 bp) as a control for generating new *ref2* mutants. PCR fragments were loaded in 2% DNA agarose. **B)** Liquid growth of wild-type strain (wt), cells lacking *REF2* (*ref2*, called YJFD1-4) and cells with either a copy of *REF2* and *ref2* deletion (*REF2/ref2*, called YJFD49-50) were inoculated at 0.02 OD₆₆₀ with YPD (pH 5.5) plus 75 mM LiCl (LiCl), 0.6 M NaCl (NaCl) and 200 mM CaCl₂ (CaCl₂). Growth at 28°C was monitored for 16 h (wt and *REF2/ref2*) or 24 h (*ref2*). Data are mean ± SEM from at least 12 independent clones.

3.3 New *ref2* mutant cells display an aneuploidy on chromosome XII

After generating new *ref2* mutants, we decided to verify the possible aneuploidy in BY4741 *ref2* strain from EUROSCARF. Initially we already described in a transcription experiment using DNA microarrays from *ref2* cells compared to wild-type strain that chromosome II and XII were overrepresented in induction genes, 39% and 51% respectively (Figure 43). For that, we designed a new approach using Comparative Genomic Hybridization microarrays (CGH). Aneuploidy has altered gene DNA copy number along an entirely chromosome. In our typical CGH measurement, total genomic DNA is isolated from test and reference yeast cells, differentially labeled and hybridizes, we are able to compare the gene

number copy of each chromosome (Bond, Neal, Donnelly, & James, 2004; Dion & Brown, 2009; Pinkel & Albertson, 2005a, 2005b).

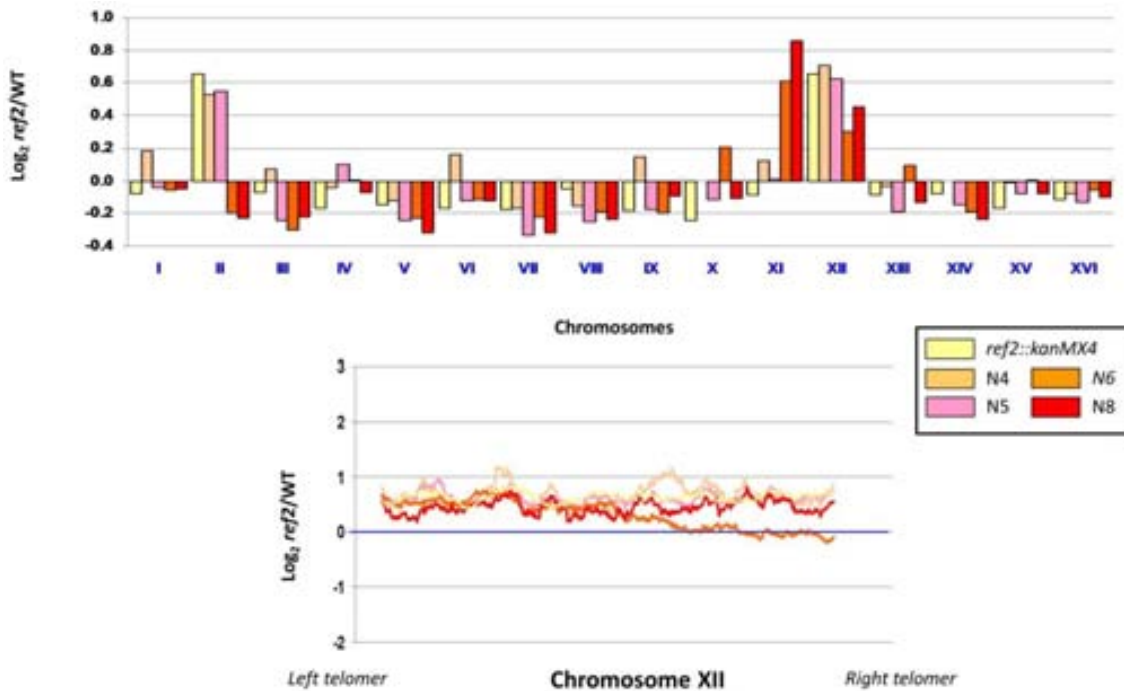


Figure 47. New *ref2* mutant generated also display aneuploidy. DNA genomic of *ref2* strain (EUROSCARF) and new *ref2* strains (YJFD1-4) was compared to wild-type strain using comparative genomic hybridization (CGH) as explained in *Experimental procedures*. The mean of each 16 yeast chromosomes is illustrated in \log_2 mutant/wild-type ratio. Below, gene distribution in chromosome XII is graphed.

As shown in *Figure 47*, *ref2* mutants display an aneuploidy due to the fact that some chromosome's means are over 1.80 folds (\log_2 ratio mutant/wild-type 0.7 approximately). Interestingly, the five strains shared the duplication of chromosome XII, but there is a divergence in the other aneuploidies: *ref2* cells plus clones N4-N5 have also chromosome II; meanwhile N6 and N8 show also chromosome XI.

We focused in chromosome XII duplication because it is common on five strains. Firstly, nearly all strains, except N6 clone the chromosome XII is induced in the whole length (*Figure 47*). We hypothesize two possible explanations: rDNA or Sen1, but we are still looking into them deeply.

Firstly, in *S. cerevisiae*, unlike in other yeasts and most other species, the tandem array of genes encoding ribosomal subunits (rDNA) is confined to a single genomic locus, on the right arm of chromosome 12 (12R) (Zimmer & Fabre, 2011). It is important to remark that correct snRNAs maturation is necessary for post-transcriptional steps in gene expression that lead to

functional ribosomes (Granneman & Baserga, 2005) which is impaired in *ref2* cells (Nedea et al., 2008). So, we decided to transform *ref2* cells with a plasmid called pRDN-wt-U which overexpresses yeast rDNA tandem (Chernoff, Vincent, & Liebman, 1994), but we were not able to rescue *ref2* strain studied phenotypes (*data not shown*). Moreover, we also transformed *tetO₇:REF2* (YJFD16) with pRDN-wt-U and, unfortunately, the overexpression of rDNA was also unable to rescue the read-through phenotype of this strain.

Secondly, in chromosome XII is located *SEN1* (YLR430W). This gene encodes a helicase protein whose basic function is interacting with the exosome to mediate 3' end formation of some mRNAs, snRNAs and snoRNAs through forming a complex with Nrd1-Nab3 (Winey & Culbertson, 1988). In (Nedea et al., 2008), Sen1 helicase is identified as a high-copy suppressor of the snoRNA termination defect; furthermore they suggest that Sen1 is a strong candidate for being a direct substrate of Glc7, potentially through the binding of Glc7 mediated by Ref2 to APT-complex. *SEN1* is an essential and, lowering the Sen1 levels with a tetO-off system is deleterious in a *ref2* strain (Nedea et al., 2008). For that, we have already designed an experiment where Sen1 is cloned in a centromeric plasmid and then transformed to *ref2* cells. We have initiated and evolutionary experiments such as (Hill, Ammar, Torti, Nislow, & Cowen, 2013; Yona et al., 2012), but we have not got any result yet.

3.4 Mutants in components of the APT-complex do not share the aneuploid-related phenotypes of the *ref2* strain

Given the aneuploidy in Ref2 described previously, as a component of the APT-complex, it was reasonable to consider whether the aneuploidy could be attributed to the role of the protein in this complex. We reasoned that, if this was the case, mutations in other components of the complex would yield phenotypes reminiscent of those of the *ref2* strain and specific for aneuploid cells. As many members of the APT-complex are essential (including Pta1), we had to resort in most cases to temperature sensitive mutants cultured at sublethal temperatures (28°C).

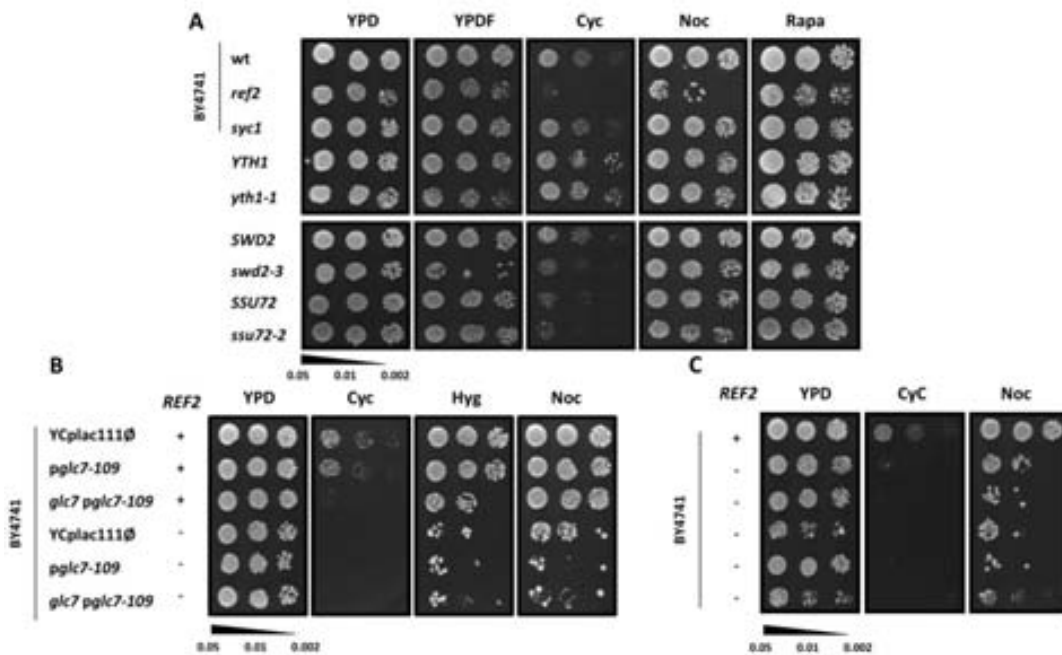


Figure 48. Mutants in components of the APT-complex do not share the aneuploid-related phenotypes of the *ref2* strain. A) Three dilutions from indicated cultures were spotted on plates containing YPD plus 3% formamide (YPDF), 0.2 μ g/ml cycloheximide (Cyc), 10 μ g/ml nocodazole (Noc), 30 μ g/ml Hygromycin B (Hyg) and 15 ng/ml rapamycin (Rap). Growth at 28°C was monitored for 2-3 days. **B)** Strains used in this dot test: BY4741 wild-type transformed with YCplac111 \emptyset (YJFD34), *pglc7-109* called pJFD11 (YJFD35) and cassette *glc7::nat1* plus *pglc7-109* (YJFD36); BY4741 *ref2* strain was equally transformed generating YJFD37, YJFD38 and YJFD39, respectively. Three dilutions from indicated cultures were spotted on plates containing YPD plus 0.2 μ g/ml cycloheximide (Cyc), 10 μ g/ml nocodazole (Noc) and 30 μ g/ml Hygromycin B (Hyg). Growth at 28°C was monitored for 2-3 days. **C)** Three dilutions from wild-type and *ref2* cells (BY4741 *ref2* and YJFD1-4) were spotted on plates containing YPD plus 0.2 μ g/ml cycloheximide (Cyc) and 10 μ g/ml nocodazole (Noc). Growth at 28°C was monitored for 2-3 days.

Aneuploid strains display several phenotypes related to the synthesis of proteins from the additional chromosomes and their presence in the cell represents an increased burden on the cell's protein production machinery which leads to a possible proteotoxic stress (Eduardo M Torres et al., 2007). As shown in *Figure 48*, *ref2* strains are hypersensitivities to protein synthesis inhibitors (cycloheximide or hygromycin B), but not to the protein synthesis inhibitor (rapamycin). Moreover, these strains display a hypersensitivity to nocodazole which depolymerizes microtubules in yeast (Solomon, 1991). Those phenotypes are not shared by APT-complex components. As displayed in *Figure 48A*, neither *syc1* nor *yth1-1* show a hypersensitive phenotype compared to its wild-type strain respectively. On the other hand, either *swd2-3* or *ssu72-2* may be slightly sensitive only to cycloheximide. This is understandable because none of the mutants at semi-restrictive temperatures displays any aneuploidy, not even at restrictive temperatures (Nedeja et al., 2003). Interestingly in *Figure 48B*, our strain *glc7-109* allele (*glc7 pglc7-109*) is also sensitive to protein synthesis inhibitors, but those phenotypes are exacerbated in *ref2* cells. *glc7-109* cells which carried a mutation at

Arg-260 found to be responsible for the sensitivity phenotypes related to ionic homeostasis through interacting with Ref2 subunit (J Ferrer-Dalmau et al., 2010; T Williams-Hart et al., 2002). For that, it is not strange that the lack of *REF2* could also relate Glc7 to protein synthesis defects.

3.5 Mutants in components of the APT-complex share a decreased biomass production than wild-type cells

Aneuploid cells exhibit increased glucose uptake, furthermore wild-type cells generate more biomass per internalized glucose molecule than aneuploids (Eduardo M Torres et al., 2007). As shown in *Figure 49*, *ref2* cells and other mutants of the APT-complex display a saturated density lower than wild-type strain, but we have not been able to observe an increased glucose uptake. Finally, in aneuploidy cells both *HXT6* and *HXT7* or specific glucose transporters are hyperactivated, but they could not be found in our *ref2* strains (Eduardo M Torres et al., 2007).

Since it is estimated that 60 to 90% of the intracellular chemical energy is devoted to protein production, gene copies in the extra-chromosomes are not only transcribed but also translated. Despite this increase protein translation, there is no increase in protein abundance, meaning that these new proteins may be degraded shortly after being produced (Schubert et al., 2000; Eduardo M Torres et al., 2007). For that, there is this increase on glucose need for aneuploid cells. However this hypothesis may explain the results for *ref2* cells which are aneuploids, APT-complex mutants do not have any aneuploidy. Our explanation may be that those mutants have defects on snoRNA maturation meaning that they are generating transcripts which cannot be processed. So, we could have three possibilities: 1) increased transcripts production to achieve normal function of ribosome production, 2) incorrect transcripts must be degraded or 3) incorrect transcripts are accumulated forming aggregates. At least, in hypothesis 1 and 2 the requirement of more glucose molecules than wild-type cells is completely justified which would imply lower biomass production.

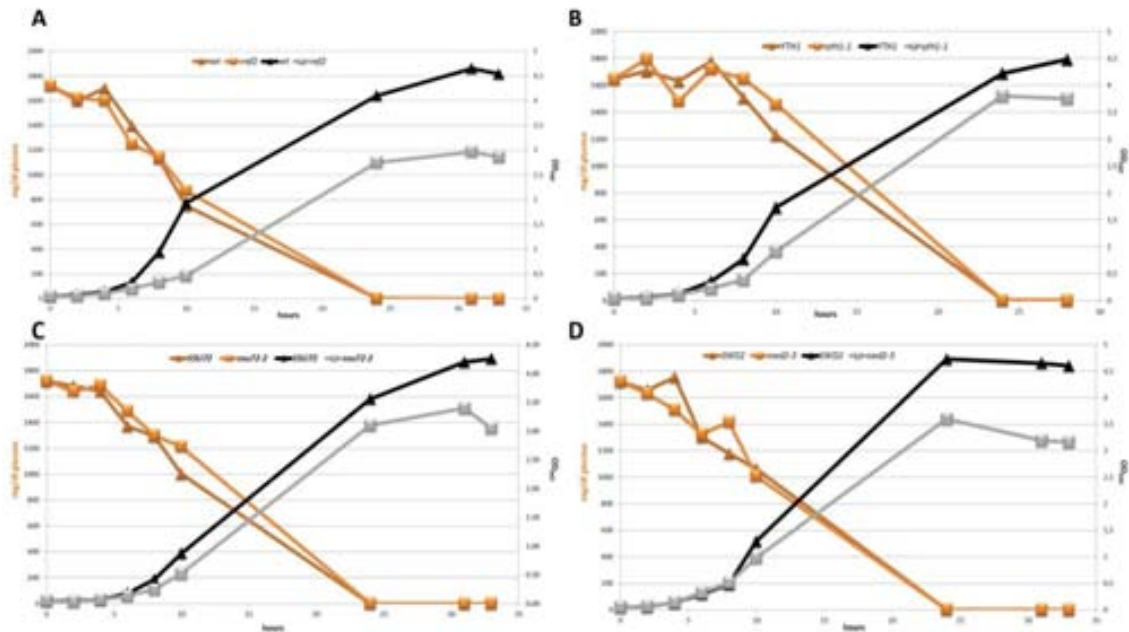


Figure 49. APT-complex strains display lower biomass production than wild-type strains. A, B, C and D) Wild-type and APT-complex mutant cells (*ref2* (A), *yth1-1* (B), *ssu72-2* (C) and *swd2-3* (D)) were grown overnight in YPD. Cells were inoculated at 0.05 OD₆₀₀ and their growth monitored for 36 h at 28°C. The amount of glucose in the medium was determined at the indicated times as explained in *Experimental procedures*.

3.6 *ref2* mutant cells in different background show similar phenotypes

As shown in *Figure 49*, the generation of new *ref2* strains in different genetic backgrounds such as 1700, CML476, FY61, TM141 and DBY746 was performed and we decided to analyze their aneuploidy phenotypes, among others. Apparently, all of them shared a hypersensitivity to protein synthesis inhibitors and a lower biomass production per molecule of glucose uptake. Meaning that *ref2* cells may also have an aneuploidy, we analyzed DBY746 *ref2* (YJFD5) and this strain had only chromosome V duplicated (*data not shown*) which may imply that each *ref2* strain has specific aneuploidies due to background.

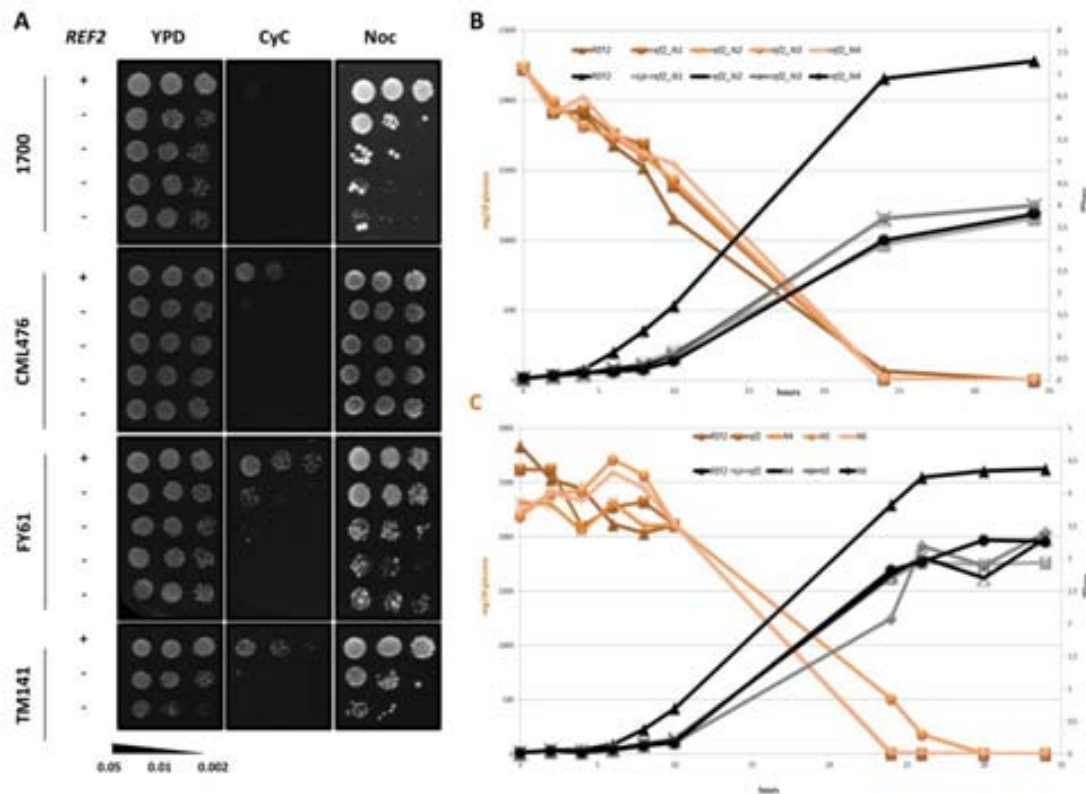


Figure 50. *ref2* mutants in new backgrounds not only display protein synthesis inhibitor stress but also lower biomass production than wild-type strain. **A)** New *ref2* strains were generated from TM141 wild-type (YJFD90), 1700 wild-type (YJFD92), CML476 wild-type (YJFD94) and FY61 wild-type (YJFD89). Three dilutions from indicated cultures were spotted on plates containing YPD plus 0.2 $\mu\text{g/ml}$ cycloheximide (Cyc) and 10 $\mu\text{g/ml}$ nocodazole (Noc). Growth at 28°C was monitored for 2-3 days. **B)** 1700 wild-type and its *ref2* derivative cells (*ref2*_N1-N4 called YJFD92) were grown overnight in YPD. Cells were inoculated at 0.05 OD_{660} and their growth monitored for 36 h at 28°C. The amount of glucose in the medium was determined at the indicated times as explained in *Experimental procedures*. **C)** BY4741 wild-type and its *ref2* derivative cells (YJFD1-4) were grown overnight in YPD. Cells were inoculated at 0.05 OD_{660} and their growth monitored for 36 h at 28°C. The amount of glucose in the medium was determined at the indicated times as explained in *Experimental procedures*.

3.7 *ref2* mutant cells apparently does not show any delay in cell cycle

Aneuploidy cells are altered in G_1 -S phase transition due to the increased doubling time and cell size in complete medium. These cells have problems to get through START to entry into cell cycle (Jorgensen & Tyers, 2004) because the presence of extra chromosome might affect Cln3-CDK function (Eduardo M Torres et al., 2007).

In (Thorburn et al., 2013), they described G1 delay in asynchronous cultures of aneuploidy cells. Collaborating with Ethel Queralt's lab from PEBC, we performed FACS experiments with *ref2* cells (Figure 51) without synchronizing yeast cultures. Our results do not show any difference between wild-type to *ref2* strains. Moreover, we also used *ref2* cells

transformed with *REF2* and *REF2*^{F374A} allele, but we are not able to see any difference between them. The only difference is between the horizontal size of peaks of *ref* cells which may be a result of cell size growing in minimum medium *Figure 51B*.

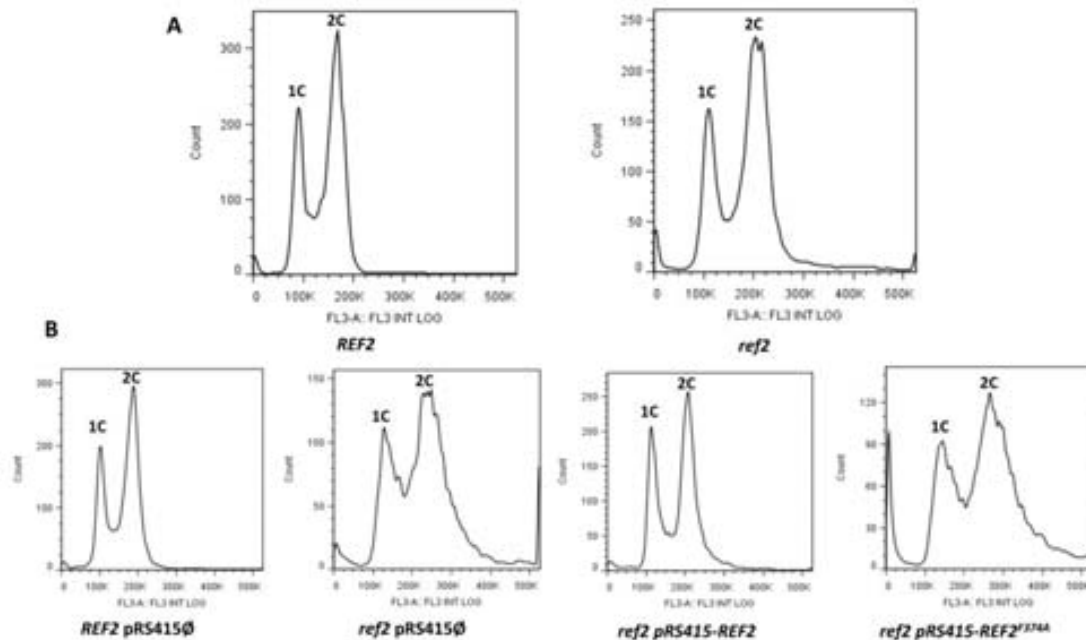


Figure 51. *ref2* cells apparently do not display a delay in G₁. **A)** Non-synchronized wild-type and its derivative *ref2* cells were grown at exponential growth and DNA content was determined by FACS. **B)** Non-synchronized wild-type and *ref2* (BY4741 *ref2*) cells transformed with plasmid containing *REF2* (pJFD1) or *REF2*^{F374A} (pJFD2) were grown in its restrictive medium (Leu⁻). DNA content was determined using FACS.

A deeply study should be done, because *ref2* strains are hypersensitive to nocodazole (*Figure 48*, *Figure 50* and *Figure 52*). This sensitivity indicates that aneuploidy strains exhibit a chromosome bi-orientation defect. This is another typical phenotype of aneuploidy cells which have chromosome missegregation due to defects in chromosome attachment to the mitotic spindle or from problems in DNA replication or repair. Moreover, defects in any of these processes delay mitosis by stabilizing the anaphase inhibitor Pds1 (securing) or a delay in anaphase through the mitotic checkpoint component Mad2 (Musacchio & Salmon, 2007; Sheltzer et al., 2011).

Surprisingly, *glc7-109* allele, which is directly related to Ref2 in ionic homeostasis regulation (J Ferrer-Dalmau et al., 2010), does not display nocodazole sensitivity (*Figure 48*). Nevertheless, Ref2 needs to be bound to Glc7 to grow properly in nocodazole (*Figure 52*).

3.8 The Ref2^{F374A} cells have an aneuploidy in chromosome XII

After describing *ref2* cells aneuploidy, we performed the same phenotypes, glucose uptakes and DNA microarray experiments with Ref2^{F374A} allele.

As observed in *Figure 52A-B*, it is important the binding of Glc7 to APT-complex through Ref2 in order to grow properly in protein synthesis inhibitor (cycloheximide) and the lower biomass produced per glucose molecules.

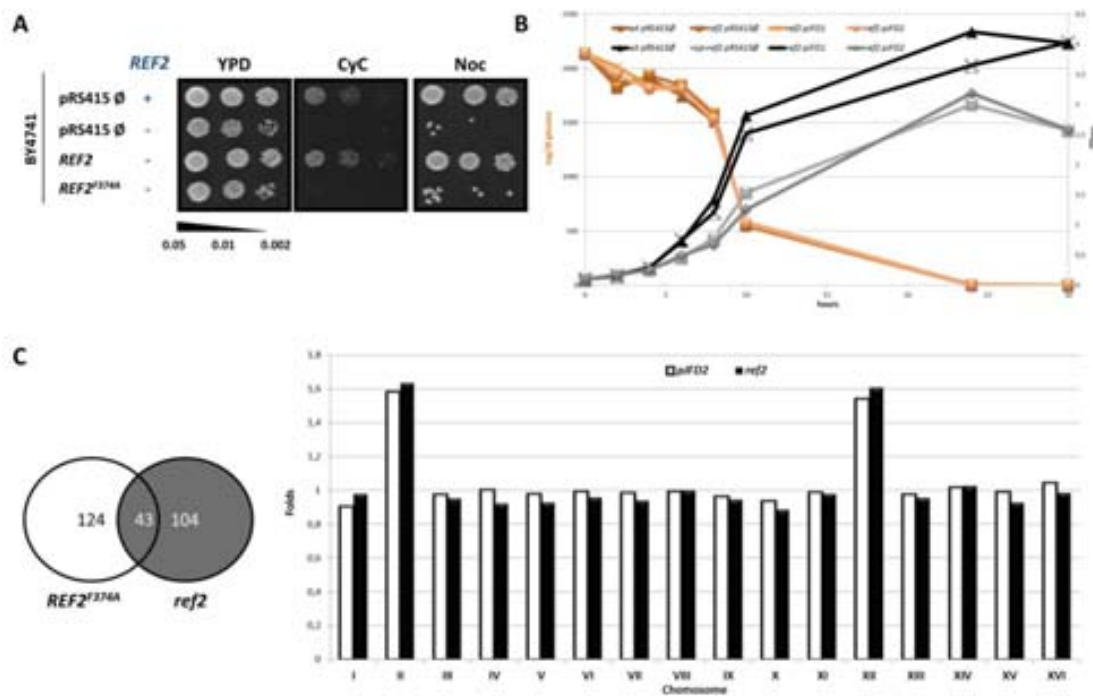


Figure 52. Mutation of Phe-374 within the Glc7-binding consensus sequence also display an aneuploidy. A) Wild-type BY4741 (+) and *ref2* strains (-) were transformed with the empty plasmid pRS415 or the same plasmid expressing the wild-type Ref2 protein (pJFD1) or the Ref2^{F374A}-mutated version (pJFD2). Three dilutions of transformants were spotted on to YPD plates plus 0.2 μ g/ml cycloheximide (Cyc) and 10 μ g/ml nocodazole (Noc). Growth at 28°C was monitored for 2-3 days. **B)** Indicated strains were saturated in the appropriate medium and then inoculated at 0.05 OD₆₆₀ and their growth monitored for 36 h at 28°C. The amount of glucose in the medium was determined at the indicated times as explained in *Experimental procedures*. **C)** Left panel, induced genes of DNA microarray experiments from *ref2* cells (grey) and *ref2* cells carrying the plasmid with the Ref2^{F374A}-mutated version (pJFD2) were classified in a Venn diagram. Right panel, once analyzed the DNA microarray experiments as explained in *Experimental procedures*, the mean of each chromosome was calculated for indicated strains and graphed in folds.

Finally, we performed a DNA microarray from *ref2* cultures transformed with REF2 (pJFD1) and REF2^{F374A} (pJFD2). As graphed in *Figure 52C*, either *ref2* or REF2^{F374A} cells display the same transcription pattern, meaning that both strains have an aneuploidy in chromosome II and XII.

In the left panel, the Venn diagram indicates that both strains have 43 induced common genes, which all of them are distributed along chromosome II or XII.

3.9 Homozygous diploid *ref2* cannot sporulate

The generation of diploids had two main goals: the analysis of aneuploidy phenotypes and the DNA analysis of daughter cells.

In *Figure 53A*, we demonstrate that mating *ref2* cells are able to generate homozygous diploids (*ref2/ref2*) which display the same phenotypes as a haploid *ref2* in ionic homeostasis and cell wall integrity stressors. Moreover, those homozygous diploids need Glc7's binding to APT-complex to properly grow in the studied stress conditions. We have not done yet the experiments with aneuploidy phenotype conditions, but it is important to remark that the proliferative disadvantage and increase in cell size were also observed in aneuploidy diploid cells, indicating that the gain of an extra chromosome interferes with cell proliferation of both haploid and diploid cells (Eduardo M Torres et al., 2007).

On the other hand, we wanted to analyze the chromosomal progeny dotation. So, we tried to sporulate those diploids generated transformed with the respective plasmids. Moreover, we did not select for any growth condition because we wanted to generate as many spores as possible. Importantly, homozygous diploids *ref2* (*ref2/ref2*) transformed with either the empty vector (pRS415 \emptyset) or pRS415-*REF*^{F374A} (pJFD2) were not able to sporulate (*Figure 53*). Moreover, a single copy of *REF2* allows a wild-type sporulation, meaning that the lack of *REF2* is deleterious for sporulation.

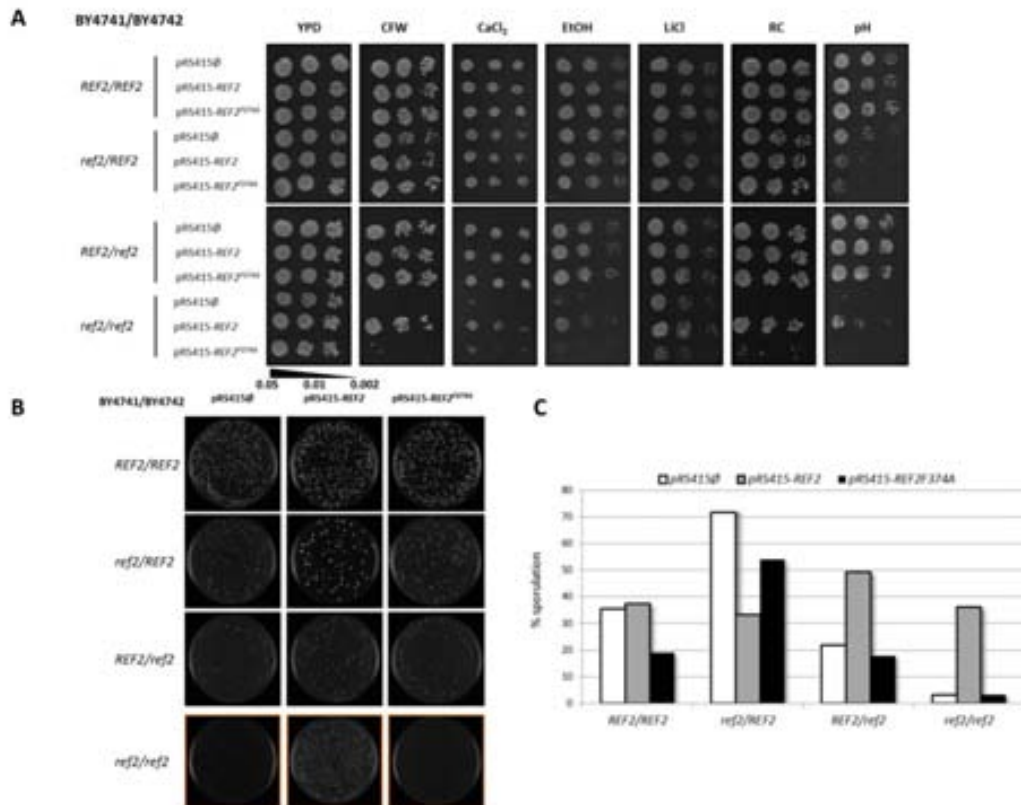


Figure 53. Diploid homozygous *ref2* is unable to sporulate. The strains used in these experiments: BY4741/BY4742 wild-types (BY4743), BY4741 *ref2*/BY4742 wild-type called YJFD70 (*ref2*/REF2), BY4741 wild-type/YJFD9 called YJFD69 (REF2/*ref2*) and BY4741 *ref2*/YJFD9 called YJFD71 (*ref2*/*ref2*) also transformed with pRS415∅ and its derivative containing REF2 (pJFD1) or REF2^{F374A} (pJFD2). **A**) Three dilutions from indicated cultures were spotted on plates containing YPD plus 5 µg/ml Calcofluor white (CFW), 200 mM CaCl₂ (CaCl₂), 100 mM LiCl (LiCl), 15 µg/ml Congo red (RC) and adjusted a pH 8 (pH); and YP plus 4% ethanol (EtOH). Growth at 28°C was monitored for 2-3 days. **B**) Random spore analysis of the indicated strains plated on YPD plates and growth monitored for 2 days and dilution 1/50, except *ref2/ref2* diploid strain which was incubated for 3 days and dilution 1/10 at 28°C. **C**) Graphic of obtained spores divided by total cells inoculation on to YPD plates.

Consequently, we started a tiny study of sporulation. In (Neiman, 2011) and summarized at Figure 54A, sporulation is described as a three stage process: early, middle and late. Basically, early phase consists on leading to exit from the mitotic cycle in G₁ and entry into premeiotic S phase with DNA replicate; then middle phase includes the major cytological events of sporulation, in which the meiotic divisions give rise to four haploid nuclei that are then packaged into daughter cells and the synthesis of prospore membrane; finally spores enter to late phase which implies spores maturation. So, these phases are regulated with two transcription factors: Ime1 and Ndt80.

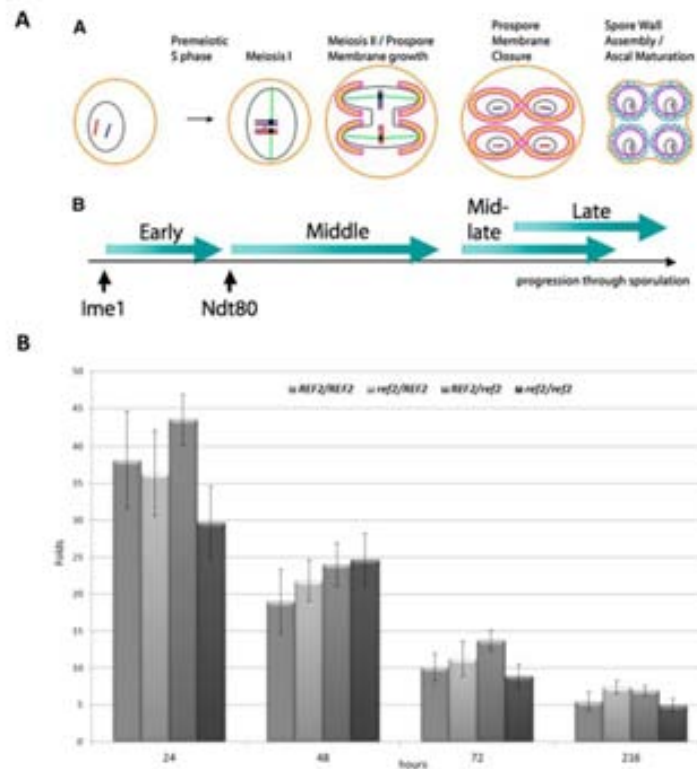


Figure 54. Diploid homozygous *ref2* has a wild-type *IME1* regulation. A) The morphogenetic events of spore formation are driven by an underlying transcriptional cascade. (A) The landmark events of meiosis and sporulation are shown in temporal order. Orange lines indicate the mother cell plasma membrane (which becomes the ascus membrane). Gray lines indicate the nuclear envelope. Blue and red lines represent homologous chromosomes. Green lines represent spindle microtubules. Prospore membranes are indicated by pink lines and the lumen of the prospore membrane is highlighted in yellow. After membrane closure, the prospore membrane is separated into two distinct membranes. The one closest to the nucleus serves as the plasma membrane of the spore, while the outer membrane, indicated by thin, dashed pink line, breaks down during spore wall assembly. Blue hatching represents the spore wall. (B) The shaded arrows indicate the relative timing of the different transcriptional classes with respect to the events in A. The black arrows indicate the points at which the transcription factors *Ime1* and *Ndt80* become active (Neiman, 2011). **B)** Wild-type and its derivative diploid strains were transformed with the construct *pIME1-lacZ* (**p1335**) and cultures were grown until reached 0.8 OD₆₆₀ in YPD (pH 5.5). Cells were transferred to sporulation medium and collected at indicated times for measuring β -galactosidase activity as described in *Experimental procedures*. Data are mean \pm SEM from at least six independent clones.

We started our analysis in *IME1*'s transcription. Expression of *IME1* is regulated at transcriptional, posttranscriptional, and post-translational levels by a variety of different factors including mating type, nitrogen source, carbon source, storage carbohydrate, and extracellular pH and needed to enter to late phase (Neiman, 2011) and, when it is degraded to let cells enter the next phase expression *Ndt80*. Using β -galactosidase report fused to *IME1* promoter (p1335), kindly provided from Angelika Amon's Lab in MIT, we analyzed the response when we induced our diploids to sporulation. In *Figure 54B*, we show that

homozygous diploids *ref2* (*ref2/ref2*) has a wild-type expression of *IME1*. Moreover, we can hardly see any difference in the activation of *IME1* and in its degradation. To sum up, diploids can enter to the early phase, so they may have defects in middle phase due to problems in meiosis. Furthermore, we have to remark that we cannot find any spores present in an optic microscopy experiment in *ref2/ref2* diploids, meaning that the spore has not generated, even one month of sporulation.

3.10 Conclusions

7. The generation of *tetO₇::REF2* strain demonstrated the defects of snoRNA maturation and processing already described as an APT-complex component. Moreover, we were not able to show the aneuploidy in this strain. One possibility it is that the experiment is not long enough, meaning that a longer treatment with doxycycline could achieve the aneuploidy.
8. All *ref2* mutant cells in BY4741 genetic background display the common aneuploidy on chromosome XII, but they have also different chromosome duplication (II and XI). Those strains also show hypersensitivity to typical phenotypes of aneuploidy cells such as protein synthesis inhibitors (cycloheximide and hygromycin B) and a lower biomass production per glucose molecules than wild-type cells.
9. Surprisingly, *ref2* mutant cells do not show a G₁ delay in cell cycle. Despite this negative result, we should repeat the experiments synchronizing the cellular culture because *ref2* mutant cells display sensitivity to nocodazole meaning a chromosome bi-orientation defect.
10. APT-complex mutants do not show an aneuploidy. Furthermore, our results indicate that these mutants need more energy for growing than wild-type strain implying a lower saturation level.
11. All the phenotypes of *ref2* mutant cells are due to the inability to bind Glc7. Despite this regulation, *glc7-109* allele which is directly regulated by Ref2 in ionic homeostasis adaptation, does not present an aneuploidy.
12. The haploid *ref2* mutant cells can generate diploids. Nevertheless, homozygous diploid *ref2* cells cannot form spores. These diploid cells can start the sporulation process by entering early phase, but then there are no visible spores, because possibly they carry a defect in meiosis.

4. Study of Unfolded Protein response in mutants on non-essential Glc7-regulatory subunits

As explained in the *Introduction, section 3.5*, since now it has ever been related a relation between Glc7, or any of its regulatory subunits, to unfolded protein response (UPR). In our work, we decided to analysis phenotypically the response of mutants on each non-essential Glc7-regulatory subunit (*Table 12*).

4.1 Phenotypical analysis of mutants on non-essential Glc7-regulatory subunits

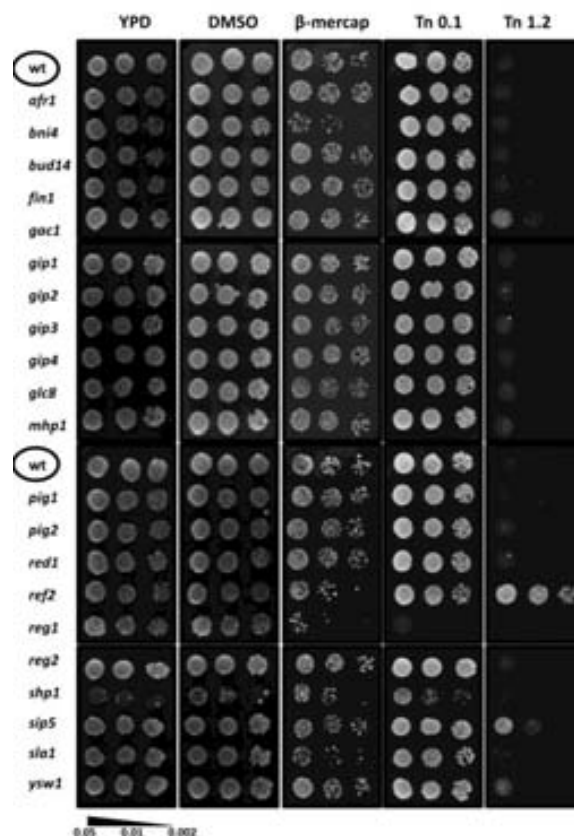


Figure 55. Effect of the mutation of several Glc7-interacting proteins on different stressors. Three dilutions from cultures of wild-type strain BY4741 (wt) and the indicated isogenic derivatives were grown on either YPD plates in the presence of β -mercap (2-Mercaptoethanol 40 mM) and Tn (Tunicamycin 0.1 / 1.2 μ g/ml). Growth at 28°C was monitored for 2-3 days.

Basically, we used tunicamycin as the main UPR inducer. As described in (Back et al., 2005), β -mercaptoethanol and Dithiothreitol (DTT) reduce disulfide bonds as a primary effect, but they show several secondary effects on yeast cell, challenging the interpretation of results,

such as: **i)** releasing proteins from the cell wall and low molecular weight compounds from the cell; **ii)** decreasing the electrochemical potential and proton gradient over plasma and vacuolar membranes and **iii)** inducing antioxidant proteins and inhibit adenosine kinase. For that, we primarily used tunicamycin an Alg7 inhibitor, which catalyzes the addition of 2-N-acetyl-D-glucosaminy-1-phosphate to dolichol phosphate; which completely blocks glycosylation of nascent polypeptides (reviewed in (Loibl & Strahl, 2013)). As a specific inhibitor, its secondary effects only include the impairing of DNA, RNA, and protein synthesis and induce RNA and DNA degradation. Finally, as shown in *Figure 55*, as in nearly all experiments, we used dimethyl sulfoxide (DMSO) plates as a control because tunicamycin stock is diluted in DMSO.

Figure 55 shows that *gac1*, *sip5* mutant cells display a slightly tolerant phenotype to tunicamycin; meanwhile *ref2* mutant cells show an accused tolerant phenotype to tunicamycin. *shp1* mutant cells display hypersensitivity to UPR inducers (Tan et al. 2009), however, deletion of *SHP1* caused a rather severe growth defect even in the absence of stress, as previously described (Zhang et al., 1995), making it difficult to assess the actual effect of the mutation under the conditions tested. On the other hand, *sla1* and *bni4* mutant cells display a slightly hypersensitive phenotype to β -mercaptoethanol. Finally, *reg1* mutant cells display an accused hypersensitivity to both tunicamycin and β -mercaptoethanol, which was already described in (Tan et al. 2009). Therefore, *ref2* and *reg1* mutant cells display the most differential phenotypes to UPR inducers than other non-essential Glc7-regulatory subunit mutant cells, which may indicate a possible regulation of UPR through Glc7.

4.2 UPRE transcriptional analysis of mutants on non-essential Glc7-regulatory subunits

Our next step consisted on evaluating the transcriptional activation unfolded protein response element (UPRE) to tunicamycin in the non-essential Glc7-regulatory subunit mutant cells. This response element is activated by Hac1, a basic leucine zipper (bZIP) transcription factor which translocates to the nucleus and activates the UPR genes (Nojima et al., 1994). To perform the experiment, Jose Antonio Prieto, Ph.D. from IATA, València, provided us the plasmid pMCZ-Y which contains UPRE fused to *lacZ* gene (Mori et al., 1996; Torres-Quiroz et al., 2010).

Firstly, as shown in *Figure 56*, *hac1* mutant cells are used as a negative control where the lack of the transcriptional factor cannot induce any response to tunicamycin through UPRE

(Mori et al., 1996). Moreover, *ptc2* and *dcr2* mutant cells, which have already been described as somehow regulators of UPR through possibly interacting with Ire1 kinase (Guo & Polymenis, 2006; Welihinda et al., 1998), display a slightly lower transcriptional activation of UPRE than wild-type cells. Importantly, *reg1* mutant cells, which are hypersensitive to tunicamycin, not only do they display the lowest basal levels in non-induced conditions but also do they have the highest levels in tunicamycin inducing conditions. Finally, *ref2* and *shp1* mutant cells show a defect in activating UPRE at wild-type levels, but phenotypically speaking *ref2* mutant cells show a tolerance to tunicamycin and *shp1* mutant cells possibly display a slightly sensitivity to tunicamycin (Figure 55).

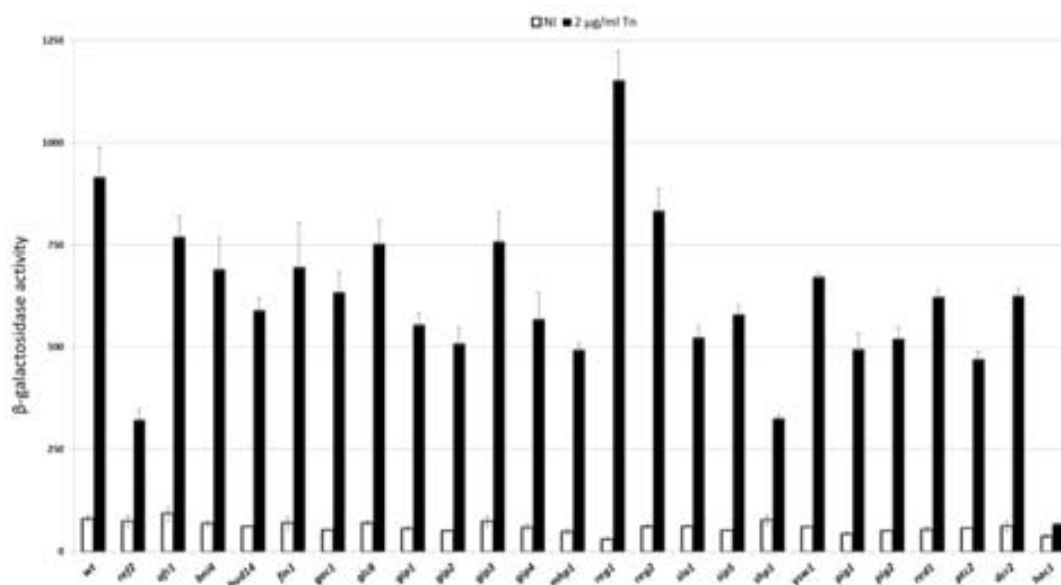


Figure 56. Evaluation of UPRE in mutants on non-essential Glc7-regulatory subunits. Wild-type and the indicated isogenic derivatives were transformed with the construct pMCZ-Y and cultures were grown until reached 0.8 OD₆₆₀ in YPD (pH 5.5). Cells were transferred to fresh YPD (NI, white bars) and with 2 µg/ml tunicamycin (2 µg/ml Tn, black bars) for 90 min at 28°C. β-galactosidase activity was measured as described in *Experimental procedures*. Data are mean ± SEM from at least six independent clones.

Therefore, increased response levels to tunicamycin, as observed in *reg1* mutant cells, may indicate a deregulation of this pathway, which may cause a hypersensitive phenotype to UPR inducers such as tunicamycin or β-mercaptoethanol.

4.3 *glc7-109* allele shows a hypersensitive phenotype to UPR inducers

Since now, no *GLC7* allele has been described as important for unfolded protein response, therefore we decided to analyze *glc7-109* allele due to the important of this allele in ionic homeostasis regulation through Ref2 subunit (Jofre Ferrer-Dalmau et al., 2010; T Williams-Hart et al., 2002). It is important to remark that *glc7-109* allele has two point

mutations (Glc7^{K259A R260A}), where Arg-260 lies in the vicinity of Phe-256 residue in the Glc7-hydrophobic channel that makes contact with the aromatic residue of the (R/K)(V/I)X(F/W) binding-partner motif which unable the binding of some Glc7-regulatory subunits (T Williams-Hart et al., 2002). Our dot test revealed that *glc7-109* allele displays hypersensitivity to UPR inducers such as tunicamycin and β -mercaptoethanol (Figure 57A). Therefore, this result indicates that the binding of Glc7-regulatory subunits to the catalytic subunit is essential for properly UPR regulation. For that we evaluated the phenotypes of both Reg1 and Ref2 point-mutation versions in the Glc7-binding motif.

Initially, we transformed *reg1* mutant cells with the LexA-Reg1 plasmids containing point mutations at phenylalanine in the putative PP-1C-binding site motif (K/R)(X)(I/V)XF. These mutations are unable either to rescue Hxk2 dephosphorylation or to restore its phosphatase activity which demonstrate that Reg1 targets PP-1C to dephosphorylate Hxk2 *in vivo* at the motif (K/R)(X)(I/V)XF (Alms et al., 1999). Figure 57B shows that *reg1* mutant cells are rescued when Reg1 is re-introduced into the cells (pLexA-Reg1), but the plasmids containing the point mutations (pLexA-Reg1^{F468D} and pLexA-Reg1^{F468R}) somewhat rescue the fitness to tunicamycin. It is interesting that wild-type LexA-Reg1 has been shown to complement the *reg1* mutant cells effectively reducing *SUC2* expression 130 folds in glucose grown *reg1* mutant cells; whereas the point mutations of LexA-Reg1 only reduce the expression of *SUC2* by 3 folds. This small activity reduction of *SUC2* is enough to increase *reg1* mutant cells fitness to tunicamycin. Definitely, the main problem in *reg1* mutant cells which may cause UPR-hypersensitivity will be the basal hyperactivation of Snf1 pathway (Alms et al., 1999; Castermans et al., 2012). On the other hand, the lack of *REF2* causes a tolerant phenotype which is impaired to a wild-type phenotype when *ref2* mutant cells are rescued with the pRS415-Ref2 (pJFD1). It has been described the importance of Phe-374 residue to bind Glc7 to APT-complex through Ref2 for either snoRNA maturation or ionic homeostasis regulation (Jofre Ferrer-Dalmau et al., 2010; Nedeá et al., 2008). So, transforming *ref2* mutant cells with pRS415-Ref2^{F374A} (pJFD2) causes a tolerant phenotype such as *ref2* mutant cells transformed with the empty plasmid. That means that somehow there is an improvement in tunicamycin resistance when Glc7 is not binding to APT-complex.

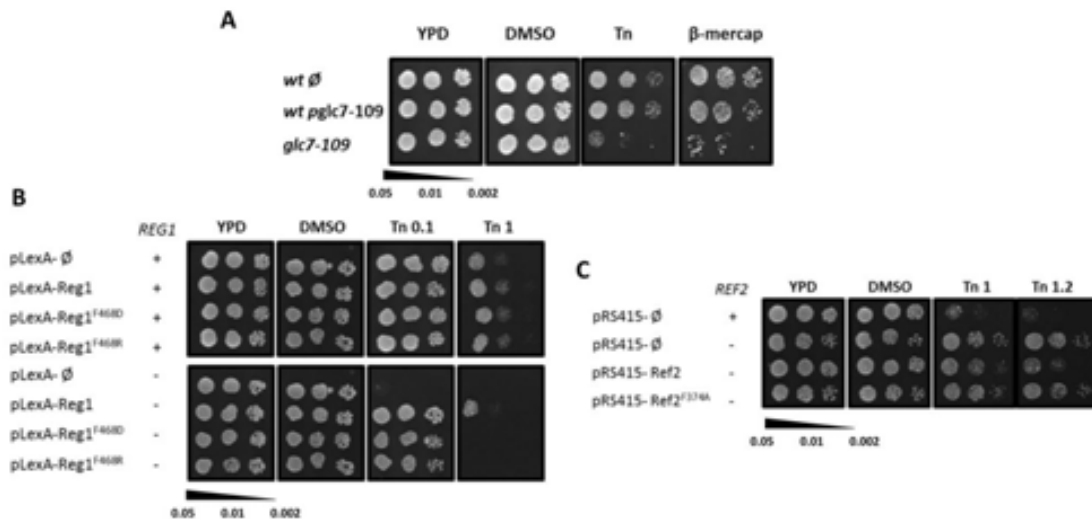


Figure 57. *GLC7* is needed for properly adaptation to UPR inducers. A) Strains used in this dot test were BY4741 wild-type transformed with YCplac111 \emptyset (YJFD34), *pglc7-109* called pJFD11 (YJFD35) and cassette *glc7::nat1* plus *pglc77-109* (YJFD36) Three dilutions from indicated cultures were spotted on plates containing YPD plus 0.8 μ g/ml tunicamycin (**Tn**) and 40 mM 2-Mercaptoethanol (**β -mercap**). Growth at 28°C was monitored for 2-3 days. **B)** Wild-type BY4741 (+) and *reg1* strains (-) were transformed with the empty plasmid pLexA or the same plasmid expressing the wild-type Reg1 protein (pLexA-Reg1, pRJ65), the Reg1^{F468D} mutated version (pLexA-Reg1^{F468D}) or the Reg1^{F468R} mutated version (pLexA-Reg2^{F468R}). Three dilutions of transformants were spotted on to YPD plates plus 0.1 μ g/ml tunicamycin (**Tn 0.1**) and 1.0 μ g/ml tunicamycin (**Tn 1.0**). Growth at 28°C was monitored for 2-3 days. **C)** Wild-type BY4741 (+) and *ref2* strains (-) were transformed with the empty plasmid pRS415 or the same plasmid expressing the wild-type Ref2 protein (pJFD1) or the Ref2^{F374A}-mutated version (pJFD2). Three dilutions of transformants were spotted on to YPD plates plus 1 μ g/ml tunicamycin (**Tn 1**) and 1.2 μ g/ml tunicamycin (**Tn 1.2**). Growth at 28°C was monitored for 2-3 days.

As performed in *Figure 56*, we followed the UPR induction under tunicamycin conditions through time in the described strains (*Figure 58*). Firstly, *reg1* mutant cells have an uncontrolled transcriptional response of UPR, meaning that the induction is always increasing even after 4 h of tunicamycin induction. On the contrary, *ref2* mutant cells display a very low UPR induction throughout experiment, but increased tunicamycin fitness (*Figure 55*). *glc7-109* allele shows a lower induction than wild-type cells, but the same induction profile. Finally, we generated *ref2 reg1* mutant cells and its response to tunicamycin is similar to *glc7-109* allele, although it displays a hypersensitive phenotype to tunicamycin such as *reg1* mutant cells (data not shown). That may indicate that both subunits are essential for UPR regulation.

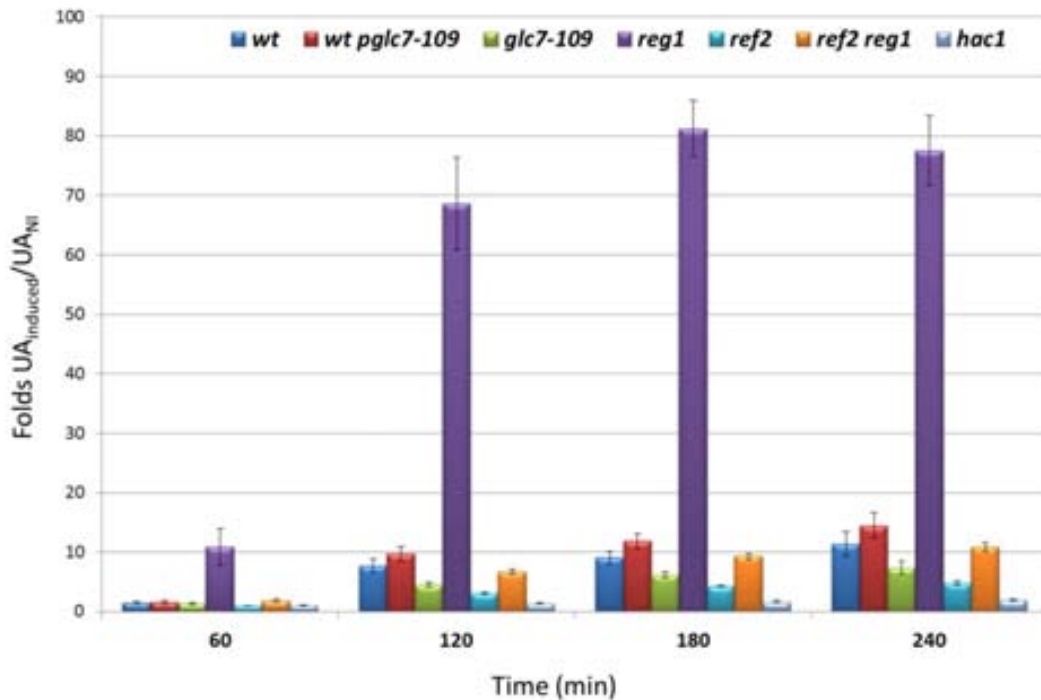


Figure 58. *reg1* mutant cells display an uncontrolled UPR. Wild-type and the indicated isogenic derivatives were transformed with the construct pMCZ-Y and cultures were grown until reached 0.8 OD₆₆₀ in YPD (pH 5.5). Cells were transferred to fresh YPD with 2 μ g/ml tunicamycin and cells collected at the indicated times at 28°C. β -galactosidase activity was measured as described in *Experimental procedures*. Data are mean \pm SEM from at least six independent clones. Folds are referred to non-induced cultures.

From this section, we will continue focus on both Glc7-regulatory subunits: Ref2 and Reg1. We will try to demonstrate that both subunits are important for UPR regulation but in different ways. Our Ref2-hypothesis is that the tolerance phenotype is due to the aneuploidy; meanwhile Reg1-hypothesis is that this subunit regulate Ire1 dephosphorylation.

4.4 Ref2, a possible UPR regulator

4.4.1 Tunicamycin tolerance Ire1-independent

Firstly, we generated a new strain *ref2 ire1* (YJFD88) in order to abolish the main UPR pathway. The lack of both *REF2* and *IRE1* causes a tolerance phenotype to tunicamycin (Figure 59A). Moreover, *ref2 ire1* mutant cells activates UPR as *ref2* mutant cells, when yeast cells are switched to UPR inducers such as tunicamycin, DTT and 2-mercaptoethanol (Figure 59B). Our results indicate that *ref2* mutant cells tolerance is not due to a specific activation of UPR through Ire1 kinase. That might imply a mechanism for *ref2* mutant cells tunicamycin tolerance Ire1-independent.

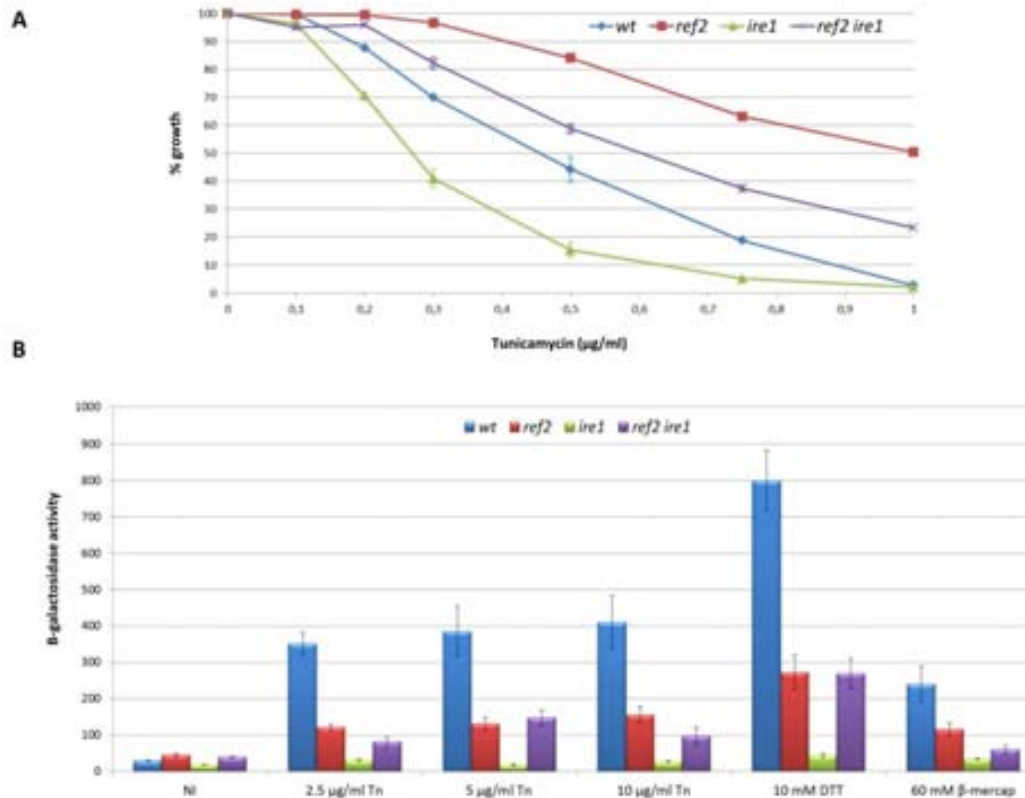


Figure 59. The lack of Ref2 causes a tolerant phenotype to ER-inducers. A) Liquid growth of wild-type strain (**wt**), cells lacking *REF2* (**ref2**) or *IRE1* (**ire1**) and cells lacking both *REF2* and *IRE1* (**ref2 ire1**; YJFD88) were inoculated at 0.02 OD₆₅₀ with YPD (pH 5.5) plus the indicated tunicamycin concentrations. Growth at 28°C was monitored for 16 h (**wt** and **ire1**) or 24 h (**ref2** and **ref2 ire1**). Data are mean ± SEM from at least 9 independent clones. **B)** Wild-type and the indicated isogenic derivatives were transformed with the construct pMCZ-Y and cultures were grown until reached 0.8 OD₆₆₀ in YPD (pH 5.5). Cells were transferred to fresh YPD with the indicated UPR inducers for 90 min at 28°C. β-galactosidase activity was measured as described in *Experimental procedures*. Data are mean ± SEM from at least six independent clones.

(Shamu & Walter, 1996) already reported, when they measured UPR transcription in *ire1* mutant cells under tunicamycin conditions, those cells still display one third of unfolded protein response which seemed Ire1-independent. Actually, (Schröder, Clark, & Kaufman, 2003) explained a plausible solution for the residual activation by demonstrating that moderate transcriptional activation of a core promoter occurs after induction of ER stress, and that the classic UPR is dispensable for this response. Furthermore, (Leber, Bernales, & Walter, 2004) hypothesize that *HAC1* mRNA transcription is regulated, resulting in control of Hac1 abundance whose regulation responds to a bipartite signal that emanates from the ER and is communicated in a Ire1-independent pathway called S-UPR; but they just propose the possible pathway not the solution. In the same issue, (Patil, Li, & Walter, 2004) demonstrates that Gcn2-Gcn4 are important and necessary for unfolded protein response through the activation of Hac1-independent genes. Basically, these two papers explain a mechanism for what the

unfolded protein response can respond to higher UPR inducers concentrations by activating not only Hac1-dependent genes but also Ire1- / Hac1-independent responses. So, this Ire1-independent response in *ref2* mutant cells might be possible to other mechanisms which may activate putative UPR genes, which may not possess a UPR element. For that *ref2* mutant cells may display lower induction to UPR-lacZ reporter than wild-type cells.

4.4.2 *ref2* cells phenotype is independent of holo-CPF

Given the tunicamycin tolerance of *ref2* mutant cells (Figure 55), as a component of the APT-complex, it is reasonable to consider whether this tolerant phenotype may be shared by other holo-CPF components. We reasoned that, if this was the case, mutations in other components of the complex would yield phenotypes reminiscent of those of the *ref2* mutant cells. As many members of the APT-complex are essential (including Pta1), we had to resort in most cases to temperature sensitive mutants cultured at sublethal temperatures (28°C or 37°C).

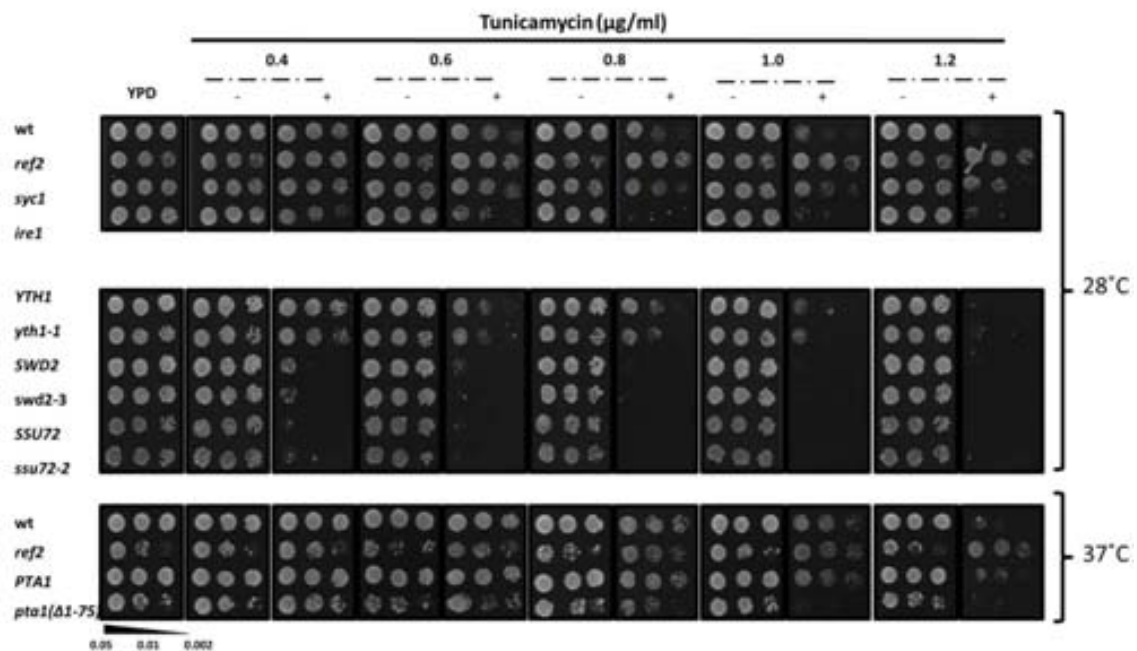


Figure 60. The *ref2* cells phenotype is not shared by other members of CPF. Three dilutions of wild-type and its isogenic derivatives were spotted on to YPD plates plus indicated tunicamycin concentrations (+) or DMSO (-). Growth at 28°C or 37 °C were monitored for 2-3 days.

Interestingly, none of the holo-CPF components display a tolerant phenotype (Figure 60). Basically, all of them seem to behave as each wild-type strain. Surprisingly, those mutants should accumulate more unfunctional RNA due to the problems on RNA or snoRNA processing and maturation. Anyone could think that this deficiency would increase the accumulation of

unfolded proteins and, then, a synthetic increase due to tunicamycin presence should cause a saturated unfolded protein response trying either to refold or to degrade those proteins implying a hypersensitive phenotype. That means that the glucose molecules spent in not producing biomass (*Figure 49*) might be due to RNA degradation.

4.4.3 *ref2* cells tolerant phenotype is genetic background specific

As previously performed in aneuploidy studies, we analyzed in drop-test the new *ref2* mutant cells generated from several genetic backgrounds. Exemplified in *Figure 61A*, *ref2* BY4741 mutant cells display a tolerant phenotype to tunicamycin, but *ref2* 1700 mutant cells behaves as its wild-type strain. Those cells have behaved similar either to all aneuploidy stressors and phenotypes or to ionic homeostasis responses. So, the difference may be the possible aneuploidy, which has not been determined yet, in *ref2* 1700 mutant cells.

Moreover, we have already described that *glc7-109* allele has an opposite phenotype than *ref2* mutant cells to tunicamycin (*Figure 57A*), but what surprised us is that the double mutant *glc7-109 ref2* mutant cells show a tolerant phenotype to tunicamycin (*Figure 61B*). Interestingly, the phenotype due to the lack of the non-essential regulatory subunit prevails over the *Glc7* allele. This situation could be explained because *ref2* mutant cells have an aneuploidy in chromosome II and XII that *glc7-109* allele cells might not display.

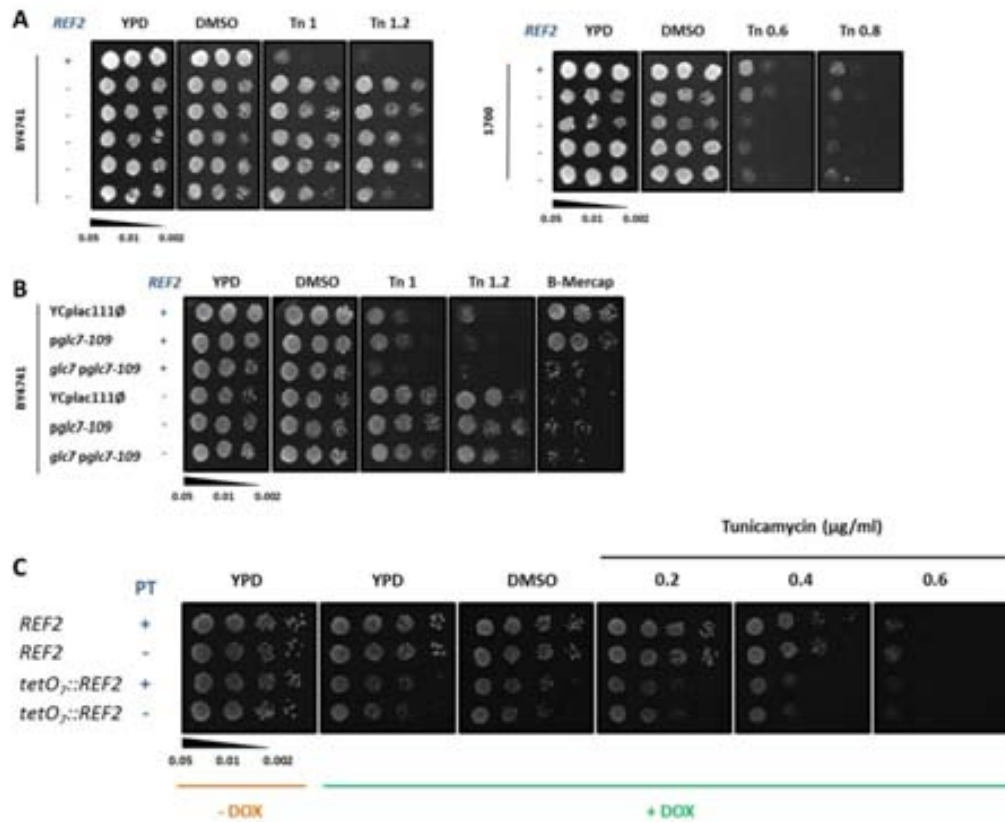


Figure 61. *ref2* cells has a unique tunicamycin tolerance in BY4741 background. **A (left panel)** Three dilutions from wild-type and *ref2* cells (BY4741 *ref2* and YJFD1-4) were spotted on plates containing YPD plus 1.0 µg/ml tunicamycin (Tn 1.0) and 1.2 µg/ml tunicamycin (Tn 1.2). Growth at 28°C was monitored after 2-3 days. **A (right panel)** 1700 wild-type and its *ref2* derivative cells (*ref2*_N1-N4; YJFD92) were spotted on plates containing YPD plus 0.6 µg/ml tunicamycin (Tn 0.6) and 0.8 µg/ml tunicamycin (Tn 0.8). Growth at 28°C was monitored after 2-3 days. **B**) Strains used in this dot test: BY4741 wild-type transformed with YCplac111Ø (YJFD34), *pglc7-109* called pJFD11 (YJFD35) and cassette *glc7::nat1* plus *pglc7-109* (YJFD36); BY4741 *ref2* strain was equally transformed generating YJFD37, YJFD38 and YJFD39, respectively. Three dilutions from indicated cultures were spotted on plates containing YPD plus: 1.0 µg/ml tunicamycin (Tn 1.0), 1.2 µg/ml tunicamycin (Tn 1.2) and 40 mM 2-Mercapethanol (β-Mercap). Growth at 28°C was monitored after 2-3 days. **C**) Three dilutions from cultures of wild-type strain CML476 and its derivative *tetO7::REF2* (YJFD16) were pre-treated with 100 µg/ml doxycycline for 8 h (PT +) or without pre-treatment (PT -) and then spotted on plates containing YPD plus either the indicated tunicamycin concentrations or presence/absence of 100 µg/ml doxycycline (+DOX/-DOX). Growth at 28°C was monitored after 2-3 days.

Finally, in *Figure 61C*, we performed a drop test of *tetO7::REF2* strain to tunicamycin. These results correlate with the lack of tunicamycin phenotype determined in holo-CPF mutants. As extensively explained in *Results and Discussion, section 3.1*, this strain only displays snoRNA maturation defects, but we could not determine any aneuploidy after 120 h treatment with doxycycline. Under tunicamycin conditions, this strain does not display any improvement in growth than wild-type strain; meaning that only defects on snoRNA processing are not enough to cause tunicamycin tolerance.

In (Steffen et al., 2012), they demonstrate that deletion on ribosomal protein genes enhances tunicamycin resistance independent of the transcription factor Hac1. Moreover, their data support a model in which reduced translation due to slow growth is protective against ER stress by a mechanism distinct from the canonical ER stress response pathway. This evidence is complemented with the idea that UPR expands the endoplasmic reticulum of yeast cells 5 folds, at least; meaning that a slow growth could help the expansion of ER (Bernales, McDonald, & Walter, 2006). This ER-expansion decreases the concentration of unfolded protein which triggers the decreasing of UPR.

To sum up, although aneuploid cells display an accumulation of unfolded proteins implying hypersensitivity to tunicamycin (Eduardo M Torres et al., 2007). Our results point out that it may be the aneuploidy that confers the tunicamycin tolerance phenotype and it is Ire1-independent.

4.4.4 Evolutionary response to tunicamycin

(Yona et al., 2012) performs dynamic and prolonged laboratory evolution experiments in yeast. They demonstrate that aneuploidy, which is rapidly gained under stress, is a transient solution that is replaced by focal, refined, and sustainable solutions that require more time to evolve. They describe that prolonged heat stress duplicates chromosome III and under alkaline pH conditions it is chromosome V duplicated, before the specific and accurate response is generated. Moreover, aneuploidy is the first step in order to more specific changes (Sheltzer et al., 2011; Eduardo M Torres et al., 2010). For that, we decided to perform an evolution experiment of wild-type strain under either 0.5 or 0.75 $\mu\text{g/ml}$ tunicamycin conditions as described in *Figure 62A*. These concentrations were defined in *Figure 59A* where the wild-type cells survival under tunicamycin conditions is 40% and 20%, respectively.

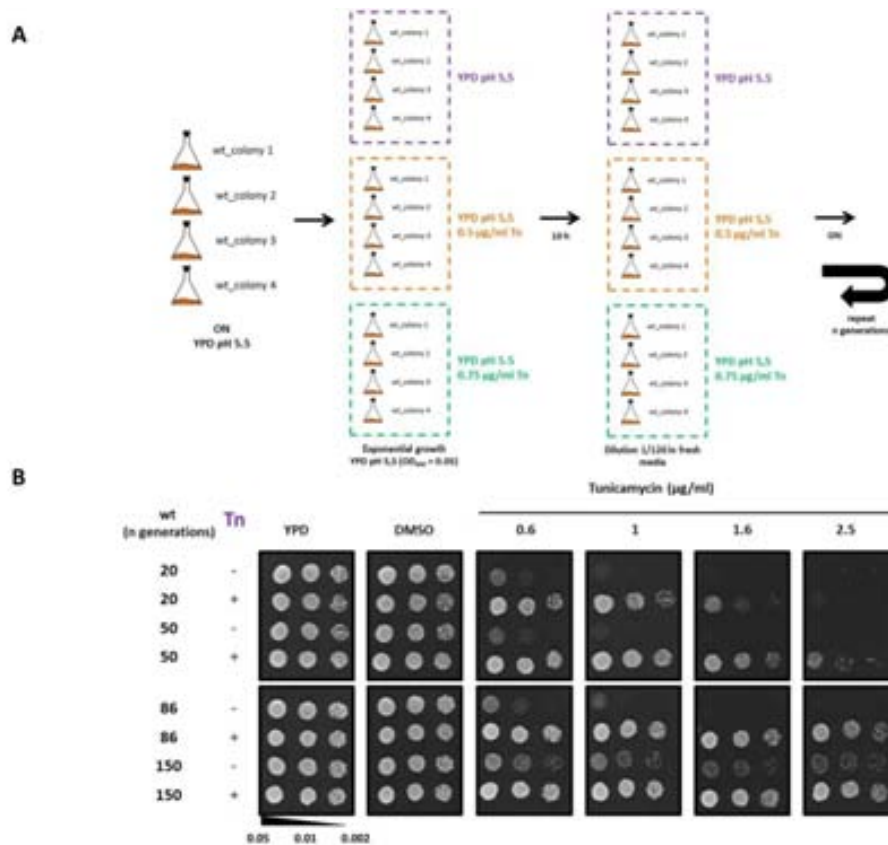


Figure 62. Our new strains treated with tunicamycin for generations show an increase in tunicamycin tolerance phenotype. **A)** Evolutionary tunicamycin experiment design. Basically, wild-type cells were treated with 0.5 / 0.75 µg/ml tunicamycin for the indicated number of generations (n). Initially, cells were inoculated on YPD (pH 5.5) at 0.05 OD₆₆₀ with presence or absence of tunicamycin, after 10 h approximately, the number of generations (n generations) was annotated and cells were diluted 1/120 in fresh YPD (pH 5.5) plus tunicamycin and incubated overnight at 28°C. The experiment was repeated until 120 yeast generations. **B)** Three dilutions from cultures of wild-type strain induced with 0.5 µg/ml tunicamycin for n generations (Tn +) or without tunicamycin treatment (Tn -) were spotted on YPD plates plus the indicated tunicamycin concentrations. Growth at 28°C was monitored after 2 days.

In order to follow the evolution experiment we performed three checkpoints: first, we determined the growth rate and cells under tunicamycin conditions grew slower than wild-type cells in YPD; secondly, we analyzed the saturation levels after overnight cultures, where initial generation strains had lower OD₆₆₀ density than last generation strains; and thirdly, we performed a drop-test at different number of generations and cells display an increase in tunicamycin tolerance phenotype (Figure 62B).

4.4.5 Tunicamycin tolerance implies a chromosome II duplication

As performed in aneuploidy experiments, we performed DNA microarray experiments of the same wild-type strain in four different number of generations (20, 50, 86 and 150 n) compared to the wild-type strain in YPD conditions (Figure 63).

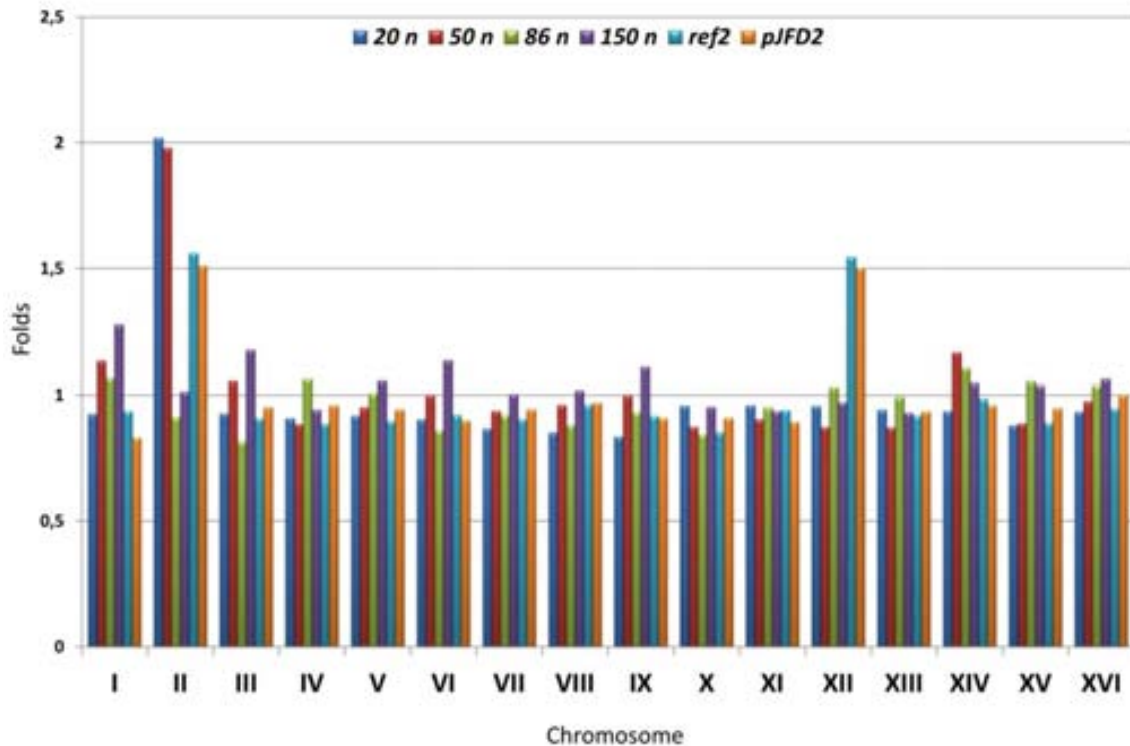


Figure 63. Strains treated with tunicamycin for 20 and 50 generations display an aneuploidy in chromosome II. Total RNA extraction from wild-type treated with 0.5 $\mu\text{g}/\text{ml}$ tunicamycin for 20, 50, 86 and 120 generations as described in *Experimental procedures*. Once analyzed the DNA microarray experiments, the mean of each chromosome was calculated for indicated strains, graphed in folds and compared to DNA microarray experiment from BY4741 *ref2* (*ref2*) and BY4741 *ref2* transformed with the plasmid which contains the mutated version $\text{Ref2}^{\text{E374A}}$ (*pJFD2*) from *Figure 52C*.

As evolution experiments done in other conditions, we have been able to follow the appearance of an aneuploidy in chromosome II and the accurate response which is observed in the 120 n strain. The comparison with *ref2* and *pJFD2* DNA experiments shows a similar profile than 20 and 50 n strains, showing a fold transcription duplication from the whole chromosome II which may indicate the double DNA dotation in this specific chromosome (Tang & Amon, 2013; E M Torres et al., 2010).

Obviously, we also analyzed the functional categories of induced and repressed genes of tunicamycin-evolution experiment together with a wild-type strain induced with 1 $\mu\text{g}/\text{ml}$ tunicamycin for 1 h (**wt Tn**) (*Table 15*). Interestingly, the induced genes in 20 n strain displays the functional category of unfolded protein response similar to the functional categories represented in **wt Tn** experiment. That possibly mean that the activation of genes of the UPR are short-term adaptation to UPR inducers, but prolonged stress implies a different response. In repressed genes, most of the strains do not show any representative functional category. Otherwise, 50 n strain repressed genes are significantly either ribosome proteins or ribosome

biogenesis which could correlate that deficiencies in ribosome protein are tunicamycin tolerant strains (Steffen et al., 2012).

A				B			
Strain	Induced Categories	P-value	Genes % Ind	Strain	Repressed Categories	P-value	Genes % Rep
20 n	Stress response	2.93E-05	248 5.94	20 n	None		279 5.73
	Cell rescue, defense and virulence	2.23E-04					
	Unfolded protein response	3.33E-04					
	Sugar, glucoside, glycol and carbohydrate anabolism	3.57E-04					
50 n	Aminoacyl-tRNA-synthetases	9.33E-05	394 10.30	50 n	Ribosomal proteins	1.96E-08	381 9.96
	Protein synthesis	1.00E-08					
86 n	Glycolysis and gluconeogenesis	7.63E-07	124 2.88		Protein synthesis	9.63E-11	
	Translation	2.26E-05					
	Energy	5.43E-06					
	Aminoacyl-tRNA-synthetases	5.57E-05					
150 n	Energy	1.49E-05	197 4.87	Electron transport and membrane-associated energy conservation	1.38E-06		
	Glycolysis and gluconeogenesis	3.77E-04					
	Amine / polyamine transport	4.83E-04					
	Fermentation	4.93E-04					
wt 7n	Protein Fate (folding, modification, destination)	2.05E-04	149 4.00	86 n	None		274 6.35
	Protein folding and stabilization	4.49E-05					
	Protein modification	1.07E-04					
	Modification with sugar residues	9.23E-04					
wt 7n				150 n	Electron transport and membrane-associated energy conservation	1.96E-08	195 4.82
				Respiration	9.25E-07		
				Energy generation (e.g. ATP synthase)	2.53E-05		
				Aerobic respiration	8.96E-05		
				Energy conversion and regeneration	2.76E-04		
				Electron transport	1.87E-04		
			wt 7n	Peroxisome reaction	8.53E-04	175 3.67	

Table 15. Characterization of induced and repressed genes in tunicamycin-evolution experiment. Analysis of induced (A) genes (relative expression > 1.80 folds) or repressed (B) genes (relative expression < 0.55 folds) of each strain were obtained by the functional categories classifier tool of MIPS (Ruepp et al., 2004). Only functional categories with P-value < 10^{-4} were characterized and either the percentage of induced genes (% Ind) or repressed genes (% Rep) were calculated respect the total of genes with existing data.

We have graphed the genes of chromosome II in to order see the distribution of induced genes in this chromosome (Figure 64). Interestingly, in 20 n strain, induced genes are nearly uniformly distributed along both arms of the chromosome II; but following the evolution experiment, in the next strain (50 n) the induced genes are mainly located in the right arm of chromosome II. Finally, both last strains (86 n and 120 n) do not show a specific distribution of induced genes in this chromosome; reaffirming that this chromosome does not display a duplication at long-time samples.

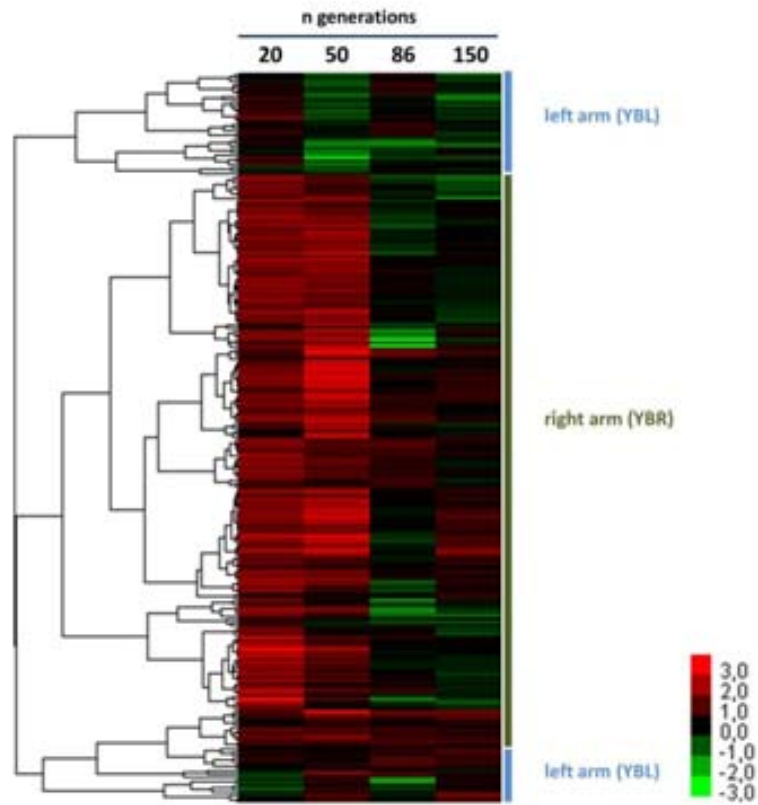


Figure 64. The right arm of chromosome II display a duplication in strains treated with tunicamycin for 20 and 50 n. DNA microarray data from gens located on chromosome II in the indicated strains were graphed using a hierarchical cluster, which was performed using array correlation parameter plus complete linkage clustering, and data was represented by Treeview toll v1.6 from Eisen's lab software.

Gene Name	Null mutant ¹	Description ¹
FES1	Viable	Hsp70 (Ssa1) nucleotide exchange factor; required for the release of misfolded proteins from the Hsp70 system to the Ub-proteasome machinery for destruction; cytosolic homolog of Sil1, which is the nucleotide exchange factor for BiP (Kar2) in the endoplasmic reticulum.
YBR287W	Viable	Protein of unknown function; green fluorescent protein (GFP)-fusion protein localizes to the ER.
SSH1	Viable	Subunit of the Ssh1 translocon complex; Sec61 homolog involved in co-translational pathway of protein translocation.
PHO5	Viable	Repressible acid phosphatase that also mediates extracellular nucleotide-derived phosphate hydrolysis; secretory pathway derived cell surface glycoprotein; induced by phosphate starvation and coordinately regulated by <i>PHO4</i> and <i>PHO2</i> .
PHO88	Viable	Probable membrane protein; involved in phosphate transport.
UTP20	Inviabile	Component of the small-subunit (<i>SSU</i>) processome, which is involved in the biogenesis of the 18S rRNA.
APD1	Viable	Protein of unknown function; required for normal localization of actin patches and for normal tolerance of sodium ions and hydrogen peroxide localized to both cytoplasm and nucleus.
AKL1	Viable	Ser-Thr protein kinase; member (with Ark1p and Prk1p) of the Ark kinase family which is involved in endocytosis and actin cytoskeleton organization
RRT2	Viable	Protein required for last step of diphthamide biosynthesis and also involved in endosomal recycling for recycling internalized cell-surface proteins.
HMT1	Viable	Nuclear SAM-dependent mono- and asymmetric methyltransferase which modifies hnRNPs, including Npl3 and Hrp1, affecting their activity and nuclear export. It also methylates U1 snRNP protein Snp1 and ribosomal protein Rps2p and interaction with Rpd3 is important for Rpd3 recruitment to the subtelomeric region.
ALG1	Inviabile	Mannosyltransferase; involved in asparagine-linked glycosylation in the endoplasmic reticulum (ER).

Table 16. Gene induced in chromosome II from the early response to tunicamycin. We compared the genes induced in chromosome II from the 20 n, 50 n, *ref2* and *pJFD2* strains (¡Error! No se encuentra el origen de la referencia.). Data from *Saccharomyces* Genome Database (SGD).

We compared the induced genes in chromosome II in the early response to tunicamycin with the induced genes in *ref2* cells and these cells containing the plasmid with point mutation of Ref2^{F374A} (*pJFD2*) triggering eleven common induced genes. Therefore, these genes cannot be classified in any functional category by MIPS. However, we can correlate both the response to tunicamycin and duplication of chromosome II.

Firstly, the overexpression of *ALG1* may suppress the effect of tunicamycin which is an inhibitor of Alg7 (Lehrman, 1991). Both genes encode ER-essential proteins and are involved in dolichol pathway of protein asparagine-linked glycosylation, whereas Alg7 transfers Glc-Nac-P (N-acetylglucosamine phosphate) from UDP-GlcNac to Dol-P (dolichol phosphate), Alg1 catalyzes the addition of the first mannose moiety to the growing lipid-linked oligosaccharide (Dol-PP-GlcNac2) (Robbins, 1991). N-linked protein glycosylation is essential for several functions in yeast cells, such as immune response, intracellular targeting, intercellular recognition, and protein folding and stability (extensively reviewed in (Weerapana & Imperiali,

2006). Therefore, the transcriptional induction of *ALG1* may maintain the N-linked protein glycosylation function under tunicamycin conditions. Additionally, listed in *Table 16*, *FES2*, *YBR287W*, *SSH1* and *PHO5* are involved either in ER functions or in protein secretory pathways of glycoproteins. Moreover, *APD1* and *AKL1* are involved in actin patches. So, all these genes work together to maintain unfolded protein response.

On the hand, *UTP20*, *HMT1* and *RRT2* encode proteins whose function is involved in rDNA regulation. Ribosome biogenesis is a complex, tightly regulated process consisting of ribosomal DNA (rDNA) transcription, ribosomal RNA (rRNA) processing, ribosomal protein synthesis, and ribosome assembly. Its regulation is important for the control of cellular growth because it dictates the availability of the number of ribosomes required for efficient protein synthesis. Of particular importance is the synthesis of rRNA by RNA polymerase I (Pol I), which comprises the majority of all transcription in growing yeast (reviewed in (Hontz, Niederer, Johnson, & Smith, 2009)) One of the common hallmarks shared by rapidly proliferating cancer cells is an increase in rDNA transcription (White, 2005) which happens in *ref2* cells (*Figure 47*). Therefore, (Hontz et al., 2009) describes new fourteen genes involved in a new function: regulators of rDNA transcription (RRT), which their transcription is induced when the levels of rDNA transcription are increased due to growth conditions. So, aneuploid cells need these genes to regulate the ribosome concentration to be able to synthesize more proteins.

4.4.6 Long-term adaptation to tunicamycin growth

We decided to analyze only induced genes on long-term strains (86 n and 120 n) (*Figure 65*), because our interests reside on looking for the accurate and specific response which deletes the duplication of chromosome II (*Figure 64*). We figure out two different categories of genes: retrotransposons and genes involved on yeast global adaptation.

Retrotransposons have broadly studied because Ty elements transpose by a mechanism similar to retrovirus reverse transcription and integration (Garfinkel, Nyswaner, Wang, & Cho, 2003; Xu & Boeke, 1987). Moreover, recently, it has been described that chromosomal rearrangements such as duplications and deletions are key factors in evolutionary processes between strains because they promote genomic plasticity processed by differences in Ty1 retrotransposon activity (Fritsch et al., 2009). Another study proposed that Ty1 integrase accepts non-Ty DNA as substrate modifying DNA genomic (Friedl, Kiechle, Maxeiner, Schiestl, & Eckardt-Schupp, 2010). So, we conclude that this induced

retrotransposon activity in long-term strains may be due to the DNA genomic modifications needed for tunicamycin adaptation.

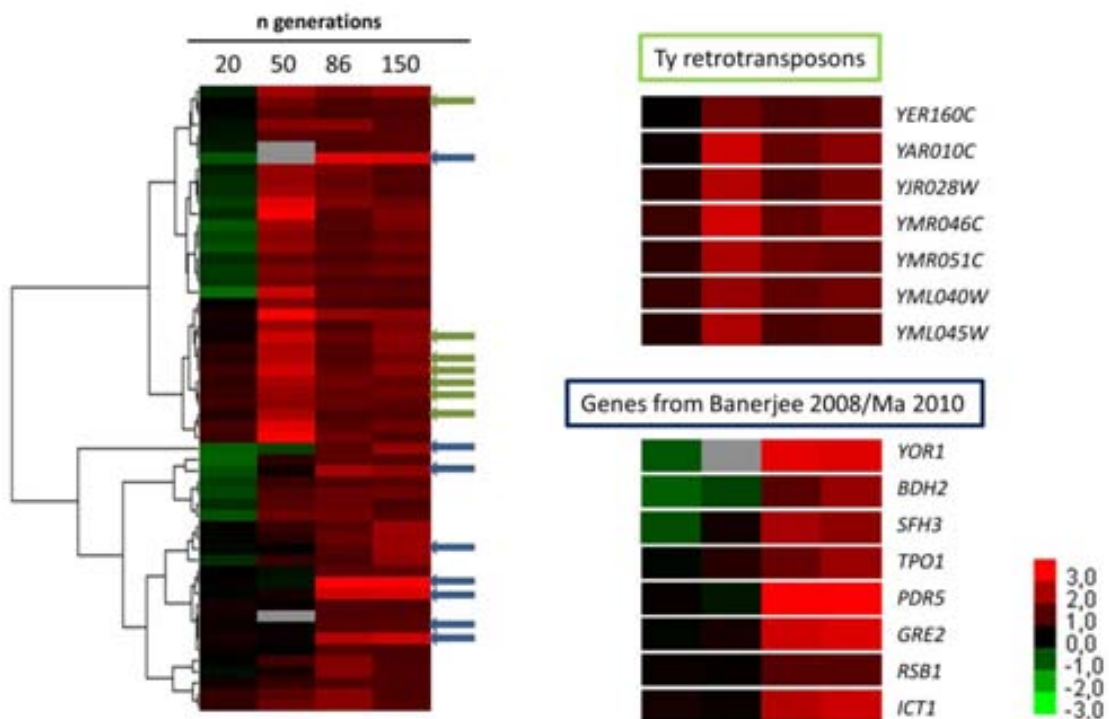


Figure 65. Wild-type strains treated with tunicamycin for 86 and 120 generations show an accurate long-term response similar to other drugs or inducers. **Left panel:** 56 selected genes by expression using the parameters: < 1.85 folds at $20n$ + > 1.85 folds at $86n$ + > 1.85 folds at $150n$ were represented in a hierarchical cluster which was performed using array correlation parameter plus complete linkage clustering, and data was represented by Treeview toll v1.6 from Eisen's lab software. **Right panel:** Characteristic genes found in the analysis with the same parameter used above: **retrotransposons** genes and **induced** genes from (Banerjee et al., 2008; Ma & Liu, 2010) are located on the hierarchical cluster representation.

On the other hand, it has been already described in different evolution experiments to several stressors (Banerjee et al., 2008; Liu, Ma, & Song, 2009; Ma & Liu, 2010). They have identified some transcription factor genes *YAP1*, *PDR1*, *PDR3*, *RPN4*, and *HSF1* were identified as key regulatory genes for yeast global adaptation regulation multidrug resistance, oxidative stress, protein degradation/protection and DNA repairing. Then, they also describe the high ratio of expression of *PDR* genes which encode plasma membrane proteins and function as transporter of ATP-binding cassette proteins. The large number of induced *PDR* genes observed by several studies suggests a hypothesis of the important *PDR* function of pumping drugs and endogenous toxic metabolites to maintain cell viability. Important *PDR* gene functions include specific transporter ATPase gene *RSB1*, toxin transporter genes *TPO1* and *TPO4*, and multiple cellular transport facilitator genes *PDR5*, *PDR12*, *PDR15*, *YOR1*, and *SNQ2*. Our strains have induced transcription from some of these genes listed in Figure 65. So, our

strains show the global transcription adaptation and possible specific induced genes due to tunicamycin adaptation. For that, we analyzed these new strains under several stress conditions (Figure 66).

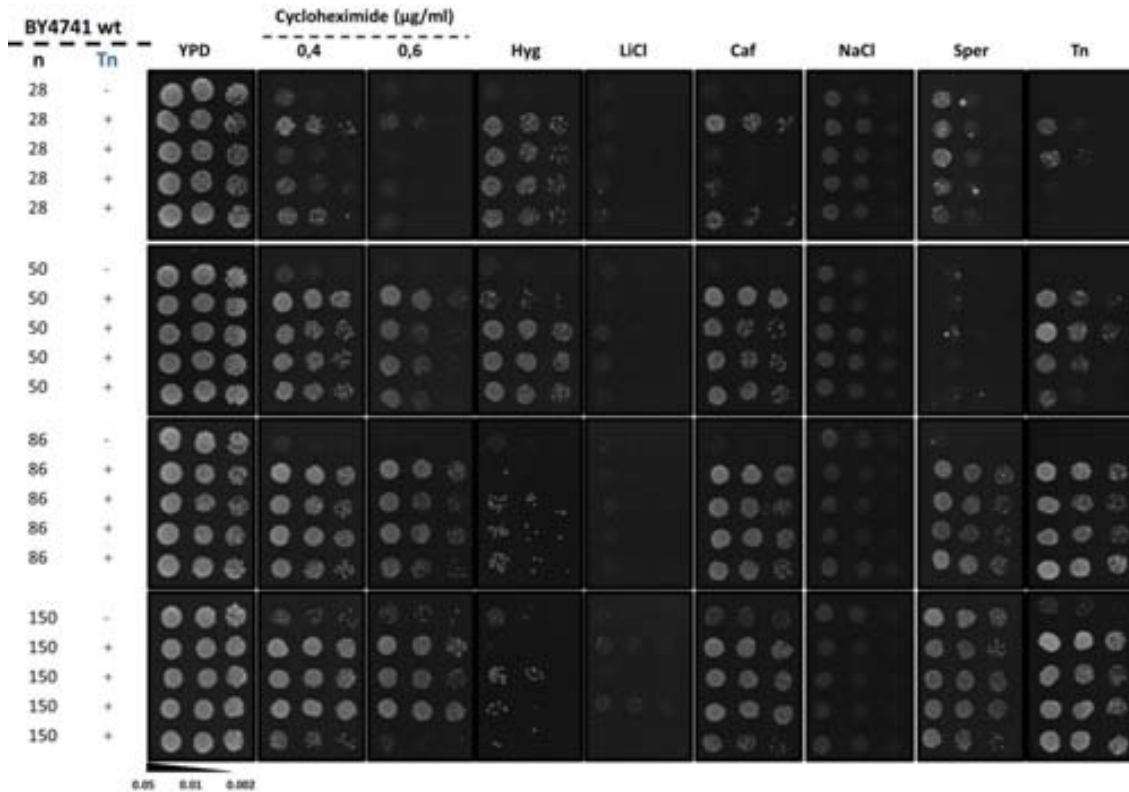


Figure 66. Wild-type strains treated with tunicamycin display different phenotypes to several drugs. Three dilutions from cultures of wild-type strain induced with 0.5 $\mu\text{g/ml}$ tunicamycin for n generations (**Tn +**) or without tunicamycin treatment (**Tn -**) were spotted on YPD plates plus the following stressors: cycloheximide at the indicated concentrations; 70 mM hygromycin B (**Hyg**); 20 mM caffeine (**Caf**); 1.2 M NaCl (**NaCl**); 200 mM LiCl (**LiCl**); 0.7 $\mu\text{g/ml}$ spermine (**Sper**) and 2 $\mu\text{g/ml}$ tunicamycin (**Tn**). Growth at 28°C was monitored after 2-3 days.

Firstly, the dot test was performed with all the colonies from wild-type used in the evolution experiment. None of these strains show a tolerant phenotype to cations (lithium and sodium), meaning that this biological adaptation follows another pathway. Two protein synthesis inhibitors (cycloheximide and hygromycin B) display different adaptation profile. Since cycloheximide is lethal for 20 n strain, which is understandable because chromosome II duplication causes this hypersensitive phenotype (Eduardo M Torres et al., 2007), but then cells display a tolerant phenotype. Moreover, strains with aneuploidy in chromosome II (20 n and 50 n) are tolerant to hygromycin B, but the loss of the aneuploidy described suppresses this phenotype. Finally, long-term strains show a tolerant phenotype to spermine and caffeine. Both synthetic stressors are not functionally linked; spermine is a polyamine which effects

growth, proliferation, differentiation, apoptosis and potential membrane (Erez & Kahana, 2001) and; caffeine causes decreased TOR activity plus increased life span (Reinke, Chen, Aronova, & Powers, 2006; Wanke et al., 2008). Additionally, (Juchimiuk et al., 2010) describes that the defect in dolichol-dependent glycosylation aggravates hypersensitivity to anti-fungal drugs, such as caspofungin and amphotericin B, due to an aberrant cell wall structure and composition. Therefore, the use of tunicamycin, an inhibitor of Alg7, may indirectly adapt yeast cells to anti-fungal drug resistance due to the secondary effects of this UPR inducer.

4.4.7 Defects either in CWI or calcium homeostasis suppresses tunicamycin tolerance phenotype in *ref2* mutant cells

It has been deeply described that unfolded protein response (UPR) is not alone in endoplasmatic reticulum homeostatic regulation. This is not strange because proper function of ER is needed to avoid unfolded proteins which appear when yeast cells are under several stresses. So far, three pathways have been reported to be essential for a proper UPR regulation and vice versa: **1**) calcineurin pathway (Myriam Bonilla, Nastase, & Cunningham, 2002; Varadarajan et al., 2013); **2**) cell wall integrity regulation (Scrimale, Didone, de Mesy Bentley, & Krysan, 2009) and **3**) osmotic Hog1 regulation (Bicknell et al., 2010; Torres-Quiroz et al., 2010). For that, we used our collection of double mutants *ref2* plus either cell wall integrity components or calcineurin regulators to perform not only a phenotypical but also the transcriptional study of UPR (Figure 67 and Figure 68).

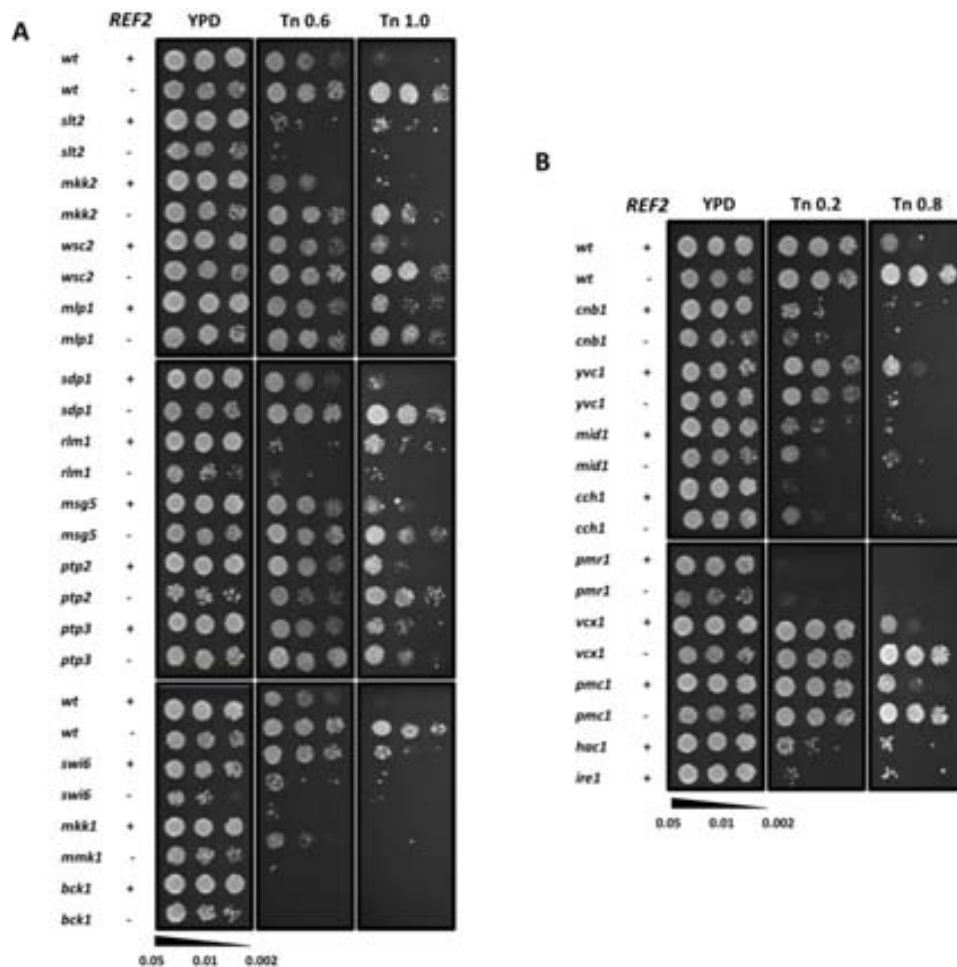


Figure 67. Phenotypal analysis of cell wall integrity pathway and calcium homeostasis in *ref2* cells. A) Three dilutions from cultures of wild-type strain and mutants from cell wall integrity components combined with disruption of *REF2* (-) were spotted on YPD plus 0.6 $\mu\text{g/ml}$ tunicamycin (**Tn 0.6**) and plus 1.0 $\mu\text{g/ml}$ tunicamycin (**Tn 1.0**). Growth at 28°C was monitored for 2-3 days. **B)** Three dilutions from cultures of wild-type strain and mutants from calcium homeostasis combined with disruption of *REF2* (-) were spotted on YPD plus 0.2 $\mu\text{g/ml}$ tunicamycin (**Tn 0.2**) and plus 0.8 $\mu\text{g/ml}$ tunicamycin (**Tn 0.8**). Growth at 28°C was monitored for 2-3 days.

As shown in *Figure 67A*, lack of *SLT2*, *MKK2*, *RLM1*, *MKK1*, *SWI6* or *BCK1* causes hypersensitivity to tunicamycin which has already described by (Chen et al., 2005). On the other hand, *ptp3* mutant cells display a tolerant phenotype to UPR inducer. As expected, not only does the deletion of *SLT2*, *BCK1* or *MKK1* in *ref2* mutant cells suppress the tolerant phenotype of the single mutant *ref2* cells but also does it imply a hypersensitive phenotype (*Figure 42*). Moreover, deletion of *REF2* in *mkk2* mutant cells restores the wild-type phenotype at UPR stressors; even so these cells become tolerant to tunicamycin. These results show that the lack of the transcription factors *RLM1* and *SWI6* causes a hypersensitive phenotype either in single or double mutants. The lack of *REF2* causes a decreased transcription of UPR under tunicamycin conditions and the response of UPR is nearly shut down in double mutants' *slt2*, *bck1* and *rlm1* combined with *ref2*.

Finally, the lack of *REF2* together with *CCH1* or *MID1* or *CNB1* or *PMR1* causes a hypersensitive phenotype. Deletion of either *CCH1* or *MID1* has already been described the unviability to growth under tunicamycin conditions (Myriam Bonilla et al., 2002), and these mutations are able to revert the *ref2* strain tunicamycin phenotype. Moreover, *CNB1* is needed to regulate the calcium channel Mid1-Cch1 (figure calcium), so *cnb1* cells also display a hypersensitive phenotype under tunicamycin conditions. Double mutants' *ref2 cnb1*, *ref2 cch1* and *ref2 mid1* have no induction of UPRE plasmid fused to *lacZ* under tunicamycin conditions, meaning that calcium is needed for ER homeostasis. Finally, ER of yeast employs Ca^{2+} for the folding or processing of secretory proteins. Previously it was shown that mutants lacking *PMR1* failed to retain a heterologous secretory protein in the ER (Rudolph et al., 1989) and failed to degrade misfolded proteins in the ER (Durr et al., 1998). Furthermore, (Yadav et al., 2007) not only described the hypersensitive tunicamycin phenotype of *pmr1* cells but also reported that tunicamycin toxicity may be exacerbated by depletion of manganese ions from the Golgi, because endoglycosidases are Mn^{2+} -requiring enzymes. For these reasons both *pmr1* and *pmr1 ref2* strains display a hypersensitive phenotype to tunicamycin, but not an impaired UPRE induction.

These results, together with the phenotypes described for *ref2 pmr1* strain (calci, lithium and CWI), confirm that there is an interaction between Ref2 and Pmr1, through a possible Glc7 regulation.

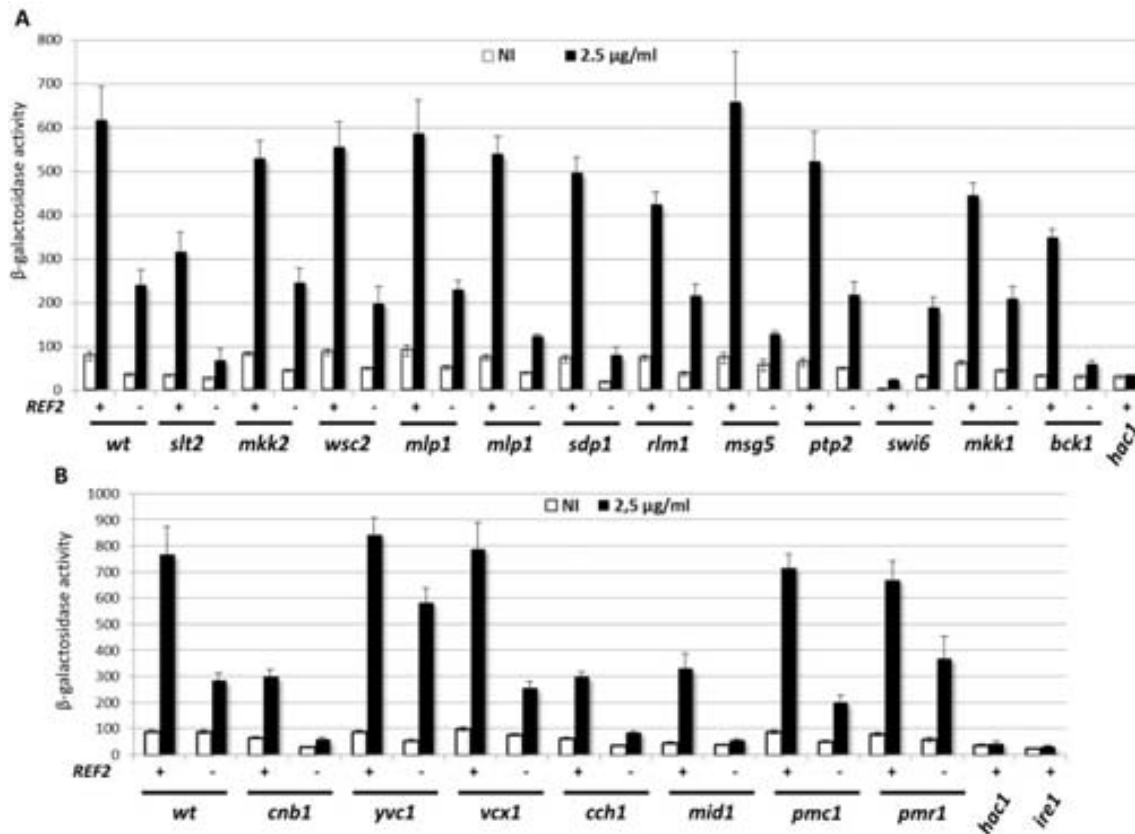


Figure 68. UPRE analysis on cell wall integrity pathway and calcium homeostasis in *ref2* cells. **A)** Wild-type and mutants on cell wall integrity components were transformed with the construct pMCZ-Y and cultures were grown until reached 0.8 OD₆₆₀ in YPD (pH 5.5). Cells were transferred to fresh YPD with 2.5 µg/ml tunicamycin for 90 min at 28°C. β-galactosidase activity was determined as described in *Experimental procedures*. Data are mean ± SEM from at least six independent clones. **B)** Wild-type and mutants on calcium homeostasis components were transformed with the construct pMCZ-Y and cultures were grown until reached 0.8 OD₆₆₀ in YPD (pH 5.5). Cells were transferred to fresh YPD with 2.5 µg/ml tunicamycin for 90 min at 28°C. β-galactosidase activity was determined as described in *Experimental procedures*. Data are mean ± SEM from at least six independent clones.

4.5 Reg1, a possible UPR regulator

4.5.1 Deletion of *SNF1* alleviates *reg1* mutant cells phenotype to tunicamycin

Our results and (S.-X. Tan, Teo, Lam, Dawes, & Perrone, 2009b) describe that *reg1* mutant cells hypersensitivity to tunicamycin compared to wild-type cells. As shown in *Figure 69A*, *snf1* mutant cells do not display any differential phenotype to wild-type cells under tunicamycin conditions. Furthermore, the deletion of *SNF1* in *reg1* cells alleviates the hypersensitivity to tunicamycin of *reg1* single mutant cells. Apart from this evidence, we analyzed the induction of UPR under tunicamycin and DTT conditions, *reg1* cells display an uncontrolled activation of UPR, but *reg1 snf1* cells show an induction equal to either wild-type or *snf1* cells. Additionally, *reg1* cells show a lower basal induction of UPR than wild-type cells,

meaning that the pathway is activated not only in β -galactosidase activity but also in folds. To sum up, it seems clear that hyperactivated *SNF1* is more deleterious for yeast cells under UPR inducers than the lack of *SNF1* itself.

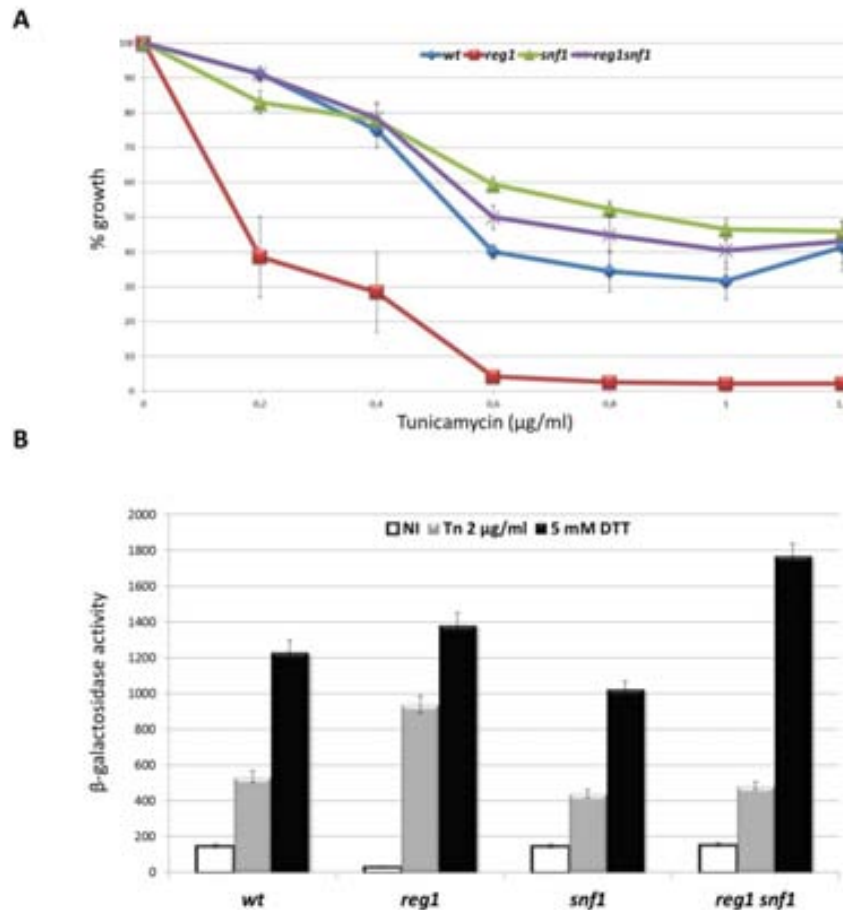


Figure 69. *reg1* cells display an uncontrolled UPRE in DBY746 background as well. A) Liquid growth of wild-type strain (**wt**), cells lacking *REG1* (**reg1**; *MP030*) or *SNF1* (**snf1**; *CCV180*) and cells lacking both (**reg1 snf1**; *CCV181*) were inoculated at 0.02 OD_{660} with YPD (pH 5.5) plus the indicated tunicamycin concentrations. Growth at 28°C was monitored for 16 h (**wt**) and for 24 h (**reg1**; **snf1** and **reg1 snf1**). Data are mean \pm S.E. from at least 12 independent clones. **B)** The indicated strains above were transformed with the construct pMCZ-Y and cultures were grown until reached 0.8 OD_{660} in YPD (pH 5.5). Cells were transferred to fresh YPD (non-induced, **NI**) with 2 $\mu\text{g/ml}$ tunicamycin (**Tn 2 $\mu\text{g/ml}$**) or 5 mM DTT for 90 minutes at 28°C. β -galactosidase activity was measured as described in *Experimental procedures*. Data are mean \pm SEM from at least nine independent clones.

4.5.2 *PTC2* do not rescue *reg1* mutant cells tunicamycin hypersensitivity

Two possible UPR regulators are Dcr2 and Ptc2, two phosphatases which cannot deactivate the Hac1 splicing possibly due to the impossibility of Ire1 dephosphorylation (Guo & Polymenis, 2006; Welihinda et al., 1998). In our lab, we own two plasmids which are overexpressing *PTC2* and *PTC3*. These genes share the majority of their known functions such as: regulation of Hog1 MAPK, dephosphorylation of Rad53 in DNA checkpoint Inactivation after

a double-strand break and regulation of cell cycle progression; and analyzing their amino acid sequence alignment shows that Ptc2 and Ptc3 have the highest degree of identity (A. Cheng, Ross, Kaldis, & Solomon, 1999; Leroy et al., 2003; Young, Mapes, Hanneman, Al Zarban, & Ota, 2002).

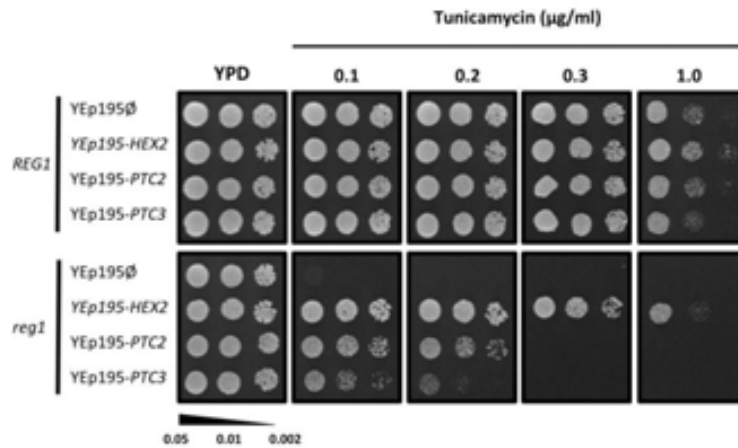


Figure 70. *PTC2* and *PTC3* partially rescue the hypersensitivity to tunicamycin of *reg1* cells. Three dilutions from cultures of wild-type and *reg1* cells transformed with YEpl95Ø, YEpl95-*HEX2*, YEpl95-*PTC2* and YEpl95-*PTC3* were spotted on YPD plus tunicamycin at the indicated concentrations. Growth at 28°C was monitored for 2-3 days.

In *Figure 70*, firstly the overexpression of *HEX2* (*REG1*) in *reg1* cells restitutes the wild-type UPR's phenotype. Moreover, the overexpression of *PTC2* and *PTC3* slight improves the *reg1* hypersensitivity to tunicamycin. Additionally, *ptc2*, *ptc3* and *ptc2 ptc3* mutant cells display the wild-type phenotype on tunicamycin plates (data not shown). Therefore, there is no link between the theoretical phosphatase involved in Ire1-dephosphorylation and hypersensitivity to UPR inducer growth; meaning that the deactivation of Ire1 may be independent of protein dephosphorylation mechanism, as postulated by (Rubio et al. 2011).

4.5.3 *reg1* mutant cells are unable to deactivate UPR

Our hypothesis is that *REG1* plays a role in Ire1 regulation by somehow being essential for the deactivation of UPR after tunicamycin stress is washed out.

Based on (Chawla et al., 2011), we designed an qRT-PCR for *KAR2* which is one of the main effectors of *HAC1* splicing and induced under tunicamycin conditions. As already described, either *HAC1* spliced form ($Hac1^i$) or *KAR2* transcription can still be seen after six hours of experiment when tunicamycin is washed from the medium. For that, our experiments are log enough that not only $Hac1^i$ is completely transformed on the unspliced form ($Hac1^u$) but also *KAR2* expression return to non-induced levels in wild-type strain, at least. In *Figure*

71A, it is shown that *reg1* cells induce *KAR2* transcription higher than wild-type strain, as it happens in β -galactosidase assay (Figure 56), but those cells are unable to feedback the UPR once tunicamycin is washed from the medium. Additionally, in Figure 71B, induction of *KAR2* transcription perfectly correlates with the appearance of Hac1ⁱ and then, both genes return to basal condition when tunicamycin is washed from the medium.

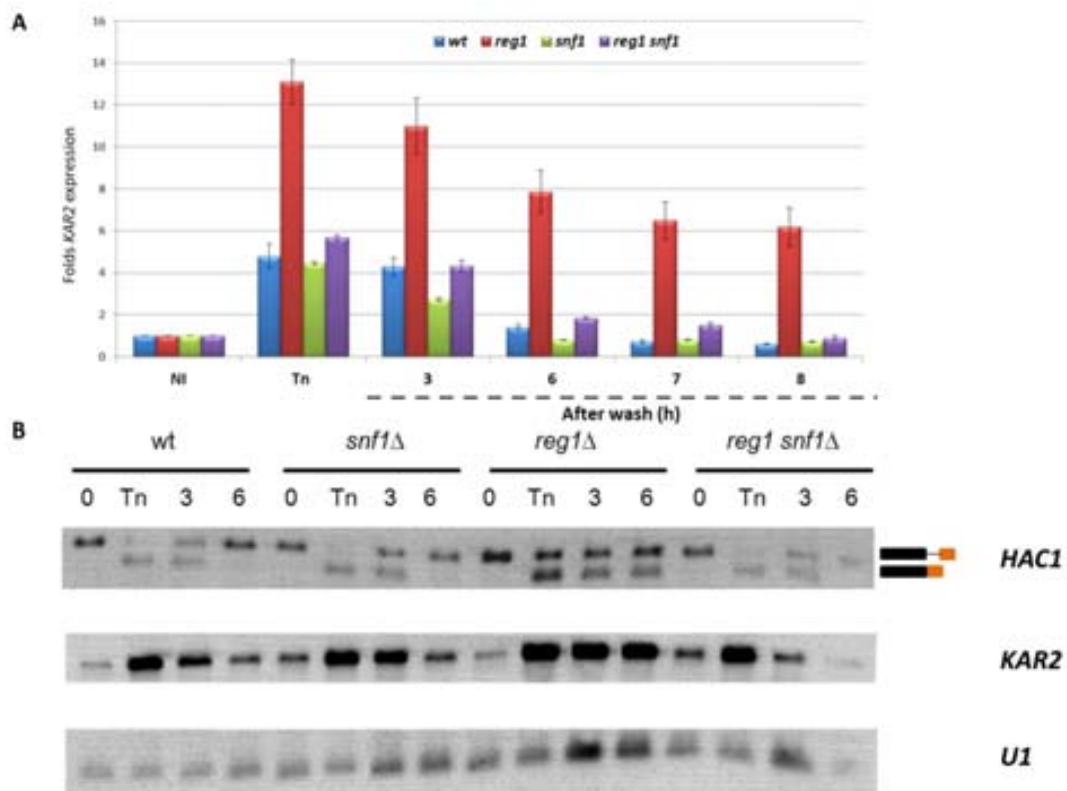


Figure 71. *reg1* cells cannot reverse the *HAC1* splicing. **A)** Wild-type strain and its isogenic derivatives *reg1*, *snf1* or *reg1 snf1* (YJFD31) were grown for until reached 0.6 OD₆₆₀ in YPD (pH 5.5) then induced with 1 μ g/ml Tunicamycin for 1 h (Tn). After induction, cells were collected, washed with fresh YPD (pH 5.5) and then resuspended in YPD (pH 5.5) and samples collected at indicated times. After total RNA extraction 15 ng total RNA were used to perform a qRT-PCR as described in the *Experimental procedures*. Folds of *KAR2* gene were calculated of each mutant as non-induced (NI) as a template. **B)** Wild-type strain and its isogenic derivatives *reg1*, *snf1* or *reg1 snf1* (YJFD31) were grown for until reached 0.6 OD₆₆₀ in YPD (pH 5.5) then induced with 1 μ g/ml tunicamycin for 1 h (Tn). After induction, cells were collected, washed with fresh YPD (pH 5.5) and then resuspended in YPD (pH 5.5) and samples collected at indicated times. After total RNA extraction, the Northern blot was performed for analyzing the indicated genes.

Despite transcriptional assays, following the experimental procedures of (Kimata et al., 2007), where they use the oligomerization of Ire1 to activate the UPR under several inducers, we repeated the conditions of the Figure 71. As shown in Figure 72, as expected, *reg1* cells

could form the Ire1's oligomers and respond to unfolded proteins, but when tunicamycin is washed from the medium, these cells were unable to unhook the Ire1-oligomers, even after 20 h of experiment.

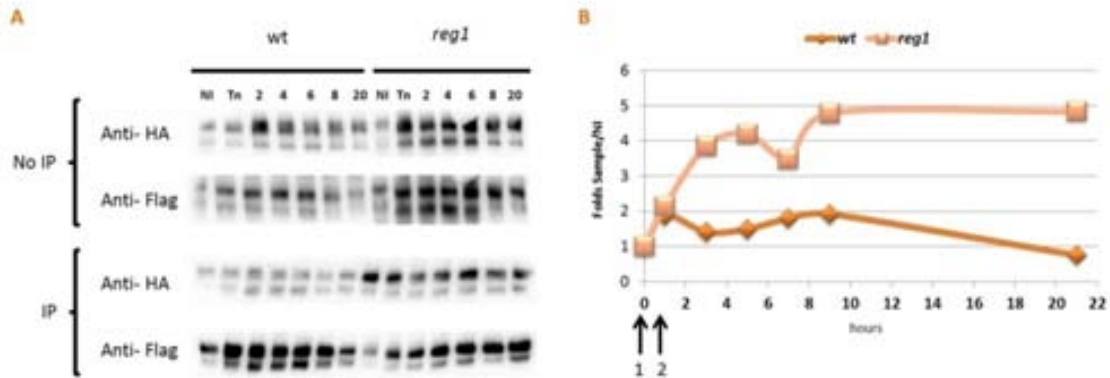


Figure 72. *reg1* cells cannot decouple Ire1 oligodimers. **A)** Wild-type and *reg1* cells were co-transformed with pRS315-*IRE1*-HA and pRS426-*IRE1*-Flag. Cultures were grown until they reached 0.6 OD₆₆₀ in YPD (pH 5.5) then induced with 1 µg/ml tunicamycin for 1 h (Tn). After induction, cells were collected, washed with fresh YPD (pH 5.5) and then resuspended in YPD (pH 5.5) and samples collected at indicated times. Protein extraction was performed as explained in *Experimental procedures*. Blots were incubated with the antibodies anti-HA or anti-Flag either before immunoprecipitation (**No IP**) or after immunoprecipitation (**IP**). **B)** Quantification from blots was performed using the GelAnalyzer 2010. Fold calculation on **IP** experiment was performed as: **1)** every sample detected with anti-Flag was divided for the same sample detected with anti-Ha and then **2)** non-induced samples (**NI**) were determined as basal level, so folds were calculated dividing a sample to wild-type non-induced or *reg1* non-induced. The starting point in the graphic is the non-induced samples (**1**) and (**2**) indicates the 1 µg/ml tunicamycin for 1 h.

So, we have demonstrated in three different ways that *reg1* cells can induce the unfolded protein response, even though in higher levels than wild-type strain, but they cannot deactivate Ire1 by unhooking the oligomers. It is absolutely plausible to hypothesize that Reg1 may be the Glc7's regulatory subunit which involves PP1 in unfolded protein response such as Ptc2 and Dcr2 phosphatase. Besides, *glc7-109* allele is hypersensitive to UPR inducers *Figure 57A*, but we have not tested in the deactivation of the pathway. Despite our results, new studies in UPR hypothesize that Ire1 deactivation is due to its hyperphosphorylation on the kinase domain (Rubio et al., 2011). That means that there is no need for a phosphatase in Ire1 regulation and, additionally, no physical interaction has ever been described between Reg1-Ire1-Glc7.

Finally, our next step was based on *reg1 snf1* cells behave as either a wild-type or *snf1* strains. So, it seems that it might be that hyperactivated response of Snf1 in *reg1* cells could be deleterious for unfolded protein response attenuation.

4.5.4 UPR does not activate Snf1 pathway

It has been deeply described that unfolded protein response (UPR) is not alone in endoplasmatic reticulum homeostatic regulation. This is not strange because properly function of ER is needed to avoid unfolded proteins which appear when yeast cells are under several stresses. So far, three pathways have been reported to be essential for a proper UPR regulation and vice versa: **1)** calcineurin pathway (Myriam Bonilla et al., 2002; Varadarajan et al., 2013); **2)** cell wall integrity regulation (Scrimale et al., 2009) and **3)** osmotic Hog1 regulation (Bicknell et al., 2010; Torres-Quiroz et al., 2010). As *reg1* cells are hypersensitive to tunicamycin and all that pathways are involved on UPR homeostasis, we had to analyze their response in *reg1* cells. In *Figure 73*, *reg1* cells do not display any deficiency in activating the compensatory pathway when UPR is activated.

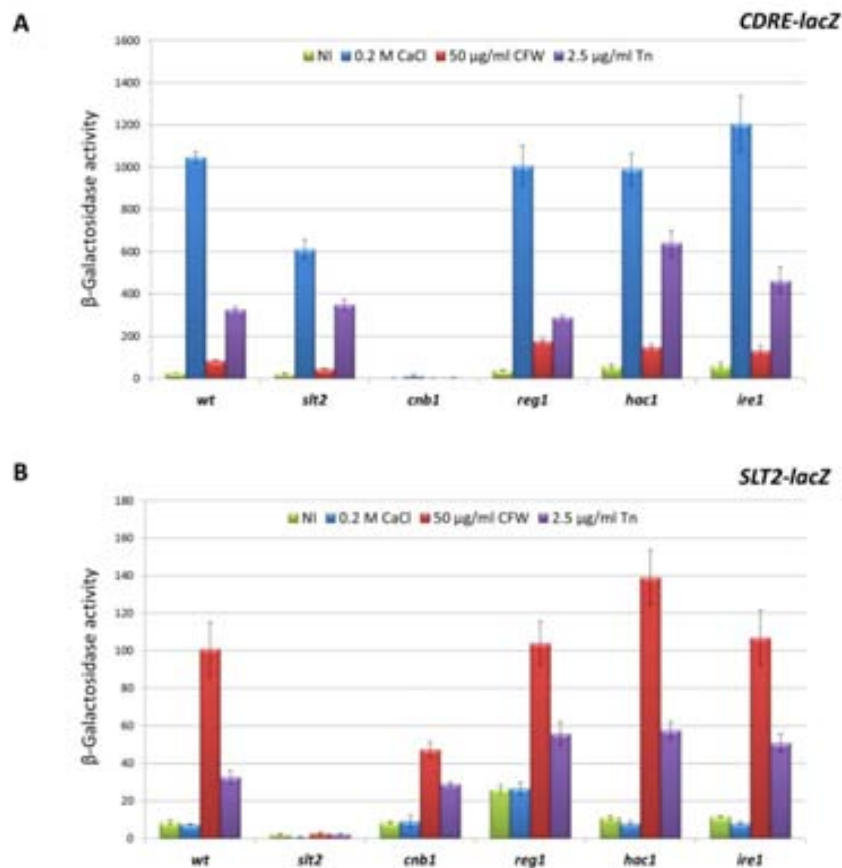


Figure 73. **reg1** cells display an unaltered either a cell wall integrity or calcium homeostasis under tunicamycin conditions. **A)** The indicated strains above were transformed with the construct containing four CDRE tandem repeats (pAMS366) and cultures were grown until reached 0.8 OD₆₆₀ in YPD (pH 5.5). Cells were transferred to fresh YPD (non-induced, **NI**) plus: 2.5 µg/ml tunicamycin (**Tn**), 50 µg/ml Calcofluor white (**CFW**) or 0.2 M **CaCl₂** for 90 minutes at 28°C. β-galactosidase activity was measured as described in *Experimental procedures*. Data are mean ± SEM from at least twelve independent clones. **B)** The indicated strains above were transformed with the construct containing the promoter of *SLT2* (p1365) and cultures were grown for until reached 0.8 OD₆₆₀ in YPD (pH 5.5). Cells were transferred to fresh YPD (non-induced, **NI**) plus: 2.5 µg/ml tunicamycin (**Tn**), 50 µg/ml Calcofluor white (**CFW**) or 0.2 M **CaCl₂** for 90 minutes at 28°C. β-galactosidase activity was measured as described in *Experimental procedures*. Data are mean ± SEM from at least twelve independent clones.

As described previously in (Alms et al., 1999; Castermans et al., 2012), *reg1* cells display a basal hyperactivation of *SUC2* because Snf1 is continuously phosphorylated. So, Snf1 pathway, which mainly means the adaptation to either non-fermentable carbon source or low glucose, is not induced under tunicamycin conditions after 3 h of treatment, at least. Moreover, both *hac1* and *ire1* do not display impairment in *SUC2* activation.

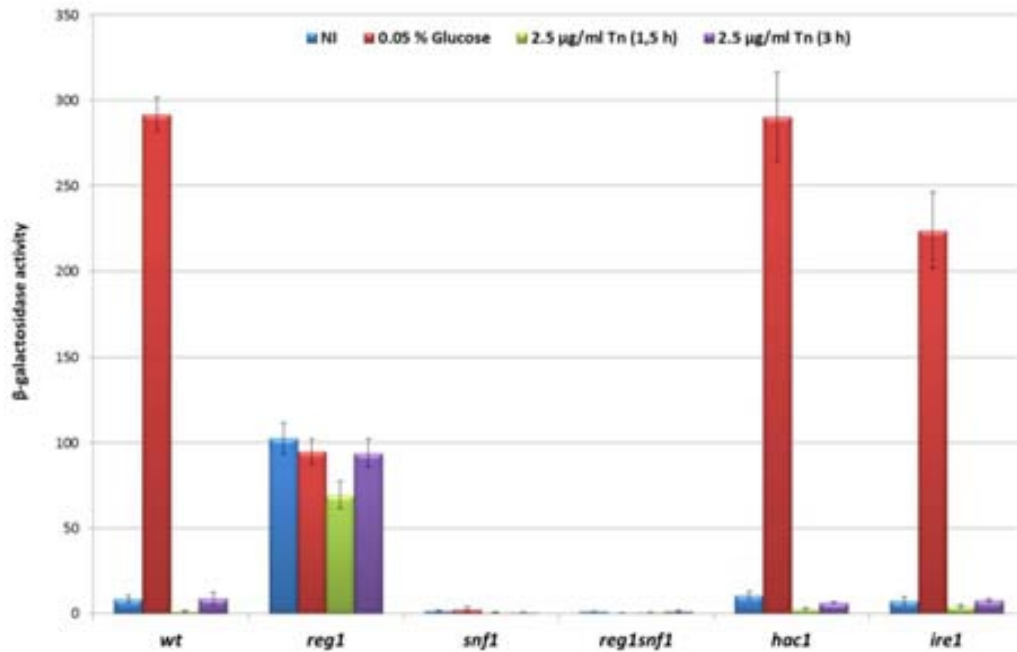


Figure 74. UPR does not activate Snf1 pathway. The indicated strains above were transformed with the construct containing the promoter of *SUC2* (YE_{p357-SUC2}) and cultures were grown until reached 0.8 OD₆₆₀ in YPD (pH 5.5). Cells were washed for eliminating glucose with YP then were transferred to YPD (non-induced, **NI**) or YP low glucose (**0.05% glucose**) plus 2.5 μg/ml tunicamycin (**Tn**) for 1.5 h or 3 h at 28°C. β-galactosidase activity was measured as described in *Experimental procedures*. Data are mean ± SEM from at least twelve independent clones.

After demonstrating that Snf1 pathway it is not induced under tunicamycin conditions, we performed the vice versa experiment: cells transformed with plasmid containing UPRE-*lacZ* were induced with low glucose conditions (0.05%). In *Figure 75A*, low glucose conditions do not activate an unfolded protein response and any strain display any difference between them. Interestingly, the combination of low glucose plus tunicamycin conditions causes a decrease in UPRE induction, meaning that the sum of both responses is deleterious for yeast cells. Moreover, this response is totally dependent of Ire1 and Hac1.

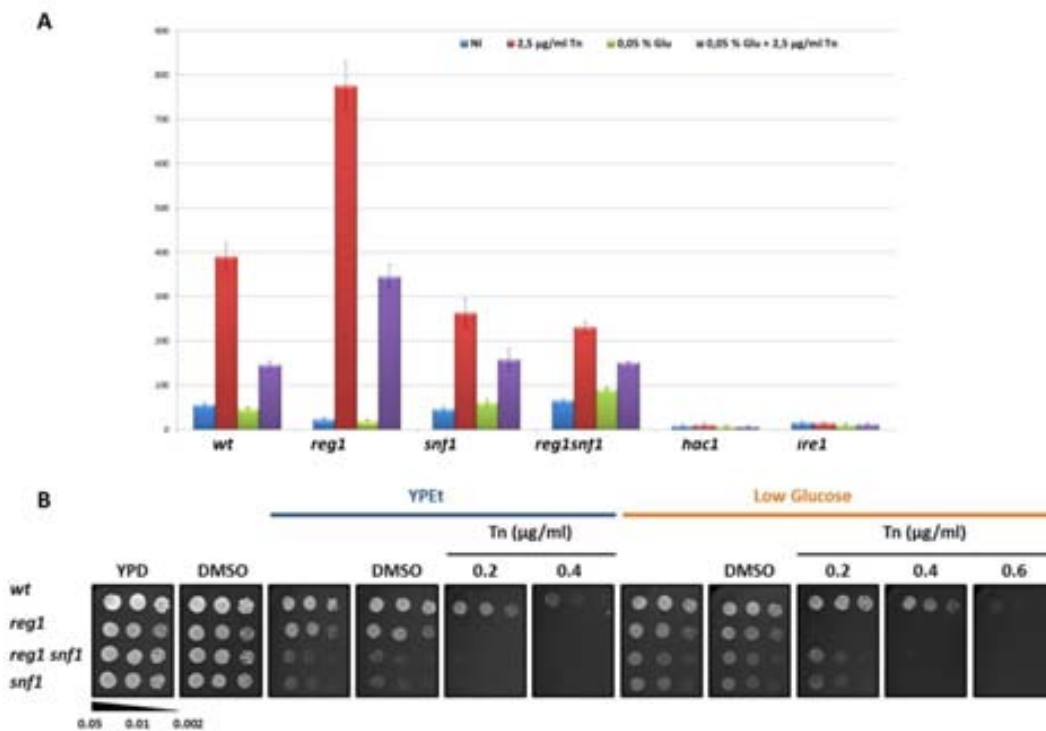


Figure 75. Low glucose does not activate UPR. A) The indicated strains were transformed with the construct pMCZ-Y (UPRE-*lacZ*) and cultures were grown until reached 0.8 OD₆₆₀ in YPD (pH 5.5). Cells were transferred to fresh YPD (non-induced, NI) with 2.5 μg/ml tunicamycin (Tn) or YP low glucose (0.05% glucose) plus 2.5 μg/ml tunicamycin (Tn) for 90 minutes at 28°C. β-galactosidase activity was measured as described in *Experimental procedures*. Data are mean ± SEM from at least eighteen independent clones. **B)** Three dilutions from the indicated cultures were spotted on YP plus 4% ethanol (EtOH) plus the indicated tunicamycin concentrations (Tn) or YP plus 0.05% glucose (Low Glucose) plus the indicated tunicamycin concentrations (Tn). Growth at 28°C was monitored for 2-3 days.

Due to these results, we performed a dot test where low glucose or ethanol was combined with several tunicamycin concentrations. Apparently, those conditions increase lethality of wild-type cells because they cannot grow at 0.4 μg/ml tunicamycin, meanwhile in YPD conditions wild-type cells are able to grow till 1 μg/ml tunicamycin, approximately. Those results perfectly correlate with the decrease in UPRE determined in *Figure 75A*.

4.5.5 Snf1 inactive alleles rescue *reg1* cells phenotype

We analyzed two types of *SNF1* alleles. Firstly, alteration of Tyr¹⁰⁶ in the αC helix relieved glucose inhibition of phosphorylation, resulting in phosphorylation of Thr²¹⁰ during growth on high levels of glucose (*SNF1-Y106A*) and substitution of Arg for Gly⁵³, at the N terminus of the kinase domain, increased activation on both high and low glucose (*SNF1-G53R*) (Momcilovic & Carlson, 2011) (*Figure 50A*). On the other hand, alteration on the conserved Thr²¹⁰ on the activation loop of the catalytic subunit Snf1 prevents phosphorylation and Snf1 activation (*SNF1-T210A*) additionally; carrying substitutions of the ATP-binding site Lys⁸⁴ suppresses Snf1 activation (*SNF1-K84R*) (Hedbacker, Hong, et al., 2004) (*Figure 50B*).

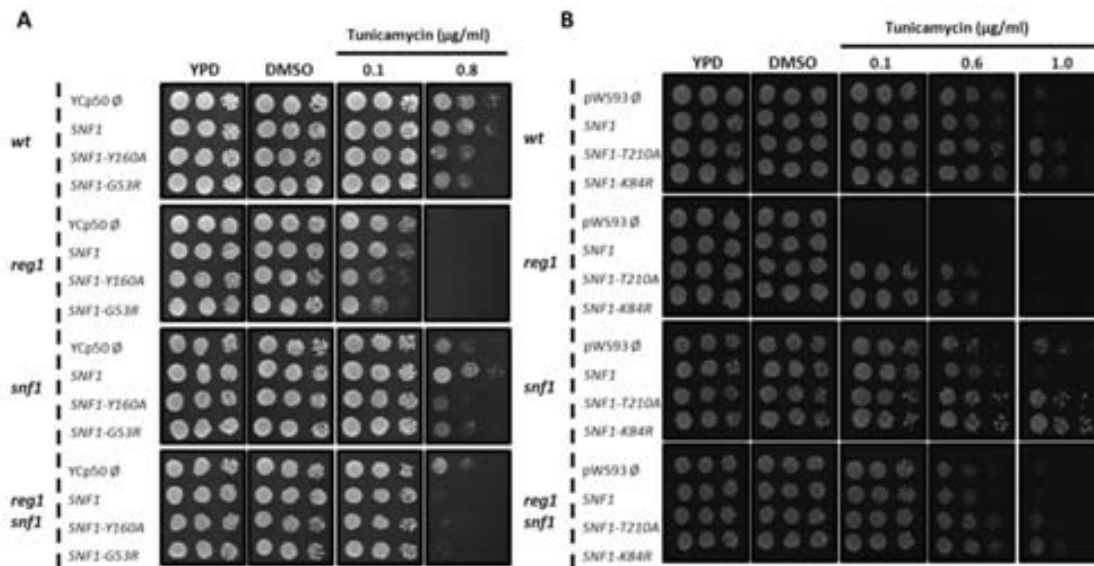


Figure 76. Snf1 inactive alleles rescue *reg1* cells hypersensitivity to tunicamycin. **A)** Wild-type strain and its isogenic derivatives *reg1*, *snf1* or *reg1 snf1* (YJFD31) were transformed with the indicated plasmids: YCp50Ø, pCE108 (*SNF1*), pCE108-Y106A (*SNF1-Y106A*) and pCE108-G53R (*SNF1-G53R*). Three dilutions from the indicated cultures were spotted on YPD (pH 5.5) plus the indicated tunicamycin concentrations (Tn). Growth at 28°C was monitored for 2-3 days. **B)** Wild-type strain and its isogenic derivatives *reg1*, *snf1* or *reg1 snf1* (YJFD31) were transformed with the indicated plasmids: pWS93Ø, pSK119 (*SNF1*), pSK119A (*SNF1-T210A*) and pSK120 (*SNF1-K84R*). Three dilutions from the indicated cultures were spotted on YPD (pH 5.5) plus the indicated tunicamycin concentrations (Tn). Growth at 28°C was monitored for 2-3 days.

Basically, overexpression of an inactive version of Snf1 (*T210A* or *K84R*) in *reg1* cells alleviates the hypersensitive phenotype to tunicamycin of these cells. Even though wild-type cells can grow in higher tunicamycin concentrations. On the contrary, hyperactivated Snf1 alleles are deleterious for yeast cells in order to grow in tunicamycin. To sum up, it seems that the main problem of *reg1* cells for growing in tunicamycin is the hyperactivation of the Snf1 pathway. This result might indicate that *REG1* does not really play a role in directly dephosphorylating Ire1 kinase, but the hyperactivation of Snf1 response is deleterious for yeast cells when UPR is also activated.

4.5.6 Analysis of Snf1's repressors

Reviewed in (Ariño et al., 2010), we have mutant strains with multiple combinations of either four theoretical transcriptional repressors regulated by Snf1 (Mig1, Mig2, Nrg1 and Nrg2) or Rim101, a transcription factor which regulates Nrg1. Only the lack of *RIM101* has already been described hypersensitivity to not only tunicamycin but also DTT and 2-mercaptoethanol in (Chen et al., 2005; Parsons et al., 2004).

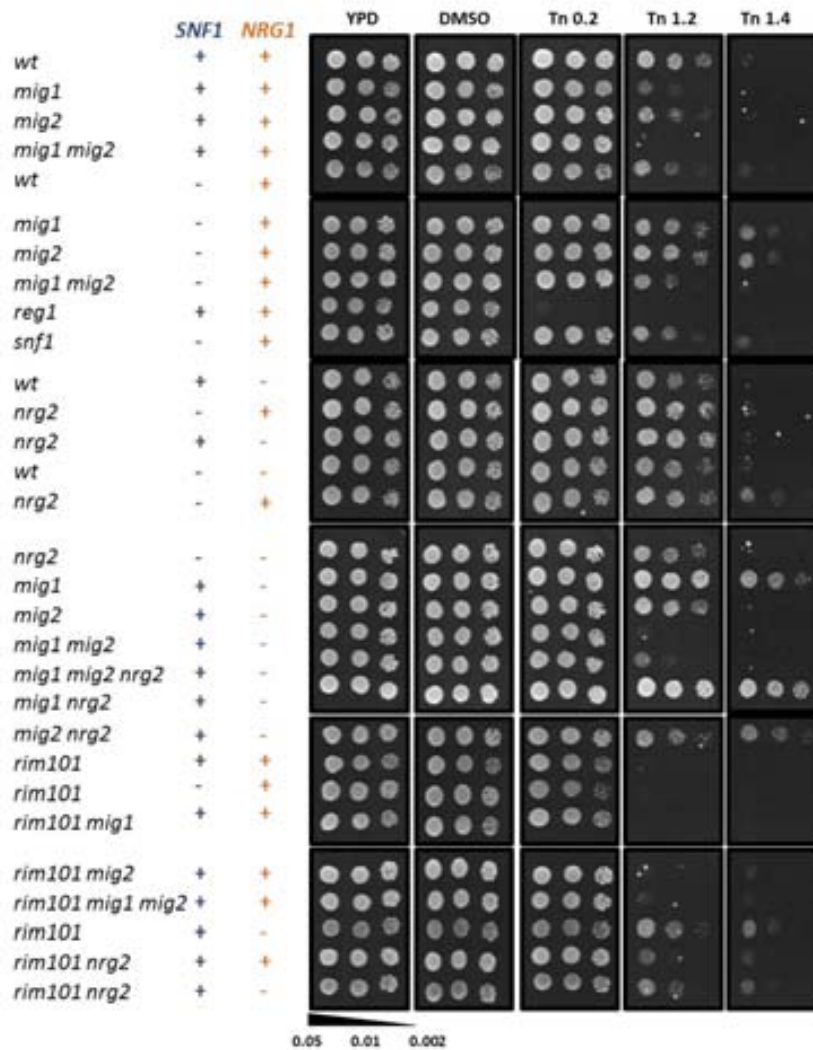


Figure 77. Phenotypal analysis of Snf1 pathway under tunicamycin conditions. Three dilutions from the indicated cultures were spotted on YPD plus 0.2 $\mu\text{g/ml}$ tunicamycin (**Tn 0.2**), 1.2 $\mu\text{g/ml}$ tunicamycin (**Tn 1.2**) and 1.4 $\mu\text{g/ml}$ tunicamycin (**Tn 1.4**). Growth at 28°C was monitored for 2-3 days.

Analyzing together the results from *Figure 77* and *Figure 78*, *mig1 mig2* strains are hypersensitive to tunicamycin, but they do not display a hyperactivation of UPRE. Additionally, deletion of *SNF1* in *mig1 mig2* cells alleviates the tunicamycin's phenotype and causes an increase in UPRE induction doubling wild-type cells response to tunicamycin. It has been reported that Mig1 and Mig2 are directly regulated by Snf1 or Cyc8 phosphorylation in glucose repression (Lutfiyya et al., 1998; J. Wu & Trumbly, 1998). The hypersensitivity could happen for derepression of glucose genes, likely what may happen with *reg1* cells, but not so exaggerate; meaning that *REG1* may have a more essential role by possible direct dephosphorylation of Ire1 kinase.

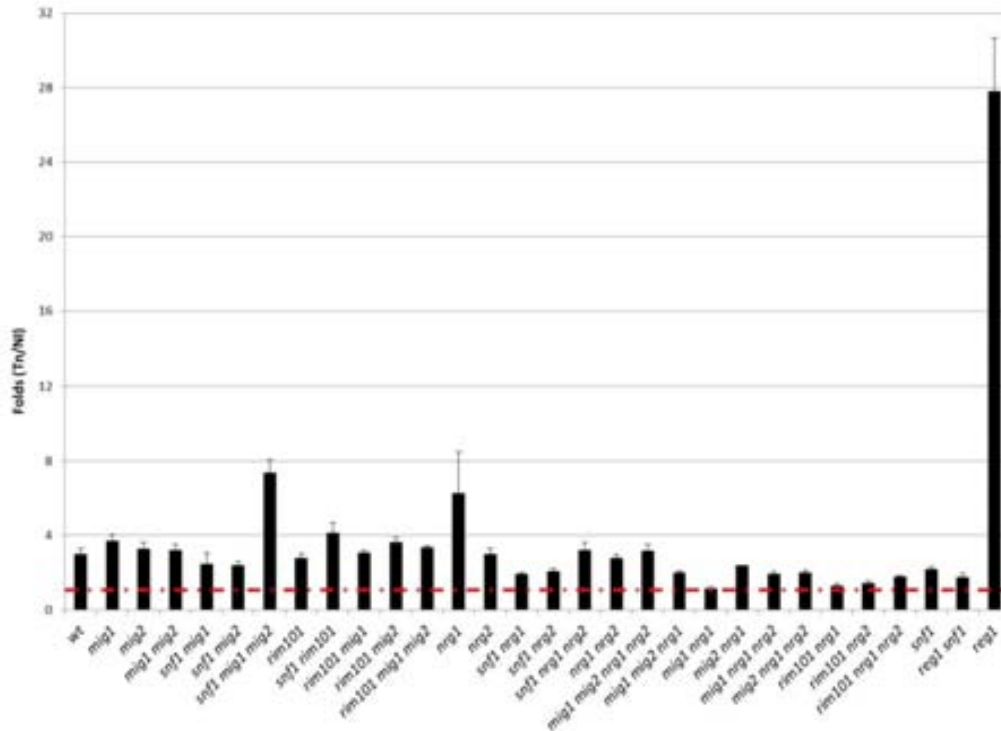


Figure 78. UPRE analysis of Snf1 pathway. The indicated strains were transformed with the construct pMCZ-Y (UPRE-*lacZ*) and cultures were grown until reached 0.8 OD₆₆₀ in YPD (pH 5.5). Cells were transferred to fresh YPD (non-induced, NI) with 2.5 µg/ml tunicamycin (Tn) for 90 minutes at 28°C. β-galactosidase activity was measured as described in *Experimental procedures*. Data are mean ± SEM from at least twelve independent clones. Folds were calculated as the ratio between non-induced conditions and the transcriptional response to tunicamycin for each strain.

The other interesting point is the hypersensitivity of *rim101* cells. Previously it has been already reported that mutants lacking *PMR1* failed to retain a heterologous secretory protein in the ER (Rudolph et al., 1989) and failed to degrade misfolded proteins in the ER (Durr et al., 1998); so *pmr1* mutant is hypersensitive to tunicamycin (Figure 67B). So, (Y. Zhao, Du, Xiong, Xu, & Jiang, 2013) describes that an uncovered function of *ESCRT* components in regulating *PMR1* expression through the Nrg1/Rim101 pathway. The endosomal sorting complex required for transport (*ESCRT*) complexes function to form multivesicular bodies for sorting of proteins destined for the yeast vacuole, they demonstrate that deleting each of these *ESCRT* genes leads to the activation of the calcium/calcineurin signaling pathway in yeast cells, but unexpectedly, reduces *PMR1* expression. The calcium hypersensitivity of these *ESCRT* mutants can be partially suppressed by expression of a constitutively active form of Rim101 or by further deletion of its downstream target *NRG1*. Further molecular analyses reveal that expression of *PMR1* is under the negative control of the Rim101/Nrg1 pathway through two Nrg1-binding sites in its promoter. For that, *rim101* cells are unable to regulate calcium homeostasis because they cannot activate the expression of *PMR1* for unfolded protein

response homeostasis and display the hypersensitive phenotype. Besides, the lack of *NRG1*, which increases the *PMR1* transcription by derepressing its promoter, alleviates *rim101* cells' phenotype to tunicamycin. Additionally, *nrg1* cells combined with deletion of *MIG1* or *MIG2* deletions (*nrg1 mig1* or *nrg1 mig2*) display tolerant phenotype to tunicamycin. On the contrary, *nrg1 mig1 mig2* cells are hypersensitive to tunicamycin, indicating that it might be that Mig1 and Mig2 act directly regulating UPR, meanwhile Nrg1 regulates calcium homeostasis which is needed for UPR homeostasis. Finally, due to the calcium regulation of Rim101/Nrg1 pathway, we are not able to see any increase in UPR induction under tunicamycin conditions. Obviously, we are just scratching the surface of a new function for Snf1 repressors and, indirectly for Rim101/Nrg1 pathway in UPR regulation.

4.6 Conclusions

13. We have demonstrated that Glc7-regulatory subunits are implicated in unfolded protein response. From those non-essential regulatory subunits, two may have significant importance: Ref2 and Reg1.
14. The lack of *REF2* displays a tolerance to tunicamycin, but not an increase in the transcription of UPR. Moreover, this function is independent of holo-CPF components, but Ref2 needs to bind Glc7 to behave as a wild-type strain. Our evolution experiment results report that the duplication in chromosome II which causes the tolerance phenotype to tunicamycin of *ref2* mutant cells.
15. Yeast cells duplicate chromosome II when are kept under tunicamycin stress. This aneuploidy is a first step to long-term accurate response. The loss of aneuploidy generates a strain which not only is tolerant to tunicamycin but also to other drugs due to the expression of specific MDR elements. Moreover, it seems that overexpression of retrotransposons genes is needed for yeast cells to modify its DNA genomic in order to adapt to these new environmental conditions.
16. The lack of *REG1* displays a hypersensitive phenotype to UPR inducers which is shared not only by its ability to bind Glc7 but also with *glc7-109* allele. Although *reg1* mutant cells can activate UPR in higher levels than wild-type strain, these cells are unable to deoligomerize Ire1 kinase.
17. Our results indicate that hyperactivation of *SUC2* in *reg1* cells, meaning that Snf1 pathway is constitutively active, plus tunicamycin induction is deleterious for yeast cells. To sum up, it seems that both pathways are not needed for their functions, as it happens with calcium homeostasis or maintenance of cell wall integrity.
18. Finally, we analyzed either Snf1 repressors or Rim101 pathway. Those results report that *rim101* mutant cells are hypersensitive to tunicamycin due to the inability to derepress Nrg1 from Pmr1 promoter which will be essential for UPR homeostasis.

Conclusions

CONCLUSIONS

1. The phenotypic analysis revealed that mutants on non-essential Glc7-regulatory subunits display a high variety of sensitive/tolerant phenotypes under stress conditions. These myriad of phenotypes also correspond to the incredible number of functions where Glc7 has been involved. Moreover, some of these phenotypes have already been described for some of the *GLC7* alleles.
2. The vacuolar analysis of those mutants showed that two new subunits, Ref2 and Red1, are involved in the proper function of vacuole, through regulating Glc7. The abnormal vacuole density in *reg1* mutant cells was already described and its role in vacuole regulation has already been demonstrated. Importantly, Ref2 seems to be involved in the endocytic pathway regulation.
3. The transcriptomical analysis demonstrated that some of the mutants in non-essential Glc7-regulatory subunits have no sufficient defects in our standard conditions (YPD pH 5.5) compared to wild-type strain, meaning that they could not be evaluated using DNA microarray experiments and growth in optimal conditions. Further analyses for some mutants in non-optimal conditions have been carried out (such as *reg1* mutant cells growing in low glucose concentration or in alkaline pH). Specifically, *ref2* mutant cells showed an aneuploidy in chromosome II and XII.
4. The results of the present study demonstrate that the role of Ref2 on cation tolerance is not attributable to its function in regulating Glc7 in the CPF complex but, instead, it suggests that Ref2 must direct Glc7 to alternative target(s); therefore Ref2 would represent a novel example of multifunctional Glc7-regulatory subunits.
5. Our results demonstrate a possible positive relation between Pmr1 and Ref2. The lack of *PMR1* in *ref2* mutant cells alleviates its phenotype in calcium and lithium, so cation homeostasis may be somehow related to the entry of cations in the endoplasmic reticulum.
6. APT-complex is needed to cell wall integrity response. Deletion of *REF2* in mutants of CWI causes an additive and synergistic phenotype to cell wall stressors, therefore these data indicate that the hypersensitivity of APT-complex is due to different substrates than a malfunctioning of CWI components
7. The generation of *tetO₇::REF2* strain demonstrated the defects of snoRNA maturation and processing already described as an APT-complex component. Moreover, we were not able to show the aneuploidy in this strain. One possibility it is that the experiment

- is not long enough, meaning that a longer treatment with doxycycline could achieve the aneuploidy.
8. All *ref2* mutant cells in BY4741 genetic background display the common aneuploidy on chromosome XII, but they have also different chromosome duplication (II and XI). Those strains also show hypersensitivity to typical phenotypes of aneuploidy cells such as protein synthesis inhibitors (cycloheximide and hygromycin B) and a lower biomass production per glucose molecules than wild-type cells.
 9. Surprisingly, *ref2* mutant cells do not show a G₁ delay in cell cycle. Despite this negative result, we should repeat the experiments synchronizing the cellular culture because *ref2* mutant cells display sensitivity to nocodazole meaning a chromosome bi-orientation defect.
 10. APT-complex mutants do not show an aneuploidy. Furthermore, our results indicate that these mutants need more energy for growing than wild-type strain implying a lower saturation level.
 11. All the phenotypes of *ref2* mutant cells are due to the inability to bind Glc7. Despite this regulation, *glc7-109* allele which is directly regulated by Ref2 in ionic homeostasis adaptation, does not present an aneuploidy.
 12. The haploid *ref2* mutant cells can generate diploids. Nevertheless, homozygous diploids *ref2* cells cannot form spores. These diploid cells can start the sporulation process by entering early phase, but then there are no visible spores, because possibly they carry a defect in meiosis.
 13. We have demonstrated that Glc7-regulatory subunits are implicated in unfolded protein response. From those non-essential regulatory subunits, two may have significant importance: Ref2 and Reg1.
 14. The lack of *REF2* displays a tolerance to tunicamycin, but not an increase in the transcription of UPR. Moreover, this function is independent of holo-CPF components, but Ref2 needs to bind Glc7 to behave as a wild-type strain. Our evolution experiment results report that the duplication in chromosome II which causes the tolerance phenotype to tunicamycin of *ref2* mutant cells.
 15. Yeast cells duplicate chromosome II when are kept under tunicamycin stress. This aneuploidy is a first step to long-term accurate response. The loss of aneuploidy generates a strain which not only is tolerant to tunicamycin but also to other drugs due to the expression of specific MDR elements. Moreover, it seems that

- overexpression of retrotransposons genes is needed for yeast cells to modify its DNA genomic in order to adapt to these new environmental conditions.
16. The lack of *REG1* displays a hypersensitive phenotype to UPR inducers which is shared not only by its ability to bind Glc7 but also with *glc7-109* allele. Although *reg1* mutant cells can activate UPR in higher levels than wild-type strain, these cells are unable to deoligomerize Ire1 kinase.
 17. Our results indicate that hyperactivation of *SUC2* in *reg1* cells, meaning that Snf1 pathway is constitutively active, plus tunicamycin induction is deleterious for yeast cells. To sum up, it seems that both pathways are not needed for their functions, as it happens with calcium homeostasis or maintenance of cell wall integrity.
 18. Finally, we analyzed either Snf1 repressors or Rim101 pathway. Those results report that *rim101* mutant cells are hypersensitive to tunicamycin due to the inability to derepress Nrg1 from Pmr1 promoter which will be essential for UPR homeostasis.

Table of contents (Figures and Tables)

TABLE OF CONTENTS (Figures and Tables)

Figure 1. Classification of Ser / Thr phosphatases. A) The three main families and the corresponding subfamilies of catalytic subunits of protein phosphatases are shown. The <i>S. cerevisiae</i> catalytic subunits of each subfamily are shown in the right column. The symbol (-) indicates that there is not a counterpart of PP7 in <i>S. cerevisiae</i> . B) Tree alignment of PP sequences of <i>S. cerevisiae</i> . Protein sequences were analyzed with ClustalW 2.0 from EMBL-EBI (Larkin et al., 2007). Hierarchical cluster was performed using array correlation parameter plus complete linkage clustering and data was represented by Treeview tool v1.6 from Eisen's lab software (Eisen, Spellman, Brown, & Botstein, 1998). Each PP family is marked with its own color such as PPP (red), PPM (blue) and Asp-based phosphatase (purple).	12
Figure 2. The crystal structure of the catalytic PP1. A) Structure of the catalytic subunit (blue) of protein phosphatase 1 (PP1) bound to okadaic acid (OA, yellow ball and stick). A Y-shaped surface groove (pink) is defined by the three domains of PP1. The two metal ions (red spheres) are Mn ²⁺ (manganese) and Fe ²⁺ (iron). This frontal view of PP1 with the catalytic site (encircled) and the three grooves that emanate from the catalytic site modified from (Shi, 2009). B) The dorsal view of the same structure. The RVXF-containing peptide is rendered as a green sticks representation. The accommodating RVXF-binding channel is lined by residues of the last strand and by adjacent residues (cyan). The protein surface near the entrance of the channel, which is thought to bind the basic residues preceding the V-position of the RVXF motif, is negatively charged due to the presence of conserved acidic residues (red and orange) modified from (Hugo Ceulemans & Bollen, 2004).	13
Figure 3. Ref2 is a key component in holo-CPF integrity. A) Scheme of the components of the holo-CPF and the proteins that compose each complex. B) Illustration of the different effects caused by deletion or the F374A point mutation of REF2.	21
Figure 4. Reg1 is the phosphatase of Snf1. Summary of the three different localizations through which Snf1 can respond in front of different stresses, associating to each β subunit, localizing differently Snf1. It also shows the key role of Reg1 being, so far, the only phosphatase of Snf1.	23
Figure 5. The major plasma membrane and intracellular cation transporters in the yeast <i>S. cerevisiae</i>. The main transporters located either in the plasma membrane or in the organelles are shown. The questions marks on the mitochondria indicate that it is not known if these proteins are transporters or they participate in their regulation (adapted from (Ariño et al., 2010)).	26
Figure 6. Schematic outline of the regulation of the ENA1 promoter in <i>S. cerevisiae</i>. Only the major components of the signal transduction pathways and the corresponding stimuli that activate them are denoted. Discontinuous lines represent inputs to the promoter that were not documented when the work started or that still remain obscure. The regulatory DNA-motifs are represented to their relative position on the promoter (which is not drawn at to scale) with basic shapes and indicated in the inset (figure based on (Amparo Ruiz & Ariño, 2007)).	27
Figure 7. Scheme of the calcineurin pathway. The main transporters involved in calcium homeostasis are depicted: Mid1-Cch1 and Yvc1 which contribute to intracellular Ca ²⁺ raises and Pmc1, Vcx1 and Pmr1 which eliminate calcium from the cytoplasm. Specific environmental conditions provoke increases of intracellular Ca ²⁺ and the phosphatase calcineurin is activated dephosphorylating Crz1 which then enters the nucleus to activate CDRE-containing genes. Deactivation of Crz1 occurs upon phosphorylation by PKA, Hrr25 and the Pho85-Pho80 CDK complex. Calcineurin activation depends on the phosphorylation state of the calci-repressin Rcn1. Adapted from Raquel Serrano's thesis.	30
Figure 8. Cell Wall Integrity pathway. Cell wall stress is perceived from the cell surface sensors Wsc1-3, Mid2 and Mtl2 and the signal is transmitted through the G-protein Rho1 to the Pkc1 protein kinase. When activated, Pkc1 in turn activates the members of the MAP kinase cascade, Bck1, Mkk1/2 and Slk2. Two transcription factors, Rlm1 and the SBF complex (Swi4/Swi6) are targets of Slk2 MAP kinase.	33
Figure 9. Domain arrangements of ABC (A) and MFS transporters (B) (R. D. Cannon et al., 2009).	37
Figure 10. The three unfolded protein response (UPR) branches in higher eukaryotes (Korennykh & Walter, 2012).	39

- Figure 11. The structure of Ire1 and its role in the activation of the UPR pathway.** **A)** Schematic representation of three transmembrane ER mammalian stress sensors: Ire1, PERK and ATF6. Thin lines indicate BiP binding regions (BiP1, assigned by yeast Ire1; BiP2, a potential binding region of human IRE1a). Bold lines represent regions that are indispensable for sensing stress (core). The broken line represents a region necessary for Golgi translocation (GLS: Golgi localization signal). Vertical bars indicate conserved cysteine residues in the ER luminal region of ATF6. S, signal sequence; T, transmembrane region; bZIP, transcription factor containing basic leucine zipper; N, amino terminus; C, carboxyl terminus; IV, yeast Ire1 subregion (Kohno, 2010). **B)** A general scheme of Ire1 activation during the UPR summarizing the key events. The kinase domain of Ire1 (K) is colored brown and the RNase domain (R) is colored purple (Korennykh et al., 2009). **C)** A diagram of yeast Ire1 luminal region where is represented the core stress-sensing region (CSSR) (Kohno, 2010). **D)** Chaperone protein Kar2 (similar to mammalian BiP) binds to Ire1 and dissociates in response to endoplasmic reticulum stress (Kimata et al., 2007)..... 40
- Figure 12. Aneuploidy induces proteotoxic stress.** (Top) An extra copy of an individual yeast chromosome, or disomy in haploid cells, causes imbalanced expression of the proteins encoded on that chromosome. Adding an inhibitor of protein synthesis, such as G418 (Geneticin), increases the errors in translation and enhances the proteotoxic stress. This stress reduces fitness and inhibits cell growth primarily during the G1 phase. (Bottom) Suppressors of proteotoxic stress, including mutations in components of ubiquitin/proteasome pathway, can ameliorate the proteomic imbalance and restore fitness (Eduardo M Torres et al., 2010). For example, disrupting the deubiquitinase *UPB6* can increase the growth rate of aneuploid cells by triggering more rapid protein degradation by the proteasome (Cetin & Cleveland, 2010). 45
- Figure 13. Effect of the mutation of Glc7-interacting proteins on different stressors or conditions.** Two dilutions from cultures of wild-type strain BY4741 (**wt**) and the indicated isogenic derivatives were grown on either YPD plates in the presence of **CFW** (Calcofluor white 50 µg/ml), **Caf** (caffeine 7 mM), **pH** (alkaline pH with TAPS 8.2), **NaCl** (0.6 M), **LiCl** (150 mM), **CaCl₂** (0.2 M), **ZnCl₂** (4 mM); or YP plates in the presence of **EtOH** (ethanol 2%), **Gly** (glycerol 2%) and **LG** (low glucose 0.05%) for 2-3 days..... 71
- Figure 14. Phenotypic array comparing multiple wild-type phenotypes with those of the non-essential regulatory subunits of Glc7 mutant strains.** Tree alignment of phenotypes of mutants of the non-essential Glc7-regulatory subunits analyzed with ClustalW 2.0 from EMBL-EBI (Larkin et al., 2007). Hierarchical cluster was performed using array correlation parameter plus complete linkage clustering and data was represented by Treeview tool v1.6 from Eisen's lab software (Eisen et al., 1998). Conditions tested to construct the array were: YP plus 0.05% glucose (1), YP plus 2% glycerol (2), 1-300 µg/ml Calcofluor white (3), 100-300 mM CaCl₂ (4), 0.4-1.2 M NaCl (5), YP plus 2% ethanol (6), 37 °C (7), 0.2-0.6 M TMA (8), 20-60 µg/ml hygromycin B (9), 0.1-0.7 mM spermine (10), 1-6 mM ZnCl₂ (11), , 50-300 mM LiCl (12), 5-40 mM 2-mercapthenol (13), pH 8.0-8.3 (14), 1-20 mM caffeine (15) and 0.1-1-4 µg/ml tunicamycin (16). Red color denote strong sensitivity (**HS**), black color correspond with wild-type behavior (**wt**) and green color indicates an hypertolerance phenotype (**TL**)..... 73
- Figure 15. Vacuolar analysis of Glc7 subunits.** **A)** Distribution of the number of vacuoles in different mutant cells on the non-essential regulatory subunits of Glc7 by using the internalization of FM4-64 fluorescent dye. The categories used for the number of vacuoles are 1, 2, 3> 3 and miscellaneous which represents no functional vacuole observed. **B)** Comparative picture of stained vacuoles in wild-type cells (**wt**) and in cells of its derivative *ref2* mutant strain (**ref2**). **C)** Three dilutions from cell cultures of the wild-type strain BY4741 (**wt**) and the indicated isogenic derivatives (**ref2**) transformed with multicopy plasmid carrying *VPS70* and *VPS73* were spotted on YPD plates in the presence of the indicated conditions. Growth at 28°C was monitored for 2-3 days. 75
- Figure 16. Glc7-regulatory subunits do not show a specific expression profile.** **A)** Wild-type and its derivative strains were transformed with the construct *pPHO84-lacZ* and cultures were grown in YPD (pH 5.5) until 0.8 OD₆₆₀ was reached. Cells were collected and β-galactosidase activity measured as described in *Experimental procedures*. Data are mean ± SEM from at least six independent clones. The β-galactosidase activity results are represented in folds increased respect that of wild-type cells (black bars). The expression data, also in fold increase respect wild-type cells, for the *PHO84* gene obtained from DNA microarray experiments is also shown (white bars). **B)**

Expression changes found in each DNA microarray experiment data from indicated strains were analyzed with Cluster tool v2.11 from Eisen's lab software (Eisen et al., 1998). Hierarchical cluster was performed using array correlation parameter plus complete linkage clustering and data was represented by TreeView toll v1.6 from Eisen's lab software. 78

Figure 17. Cells lacking REF2 show a possible aneuploidy in chromosome II and XII. Once analyzed the DNA microarray experiments as explained in *Experimental procedures*. The mean of the expression values (in log₂) for the genes of each chromosome was calculated and represented for some of the analyzed mutants as fold change. 79

Figure 18. Phylome of *S.cerevisiae* Ref2. Protein Ref2 is compared to Yeast Phylome 60 database (Marcet-Houben & Gabaldón, 2009) to find protein orthologs using PhylomeDB (Huerta-Cepas et al., 2011, 2008) with the Blosum62 comparative method. 80

Figure 19. Effect of the mutation of several Glc7-interacting proteins on cation-related phenotypes. Two dilutions from cultures of wild-type strain BY4741 (**wt**) and the indicated isogenic derivatives were grown on YPD plates in the presence of 0.6 M NaCl, 50 mM LiCl, 0.2 M CaCl₂ or at alkaline pH (**pH 8.0**) for 2 days. 83

Figure 20. ref2 mutant cells show phenotypes of hypersensitivity to Na⁺ and Li⁺ and also defective cations efflux. A) Three dilutions from the indicated cultures were spotted on YPD plus the indicated concentrations either of NaCl or LiCl. Growth at 28°C was monitored for 2-3 days. **B)** Wild-type BY4741 cells (white bars) and the *ref2* derivative (black bars) were incubated with 25 or 50 mM LiCl as described in the *Experimental procedures section 19* and the intracellular content of lithium ions measured. Results are means ± SEM for at least six independent determinations. **C)** Strains BY4741 and its isogenic derivative *ref2* were loaded with 75 mM LiCl, samples taken at different times and the efflux of the cation determined as described in the *Experimental procedures section 19*. Results are expressed as a percentage of the intracellular lithium content for each strain at the start of the experiment and are means ± SEM for at least six independent assays. 84

Figure 21. Mutation of REF2 increases potassium requirements for growth. Cultures of wild-type strain BY4741 (white bars) and its *ref2* derivative (black bars) were inoculated at an OD₆₆₀ of 0.004 in Translucent K-free medium, supplemented with the indicated amounts of KCl, and grown for 16 h. Results are represented as a percentage of growth compared with cells incubated with 50 mM KCl and are means ± S.E.M. for three independent cultures. 85

Figure 22. Mutation of Phe-374 within the Glc7-binding consensus sequence abolishes the function of Ref2 in cation tolerance. A) Wild-type BY4741 (+) and *ref2* strains (-) were transformed with the empty plasmid pRS415 or the same plasmid expressing the wild-type Ref2 protein (pJFD1) or the Ref2^{F374A}-mutated version (pJFD2). Transformants were spotted on to YPD plates, which were adjusted to pH 8.1 or contained LiCl (150 mM), NaCl (1 M), TMA (0.3 M), Spermine (0.6 mM) or Hygromycin B (20 µg/ml) as indicated. Growth was monitored after 3 days, except for the LiCl and NaCl conditions when growth was monitored after 6 days. **B)** Wild-type (+) and *ref2* (-) strains were transformed with the indicated plasmids and growth was tested at a limiting concentration of external potassium (1 mM). Experimental conditions were as described in *Figure 21*. 86

Figure 23. Effects of overexpression of Glc7 on Ref2-deficient S. cerevisiae strains. A) Wild-type strain BY4741 (WT) and its *ref2* derivative were co-transformed with the indicated plasmids. Three dilutions of the cultures were plated in the conditions indicated. Growth at 28°C was recorded after 4 days. **B)** Strains carrying wild-type (KT1112) and mutated forms of Glc7 (KT1935 or KT2210) were transformed with the indicated plasmid and spotted on YPD plates. Growth at 28° was recorded after 3 days. 87

Figure 24. Mutation of Ref2 affects expression of the ENA1 ATPase gene under saline and alkaline pH stresses. A) Wild-type strain BY4741 (**wt**) and its *ref2* derivative (**ref2**) were transformed with pKC201 (*ENA1-lacZ*) and cultures were grown until reached 0.8 OD₆₆₀ in YPD (pH 5.5). Cells were transferred to fresh YPD (non-induced, **NI**) with 0.4 M NaCl, 0.05% glucose, 0.2 M LiCl and alkaline pH 8.2 for 90 min and, YPD plus 0.9 M NaCl for 4 h at 28°C. β-galactosidase activity was measured as described in *Experimental procedures*. Data are mean ± SEM from at least twelve independent clones. **B)** Folds were calculated dividing each stress condition to non-induced response activity for each strain. 88

Figure 25. Effects of the ref2 mutation in wild-type and cnb1 strains on the ENA1 promoter activity. A) The indicated strains were transformed with plasmids pKC201, carrying the entire *ENA1* ATPase

- gene promoter, or plasmids pMRK212 or pMRK213, which contain specific regions of the *ENA1* promoter, as indicated in the diagram at the top of the panel. MIG, Mig1/2 binding sequence; CRE, cAMP regulatory element. Cells received no treatment (NI), were shifted to pH 8.2 (pH) or were exposed to 0.4 M NaCl (Na⁺) or 0.2 M LiCl (Li⁺) for 1 h. β -Galactosidase activity was measured in permeabilized cells as described in the *Experimental procedures*. Results are means \pm SEM for eight or nine independent transformants. **B)** Three dilutions of the indicated cultures were spotted on to plates at the conditions YPD plus 50 mM LiCl (LiCl) and 0.6 M NaCl (NaCl) and growth recorded after 72 h (LiCl and NaCl) or 48 h (alkaline pH).....90
- Figure 26. Lack of *REF2* results in altered calcium homeostasis and vacuolar morphology.** **A)** The indicated strains were grown in the presence or absence of calcium cations (300 mM CaCl₂) and growth was monitored after 72 h. **B)** Yeast strains were transformed with plasmid pAMS366, which contains a tandem-repeat of four CDREs fused to a *lacZ* reporter (CDRE-*lacZ*), and incubated for 1 h in the absence (white bars) or presence (black bars) of 0.2 M CaCl₂. β -Galactosidase activity was measured as described in the *Experimental procedures*. Results are means \pm SEM for six independent transformants. **C)** Vacuolar staining of wild-type BY4741 (*wt*), *ref2::kanMX4* (*ref2*), YJFD17 (*glc7-109*) and YJFD18 (*ref2 glc7-109*) strains with the fluorescent dye FM4-64 was performed as described in the *Experimental procedures* for 30 min and monitored by fluorescence microscopy.....91
- Figure 27. Mutation of Phe-374 within the Glc7-binding motif abolishes the function of Ref2 in calcium tolerance.** **A)** BY4741 wild-type and *ref2* strains were transformed with the empty plasmid pRS415 or the same plasmid harboring the wild-type Ref2 protein (pJFD1) or the Phe-374 mutated version (pJFD2). Yeast strains were transformed with plasmid pAMS366, which contains a tandem of four CDREs, and incubated for 1 h in the absence or presence of 0.2 M CaCl₂. β -galactosidase activity was measured as described in *Experimental procedures*. Data are mean \pm SEM from 9 independent transformants. **B)** BY4741 wild-type and *ref2* strains were transformed with the empty plasmid pRS415 or the same plasmid harboring the wild-type Ref2 protein (pJFD1) or the Phe-374 mutated version (pJFD2). Three dilutions of transformants were spotted on plates containing a rank of calcium concentrations and growth was monitored after 3-4 days.....93
- Figure 28. The lack of Ref2 increases the calcium hypersensitivity of a Glc7 allele unable to interact with its regulatory subunits (*glc7-109*).** To generate the strains, a deletion cassette for *GLC7* and a plasmid YCplac111 harbouring the *glc7-109* allele (pJFD11) were cotransformed in BY4741 wild-type (YJFD36) and *ref2* mutant (YJFD39). **A)** Yeast strains were transformed with plasmid pAMS366, which contains a tandem of four CDREs, and incubated for 1 h in the absence (white bars) or presence of 0.2 M CaCl₂ (black bars). β -galactosidase activity was measured as described in *Experimental procedures*. Data are mean \pm SEM from 9 independent transformants. Folds were calculated dividing each sample to wild-type strain in non-induced conditions. **B)** Three dilutions of transformants were spotted on plates containing a rank of calcium concentrations and growth was monitored after 3-4 days.....95
- Figure 29. Comparison of *ref2* phenotypes with those of diverse APT-related mutants.** **A)** Three dilutions of the strains indicated to the left of the panel were spotted on to plates and grown at the temperatures indicated to the right of the panel for 3 days. Conditions used were: YPDF, YPD plus 3% formamide; LiCl, 100 mM LiCl (30°C) or 150 LiCl mM (37°C); NaCl, 800 mM NaCl; pH 8.2; CaCl₂, 200 mM CaCl₂. **B)** Phenotypic array comparing multiple *ref2* phenotypes with those of other APT-related mutants. Growth of each mutant was compared with that of the corresponding wild-type strain grown under the same set of conditions. Black squares denote strong sensitivity, grey squares indicate a mild phenotype and white squares correspond with wild-type behaviour. Conditions tested to construct the array were: LiCl, 50–200 mM LiCl; NaCl, 0.4–1.2 M NaCl; high pH, pH 8.0–8.3; Ca²⁺, 100–300 mM CaCl₂, YPDF, YPD plus 3% formamide; YPGly, YP plus 2% glycerol; YP-EtOH, YP plus 2% ethanol; YP-LowGlu, YP plus 0.05% glucose; Hyg B, 20–60 μ g/ml hygromycin B; TMA, 0.2–0.6 M TMA.....96
- Figure 30. Expression of *ENA1* under saline stress in diverse APT-related mutants.** The indicated mutants and their corresponding wild-type strains (the bars show isogenic strains) were transformed with plasmid pKC201, carrying the entire *ENA1* ATPase gene promoter. Stress conditions were as in described in *Figure 25*, except that the growth temperature was 30°C for all strains but PTA1 and *pta1 Δ 1–75*, which were grown at 37°C. Results are means \pm SEM for 12 independent transformants.97

- Figure 31. APT-related mutants display a hyperactive calcineurin-dependent response element in basal conditions.** **A)** APT-related mutants were transformed with pAMS366 (*CDRE-lacZ*) and cultures were grown until OD₆₆₀ 0.8 in YPD (pH 5.5) at their semi-permissive temperatures. β -galactosidase activity was measured as described in *Experimental procedures*. Data are mean \pm SEM from twelve independent transformants. Folds were calculated dividing each sample to wild-type strain in non-induced conditions. **B)** Vacuolar staining of APT-related mutant strains with the fluorescent dye FM4-64 was performed as described in the Experimental section for 30 min and monitored by fluorescence microscopy. Color blue indicates the vacuole class (Patricia M Kane, 2006).....98
- Figure 32. Analysis of the calcium homeostasis in *ref2* mutant.** We combined the deletion of *REF2* with several components of the calcium homeostasis machinery. Using the generated strains, three μ l of the indicated dilutions of each strain were inoculated on YPD plates containing different concentrations of calcium (100-300 mM calcium) or 150 mM LiCl and growth was monitored after 2-4 days.....100
- Figure 33. Analysis of the calcium homeostasis in *ref2* mutant.** We combined the deletion of *REF2* with several components of the calcium homeostasis machinery. The generated strains were transformed with plasmid pAMS366 (*CDRE-lacZ*) and incubated for 1 h in the absence (white bars) or presence of 0.2 M CaCl₂ (black bars). β -galactosidase activity was measured as described in *Experimental procedures*. Data are mean \pm SEM from twelve independent transformants.101
- Figure 34. Analysis of the calcium homeostasis in *ref2* mutant under cell wall integrity stressors.** We combined the deletion of *REF2* with several components of the calcium homeostasis machinery. Using the generated strains, dilutions of each strain were inoculated on YPD plates containing different concentrations of Calcofluor white (CFW) and Congo red (CR) and growth was monitored after 2-4 days.....102
- Figure 35. The sensitivity to CWI stressors of *ref2* mutant is only shared by *sla1* mutant.** Three μ l of different dilutions of each BY4741 background strain were inoculated on YPD plates containing different cell wall integrity (CWI) stressors: 50 μ g/ml Calcofluor white (CFW), 7 mM caffeine (Caf), alkaline pH (pH 8) and 1 M sorbitol (1 M Sorb) and incubated at 30°C or 37°C as indicated for 2 - 3 days.....104
- Figure 36. *ref2* cells show a wild-type induction of cell wall integrity pathway.** **A)** The indicated yeast strains were transformed with plasmid p1365, which contains the promoter of *SLT2* driving the expression of the *lacZ* gene, and incubated for 2 h in the absence or presence of 40 μ g/ml Calcofluor white (CFW) and 40 μ g/ml Congo red (CR). β -galactosidase activity was measured as described in *Experimental procedures*. Data are mean \pm SEM from 9 independent transformants. **B)** Yeast strains were transformed with plasmid p2052, which contains the reporter for the *FKS2* promoter and incubated for 16 h at 39°C. β -galactosidase activity was measured as described in *Experimental procedures*. Folds were calculated as the ratio of 39°C /28°C β -galactosidase activities for each strain. Data are mean \pm SEM from 12 independent transformants.106
- Figure 37.** The analysis of different mutants for the subunits of the holo-CPF was performed using a liquid growth test which was initialized at OD₆₆₀ 0.025 and an increasing rank of concentrations of Congo red (A) and Calcofluor white (B). Growth was monitored after 17-24 h. Plates were incubated at 30°C or 37°C, semi-permissive temperatures for the thermo-sensitive mutants used. Brackets have been used to group the wild-type strain (the first in each bracket) with its mutant derivatives, shown as discontinuous lines. Data are mean \pm SEM from 9 independent cultures. ...107
- Figure 38. APT-related mutant strains does not show an induction of the transcriptional response driven by Rlm1.** Semi-quantitative analysis of the *CRH1* expression levels was performed in yeast strains which were grown in YPD until exponential phase at semi-permissive temperatures, then RNA purification was made using RiboPure-Yeast kit (Ambion). Semi-quantitative RT-PCR was performed with *Ready-to-Go* RT-PCR Beads kit (Amersham) loading 50 ng of total RNA of each sample with 23 cycles of amplification and using specific primers to amplify *CRH1* and *ACT1*, which was used as a loading control.108
- Figure 39. Mutation of Phe-374 within the Glc7-binding motif mimics the phenotypes of cells lacking Ref2.** BY4741 wild-type and *ref2* strains were transformed with the empty plasmid pRS415 or the same plasmid harboring the wild-type Ref2 protein (pJFD1) or the Phe-374 mutated version (pJFD2). Liquid growth test was initialized at OD₆₆₀ 0.01 using an increasing rank of concentrations

of Calcofluor white (A) and Congo red (B). Growth was monitored for 17-24 h. Data are the mean \pm SEM from 12 independent cultures.	109
Figure 40. The Phe-374, within the Glc7-binding motif of Ref2, is not important for the transcriptional response driven by Rlm1. BY4741 wild-type and <i>ref2</i> strains were transformed with the empty plasmid pRS415 or the same plasmid harbouring the wild-type Ref2 protein (pJFD1) or the Phe-374 mutated version (pJFD2). A) Yeast strains were transformed with plasmid pLT12, which contains the promoter of <i>CRH1</i> , and incubated for 2 h in the absence or presence of 40 μ g/ml Calcofluor white (CFW) and 40 μ g/ml Congo red (CR). β -galactosidase activity was measured as described in <i>Experimental procedures</i> . Data are mean \pm SEM from 9 independent transformants. B) Yeast strains were transformed with plasmid p1365, which contains the promoter of <i>SLT2</i> , and incubated for 2 h in the absence or presence of 40 μ g/ml Calcofluor white (CFW) and 40 μ g/ml Congo red (CR). β -galactosidase activity was measured as described in <i>Experimental procedures</i> . Data are mean \pm SEM from 9 independent transformants.	110
Figure 41. The lack of Ref2 aggravates the CWI stressors hypersensitivity of a Glc7 allele unable to interact with its regulatory subunits (<i>glc7-109</i>). To generate the strains, a deletion cassette for <i>GLC7</i> and a plasmid YCplac111 harbouring the <i>glc7-109</i> allele (<i>pglc7-109</i> , pJFD11) were cotransformed in BY4741 wild-type (YJFD36) and <i>ref2</i> mutant (YJFD39). Liquid growth test was initialized at OD ₆₆₀ 0.01 using an increasing rank of concentrations of Calcofluor white (A) and Congo red (B), respectively. Growth was monitored for 17-24 h. Data is mean \pm SEM from 12 independent cultures.	111
Figure 42. Analysis of the CWI pathway in <i>ref2</i> mutant. We combined the deletion of <i>REF2</i> with several components of the cell wall integrity response machinery. Using the generated strains, three μ l of different dilutions of each strain were inoculated on YPD plates containing different concentrations of Calcofluor white (CFW), Congo red (CR) and Lithium (LiCl) and growth was monitored after 2-4 days.	113
Figure 43. Gene copy-number analysis determines the aneuploidy on chromosome II and XII. A) Distribution of induced genes through chromosomes of <i>ref2</i> cells (black bars) and theoretical distribution due to chromosome size of induced genes in <i>ref2</i> cells (white bars). B) Representative data from semi-quantitative RT-PCR compared with the DNA microarray values, where OR means out of range.	115
Figure 44. CML476 tetO₇:REF2 works properly inhibiting REF2 when doxycycline is added. A) Three dilutions from cultures of wild-type strain CML476 and its derivative tetO ₇ :REF2 were spotted on plates containing YPD plus calcofluor-white (CFW) with or without doxycycline as indicated. Growth at 28°C was monitored for 2-3 days. B) Monitored liquid growth of CML476 wild-type and its derivative tetO ₇ :REF2 strain in YPD was followed during 120 h at OD ₆₆₀ . Orange arrows indicated the addition of 100 μ g/ml doxycycline and cells were inoculated at 0.01 OD ₆₆₀ ; green arrows indicated the addition of 100 μ g/ml doxycycline. C) Semi-quantitative RT-PCR of <i>REF2</i> and <i>ACT1</i> (used as a loading control) was performed in each sample treated with doxycycline (-) or untreated with doxycycline (+).	117
Figure 45. After 120 h, cells treated with doxycycline do not show any aneuploidy. A) Once analyzed the DNA microarray experiments, the mean of each chromosome was calculated in tetO ₇ :REF2 (8, 24, 32, 48, 72, 96 and 120 h) and <i>ref2</i> mutant from EUROSCARF and graphed in folds. B) DNA microarray data from indicated strains was analyzed with Cluster tool v2.11 from Eisen's lab software (Eisen et al., 1998). Hierarchical cluster was performed using array correlation parameter plus complete linkage clustering and data was represented by Treeview toll v1.6 from Eisen's lab software.	118
Figure 46. The generation of new <i>ref2</i> strains is difficult due to genomic duplication of REF2 itself. A) Test colony PCR amplifying the <i>REF2</i> ORF with primers OJFD20 and OJFD23 (220 bp) and <i>REF2</i> deletion with primers OJFD20 and nat1-3' (700 bp) as a control for generating new <i>ref2</i> mutants. PCR fragments were loaded in 2% DNA agarose. B) Liquid growth of wild-type strain (wt), cells lacking <i>REF2</i> (<i>ref2</i> , called YJFD1-4) and cells with either a copy of <i>REF2</i> and <i>ref2</i> deletion (<i>REF2/ref2</i> , called YJFD49-50) were inoculated at 0.02 OD ₆₆₀ with YPD (pH 5.5) plus 75 mM LiCl (LiCl), 0.6 M NaCl (NaCl) and 200 mM CaCl ₂ (CaCl ₂). Growth at 28°C was monitored for 16 h (wt and <i>REF2/ref2</i>) or 24 h (<i>ref2</i>). Data are mean \pm SEM from at least 12 independent clones.	122
Figure 47. New <i>ref2</i> mutant generated also display aneuploidy. DNA genomic of <i>ref2</i> strain (EUROSCARF) and new <i>ref2</i> strains (YJFD1-4) was compared to wild-type strain using comparative	

- genomic hybridization (CGH) as explained in *Experimental procedures*. The mean of each 16 yeast chromosomes is illustrated in log₂ mutant/wild-type ratio. Below, gene distribution in chromosome XII is graphed. 123
- Figure 48. Mutants in components of the APT-complex do not share the aneuploid-related phenotypes of the *ref2* strain.** **A)** Three dilutions from indicated cultures were spotted on plates containing YPD plus 3% formamide (YPDF), 0.2 µg/ml cycloheximide (Cyc), 10 µg/ml nocodazole (Noc), 30 µg/ml Hygromycin B (Hyg) and 15 ng/ml rapamycin (Rap). Growth at 28°C was monitored for 2-3 days. **B)** Strains used in this dot test: BY4741 wild-type transformed with YCplac111Ø (YJFD34), *pglc7-109* called pJFD11 (YJFD35) and cassette *glc7::nat1* plus *pglc77-109* (YJFD36); BY4741 *ref2* strain was equally transformed generating YJFD37, YJFD38 and YJFD39, respectively. Three dilutions from indicated cultures were spotted on plates containing YPD plus 0.2 µg/ml cycloheximide (Cyc), 10 µg/ml nocodazole (Noc) and 30 µg/ml Hygromycin B (Hyg). Growth at 28°C was monitored for 2-3 days. **C)** Three dilutions from wild-type and *ref2* cells (BY4741 *ref2* and YJFD1-4) were spotted on plates containing YPD plus 0.2 µg/ml cycloheximide (Cyc) and 10 µg/ml nocodazole (Noc). Growth at 28°C was monitored for 2-3 days. 125
- Figure 49. APT-complex strains display lower biomass production than wild-type strains.** **A, B, C and D)** Wild-type and APT-complex mutant cells (*ref2* (A), *yth1-1* (B), *ssu72-2* (C) and *swd2-3* (D)) were grown overnight in YPD. Cells were inoculated at 0.05 OD₆₆₀ and their growth monitored for 36 h at 28°C. The amount of glucose in the medium was determined at the indicated times as explained in *Experimental procedures*. 127
- Figure 50. *ref2* mutants in new backgrounds not only display protein synthesis inhibitor stress but also lower biomass production than wild-type strain.** **A)** New *ref2* strains were generated from TM141 wild-type (YJFD90), 1700 wild-type (YJFD92), CML476 wild-type (YJFD94) and FY61 wild-type (YJFD89). Three dilutions from indicated cultures were spotted on plates containing YPD plus 0.2 µg/ml cycloheximide (Cyc) and 10 µg/ml nocodazole (Noc). Growth at 28°C was monitored for 2-3 days. **B)** 1700 wild-type and its *ref2* derivative cells (*ref2*_N1-N4 called YJFD92) were grown overnight in YPD. Cells were inoculated at 0.05 OD₆₆₀ and their growth monitored for 36 h at 28°C. The amount of glucose in the medium was determined at the indicated times as explained in *Experimental procedures*. **C)** BY4741 wild-type and its *ref2* derivative cells (YJFD1-4) were grown overnight in YPD. Cells were inoculated at 0.05 OD₆₆₀ and their growth monitored for 36 h at 28°C. The amount of glucose in the medium was determined at the indicated times as explained in *Experimental procedures*. 128
- Figure 51. *ref2* cells apparently do not display a delay in G₁.** **A)** Non-synchronized wild-type and its derivative *ref2* cells were grown at exponential growth and DNA content was determined by FACS. **B)** Non-synchronized wild-type and *ref2* (BY4741 *ref2*) cells transformed with plasmid containing *REF2* (pJFD1) or *REF2*^{F374A} (pJFD2) were grown in its restrictive medium (Leu⁻). DNA content was determined using FACS. 129
- Figure 52. Mutation of Phe-374 within the Glc7-binding consensus sequence also display an aneuploidy.** **A)** Wild-type BY4741 (+) and *ref2* strains (-) were transformed with the empty plasmid pRS415 or the same plasmid expressing the wild-type Ref2 protein (pJFD1) or the Ref2^{F374A}-mutated version (pJFD2). Three dilutions of transformants were spotted on to YPD plates plus 0.2 µg/ml cycloheximide (Cyc) and 10 µg/ml nocodazole (Noc). Growth at 28°C was monitored for 2-3 days. **B)** Indicated strains were saturated in the appropriate medium and then inoculated at 0.05 OD₆₆₀ and their growth monitored for 36 h at 28°C. The amount of glucose in the medium was determined at the indicated times as explained in *Experimental procedures*. **C) Left panel**, induced genes of DNA microarray experiments from *ref2* cells (grey) and *ref2* cells carrying the plasmid with the Ref2^{F374A}-mutated version (pJFD2) were classified in a Venn diagram. **Right panel**, once analyzed the DNA microarray experiments as explained in *Experimental procedures*, the mean of each chromosome was calculated for indicated strains and graphed in folds. 130
- Figure 53. Diploid homozygous *ref2* is unable to sporulate.** The strains used in these experiments: BY4741/BY4742 wild-types (BY4743), BY4741 *ref2*/BY4742 wild-type called YJFD70 (*ref2*/*REF2*), BY4741 wild-type/YJFD9 called YJFD69 (*REF2*/*ref2*) and BY4741 *ref2*/YJFD9 called YJFD71 (*ref2*/*ref2*) also transformed with pRS415Ø and its derivative containing *REF2* (pJFD1) or *REF2*^{F374A} (pJFD2). **A)** Three dilutions from indicated cultures were spotted on plates containing YPD plus 5 µg/ml Calcofluor white (CFW), 200 mM CaCl₂ (CaCl₂), 100 mM LiCl (LiCl), 15 µg/ml Congo red (RC) and adjusted a pH 8 (pH); and YP plus 4% ethanol (EtOH). Growth at 28°C was monitored for 2-3

- days. B) Random spore analysis of the indicated strains plated on YPD plates and growth monitored for 2 days and dilution 1/50, except *ref2/ref2* diploid strain which was incubated for 3 days and dilution 1/10 at 28°C. C) Graphic of obtained spores divided by total cells inoculation on to YPD plates.....132
- Figure 54. Diploid homozygous *ref2* has a wild-type *IME1* regulation.** A) The morphogenetic events of spore formation are driven by an underlying transcriptional cascade. (A) The landmark events of meiosis and sporulation are shown in temporal order. Orange lines indicate the mother cell plasma membrane (which becomes the ascus membrane). Gray lines indicate the nuclear envelope. Blue and red lines represent homologous chromosomes. Green lines represent spindle microtubules. Prospore membranes are indicated by pink lines and the lumen of the prospore membrane is highlighted in yellow. After membrane closure, the prospore membrane is separated into two distinct membranes. The one closest to the nucleus serves as the plasma membrane of the spore, while the outer membrane, indicated by thin, dashed pink line, breaks down during spore wall assembly. Blue hatching represents the spore wall. (B) The shaded arrows indicate the relative timing of the different transcriptional classes with respect to the events in A. The black arrows indicate the points at which the transcription factors *Ime1* and *Ndt80* become active (Neiman, 2011). B) Wild-type and its derivative diploid strains were transformed with the construct *pIME1-lacZ* (p1335) and cultures were grown until reached 0.8 OD₆₆₀ in YPD (pH 5.5). Cells were transferred to sporulation medium and collected at indicated times for measuring β-galactosidase activity as described in *Experimental procedures*. Data are mean ± SEM from at least six independent clones.133
- Figure 55. Effect of the mutation of several *Glc7*-interacting proteins on different stressors.** Three dilutions from cultures of wild-type strain BY4741 (wt) and the indicated isogenic derivatives were grown on either YPD plates in the presence of β-mercap (2-Mercaptoethanol 40 mM) and Tn (Tunicamycin 0.1 / 1.2 μg/ml). Growth at 28°C was monitored for 2-3 days.....136
- Figure 56. Evaluation of UPRE in mutants on non-essential *Glc7*-regulatory subunits.** Wild-type and the indicated isogenic derivatives were transformed with the construct *pMCZ-Y* and cultures were grown until reached 0.8 OD₆₆₀ in YPD (pH 5.5). Cells were transferred to fresh YPD (NI, white bars) and with 2 μg/ml tunicamycin (2 μg/ml Tn, black bars) for 90 min at 28°C. β-galactosidase activity was measured as described in *Experimental procedures*. Data are mean ± SEM from at least six independent clones.138
- Figure 57. *GLC7* is needed for properly adaptation to UPR inducers.** A) Strains used in this dot test were BY4741 wild-type transformed with *YCplac111* (YJFD34), *pglc7-109* called pJFD11 (YJFD35) and cassette *glc7::nat1* plus *pglc77-109* (YJFD36) Three dilutions from indicated cultures were spotted on plates containing YPD plus 0.8 μg/ml tunicamycin (Tn) and 40 mM 2-Mercaptoethanol (β-mercap). Growth at 28°C was monitored for 2-3 days. B) Wild-type BY4741 (+) and *reg1* strains (-) were transformed with the empty plasmid pLexA or the same plasmid expressing the wild-type *Reg1* protein (pLexA-*Reg1*, pRJ65), the *Reg1*^{F468D} mutated version (pLexA-*Reg1*^{F468D}) or the *Reg1*^{F468R} mutated version (pLexA-*Reg2*^{F468R}). Three dilutions of transformants were spotted on to YPD plates plus 0.1 μg/ml tunicamycin (Tn 0.1) and 1.0 μg/ml tunicamycin (Tn 1.0). Growth at 28°C was monitored for 2-3 days. C) Wild-type BY4741 (+) and *ref2* strains (-) were transformed with the empty plasmid pRS415 or the same plasmid expressing the wild-type *Ref2* protein (pJFD1) or the *Ref2*^{F374A}-mutated version (pJFD2). Three dilutions of transformants were spotted on to YPD plates plus 1 μg/ml tunicamycin (Tn 1) and 1.2 μg/ml tunicamycin (Tn 1.2). Growth at 28°C was monitored for 2-3 days.140
- Figure 58. *reg1* mutant cells display an uncontrolled UPRE.** Wild-type and the indicated isogenic derivatives were transformed with the construct *pMCZ-Y* and cultures were grown until reached 0.8 OD₆₆₀ in YPD (pH 5.5). Cells were transferred to fresh YPD with 2 μg/ml tunicamycin and cells collected at the indicated times at 28°C. β-galactosidase activity was measured as described in *Experimental procedures*. Data are mean ± SEM from at least six independent clones. Folds are referred to non-induced cultures.....141
- Figure 59. The lack of *Ref2* causes a tolerant phenotype to ER-inducers.** A) Liquid growth of wild-type strain (wt), cells lacking *REF2* (*ref2*) or *IRE1* (*ire1*) and cells lacking both *REF2* and *IRE1* (*ref2 ire1*; YJFD88) were inoculated at 0.02 OD₆₅₀ with YPD (pH 5.5) plus the indicated tunicamycin concentrations. Growth at 28°C was monitored for 16 h (wt and *ire1*) or 24 h (*ref2* and *ref2 ire1*). Data are mean ± SEM from at least 9 independent clones. B) Wild-type and the indicated isogenic

- derivatives were transformed with the construct pMCZ-Y and cultures were grown for until reached 0.8 OD₆₆₀ in YPD (pH 5.5). Cells were transferred to fresh YPD with the indicated UPR inducers for 90 min at 28°C. β -galactosidase activity was measured as described in *Experimental procedures*. Data are mean \pm SEM from at least six independent clones.142
- Figure 60. The *ref2* cells phenotype is not shared by other members of CPF.** Three dilutions of wild-type and its isogenic derivatives were spotted on to YPD plates plus indicated tunicamycin concentrations (+) or DMSO (-). Growth at 28°C or 37 °C were monitored for 2-3 days.143
- Figure 61. *ref2* cells has a unique tunicamycin tolerance in BY4741 background. A (left panel)** Three dilutions from wild-type and *ref2* cells (BY4741 *ref2* and YJFD1-4) were spotted on plates containing YPD plus 1.0 μ g/ml tunicamycin (**Tn 1.0**) and 1.2 μ g/ml tunicamycin (**Tn 1.2**). Growth at 28°C was monitored after 2-3 days. **A (right panel)** 1700 wild-type and its *ref2* derivative cells (*ref2*_N1-N4; **YJFD92**) were spotted on plates containing YPD plus 0.6 μ g/ml tunicamycin (**Tn 0.6**) and 0.8 μ g/ml tunicamycin (**Tn 0.8**). Growth at 28°C was monitored after 2-3 days. **B)** Strains used in this dot test: BY4741 wild-type transformed with YCplac111 \emptyset (YJFD34), *pglc7-109* called pJFD11 (YJFD35) and cassette *glc7::nat1* plus *pglc7-109* (YJFD36); BY4741 *ref2* strain was equally transformed generating YJFD37, YJFD38 and YJFD39, respectively. Three dilutions from indicated cultures were spotted on plates containing YPD plus: 1.0 μ g/ml tunicamycin (**Tn 1.0**), 1.2 μ g/ml tunicamycin (**Tn 1.2**) and 40 mM 2-Mercapethanol (**β -Mercap**). Growth at 28°C was monitored after 2-3 days. **C)** Three dilutions from cultures of wild-type strain CML476 and its derivative *tetO7:REF2* (YJFD16) were pre-treated with 100 μ g/ml doxycycline for 8 h (**PT +**) or without pre-treatment (**PT -**) and then spotted on plates containing YPD plus either the indicated tunicamycin concentrations or presence/absence of 100 μ g/ml doxycycline (**+DOX/-DOX**). Growth at 28°C was monitored after 2-3 days.145
- Figure 62. Our new strains treated with tunicamycin for generations show an increase in tunicamycin tolerance phenotype. A)** Evolutionary tunicamycin experiment design. Basically, wild-type cells were treated with 0.5 / 0.75 μ g/ml tunicamycin for the indicated number of generations (n). Initially, cells were inoculated on YPD (pH 5.5) at 0.05 OD₆₆₀ with presence or absence of tunicamycin, after 10 h approximately, the number of generations (n generations) was annotated and cells were diluted 1/120 in fresh YPD (pH 5.5) plus tunicamycin and incubated overnight at 28°C. The experiment was repeated until 120 yeast generations. **B)** Three dilutions from cultures of wild-type strain induced with 0.5 μ g/ml tunicamycin for n generations (Tn +) or without tunicamycin treatment (Tn -) were spotted on YPD plates plus the indicated tunicamycin concentrations. Growth at 28°C was monitored after 2 days.147
- Figure 63. Strains treated with tunicamycin for 20 and 50 generations display an aneuploidy in chromosome II.** Total RNA extraction from wild-type treated with 0.5 μ g/ml tunicamycin for 20, 50, 86 and 120 generations as described in *Experimental procedures*. Once analyzed the DNA microarray experiments, the mean of each chromosome was calculated for indicated strains, graphed in folds and compared to DNA microarray experiment from BY4741 *ref2* (*ref2*) and BY4741 *ref2* transformed with the plasmid which contains the mutated version Ref2^{F374A} (pJFD2) from *Figure 52C*.148
- Figure 64. The right arm of chromosome II display a duplication in strains treated with tunicamycin for 20 and 50 n.** DNA microarray data from gens located on chromosome II in the indicated strains were graphed using a hierarchical cluster, which was performed using array correlation parameter plus complete linkage clustering, and data was represented by Treeview toll v1.6 from Eisen's lab software.150
- Figure 65. Wild-type strains treated with tunicamycin for 86 and 120 generations show an accurate long-term response similar to other drugs or inducers. Left panel:** 56 selected genes by expression using the parameters: < 1.85 folds at 20n + > 1.85 folds at 86n + > 1.85 folds at 150n were represented in a hierarchical cluster which was performed using array correlation parameter plus complete linkage clustering, and data was represented by Treeview toll v1.6 from Eisen's lab software. **Right panel:** Characteristic genes found in the analysis with the same parameter used above: retrotransposons genes and *induced* genes from (Banerjee et al., 2008; Ma & Liu, 2010) are located on the hierarchical cluster representation.153
- Figure 66. Wild-type strains treated with tunicamycin display different phenotypes to several drugs.** Three dilutions from cultures of wild-type strain induced with 0.5 μ g/ml tunicamycin for n generations (**Tn +**) or without tunicamycin treatment (**Tn -**) were spotted on YPD plates plus the

following stressors: cycloheximide at the indicated concentrations; 70 mM hygromycin B (**Hyg**); 20 mM caffeine (**Caf**); 1.2 M NaCl (**NaCl**); 200 mM LiCl (**LiCl**); 0.7 µg/ml spermine (**Sper**) and 2 µg/ml tunicamycin (**Tn**). Growth at 28°C was monitored after 2-3 days. 154

Figure 67. Phenotypical analysis of cell wall integrity pathway and calcium homeostasis in *ref2* cells. A) Three dilutions from cultures of wild-type strain and mutants from cell wall integrity components combined with disruption of *REF2* (-) were spotted on YPD plus 0.6 µg/ml tunicamycin (**Tn 0.6**) and plus 1.0 µg/ml tunicamycin (**Tn 1.0**). Growth at 28°C was monitored for 2-3 days. **B)** Three dilutions from cultures of wild-type strain and mutants from calcium homeostasis combined with disruption of *REF2* (-) were spotted on YPD plus 0.2 µg/ml tunicamycin (**Tn 0.2**) and plus 0.8 µg/ml tunicamycin (**Tn 0.8**). Growth at 28°C was monitored for 2-3 days. 156

Figure 68. UPRE analysis on cell wall integrity pathway and calcium homeostasis in *ref2* cells. A) Wild-type and mutants on cell wall integrity components were transformed with the construct pMCZ-Y and cultures were grown for until reached 0.8 OD₆₆₀ in YPD (pH 5.5). Cells were transferred to fresh YPD with 2.5 µg/ml tunicamycin for 90 min at 28°C. β-galactosidase activity was determined as described in *Experimental procedures*. Data are mean ± SEM from at least six independent clones. **B)** Wild-type and mutants on calcium homeostasis components were transformed with the construct pMCZ-Y and cultures were grown for until reached 0.8 OD₆₆₀ in YPD (pH 5.5). Cells were transferred to fresh YPD with 2.5 µg/ml tunicamycin for 90 min at 28°C. β-galactosidase activity was determined as described in *Experimental procedures*. Data are mean ± SEM from at least six independent clones. 158

Figure 69. *reg1* cells display an uncontrolled UPRE in DBY746 background as well. A) Liquid growth of wild-type strain (**wt**), cells lacking *REG1* (**reg1**; *MPO30*) or *SNF1* (**snf1**; *CCV180*) and cells lacking both (**reg1 snf1**; *CCV181*) were inoculated at 0.02 OD₆₆₀ with YPD (pH 5.5) plus the indicated tunicamycin concentrations. Growth at 28°C was monitored for 16 h (**wt**) and for 24 h (**reg1**; **snf1** and **reg1 snf1**). Data are mean ± S.E. from at least 12 independent clones. **B)** The indicated strains above were transformed with the construct pMCZ-Y and cultures were grown for until reached 0.8 OD₆₆₀ in YPD (pH 5.5). Cells were transferred to fresh YPD (non-induced, **NI**) with 2 µg/ml tunicamycin (**Tn 2 µg/ml**) or 5 mM **DTT** for 90 minutes at 28°C. β-galactosidase activity was measured as described in *Experimental procedures*. Data are mean ± SEM from at least nine independent clones. 159

Figure 70. *PTC2* and *PTC3* partially rescue the hypersensitivity to tunicamycin of *reg1* cells. Three dilutions from cultures of wild-type and *reg1* cells transformed with YEp195∅, YEp195-*HEX2*, YEp195-*PTC2* and YEp195-*PTC3* were spotted on YPD plus tunicamycin at the indicated concentrations. Growth at 28°C was monitored for 2-3 days. 160

Figure 71. *reg1* cells cannot reverse the *HAC1* splicing. A) Wild-type strain and its isogenic derivatives *reg1*, *snf1* or *reg1 snf1* (YJFD31) were grown for until reached 0.6 OD₆₆₀ in YPD (pH 5.5) then induced with 1 µg/ml Tunicamycin for 1 h (**Tn**). After induction, cells were collected, washed with fresh YPD (pH 5.5) and then resuspended in YPD (pH 5.5) and samples collected at indicated times. After total RNA extraction 15 ng total RNA were used to perform a qRT-PCR as described in the *Experimental procedures*. Folds of *KAR2* gene were calculated of each mutant as non-induced (**NI**) as a template. **B)** Wild-type strain and its isogenic derivatives *reg1*, *snf1* or *reg1 snf1* (YJFD31) were grown for until reached 0.6 OD₆₆₀ in YPD (pH 5.5) then induced with 1 µg/ml tunicamycin for 1 h (**Tn**). After induction, cells were collected, washed with fresh YPD (pH 5.5) and then resuspended in YPD (pH 5.5) and samples collected at indicated times. After total RNA extraction, the Northern blot was performed for analyzing the indicated genes. 161

Figure 72. *reg1* cells cannot decouple *Ire1* oligodimers. A) Wild-type and *reg1* cells were co-transformed with pRS315-*IRE1*-HA and pRS426-*IRE1*-Flag. Cultures were grown for until reached 0.6 OD₆₆₀ in YPD (pH 5.5) then induced with 1 µg/ml tunicamycin for 1 h (**Tn**). After induction, cells were collected, washed with fresh YPD (pH 5.5) and then resuspended in YPD (pH 5.5) and samples collected at indicated times. Protein extraction was performed as explained in *Experimental procedures*. Blots were incubated with the antibodies anti-HA or anti-Flag either before immunoprecipitation (**No IP**) or after immunoprecipitation (**IP**). **B)** Quantification from blots was performed using the GelAnalyzer 2010. Fold calculation on **IP** experiment was performed as: **1)** every sample detected with anti-Flag was divided for the same sample detected with anti-Ha and then **2)** non-induced samples (**NI**) were determined as basal level, so folds were calculated dividing

- a sample to wild-type non-induced or *reg1* non-induced. The starting point in the graphic is the non-induced samples (1) and (2) indicates the 1 µg/ml tunicamycin for 1 h.162
- Figure 73. *reg1* cells display an unaltered either a cell wall integrity or calcium homeostasis under tunicamycin conditions.** **A)** The indicated strains above were transformed with the construct containing four CDRE tandem repeats (pAMS366) and cultures were grown until reached 0.8 OD₆₆₀ in YPD (pH 5.5). Cells were transferred to fresh YPD (non-induced, NI) plus: 2.5 µg/ml tunicamycin (Tn), 50 µg/ml Calcofluor white (CFW) or 0.2 M CaCl₂ for 90 minutes at 28°C. β-galactosidase activity was measured as described in *Experimental procedures*. Data are mean ± SEM from at least twelve independent clones. **B)** The indicated strains above were transformed with the construct containing the promoter of *SLT2* (p1365) and cultures were grown for until reached 0.8 OD₆₆₀ in YPD (pH 5.5). Cells were transferred to fresh YPD (non-induced, NI) plus: 2.5 µg/ml tunicamycin (Tn), 50 µg/ml Calcofluor white (CFW) or 0.2 M CaCl₂ for 90 minutes at 28°C. β-galactosidase activity was measured as described in *Experimental procedures*. Data are mean ± SEM from at least twelve independent clones.164
- Figure 74. UPR does not activate Snf1 pathway.** The indicated strains above were transformed with the construct containing the promoter of *SUC2* (YEp357-*SUC2*) and cultures were grown until reached 0.8 OD₆₆₀ in YPD (pH 5.5). Cells were washed for eliminating glucose with YP then were transferred to YPD (non-induced, NI) or YP low glucose (0.05% glucose) plus 2.5 µg/ml tunicamycin (Tn) for 1.5 h or 3 h at 28°C. β-galactosidase activity was measured as described in *Experimental procedures*. Data are mean ± SEM from at least twelve independent clones.165
- Figure 75. Low glucose does not activate UPR.** **A)** The indicated strains were transformed with the construct pMCZ-Y (UPRE-*lacZ*) and cultures were grown for until reached 0.8 OD₆₆₀ in YPD (pH 5.5). Cells were transferred to fresh YPD (non-induced, NI) with 2.5 µg/ml tunicamycin (Tn) or YP low glucose (0.05% glucose) plus 2.5 µg/ml tunicamycin (Tn) for 90 minutes at 28°C. β-galactosidase activity was measured as described in *Experimental procedures*. Data are mean ± SEM from at least eighteen independent clones. **B)** Three dilutions from the indicated cultures were spotted on YP plus 4% ethanol (EtOH) plus the indicated tunicamycin concentrations (Tn) or YP plus 0.05% glucose (Low Glucose) plus the indicated tunicamycin concentrations (Tn). Growth at 28°C was monitored for 2-3 days.166
- Figure 76. Snf1 inactive alleles rescue *reg1* cells hypersensitivity to tunicamycin.** **A)** Wild-type strain and its isogenic derivatives *reg1*, *snf1* or *reg1 snf1* (YJFD31) were transformed with the indicated plasmids: YCp50Ø, pCE108 (**SNF1**), pCE108-Y106A (**SNF1-Y106A**) and pCE108-G53R (**SNF1-G53R**). Three dilutions from the indicated cultures were spotted on YPD (pH 5.5) plus the indicated tunicamycin concentrations (Tn). Growth at 28°C was monitored for 2-3 days. **B)** Wild-type strain and its isogenic derivatives *reg1*, *snf1* or *reg1 snf1* (YJFD31) were transformed with the indicated plasmids: pWS93Ø, pSK119 (**SNF1**), pSK119A (**SNF1-T210A**) and pSK120 (**SNF1-K84R**). Three dilutions from the indicated cultures were spotted on YPD (pH 5.5) plus the indicated tunicamycin concentrations (Tn). Growth at 28°C was monitored for 2-3 days.167
- Figure 77. Phenotypical analysis of Snf1 pathway under tunicamycin conditions.** Three dilutions from the indicated cultures were spotted on YPD plus 0.2 µg/ml tunicamycin (Tn 0.2), 1.2 µg/ml tunicamycin (Tn 1.2) and 1.4 µg/ml tunicamycin (Tn 1.4). Growth at 28°C was monitored for 2-3 days.168
- Figure 78. UPRE analysis of Snf1 pathway.** The indicated strains were transformed with the construct pMCZ-Y (UPRE-*lacZ*) and cultures were grown for until reached 0.8 OD₆₆₀ in YPD (pH 5.5). Cells were transferred to fresh YPD (non-induced, NI) with 2.5 µg/ml tunicamycin (Tn) for 90 minutes at 28°C. β-galactosidase activity was measured as described in *Experimental procedures*. Data are mean ± SEM from at least twelve independent clones. Folds were calculated as the ratio between non-induced conditions and the transcriptional response to tunicamycin for each strain.169

Table 1. Known Glc7-regulatory subunits. The underlined residues were mutated and found to be important for Glc7 binding. The Glc7 regulatory subunits analysed on this thesis are marked in blue	18
Table 2. <i>S. cerevisiae</i> strains derived from BY4741 (MAT a <i>his3Δ1 leu2Δ met15Δ ura3Δ</i>) genetic background from EUROFAN (continue Table 3) ¹ Strains checked for correct gene deletion.	50
Table 3. <i>S. cerevisiae</i> strains derived from BY4741 (MAT a <i>his3Δ1 leu2Δ met15Δ ura3Δ</i>) genetic background.	51
Table 4. <i>S. cerevisiae</i> strains derived from BY4741 (MAT a <i>his3Δ1 leu2Δ met15Δ ura3Δ</i>) genetic background generated from the disruption cassettes.	51
Table 5. <i>S. cerevisiae</i> strains generated from the deletion cassette <i>ref2::nat1</i> in several genetic backgrounds. Diploid strains derived from BY4743 (MATa/MATα <i>his3Δ/his3Δ; leu2Δ/leu2Δ; met15Δ0/MET15; LYS2/lys2Δ; ura3Δ/ura3Δ</i>) genetic backgrounds.	52
Table 6. <i>S. cerevisiae</i> strains derived from DBY746 (MATα <i>leu2-3, 112 his3-Δ1 trp1-Δ289 ura3-52</i>) genetic background from our laboratory's database.	53
Table 7. <i>S. cerevisiae</i> strains from different genetic backgrounds kindly provided by international laboratories.	54
Table 8. <i>S. cerevisiae</i> diploid strains generated in this thesis.	54
Table 9. Oligonucleotides used in this work for generation and verification of genes disruptions.	55
Table 10. Oligonucleotides used for plasmid constructions.	60
Table 11. Oligonucleotides used in qRT-PCR, RT-PCR and Northern blot experiments. Orange indicates 5'-primers.	64
Table 12. Phenotypic array comparing multiple wild-type phenotypes with those of the non-essential regulatory subunits of Glc7 mutant strains. Growth of each mutant was compared with that of the corresponding wild-type strain grown under the same set of conditions. Black squares denote strong sensitivity (SS), grey squares indicate mild phenotype (MS), white squares correspond with wild-type behavior (WT) and red square indicates an hypertolerance phenotype (HT). Conditions tested to construct the array were: LiCl, 50–300 mM LiCl; NaCl, 0.4–1.2 M NaCl; high pH, pH 8.0–8.3; CaCl ₂ , 100–300 mM CaCl ₂ ; ZnCl ₂ , 1–6 mM ZnCl ₂ ; CFW, 1-300 µg/ml Calcofluor white; Caf, 1-20 mM caffeine; Tn, 0.1-1-4 µg/ml tunicamycin; β-merp, 5-40 mM β-mercapthenol; Hyg B, 20–60 µg/ml hygromycin B; TMA, 0.2–0.6 M TMA; Sper, 0.1-0.7 mM spermine; YPGly, YP plus 2% glycerol; YP-EtOH, YP plus 2% ethanol; YP-LowGlu, YP plus 0.05% glucose.	72
Table 13. Functional characterization of induced and repressed genes in the mutants of the Glc7-regulatory subunits analyzed. Analysis of induced genes (relative expression > 1.80 folds) or repressed genes (relative expression < 0.55 folds) of each strain were obtained by the functional categories classifier (Functat) tool of MIPS (Ruepp et al., 2004). Only functional categories with P-value < 10 ⁻³ are shown and either the percentage of induced genes (% Ind) or repressed genes (% Rep) were calculated respect the total of genes with existing data.	77
Table 14. Distribution of snoRNA read-throughs due to the lack of REF2 transcription. Array of genes located downstream of snoRNA loci whose expression is increased more than 1.75-fold (grey) or 2.0-fold (black) by tetO ₇ :REF2 strain (8, 24, 32, 48, 72, 96 and 120 h) and <i>ref2</i> cells as a result of read-through. Colors indicate a comparison between different strains: <i>ssu72-2</i> data from (Nedea et al., 2003) (orange); <i>ssu72-2</i> data from our experiment (yellow) and data from both strains (red).	120
Table 15. Characterization of induced and repressed genes in tunicamycin-evolution experiment. Analysis of induced (A) genes (relative expression > 1.80 folds) or repressed (B) genes (relative expression < 0.55 folds) of each strain were obtained by the functional categories classifier tool of MIPS (Ruepp et al., 2004). Only functional categories with P-value < 10 ⁻⁴ were characterized and either the percentage of induced genes (% Ind) or repressed genes (% Rep) were calculated respect the total of genes with existing data.	149
Table 16. Gene induced in chromosome II from the early response to tunicamycin. We compared the genes induced in chromosome II from the 20 n, 50 n, <i>ref2</i> and <i>pJFD2</i> strains (Figure 63). Data from <i>Saccharomyces</i> Genome Database (SGD).	151

Bibliography

REFERENCES

- Adams, A., Gottschling, D. E., Kaiser, C. A., & Stearns, T. (1997). *Methods in Yeast Genetics*. Cold Spring Harbor, NY: Cold Spring Harbor Laboratory Press, NY.
- Ahmed, A., Sesti, F., Ilan, N., Shih, T. M., Sturley, S. L., & Goldstein, S. A. (1999). A molecular target for viral killer toxin: TOK1 potassium channels. *Cell*, *99*(0092-8674; 3), 283–291.
- Alberola, T. M., Garcia-Martinez, J., Antunez, O., Viladevall, L., Barcelo, A., Arino, J., & Perez-Ortin, J. E. (2004). A new set of DNA macrochips for the yeast *Saccharomyces cerevisiae*: features and uses. *International microbiology: the official journal of the Spanish Society for Microbiology*, *7*(1139-6709; 3), 199–206.
- Alepuz, P. M., Cunningham, K. W., & Estruch, F. (1997). Glucose repression affects ion homeostasis in yeast through the regulation of the stress-activated *ENA1* gene. *Molecular microbiology*, *26*(0950-382; 1), 91–98.
- Alms, G. R., Sanz, P., Carlson, M., & Haystead, T. A. (1999). Reg1p targets protein phosphatase 1 to dephosphorylate hexokinase II in *Saccharomyces cerevisiae*: characterizing the effects of a phosphatase subunit on the yeast proteome. *The EMBO journal*, *18*(15), 4157–68. doi:10.1093/emboj/18.15.4157
- Andrews, P. D., & Stark, M. J. (2000). Type 1 protein phosphatase is required for maintenance of cell wall integrity, morphogenesis and cell cycle progression in *Saccharomyces cerevisiae*. *J. Cell Sci.*, *113* (Pt 3(0021-9533), 507–520.
- Arino, J. (2002). Novel protein phosphatases in yeast. *European journal of biochemistry / FEBS*, *269*(0014-2956; 4), 1072–1077.
- Ariño, J., Ramos, J., & Sychrová, H. (2010). Alkali metal cation transport and homeostasis in yeasts. *Microbiology and molecular biology reviews : MMBR*, *74*(1), 95–120.
- Arino, J., Casamayor, A., & Gonzalez, A. (2011). Type 2C protein phosphatases in fungi. *Eukaryotic cell*, *10*(1), 21–33.
- Ayllón, V., Cayla, X., García, A., Fleischer, A., & Rebollo, A. (2002). The anti-apoptotic molecules Bcl-xL and Bcl-w target protein phosphatase 1α to Bad. *European journal of immunology*, *32*(7), 1847–55.
- Ayscough, K. R., Eby, J. J., Lila, T., Dewar, H., Kozminski, K. G., & Drubin, D. G. (1999). Sla1p is a functionally modular component of the yeast cortical actin cytoskeleton required for correct localization of both Rho1p-GTPase and Sla2p, a protein with talin homology. *Molecular biology of the cell*, *10*(4), 1061–75.
- Back, S. H., Schröder, M., Lee, K., Zhang, K., & Kaufman, R. J. (2005). ER stress signaling by regulated splicing: *IRE1/HAC1/XBP1*. *Methods (San Diego, Calif.)*, *35*(4), 395–416.
- Bailis, J. M., & Roeder, G. S. (2000). Pachytene exit controlled by reversal of Mek1-dependent phosphorylation. *Cell*, *101*(2), 211–21.
- Balzi, E., Wang, M., Leterme, S., Van Dyck, L., & Goffeau, A. (1994). *PDR5*, a novel yeast multidrug resistance conferring transporter controlled by the transcription regulator *PDR1*. *The Journal of biological chemistry*, *269*(3), 2206–14.
- Banerjee, D., Lelandais, G., Shukla, S., Mukhopadhyay, G., Jacq, C., Devaux, F., & Prasad, R. (2008). Responses of pathogenic and nonpathogenic yeast species to steroids reveal the functioning and evolution of multidrug resistance transcriptional networks. *Eukaryotic cell*, *7*(1), 68–77.
- Barabino, S. M., Hübner, W., Jenny, A., Minvielle-Sebastia, L., & Keller, W. (1997). The 30-kD subunit of mammalian cleavage and polyadenylation specificity factor and its yeast homolog are RNA-binding zinc finger proteins. *Genes & development*, *11*(13), 1703–16.

- Barham, D., & Trinder, P. (1972). An improved colour reagent for the determination of blood glucose by the oxidase system. *The Analyst*, *97*(151), 142–5.
- Batisse, J., Batisse, C., Budd, A., Böttcher, B., & Hurt, E. (2009). Purification of nuclear poly(A)-binding protein Nab2 reveals association with the yeast transcriptome and a messenger ribonucleoprotein core structure. *The Journal of biological chemistry*, *284*(50), 34911–7.
- Batiza, A. F., Schulz, T., & Masson, P. H. (1996). Yeast respond to hypotonic shock with a calcium pulse. *Journal of Biological Chemistry*, *271*(0021-9258; 38), 23357–23362.
- Benito, B., Garciadeblás, B., & Rodríguez-Navarro, A. (2002). Potassium- or sodium-efflux ATPase, a key enzyme in the evolution of fungi. *Microbiology (Reading, England)*, *148*(Pt 4), 933–41.
- Bermejo, C., Rodriguez, E., Garcia, R., Rodriguez-Pena, J. M., Rodriguez de la Concepcion, M. L., Rivas, C., Arroyo, J. (2008). The sequential activation of the yeast HOG and *SLT2* pathways is required for cell survival to cell wall stress. *Molecular biology of the cell*, *19*(3), 1113–1124.
- Bernales, S., McDonald, K. L., & Walter, P. (2006). Autophagy counterbalances endoplasmic reticulum expansion during the unfolded protein response. *PLoS biology*, *4*(12), e423.
- Bertolotti, A., Zhang, Y., Hendershot, L. M., Harding, H. P., & Ron, D. (2000). Dynamic interaction of BiP and ER stress transducers in the unfolded-protein response. *Nature cell biology*, *2*(6), 326–32.
- Bertram, P. G., Choi, J. H., Carvalho, J., Chan, T.-F., Ai, W., & Zheng, X. F. S. (2002). Convergence of TOR-nitrogen and Snf1-glucose signaling pathways onto Gln3. *Molecular and cellular biology*, *22*(4), 1246–52.
- Bharucha, J. P., Larson, J. R., Gao, L., Daves, L. K., & Tatchell, K. (2008). Ypi1, a positive regulator of nuclear protein phosphatase type 1 activity in *Saccharomyces cerevisiae*. *Molecular biology of the cell*, *19*(3), 1032–45.
- Bharucha, J. P., Larson, J. R., Konopka, J. B., & Tatchell, K. (2008). *Saccharomyces cerevisiae* Afr1 protein is a protein phosphatase 1/Glc7-targeting subunit that regulates the septin cytoskeleton during mating. *Eukaryotic cell*, *7*(8), 1246–55.
- Bianchi, M. M., Costanzo, G., Chelstowska, A., Grabowska, D., Mazzoni, C., Piccinni, E., ... Negri, R. (2004). The bromodomain-containing protein Bdf1p acts as a phenotypic and transcriptional multicopy suppressor of *YAF9* deletion in yeast. *Molecular microbiology*, *53*(3), 953–68.
- Bicknell, A. A., Tourtellotte, J., & Niwa, M. (2010). Late phase of the endoplasmic reticulum stress response pathway is regulated by Hog1 MAP kinase. *The Journal of biological chemistry*, *285*(23), 17545–55.
- Birchwood, C. J., Saba, J. D., Dickson, R. C., & Cunningham, K. W. (2001). Calcium influx and signaling in yeast stimulated by intracellular sphingosine 1-phosphate accumulation. *Journal of Biological Chemistry*, *276*(0021-9258; 15), 11712–11718.
- Bissinger, P. H., & Kuchler, K. (1994). Molecular cloning and expression of the *Saccharomyces cerevisiae* *STS1* gene product. A yeast ABC transporter conferring mycotoxin resistance. *The Journal of biological chemistry*, *269*(6), 4180–6.
- Bloecher, A., & Tatchell, K. (2000). Dynamic localization of protein phosphatase type 1 in the mitotic cell cycle of *Saccharomyces cerevisiae*. *The Journal of cell biology*, *149*(1), 125–40.
- Bollen, M. (2001). Combinatorial control of protein phosphatase-1. *Trends Biochem.Sci.*, *26*(0968-0004; 7), 426–431.
- Bond, U. (2006). Stressed out! Effects of environmental stress on mRNA metabolism. *FEMS yeast research*, *6*(2), 160–70.
- Bond, U., Neal, C., Donnelly, D., & James, T. C. (2004). Aneuploidy and copy number breakpoints in the genome of lager yeasts mapped by microarray hybridisation. *Current genetics*, *45*(6), 360–70.
- Bonilla, M., & Cunningham, K. W. (2002). Calcium release and influx in yeast: TRPC and VGCC rule another kingdom. *Sci.STKE*, *2002*(1525-8882; 127), E17.

- Bonilla, M, Nastase, K. K., & Cunningham, K. W. (2002). Essential role of calcineurin in response to endoplasmic reticulum stress. *The EMBO journal*, 21(0261-4189; 10), 2343–2353.
- Bonilla, Myriam, Nastase, K. K., & Cunningham, K. W. (2002). Essential role of calcineurin in response to endoplasmic reticulum stress. *The EMBO journal*, 21(10), 2343–53.
- Bonilla, Myriam, & Cunningham, K. W. (2003). Mitogen-activated protein kinase stimulation of Ca(2+) signaling is required for survival of endoplasmic reticulum stress in yeast. *Molecular biology of the cell*, 14(10), 4296–305.
- Boustany, L. M., & Cyert, M. S. (2002). Calcineurin-dependent regulation of Crz1p nuclear export requires Msn5p and a conserved calcineurin docking site. *Genes Dev.*, 16(0890-9369; 5), 608–619.
- Bredden, L. L. (2003). Periodic transcription: a cycle within a cycle. *Current biology : CB*, 13(1), R31–8.
- Cannon, J. F. (2010). Function of protein phosphatase-1, Glc7, in *Saccharomyces cerevisiae*. *Advances in applied microbiology*, 73, 27–59.
- Cannon, R. D., Lamping, E., Holmes, A. R., Niimi, K., Baret, P. V., Keniya, M. V, Monk, B. C. (2009). Efflux-mediated antifungal drug resistance. *Clinical microbiology reviews*, 22(2), 291–321.
- Cappellaro, C., Baldermann, C., Rachel, R., & Tanner, W. (1994). Mating type-specific cell-cell recognition of *Saccharomyces cerevisiae*: cell wall attachment and active sites of a- and alpha-agglutinin 1. *The EMBO journal*, 13(0261-4189; 20), 4737–4744.
- Casagrande, V., Del Vescovo, V., Militti, C., Mangiapelo, E., Frontali, L., Negri, R., & Bianchi, M. M. (2009). Cesium chloride sensing and signaling in *Saccharomyces cerevisiae*: an interplay among the HOG and CWI MAPK pathways and the transcription factor Yaf9. *FEMS yeast research*, 9(3), 400–10.
- Castermans, D., Somers, I., Kriel, J., Louwet, W., Wera, S., Versele, M., ... Thevelein, J. M. (2012). Glucose-induced posttranslational activation of protein phosphatases PP2A and PP1 in yeast. *Cell research*.
- Celenza, J. L., & Carlson, M. (1989). Mutational analysis of the *Saccharomyces cerevisiae* SNF1 protein kinase and evidence for functional interaction with the SNF4 protein. *Molecular and cellular biology*, 9(11), 5034–44.
- Cetin, B., & Cleveland, D. W. (2010). How to survive aneuploidy. *Cell*, 143(1), 27–9.
- Ceulemans, H, Vulsteke, V., De Maeyer, M., Tatchell, K., Stalmans, W., & Bollen, M. (2002). Binding of the concave surface of the Sds22 superhelix to the alpha 4/alpha 5/alpha 6-triangle of protein phosphatase-1. *Journal of Biological Chemistry*, 277(0021-9258; 49), 47331–47337.
- Ceulemans, Hugo, & Bollen, M. (2004). Functional diversity of protein phosphatase-1, a cellular economizer and reset button. *Physiological reviews*, 84(1), 1–39.
- Ceulemans, Hugo, Vulsteke, V., De Maeyer, M., Tatchell, K., Stalmans, W., & Bollen, M. (2002). Binding of the concave surface of the Sds22 superhelix to the alpha 4/alpha 5/alpha 6-triangle of protein phosphatase-1. *The Journal of biological chemistry*, 277(49), 47331–7.
- Chang, J. S., Henry, K., Wolf, B. L., Geli, M., & Lemmon, S. K. (2002). Protein phosphatase-1 binding to scd5p is important for regulation of actin organization and endocytosis in yeast. *The Journal of biological chemistry*, 277(50), 48002–8. doi:10.1074/jbc.M208471200
- Chawla, A., Chakrabarti, S., Ghosh, G., & Niwa, M. (2011). Attenuation of yeast UPR is essential for survival and is mediated by IRE1 kinase. *The Journal of cell biology*, 193(1), 41–50.
- Chen, Y., Feldman, D. E., Deng, C., Brown, J. A., De Giacomo, A. F., Gaw, A. F., Koong, A. C. (2005). Identification of mitogen-activated protein kinase signaling pathways that confer resistance to endoplasmic reticulum stress in *Saccharomyces cerevisiae*. *Molecular cancer research : MCR*, 3(12), 669–77.
- Cheng, A., Ross, K. E., Kaldis, P., & Solomon, M. J. (1999). Dephosphorylation of cyclin-dependent kinases by type 2C protein phosphatases. *Genes Dev.*, 13(0890-9369; 22), 2946–2957.

- Cheng, C., Huang, D., & Roach, P. J. (1997). The 18th International Conference on Yeast Genetics and Molecular Biology. Stellenbosch, South Africa, March 31-April 5, 1997. Abstracts. *Yeast (Chichester, England)*, 13 Spec No(1), S1–266.
- Cheng, H., He, X., & Moore, C. (2004). The essential WD repeat protein Swd2 has dual functions in RNA polymerase II transcription termination and lysine 4 methylation of histone H3. *Molecular and cellular biology*, 24(7), 2932–43.
- Chernoff, Y. O., Vincent, A., & Liebman, S. W. (1994). Mutations in eukaryotic 18S ribosomal RNA affect translational fidelity and resistance to aminoglycoside antibiotics. *The EMBO journal*, 13(4), 906–13.
- Chesarone, M., Gould, C. J., Moseley, J. B., & Goode, B. L. (2009). Displacement of formins from growing barbed ends by Bud14 is critical for actin cable architecture and function. *Developmental cell*, 16(2), 292–302.
- Christianson, T. W., Sikorski, R. S., Dante, M., Shero, J. H., & Hieter, P. (1992). Multifunctional yeast high-copy-number shuttle vectors. *Gene*, 110(1), 119–22.
- Clotet, J., Posas, F., Casamayor, A., Schaaff-Gerstenschlager, I., & Arino, J. (1991). The gene *DIS2S1* is essential in *Saccharomyces cerevisiae* and is involved in glycogen phosphorylase activation. *Current genetics*, 19(0172-8083; 5), 339–342.
- Cohen, P. (1991). Classification of protein-serine/threonine phosphatases: identification and quantitation in cell extracts. *Methods in enzymology*, 201, 389–98.
- Cohen, P. T. (1997). Novel protein serine/threonine phosphatases: variety is the spice of life 2. *Trends Biochem.Sci.*, 22(0968-0004; 7), 245–251.
- Cohen, P. T. (2002). Protein phosphatase 1--targeted in many directions. *J.Cell Sci.*, 115(0021-9533), 241–256.
- Collister, M., Didmon, M. P., MacIsaac, F., Stark, M. J., MacDonald, N. Q., & Keyse, S. M. (2002). YIL113w encodes a functional dual-specificity protein phosphatase which specifically interacts with and inactivates the Slr2/Mpk1p MAP kinase in *S. cerevisiae*. *FEBS letters*, 527(0014-5793; 1-3), 186–192.
- Connor, J. H., Kleeman, T., Barik, S., Honkanen, R. E., & Shenolikar, S. (1999). Importance of the beta12-beta13 loop in protein phosphatase-1 catalytic subunit for inhibition by toxins and mammalian protein inhibitors. *The Journal of biological chemistry*, 274(32), 22366–72.
- Cowen, L. E. (2008). The evolution of fungal drug resistance: modulating the trajectory from genotype to phenotype. *Nature reviews. Microbiology*, 6(3), 187–98.
- Cowen, L. E., & Steinbach, W. J. (2008). Stress, drugs, and evolution: the role of cellular signaling in fungal drug resistance. *Eukaryotic cell*, 7(5), 747–64.
- Cox, J. S., Shamu, C. E., & Walter, P. (1993). Transcriptional induction of genes encoding endoplasmic reticulum resident proteins requires a transmembrane protein kinase. *Cell*, 73(6), 1197–206.
- Credle, J. J., Finer-Moore, J. S., Papa, F. R., Stroud, R. M., & Walter, P. (2005). On the mechanism of sensing unfolded protein in the endoplasmic reticulum. *Proceedings of the National Academy of Sciences of the United States of America*, 102(52), 18773–84.
- Crespo, J. L., Daicho, K., Ushimaru, T., & Hall, M. N. (2001). The GATA transcription factors GLN3 and GAT1 link TOR to salt stress in *Saccharomyces cerevisiae* 5. *Journal of Biological Chemistry*, 276(0021-9258; 37), 34441–34444.
- Cui, D.-Y., Brown, C. R., & Chiang, H.-L. (2004). The type 1 phosphatase Reg1p-Glc7p is required for the glucose-induced degradation of fructose-1,6-bisphosphatase in the vacuole. *The Journal of biological chemistry*, 279(11), 9713–24.
- Cullen, P. J., & Sprague, G. F. (2002). The Glc7p-interacting protein Bud14p attenuates polarized growth, pheromone response, and filamentous growth in *Saccharomyces cerevisiae*. *Eukaryotic cell*, 1(6), 884–94.

- Cunningham, K. W., & Fink, G. R. (1994). Calcineurin-dependent growth control in *Saccharomyces cerevisiae* mutants lacking *PMC1*, a homolog of plasma membrane Ca²⁺ ATPases. *J. Cell Biol.*, 124(0021-9525; 3), 351–363.
- Cunningham, K. W., & Fink, G. R. (1996). Calcineurin inhibits VCX1-dependent H⁺/Ca²⁺ exchange and induces Ca²⁺ ATPases in *Saccharomyces cerevisiae*. *Molecular and cellular biology*, 16(5), 2226–37.
- Cyert, M. S. (2003). Calcineurin signaling in *Saccharomyces cerevisiae*: how yeast go crazy in response to stress. *Biochemical and biophysical research communications*, 311(0006-291; 4), 1143–1150.
- Cyert, M. S., Kunisawa, R., Kaim, D., & Thorner, J. (1991). Yeast has homologs (*CNA1* and *CNA2* gene products) of mammalian calcineurin, a calmodulin-regulated phosphoprotein phosphatase. *Proceedings of the National Academy of Sciences of the United States of America*, 88(0027-8424; 16), 7376–7380.
- Daniel, J. A., & Grant, P. A. (2007). Multi-tasking on chromatin with the SAGA coactivator complexes. *Mutation research*, 618(1-2), 135–48. doi:10.1016/j.mrfmmm.2006.09.008
- De Groot, P. W. J., Ruiz, C., de Aldana, C. R. V., Duenas, E., Cid, V. J., Del Rey, F., Klis, F. M. (2001). A genomic approach for the identification and classification of genes involved in cell wall formation and its regulation in *Saccharomyces cerevisiae*. *Comparative and Functional Genomics*, 2(3), 124–142.
- Decottignies, A., Owsianik, G., & Ghislain, M. (1999). Casein kinase I-dependent phosphorylation and stability of the yeast multidrug transporter Pdr5p. *The Journal of biological chemistry*, 274(52), 37139–46.
- Dehé, P.-M., Dichtl, B., Schaft, D., Roguev, A., Pamblanco, M., Lebrun, R., Géli, V. (2006). Protein interactions within the Set1 complex and their roles in the regulation of histone 3 lysine 4 methylation. *The Journal of biological chemistry*, 281(46), 35404–12.
- Dehé, P.-M., & Géli, V. (2006). The multiple faces of Set1. *Biochemistry and cell biology = Biochimie et biologie cellulaire*, 84(4), 536–48.
- Denis, V., & Cyert, M. S. (2002). Internal Ca²⁺ release in yeast is triggered by hypertonic shock and mediated by a TRP channel homologue. *J. Cell Biol.*, 156(0021-9525; 1), 29–34.
- Denis, Valerie, & Cyert, M. S. (2002). Internal Ca²⁺ release in yeast is triggered by hypertonic shock and mediated by a TRP channel homologue. *The Journal of cell biology*, 156(1), 29–34.
- DeVit, M. J., & Johnston, M. (1999). The nuclear exportin Msn5 is required for nuclear export of the Mig1 glucose repressor of *Saccharomyces cerevisiae*. *Current biology : CB*, 9(21), 1231–41.
- Dheur, S., Vo, L. T. A., Voisinet-Hakil, F., Minet, M., Schmitter, J.-M., Lacroute, F., Minvielle-Sebastia, L. (2003). Pti1p and Ref2p found in association with the mRNA 3' end formation complex direct snoRNA maturation. *The EMBO journal*, 22(11), 2831–40.
- Dichtl, B., Aasland, R., & Keller, W. (2004). Functions for *S. cerevisiae* Swd2p in 3' end formation of specific mRNAs and snoRNAs and global histone 3 lysine 4 methylation. *RNA (New York, N.Y.)*, 10(6), 965–77.
- Dichtl, B., Blank, D., Ohnacker, M., Friedlein, A., Roeder, D., Langen, H., & Keller, W. (2002). A role for SSU72 in balancing RNA polymerase II transcription elongation and termination. *Molecular cell*, 10(5), 1139–50.
- Dion, B., & Brown, G. W. (2009). Comparative genome hybridization on tiling microarrays to detect aneuploidies in yeast. *Methods in molecular biology (Clifton, N.J.)*, 548, 1–18.
- Doi, K., Gartner, A., Ammerer, G., Errede, B., Shinkawa, H., Sugimoto, K., & Matsumoto, K. (1994). *MSG5*, a novel protein phosphatase promotes adaptation to pheromone response in *S. cerevisiae*. *The EMBO journal*, 13(0261-4189; 1), 61–70.

- Dombek, K M, Voronkova, V., Raney, A., & Young, E. T. (1999). Functional analysis of the yeast Glc7-binding protein Reg1 identifies a protein phosphatase type 1-binding motif as essential for repression of *ADH2* expression. *Molecular and cellular biology*, *19*(9), 6029–40.
- Dombek, Kenneth M, Kacherovsky, N., & Young, E. T. (2004). The Reg1-interacting proteins, Bmh1, Bmh2, Ssb1, and Ssb2, have roles in maintaining glucose repression in *Saccharomyces cerevisiae*. *The Journal of biological chemistry*, *279*(37), 39165–74.
- Dudley, A. M., Janse, D. M., Tanay, A., Shamir, R., & Church, G. M. (2005). A global view of pleiotropy and phenotypically derived gene function in yeast. *Molecular systems biology*, *1*, 2005.0001.
- Durr, G., Strayle, J., Plemper, R., Elbs, S., Klee, S. K., Catty, P., Rudolph, H. K. (1998). The medial-Golgi ion pump Pmr1 supplies the yeast secretory pathway with Ca²⁺ and Mn²⁺ required for glycosylation, sorting, and endoplasmic reticulum-associated protein degradation 1. *Mol.Biol.Cell*, *9*(1059-1524; 5), 1149–1162.
- Egloff, M. P., Cohen, P. T., Reinemer, P., & Barford, D. (1995). Crystal structure of the catalytic subunit of human protein phosphatase 1 and its complex with tungstate. *J.Mol.Biol.*, *254*(0022-2836; 5), 942–959.
- Egloff, M. P., Johnson, D. F., Moorhead, G., Cohen, P. T., Cohen, P., & Barford, D. (1997). Structural basis for the recognition of regulatory subunits by the catalytic subunit of protein phosphatase 1. *The EMBO journal*, *16*(0261-4189; 8), 1876–1887.
- Eisen, M. B., Spellman, P. T., Brown, P. O., & Botstein, D. (1998). Cluster analysis and display of genome-wide expression patterns. *Proceedings of the National Academy of Sciences of the United States of America*, *95*(0027-8424; 25), 14863–14868.
- Erez, O., & Kahana, C. (2001). Screening for modulators of spermine tolerance identifies Sky1, the SR protein kinase of *Saccharomyces cerevisiae*, as a regulator of polyamine transport and ion homeostasis. *Molecular and cellular biology*, *21*(0270-7306; 1), 175–184.
- Farcasanu, I. C., Hirata, D., Tsuchiya, E., Nishiyama, F., & Miyakawa, T. (1995). Protein phosphatase 2B of *Saccharomyces cerevisiae* is required for tolerance to manganese, in blocking the entry of ions into the cells 1. *European journal of biochemistry / FEBS*, *232*(0014-2956; 3), 712–717.
- Fatica, A., Morlando, M., & Bozzoni, I. (2000). Yeast snoRNA accumulation relies on a cleavage-dependent/polyadenylation-independent 3'-processing apparatus. *The EMBO journal*, *19*(22), 6218–29.
- Feng, Z. H., Wilson, S. E., Peng, Z. Y., Schlender, K. K., Reimann, E. M., & Trumbly, R. J. (1991a). The yeast *GLC7* gene required for glycogen accumulation encodes a type 1 protein phosphatase 1. *Journal of Biological Chemistry*, *266*(0021-9258; 35), 23796–23801.
- Ferrer-Dalmau, J, Gonzalez, A., Platara, M., Navarrete, C., Martinez, J. L., Barreto, L., Casamayor, A. (2010). Ref2, a regulatory subunit of the yeast protein phosphatase 1, is a novel component of cation homeostasis. *The Biochemical journal*, *426*(3), 355–364.
- Flandez, M., Cosano, I. C., Nombela, C., Martin, H., & Molina, M. (2004). Reciprocal regulation between Slt2 MAPK and isoforms of Msg5 dual-specificity protein phosphatase modulates the yeast cell integrity pathway. *Journal of Biological Chemistry*, *279*(0021-9258; 12), 11027–11034.
- Fling, M. E., Kopf, J., Tamarkin, A., Gorman, J. A., Smith, H. A., & Koltin, Y. (1991). Analysis of a *Candida albicans* gene that encodes a novel mechanism for resistance to benomyl and methotrexate. *Molecular & general genetics : MGG*, *227*(2), 318–29. R
- Foor, F., Parent, S. A., Morin, N., Dahl, A. M., Ramadan, N., Chrebet, G., Nielsen, J. B. (1992). Calcineurin mediates inhibition by FK506 and cyclosporin of recovery from alpha-factor arrest in yeast. *Nature*, *360*(6405), 682–4.
- François, J. M., Thompson-Jaeger, S., Skroch, J., Zellenka, U., Spevak, W., & Tatchell, K. (1992). *GAC1* may encode a regulatory subunit for protein phosphatase type 1 in *Saccharomyces cerevisiae*. *The EMBO journal*, *11*(1), 87–96.

- Frederick, D. L., & Tatchell, K. (1996). The *REG2* gene of *Saccharomyces cerevisiae* encodes a type 1 protein phosphatase-binding protein that functions with Reg1p and the Snf1 protein kinase to regulate growth. *Molecular and cellular biology*, *16*(6), 2922–31.
- Free, S. J. (2013). Fungal cell wall organization and biosynthesis. *Advances in genetics*, *81*, 33–82.
- Friedl, A. A., Kiechle, M., Maxeiner, H. G., Schiestl, R. H., & Eckardt-Schupp, F. (2010). Ty1 integrase overexpression leads to integration of non-Ty1 DNA fragments into the genome of *Saccharomyces cerevisiae*. *Molecular genetics and genomics : MGG*, *284*(4), 231–42.
- Fritsch, E. S., Schacherer, J., Bleykasten-Grosshans, C., Souciet, J.-L., Potier, S., & de Montigny, J. (2009). Influence of genetic background on the occurrence of chromosomal rearrangements in *Saccharomyces cerevisiae*. *BMC genomics*, *10*, 99.
- Gancedo, J M. (1998). Yeast carbon catabolite repression. *Microbiology and molecular biology reviews : MMBR*, *62*(2), 334–61.
- Gancedo, Juana M. (2008). The early steps of glucose signalling in yeast. *FEMS microbiology reviews*, *32*(4), 673–704.
- Garcia, R., Bermejo, C., Grau, C., Perez, R., Rodriguez-Pena, J. M., Francois, J., Arroyo, J. (2004). The global transcriptional response to transient cell wall damage in *Saccharomyces cerevisiae* and its regulation by the cell integrity signaling pathway. *Journal of Biological Chemistry*, *279*(0021-9258; 15), 15183–15195.
- García, R., Rodríguez-Peña, J. M., Bermejo, C., Nombela, C., & Arroyo, J. (2009). The high osmotic response and cell wall integrity pathways cooperate to regulate transcriptional responses to zymolyase-induced cell wall stress in *Saccharomyces cerevisiae*. *The Journal of biological chemistry*, *284*(16), 10901–11.
- Garcia-deblas, B., Rubio, F., Quintero, F. J., Banuelos, M. A., Haro, R., & Rodriguez-Navarro, A. (1993). Differential expression of two genes encoding isoforms of the ATPase involved in sodium efflux in *Saccharomyces cerevisiae*. *Mol.Gen.Genet.*, *236*(0026-8925; 2-3), 363–368.
- Garcia-Gimeno, M. A., Munoz, I., Arino, J., & Sanz, P. (2003). Molecular characterization of Ypi1, a novel *Saccharomyces cerevisiae* type 1 protein phosphatase inhibitor. *Journal of Biological Chemistry*, *278*(0021-9258; 48), 47744–47752.
- Gardiner, F. C., Costa, R., & Ayscough, K. R. (2007). Nucleocytoplasmic trafficking is required for functioning of the adaptor protein Sla1p in endocytosis. *Traffic (Copenhagen, Denmark)*, *8*(4), 347–58.
- Gardner, B. M., Pincus, D., Gotthardt, K., Gallagher, C. M., & Walter, P. (2013). Endoplasmic reticulum stress sensing in the unfolded protein response. *Cold Spring Harbor perspectives in biology*, *5*(3), a013169.
- Garfinkel, D. J., Nyswaner, K., Wang, J., & Cho, J.-Y. (2003). Post-transcriptional cosuppression of Ty1 retrotransposition. *Genetics*, *165*(1), 83–99.
- Garrett-Engele, P., Moilanen, B., & Cyert, M. S. (1995). Calcineurin, the Ca²⁺/calmodulin-dependent protein phosphatase, is essential in yeast mutants with cell integrity defects and in mutants that lack a functional vacuolar H(+)-ATPase. *Molecular and cellular biology*, *15*(0270-7306; 8), 4103–4114.
- Gavin, A.-C., Bösch, M., Krause, R., Grandi, P., Marzioch, M., Bauer, A., Superti-Furga, G. (2002). Functional organization of the yeast proteome by systematic analysis of protein complexes. *Nature*, *415*(6868), 141–7.
- Geigl, J. B., Obenauf, A. C., Schwarzbraun, T., & Speicher, M. R. (2008). Defining “chromosomal instability”. *Trends in genetics : TIG*, *24*(2), 64–9.
- Gething, M. J., & Sambrook, J. (1992). Protein folding in the cell. *Nature*, *355*(6355), 33–45.

- Ghazy, M. A., He, X., Singh, B. N., Hampsey, M., & Moore, C. (2009). The essential N terminus of the Pta1 scaffold protein is required for snoRNA transcription termination and Ssu72 function but is dispensable for pre-mRNA 3'-end processing. *Molecular and cellular biology*, *29*(8), 2296–307.
- Giaever, G., Chu, A. M., Ni, L., Connelly, C., Riles, L., Veronneau, S., Andre, B. (2002). Functional profiling of the *Saccharomyces cerevisiae* genome. *Nature*, *418*(0028-0836; 6896), 387–391.
- Gietz, R. D., & Sugino, A. (1988). New yeast-Escherichia coli shuttle vectors constructed with in vitro mutagenized yeast genes lacking six-base pair restriction sites. *Gene*, *74*(2), 527–34.
- Gilbert, W., & Guthrie, C. (2004). The Glc7p nuclear phosphatase promotes mRNA export by facilitating association of Mex67p with mRNA. *Molecular cell*, *13*(2), 201–12.
- Goffeau, A., Barrell, B. G., Bussey, H., Davis, R. W., Dujon, B., Feldmann, H., Oliver, S. G. (1996). Life with 6000 Genes. *Science*, *274*(5287), 546–567.
- Goldberg, J., Huang, H. B., Kwon, Y. G., Greengard, P., Nairn, A. C., & Kuriyan, J. (1995). Three-dimensional structure of the catalytic subunit of protein serine/threonine phosphatase-1. *Nature*, *376*(0028-0836; 6543), 745–753.
- Gomez, M. J., Luyten, K., & Ramos, J. (1996). The capacity to transport potassium influences sodium tolerance in *Saccharomyces cerevisiae*. *FEMS Microbiol.Lett.*, *135*(0378-1097; 2-3), 157–160.
- Gonzalez, A., Ruiz, A., Serrano, R., Arino, J., & Casamayor, A. (2006). Transcriptional profiling of the protein phosphatase 2C family in yeast provides insights into the unique functional roles of Ptc1. *Journal of Biological Chemistry*, *281*(0021-9258; 46), 35057–35069.
- Gonzalez, T. N., Sidrauski, C., Dörfler, S., & Walter, P. (1999). Mechanism of non-spliceosomal mRNA splicing in the unfolded protein response pathway. *The EMBO journal*, *18*(11), 3119–32.
- Granneman, S., & Baserga, S. J. (2005). Crosstalk in gene expression: coupling and co-regulation of rDNA transcription, pre-ribosome assembly and pre-rRNA processing. *Current opinion in cell biology*, *17*(3), 281–6.
- Guarente, L., & Mason, T. (1983). Heme regulates transcription of the *CYC1* gene of *S. cerevisiae* via an upstream activation site. *Cell*, *32*(4), 1279–86.
- Guo, J., & Polymenis, M. (2006). Dcr2 targets Ire1 and downregulates the unfolded protein response in *Saccharomyces cerevisiae*. *EMBO reports*, *7*(11), 1124–7.
- Hahn, J. S., & Thiele, D. J. (2002). Regulation of the *Saccharomyces cerevisiae* Slt2 kinase pathway by the stress-inducible Sdp1 dual specificity phosphatase. *Journal of Biological Chemistry*, *277*(0021-9258; 24), 21278–21284.
- Hahn, J.-S., & Thiele, D. J. (2004). Activation of the *Saccharomyces cerevisiae* heat shock transcription factor under glucose starvation conditions by Snf1 protein kinase. *The Journal of biological chemistry*, *279*(7), 5169–76.
- Halachmi, D., & Eilam, Y. (1989). Cytosolic and vacuolar Ca²⁺ concentrations in yeast cells measured with the Ca²⁺-sensitive fluorescence dye indo-1. *FEBS letters*, *256*(0014-5793; 1-2), 55–61.
- Hardie, D. G. (2007). AMP-activated/SNF1 protein kinases: conserved guardians of cellular energy. *Nature reviews. Molecular cell biology*, *8*(1471-0080; 10), 774–785.
- Hardy, T. A., & Roach, P. J. (1993). Control of yeast glycogen synthase-2 by COOH-terminal phosphorylation 1. *Journal of Biological Chemistry*, *268*(0021-9258; 32), 23799–23805.
- Haro, R., Garcíadeblas, B., & Rodríguez-Navarro, A. (1991). A novel P-type ATPase from yeast involved in sodium transport. *FEBS letters*, *291*(0014-5793; 2), 189–191.
- Hassold, T. J., & Jacobs, P. A. (1984). Trisomy in man. *Annual review of genetics*, *18*, 69–97.
- He, X., & Moore, C. (2005). Regulation of yeast mRNA 3' end processing by phosphorylation. *Molecular cell*, *19*(5), 619–29.
- Hedbacker, K., & Carlson, M. (2006). Regulation of the nucleocytoplasmic distribution of Snf1-Gal83 protein kinase. *Eukaryotic cell*, *5*(12), 1950–6.

- Hedbacker, K., & Carlson, M. (2008). SNF1/AMPK pathways in yeast. *Frontiers in bioscience : a journal and virtual library*, *13*, 2408–20.
- Hedbacker, K., Hong, S.-P., & Carlson, M. (2004). Pak1 protein kinase regulates activation and nuclear localization of Snf1-Gal83 protein kinase. *Molecular and cellular biology*, *24*(18), 8255–63.
- Hedbacker, K., Townley, R., & Carlson, M. (2004). Cyclic AMP-dependent protein kinase regulates the subcellular localization of Snf1-Sip1 protein kinase. *Molecular and cellular biology*, *24*(5), 1836–43.
- Hedges, D., Proft, M., & Entian, K. D. (1995). CAT8, a new zinc cluster-encoding gene necessary for derepression of gluconeogenic enzymes in the yeast *Saccharomyces cerevisiae*. *Molecular and cellular biology*, *15*(4), 1915–22.
- Henras, A. K., Dez, C., & Henry, Y. (2004). RNA structure and function in C/D and H/ACA s(no)RNPs. *Current opinion in structural biology*, *14*(3), 335–43.
- Hill, J. A., Ammar, R., Torti, D., Nislow, C., & Cowen, L. E. (2013). Genetic and genomic architecture of the evolution of resistance to antifungal drug combinations. *PLoS genetics*, *9*(4), e1003390.
- Hirata, D., Yano, K., Miyahara, K., & Miyakawa, T. (1994). *Saccharomyces cerevisiae* YDR1, which encodes a member of the ATP-binding cassette (ABC) superfamily, is required for multidrug resistance. *Current genetics*, *26*(4), 285–94.
- Hisamoto, N., Sugimoto, K., & Matsumoto, K. (1994). The Glc7 type 1 protein phosphatase of *Saccharomyces cerevisiae* is required for cell cycle progression in G2/M 1. *Molecular and cellular biology*, *14*(0270-7306; 5), 3158–3165.
- Ho, Y., Gruhler, A., Heilbut, A., Bader, G. D., Moore, L., Adams, S.-L., Tyers, M. (2002). Systematic identification of protein complexes in *Saccharomyces cerevisiae* by mass spectrometry. *Nature*, *415*(6868), 180–3.
- Hochwagen, A., Tham, W.-H., Brar, G. A., & Amon, A. (2005). The FK506 binding protein Fpr3 counteracts protein phosphatase 1 to maintain meiotic recombination checkpoint activity. *Cell*, *122*(6), 861–73.
- Holland, A. J., & Cleveland, D. W. (2009). Boveri revisited: chromosomal instability, aneuploidy and tumorigenesis. *Nature reviews. Molecular cell biology*, *10*(7), 478–87.
- Hong, G., Trumbly, R. J., Reimann, E. M., & Schlender, K. K. (2000). Sds22p is a subunit of a stable isolatable form of protein phosphatase 1 (Glc7p) from *Saccharomyces cerevisiae*. *Archives of biochemistry and biophysics*, *376*(2), 288–98.
- Hontz, R. D., Niederer, R. O., Johnson, J. M., & Smith, J. S. (2009). Genetic identification of factors that modulate ribosomal DNA transcription in *Saccharomyces cerevisiae*. *Genetics*, *182*(1), 105–19.
- Howard, J. P., Hutton, J. L., Olson, J. M., & Payne, G. S. (2002). Sla1p serves as the targeting signal recognition factor for NPF(1,2)D-mediated endocytosis. *The Journal of cell biology*, *157*(2), 315–26.
- Huang, H. B., Horiuchi, A., Watanabe, T., Shih, S. R., Tsay, H. J., Li, H. C., ... Nairn, A. C. (1999). Characterization of the inhibition of protein phosphatase-1 by DARPP-32 and inhibitor-2. *The Journal of biological chemistry*, *274*(12), 7870–8.
- Huang, P. H., & Chiang, H. L. (1997). Identification of novel vesicles in the cytosol to vacuole protein degradation pathway. *The Journal of cell biology*, *136*(4), 803–10.
- Huerta-Cepas, J., Bueno, A., Dopazo, J., & Gabaldón, T. (2008). PhylomeDB: a database for genome-wide collections of gene phylogenies. *Nucleic acids research*, *36*(Database issue), D491–6.
- Huerta-Cepas, J., Capella-Gutierrez, S., Pryszcz, L. P., Denisov, I., Kormes, D., Marcet-Houben, M., & Gabaldón, T. (2011). PhylomeDB v3.0: an expanding repository of genome-wide collections of trees, alignments and phylogeny-based orthology and paralogy predictions. *Nucleic acids research*, *39*(Database issue), D556–60.

- Hughes, T. R., Roberts, C. J., Dai, H., Jones, A. R., Meyer, M. R., Slade, D., Marton, M. J. (2000). Widespread aneuploidy revealed by DNA microarray expression profiling. *Nature genetics*, 25(3), 333–7.
- Idrissi, F. Z., Fernández-Larrea, J. B., & Piña, B. (1998). Structural and functional heterogeneity of Rap1p complexes with telomeric and UASrpg-like DNA sequences. *Journal of molecular biology*, 284(4), 925–35.
- Iida, H., Nakamura, H., Ono, T., Okumura, M. S., & Anraku, Y. (1994). *MID1*, a novel *Saccharomyces cerevisiae* gene encoding a plasma membrane protein, is required for Ca²⁺ influx and mating. *Molecular and cellular biology*, 14(0270-7306; 12), 8259–8271.
- Iida, H., Yagawa, Y., & Anraku, Y. (1990). Essential role for induced Ca²⁺ influx followed by [Ca²⁺]_i rise in maintaining viability of yeast cells late in the mating pheromone response pathway. A study of [Ca²⁺]_i in single *Saccharomyces cerevisiae* cells with imaging of fura-2. *Journal of Biological Chemistry*, 265(0021-9258; 22), 13391–13399.
- Ingebritsen, T. S., & Cohen, P. (1983). Protein phosphatases: properties and role in cellular regulation 1. *Science*, 221(0036-8075; 4608), 331–338.
- Irminger-Finger, I., & Mathis, N. (1998). Effect of microtubule-associated protein *MHP1* on microtubule assembly and cell cycle progression in *Saccharomyces cerevisiae*. *Cell structure and function*, 23(4), 209–19.
- Ishihara, M., Suda, Y., Inoue, I., Tanaka, T., Takahashi, T., Gao, X.-D., ... Tachikawa, H. (2009). Protein phosphatase type 1-interacting protein Ysw1 is involved in proper septin organization and prospore membrane formation during sporulation. *Eukaryotic cell*, 8(7), 1027–37.
- Ito, H., Fukuda, Y., Murata, K., & Kimura, A. (1983). Transformation of intact yeast cells treated with alkali cations. *Journal of Bacteriology*, 153, 163–168.
- Jiang, R., & Carlson, M. (1996). Glucose regulates protein interactions within the yeast SNF1 protein kinase complex. *Genes & development*, 10(24), 3105–15. R
- Jimenez-Sanchez, M., Cid, V. J., & Molina, M. (2007). Retrophosphorylation of Mkk1 and Mkk2 MAPKKs by the Slt2 MAPK in the yeast cell integrity pathway. *Journal of Biological Chemistry*, 282(0021-9258; 43), 31174–31185.
- Johnson, D. F., Moorhead, G., Caudwell, F. B., Cohen, P., Chen, Y. H., Chen, M. X., & Cohen, P. T. (1996). Identification of protein-phosphatase-1-binding domains on the glycogen and myofibrillar targeting subunits. *European journal of biochemistry / FEBS*, 239(2), 317–25.
- Johnson, S. A., & Hunter, T. (2005). Kinomics: methods for deciphering the kinome. *Nature methods*, 2(1), 17–25.
- Jones, J. S., & Prakash, L. (n.d.). Yeast *Saccharomyces cerevisiae* selectable markers in pUC18 polylinkers. *Yeast (Chichester, England)*, 6(5), 363–6.
- Jorgensen, P., & Tyers, M. (2004). How cells coordinate growth and division. *Current biology : CB*, 14(23), R1014–27.
- Jung, U S, & Levin, D. E. (1999). Genome-wide analysis of gene expression regulated by the yeast cell wall integrity signalling pathway. *Molecular microbiology*, 34(0950-382; 5), 1049–1057.
- Jung, U S, Sobering, A. K., Romeo, M. J., & Levin, D. E. (2002). Regulation of the yeast Rlm1 transcription factor by the Mpk1 cell wall integrity MAP kinase. *Molecular microbiology*, 46(0950-382; 3), 781–789.
- Jung, Un Sung, Sobering, A. K., Romeo, M. J., & Levin, D. E. (2002). Regulation of the yeast Rlm1 transcription factor by the Mpk1 cell wall integrity MAP kinase. *Molecular microbiology*, 46(3), 781–9.
- Kafadar, K. A., & Cyert, M. S. (2004). Integration of stress responses: modulation of calcineurin signaling in *Saccharomyces cerevisiae* by protein kinase A. *Eukaryot.Cell*, 3(1535-9778; 5), 1147–1153.

- Kafadar, K. A., Zhu, H., Snyder, M., & Cyert, M. S. (2003). Negative regulation of calcineurin signaling by Hrr25p, a yeast homolog of casein kinase I. *Genes Dev.*, *17*(0890-9369; 21), 2698–2708.
- Kamada, Y., Jung, U. S., Piotrowski, J., & Levin, D. E. (1995). The protein kinase C-activated MAP kinase pathway of *Saccharomyces cerevisiae* mediates a novel aspect of the heat shock response. *Genes Dev.*, *9*(0890-9369; 13), 1559–1571.
- Kane, P. M. (2006). The where, when, and how of organelle acidification by the yeast vacuolar H⁺-ATPase. *Microbiology and molecular biology reviews : MMBR*, *70*(1), 177–191.
- Kane, Patricia M. (2006). The where, when, and how of organelle acidification by the yeast vacuolar H⁺-ATPase. *Microbiology and molecular biology reviews : MMBR*, *70*(1), 177–91.
- Kawaguchi, S., & Ng, D. T. W. (2011). Cell biology. Sensing ER stress. *Science (New York, N.Y.)*, *333*(6051), 1830–1.
- Kawahara, T., Yanagi, H., Yura, T., & Mori, K. (1998). Unconventional splicing of *HAC1/ERN4* mRNA required for the unfolded protein response. Sequence-specific and non-sequential cleavage of the splice sites. *The Journal of biological chemistry*, *273*(3), 1802–7. R
- Ketela, T., Green, R., & Bussey, H. (1999). *Saccharomyces cerevisiae* Mid2p is a potential cell wall stress sensor and upstream activator of the *PKC1-MPK1* cell integrity pathway. *Journal of Bacteriology*, *181*(0021-9193; 11), 3330–3340.
- Kim, K. Y., Truman, A. W., & Levin, D. E. (2008). Yeast Mpk1 mitogen-activated protein kinase activates transcription through Swi4/Swi6 by a noncatalytic mechanism that requires upstream signal. *Molecular and cellular biology*, *28*(1098-5549; 8), 2579–2589.
- Kim, K.-Y., & Levin, D. E. (2010). Transcriptional reporters for genes activated by cell wall stress through a non-catalytic mechanism involving Mpk1 and SBF. *Yeast (Chichester, England)*, *27*(8), 541–8.
- Kim, K.-Y., Truman, A. W., Caesar, S., Schlenstedt, G., & Levin, D. E. (2010). Yeast Mpk1 cell wall integrity mitogen-activated protein kinase regulates nucleocytoplasmic shuttling of the Swi6 transcriptional regulator. *Molecular biology of the cell*, *21*(9), 1609–19.
- Kim, K.-Y., Truman, A. W., & Levin, D. E. (2008). Yeast Mpk1 mitogen-activated protein kinase activates transcription through Swi4/Swi6 by a noncatalytic mechanism that requires upstream signal. *Molecular and cellular biology*, *28*(8), 2579–89.
- Kimata, Y., Ishiwata-Kimata, Y., Ito, T., Hirata, A., Suzuki, T., Oikawa, D., Kohno, K. (2007). Two regulatory steps of ER-stress sensor Ire1 involving its cluster formation and interaction with unfolded proteins. *The Journal of cell biology*, *179*(1), 75–86.
- Kimata, Y., Kimata, Y. I., Shimizu, Y., Abe, H., Farcasanu, I. C., Takeuchi, M., Kohno, K. (2003). Genetic evidence for a role of BiP/Kar2 that regulates Ire1 in response to accumulation of unfolded proteins. *Molecular biology of the cell*, *14*(6), 2559–69.
- Kimata, Y., Oikawa, D., Shimizu, Y., Ishiwata-Kimata, Y., & Kohno, K. (2004). A role for BiP as an adjustor for the endoplasmic reticulum stress-sensing protein Ire1. *The Journal of cell biology*, *167*(3), 445–56.
- Kiss, T. (2002). Small nucleolar RNAs: an abundant group of noncoding RNAs with diverse cellular functions. *Cell*, *109*(2), 145–8.
- Klis, F. M., Boorsma, A., & De Groot, P. W. (2006). Cell wall construction in *Saccharomyces cerevisiae*. *Yeast (Chichester, West Sussex)*, *23*(0749-503; 3), 185–202.
- Klis, F. M., Mol, P., Hellingwerf, K., & Brul, S. (2002). Dynamics of cell wall structure in *Saccharomyces cerevisiae*. *FEMS Microbiol.Rev.*, *26*(0168-6445; 3), 239–256.
- Kohno, K. (2010). Stress-sensing mechanisms in the unfolded protein response: similarities and differences between yeast and mammals. *Journal of biochemistry*, *147*(1), 27–33.
- Korennykh, A., & Walter, P. (2012). Structural basis of the unfolded protein response. *Annual review of cell and developmental biology*, *28*, 251–77.

- Korennykh, A. V., Egea, P. F., Korostelev, A. A., Finer-Moore, J., Zhang, C., Shokat, K. M., Walter, P. (2009). The unfolded protein response signals through high-order assembly of Ire1. *Nature*, *457*(7230), 687–93.
- Kozubowski, L., Panek, H., Rosenthal, A., Bloecher, A., DeMarini, D. J., & Tatchell, K. (2003). A Bni4-Glc7 phosphatase complex that recruits chitin synthase to the site of bud emergence. *Molecular biology of the cell*, *14*(1), 26–39.
- Kuranda, K., Leberre, V., Sokol, S., Palamarczyk, G., & Francois, J. (2006). Investigating the caffeine effects in the yeast *Saccharomyces cerevisiae* brings new insights into the connection between TOR, PKC and Ras/cAMP signalling pathways. *Molecular microbiology*, *61*(0950-382; 5), 1147–1166.
- Lamping, E., Baret, P. V., Holmes, A. R., Monk, B. C., Goffeau, A., & Cannon, R. D. (2010). Fungal PDR transporters: Phylogeny, topology, motifs and function. *Fungal genetics and biology: FG & B*, *47*(2), 127–42.
- Larkin, M. A., Blackshields, G., Brown, N. P., Chenna, R., McGettigan, P. A., McWilliam, H., Higgins, D. G. (2007). Clustal W and Clustal X version 2.0. *Bioinformatics (Oxford, England)*, *23*(21), 2947–8.
- Larson, J. R., Bharucha, J. P., Ceaser, S., Salamon, J., Richardson, C. J., Rivera, S. M., & Tatchell, K. (2008). Protein phosphatase type 1 directs chitin synthesis at the bud neck in *Saccharomyces cerevisiae*. *Molecular biology of the cell*, *19*(7), 3040–51.
- Leber, J. H., Bernales, S., & Walter, P. (2004). *IRE1*-independent gain control of the unfolded protein response. *PLoS biology*, *2*(8), E235.
- Lee, J.-S., Shukla, A., Schneider, J., Swanson, S. K., Washburn, M. P., Florens, L., Shilatifard, A. (2007). Histone crosstalk between H2B monoubiquitination and H3 methylation mediated by COMPASS. *Cell*, *131*(6), 1084–96.
- Lee, K. S., Hines, L. K., & Levin, D. E. (1993). A pair of functionally redundant yeast genes (*PPZ1* and *PPZ2*) encoding type 1-related protein phosphatases function within the PKC1-mediated pathway. *Molecular and cellular biology*, *13*(0270-7306; 9), 5843–5853.
- Lehrman, M. A. (1991). Biosynthesis of N-acetylglucosamine-P-P-dolichol, the committed step of asparagine-linked oligosaccharide assembly. *Glycobiology*, *1*(6), 553–62.
- Leroy, C., Lee, S. E., Vaze, M. B., Ochsenbien, F., Guerois, R., Haber, J. E., & Marsolier-Kergoat, M. C. (2003). PP2C phosphatases Ptc2 and Ptc3 are required for DNA checkpoint inactivation after a double-strand break. *Mol. Cell*, *11*(1097-2765; 3), 827–835.
- Lesage, G., & Bussey, H. (2006). Cell wall assembly in *Saccharomyces cerevisiae*. *Microbiol.Mol.Biol.Rev.*, *70*(1092-2172; 2), 317–343.
- Lesage, P., Yang, X., & Carlson, M. (1996). Yeast *SNF1* protein kinase interacts with *SIP4*, a C6 zinc cluster transcriptional activator: a new role for *SNF1* in the glucose response. *Molecular and cellular biology*, *16*(5), 1921–8.
- Leung, A., Cajigas, I., Jia, P., Ezhkova, E., Brickner, J. H., Zhao, Z., Tansey, W. P. (2011). Histone H2B ubiquitylation and H3 lysine 4 methylation prevent ectopic silencing of euchromatic loci important for the cellular response to heat. *Molecular biology of the cell*, *22*(15), 2741–53.
- Levin, D E. (2005). Cell wall integrity signaling in *Saccharomyces cerevisiae*. *Microbiol.Mol.Biol.Rev.*, *69*(1092-2172; 2), 262–291.
- Levin, D E, & Bartlett-Heubusch, E. (1992). Mutants in the *S. cerevisiae* *PKC1* gene display a cell cycle-specific osmotic stability defect. *The Journal of cell biology*, *116*(5), 1221–9.
- Levin, David E. (2011). Regulation of cell wall biogenesis in *Saccharomyces cerevisiae*: the cell wall integrity signaling pathway. *Genetics*, *189*(4), 1145–75.
- Lin, J. H., Li, H., Yasumura, D., Cohen, H. R., Zhang, C., Panning, B., Walter, P. (2007). *IRE1* signaling affects cell fate during the unfolded protein response. *Science (New York, N.Y.)*, *318*(5852), 944–9.

- Liu, Z. L., Ma, M., & Song, M. (2009). Evolutionarily engineered ethanologenic yeast detoxifies lignocellulosic biomass conversion inhibitors by reprogrammed pathways. *Molecular genetics and genomics : MGG*, 282(3), 233–44.
- Lo, W. S., Duggan, L., Emre, N. C., Belotserkovskya, R., Lane, W. S., Shiekhattar, R., & Berger, S. L. (2001). Snf1--a histone kinase that works in concert with the histone acetyltransferase Gcn5 to regulate transcription. *Science (New York, N.Y.)*, 293(5532), 1142–6.
- Loibl, M., & Strahl, S. (2013). Protein O-mannosylation: what we have learned from baker's yeast. *Biochimica et biophysica acta*, 1833(11), 2438–46.
- Lutfiyya, L. L., Iyer, V. R., DeRisi, J., DeVit, M. J., Brown, P. O., & Johnston, M. (1998). Characterization of three related glucose repressors and genes they regulate in *Saccharomyces cerevisiae*. *Genetics*, 150(4), 1377–91.
- Lyne, R., Burns, G., Mata, J., Penkett, C. J., Rustici, G., Chen, D., Bähler, J. (2003). Whole-genome microarrays of fission yeast: characteristics, accuracy, reproducibility, and processing of array data. *BMC genomics*, 4(1), 27.
- Ma, M., & Liu, L. Z. (2010). Quantitative transcription dynamic analysis reveals candidate genes and key regulators for ethanol tolerance in *Saccharomyces cerevisiae*. *BMC microbiology*, 10, 169.
- Madden, K., Sheu, Y. J., Baetz, K., Andrews, B., & Snyder, M. (1997). SBF cell cycle regulator as a target of the yeast PKC-MAP kinase pathway. *Science*, 275(0036-8075; 5307), 1781–1784.
- Manning, G., Plowman, G. D., Hunter, T., & Sudarsanam, S. (2002). Evolution of protein kinase signaling from yeast to man. *Trends in biochemical sciences*, 27(10), 514–520.
- Marcet-Houben, M., & Gabaldón, T. (2009). The tree versus the forest: the fungal tree of life and the topological diversity within the yeast phylome. *PLoS one*, 4(2), e4357.
- Marquez, J. A., & Serrano, R. (1996). Multiple transduction pathways regulate the sodium-extrusion gene *PMR2/ENA1* during salt stress in yeast. *FEBS letters*, 382(0014-5793; 1-2), 89–92.
- Marquina, M., González, A., Barreto, L., Gelis, S., Muñoz, I., Ruiz, A., ... Ariño, J. (2012). Modulation of yeast alkaline cation tolerance by Ypi1 requires calcineurin. *Genetics*, 190(4), 1355–64.
- Matheos, D. P., Kingsbury, T. J., Ahsan, U. S., & Cunningham, K. W. (1997). Tcn1p/Crz1p, a calcineurin-dependent transcription factor that differentially regulates gene expression in *Saccharomyces cerevisiae*. *Genes Dev.*, 11(0890-9369; 24), 3445–3458.
- Matsumoto, T. K., Ellsmore, A. J., Cessna, S. G., Low, P. S., Pardo, J. M., Bressan, R. A., & Hasegawa, P. M. (2002). An osmotically induced cytosolic Ca²⁺ transient activates calcineurin signaling to mediate ion homeostasis and salt tolerance of *Saccharomyces cerevisiae*. *Journal of Biological Chemistry*, 277(0021-9258; 36), 33075–33080.
- Mattison, C. P., Spencer, S. S., Kresge, K. A., Lee, J., & Ota, I. M. (1999). Differential regulation of the cell wall integrity mitogen-activated protein kinase pathway in budding yeast by the protein tyrosine phosphatases Ptp2 and Ptp3. *Molecular and cellular biology*, 19(0270-7306; 11), 7651–7660.
- Mayordomo, I., Estruch, F., & Sanz, P. (2002). Convergence of the target of rapamycin and the Snf1 protein kinase pathways in the regulation of the subcellular localization of Msn2, a transcriptional activator of STRE (Stress Response Element)-regulated genes. *The Journal of biological chemistry*, 277(38), 35650–6.
- Mayordomo, I., & Sanz, P. (2002). The *Saccharomyces cerevisiae* 14-3-3 protein Bmh2 is required for regulation of the phosphorylation status of Fin1, a novel intermediate filament protein. *The Biochemical journal*, 365(Pt 1), 51–6.
- Medina, I., Carbonell, J., Pulido, L., Madeira, S. C., Goetz, S., Conesa, A., Dopazo, J. (2010). Babelomics: an integrative platform for the analysis of transcriptomics, proteomics and genomic data with advanced functional profiling. *Nucleic acids research*, 38(Web Server issue), W210–3.

- Meiselbach, H., Sticht, H., & Enz, R. (2006). Structural analysis of the protein phosphatase 1 docking motif: molecular description of binding specificities identifies interacting proteins. *Chemistry & biology*, 13(1), 49–59.
- Mendoza, I., Rubio, F., Rodriguez-Navarro, A., & Pardo, J. M. (1994). The protein phosphatase calcineurin is essential for NaCl tolerance of *Saccharomyces cerevisiae*. *The Journal of biological chemistry*, 269(12), 8792–6.
- Mizrahi, N., & Moore, C. (2000). Posttranslational phosphorylation and ubiquitination of the *Saccharomyces cerevisiae* Poly(A) polymerase at the S/G(2) stage of the cell cycle. *Molecular and cellular biology*, 20(8), 2794–802.
- Momcilovic, M., & Carlson, M. (2011). Alterations at dispersed sites cause phosphorylation and activation of *SNF1* protein kinase during growth on high glucose. *The Journal of biological chemistry*, 286(26), 23544–51.
- Momcilovic, M., Iram, S. H., Liu, Y., & Carlson, M. (2008). Roles of the glycogen-binding domain and Snf4 in glucose inhibition of *SNF1* protein kinase. *The Journal of biological chemistry*, 283(28), 19521–9.
- Montaner, D., Tárraga, J., Huerta-Cepas, J., Burguet, J., Vaquerizas, J. M., Conde, L., Dopazo, J. (2006). Next station in microarray data analysis: GEPAS. *Nucleic acids research*, 34(Web Server issue),
- Moorhead, G. B. G., De Wever, V., Templeton, G., & Kerk, D. (2009). Evolution of protein phosphatases in plants and animals. *The Biochemical journal*, 417(2), 401–9.
- Moorhead, G. B. G., Trinkle-Mulcahy, L., & Ulke-Lemée, A. (2007). Emerging roles of nuclear protein phosphatases. *Nature reviews. Molecular cell biology*, 8(3), 234–44.
- Mori, K., Kawahara, T., Yoshida, H., Yanagi, H., & Yura, T. (1996). Signalling from endoplasmic reticulum to nucleus: transcription factor with a basic-leucine zipper motif is required for the unfolded protein-response pathway. *Genes to cells : devoted to molecular & cellular mechanisms*, 1(9), 803–17.
- Mori, K., Ma, W., Gething, M. J., & Sambrook, J. (1993). A transmembrane protein with a cdc2+/CDC28-related kinase activity is required for signaling from the ER to the nucleus. *Cell*, 74(4), 743–56. 4
- Mori, K., Ogawa, N., Kawahara, T., Yanagi, H., & Yura, T. (1998). Palindrome with spacer of one nucleotide is characteristic of the cis-acting unfolded protein response element in *Saccharomyces cerevisiae*. *The Journal of biological chemistry*, 273(16), 9912–20.
- Mori, K., Sant, A., Kohno, K., Normington, K., Gething, M. J., & Sambrook, J. F. (1992). A 22 bp cis-acting element is necessary and sufficient for the induction of the yeast *KAR2* (BiP) gene by unfolded proteins. *The EMBO journal*, 11(7), 2583–93.
- Morlando, M., Greco, P., Dichtl, B., Fatica, A., Keller, W., & Bozzoni, I. (2002). Functional analysis of yeast snoRNA and snRNA 3'-end formation mediated by uncoupling of cleavage and polyadenylation. *Molecular and cellular biology*, 22(5), 1379–89.
- Morrison, D. K., Murakami, M. S., & Cleghon, V. (2000). Protein kinases and phosphatases in the *Drosophila* genome. *The Journal of cell biology*, 150(2), F57–62.
- Munoz, I., Simon, E., Casals, N., Clotet, J., & Arino, J. (2003). Identification of multicopy suppressors of cell cycle arrest at the G1-S transition in *Saccharomyces cerevisiae*. *Yeast (Chichester, West Sussex)*, 20(0749-503; 2), 157–169.
- Musacchio, A., & Salmon, E. D. (2007). The spindle-assembly checkpoint in space and time. *Nature reviews. Molecular cell biology*, 8(5), 379–93.
- Nakajima-Shimada, J., Iida, H., Tsuji, F. I., & Anraku, Y. (1991). Galactose-dependent expression of the recombinant Ca2(+)-binding photoprotein aequorin in yeast. *Biochemical and biophysical research communications*, 174(1), 115–22.
- Nedea, E., He, X., Kim, M., Pootoolal, J., Zhong, G., Canadien, V., Greenblatt, J. (2003). Organization and function of APT, a subcomplex of the yeast cleavage and polyadenylation factor involved in the

- formation of mRNA and small nucleolar RNA 3'-ends. *The Journal of biological chemistry*, 278(35), 33000–10.
- Nedea, E., Nalbant, D., Xia, D., Theoharis, N. T., Suter, B., Richardson, C. J., Nagy, P. L. (2008). The Glc7 phosphatase subunit of the cleavage and polyadenylation factor is essential for transcription termination on snoRNA genes. *Molecular cell*, 29(5), 577–87.
- Neiman, A. M. (2011). Sporulation in the budding yeast *Saccharomyces cerevisiae*. *Genetics*, 189(3), 737–65.
- Nigavekar, S. S., Tan, Y. S. H., & Cannon, J. F. (2002). Glc8 is a glucose-repressible activator of Glc7 protein phosphatase-1. *Archives of biochemistry and biophysics*, 404(1), 71–9.
- Nikawa, J., & Yamashita, S. (1992). *IRE1* encodes a putative protein kinase containing a membrane-spanning domain and is required for inositol phototrophy in *Saccharomyces cerevisiae*. *Molecular microbiology*, 6(11), 1441–6.
- Nishimura, K., Yasumura, K., Igarashi, K., Harashima, S., & Kakinuma, Y. (1999). Transcription of some PHO genes in *Saccharomyces cerevisiae* is regulated by spt7p. *Yeast (Chichester, England)*, 15(16), 1711–7.
- Nojima, H., Leem, S. H., Araki, H., Sakai, A., Nakashima, N., Kanaoka, Y., & Ono, Y. (1994). Hac1: a novel yeast bZIP protein binding to the CRE motif is a multicopy suppressor for cdc10 mutant of *Schizosaccharomyces pombe*. *Nucleic acids research*, 22(24), 5279–88.
- Ohkura, H., Kinoshita, N., Miyatani, S., Toda, T., & Yanagida, M. (1989). The fission yeast *dis2+* gene required for chromosome disjoining encodes one of two putative type 1 protein phosphatases. *Cell*, 57(6), 997–1007.
- Olsen, J. V., Blagoev, B., Gnadt, F., Macek, B., Kumar, C., Mortensen, P., & Mann, M. (2006). Global, in vivo, and site-specific phosphorylation dynamics in signaling networks. *Cell*, 127(3), 635–648.
- Oromendia, A. B., Dodgson, S. E., & Amon, A. (2012). Aneuploidy causes proteotoxic stress in yeast. *Genes & development*, 26(24), 2696–708.
- Paidhungat, M., & Garrett, S. (1997). A homolog of mammalian, voltage-gated calcium channels mediates yeast pheromone-stimulated Ca²⁺ uptake and exacerbates the cdc1(Ts) growth defect. *Molecular and cellular biology*, 17(12), 6339–6347.
- Panadero, J., Pallotti, C., Rodríguez-Vargas, S., Rande-Gil, F., & Prieto, J. A. (2006). A downshift in temperature activates the high osmolarity glycerol (HOG) pathway, which determines freeze tolerance in *Saccharomyces cerevisiae*. *The Journal of biological chemistry*, 281(8), 4638–45.
- Papa, F. R., Zhang, C., Shokat, K., & Walter, P. (2003). Bypassing a kinase activity with an ATP-competitive drug. *Science (New York, N.Y.)*, 302(5650), 1533–7.
- Papamichos-Chronakis, M., Gligoris, T., & Tzamarias, D. (2004). The Snf1 kinase controls glucose repression in yeast by modulating interactions between the Mig1 repressor and the Cyc8-Tup1 co-repressor. *EMBO reports*, 5(4), 368–72.
- Park, K. C., Woo, S. K., Yoo, Y. J., Wyndham, A. M., Baker, R. T., & Chung, C. H. (1997). Purification and characterization of UBP6, a new ubiquitin-specific protease in *Saccharomyces cerevisiae*. *Archives of biochemistry and biophysics*, 347(1), 78–84.
- Parsons, A. B., Brost, R. L., Ding, H., Li, Z., Zhang, C., Sheikh, B., Boone, C. (2004). Integration of chemical-genetic and genetic interaction data links bioactive compounds to cellular target pathways. *Nat. Biotechnol.*, 22(10), 62–69.
- Patil, C. K., Li, H., & Walter, P. (2004). Gcn4p and novel upstream activating sequences regulate targets of the unfolded protein response. *PLoS biology*, 2(8), E246.
- Pedelini, L., Marquina, M., Ariño, J., Casamayor, A., Sanz, L., Bollen, M., Garcia-Gimeno, M. A. (2007). *YPI1* and *SDS22* proteins regulate the nuclear localization and function of yeast type 1 phosphatase Glc7. *The Journal of biological chemistry*, 282(5), 3282–92.

- Peggie, M. W., MacKelvie, S. H., Bloecher, A., Knatko, E. V., Tatchell, K., & Stark, M. J. R. (2002). Essential functions of Sds22p in chromosome stability and nuclear localization of PP1. *Journal of cell science*, *115*(Pt 1), 195–206.
- Peng, W. T., Robinson, M. D., Mnaimneh, S., Krogan, N. J., Cagney, G., Morris, Q., Hughes, T. R. (2003). A panoramic view of yeast noncoding RNA processing. *Cell*, *113*(7), 919–33. R
- Perepnikhatka, V., Fischer, F. J., Niimi, M., Baker, R. A., Cannon, R. D., Wang, Y. K., Rustchenko, E. (1999). Specific chromosome alterations in fluconazole-resistant mutants of *Candida albicans*. *Journal of bacteriology*, *181*(13), 4041–9.
- Peters, C., Andrews, P. D., Stark, M. J., Cesaro-Tadic, S., Glatz, A., Podtelejnikov, A., Mayer, A. (1999). Control of the terminal step of intracellular membrane fusion by protein phosphatase 1. *Science (New York, N.Y.)*, *285*(5430), 1084–7.
- Pfau, S. J., & Amon, A. (2012). Chromosomal instability and aneuploidy in cancer: from yeast to man. *EMBO reports*, *13*(6), 515–27.
- Piao, H. L., Machado, I. M. P., & Payne, G. S. (2007). NPFxD-mediated endocytosis is required for polarity and function of a yeast cell wall stress sensor. *Molecular biology of the cell*, *18*(1), 57–65.
- Piekna-Przybylska, D., Decatur, W. A., & Fournier, M. J. (2007). New bioinformatic tools for analysis of nucleotide modifications in eukaryotic rRNA. *RNA (New York, N.Y.)*, *13*(3), 305–12.
- Pincus, D., Chevalier, M. W., Aragón, T., van Anken, E., Vidal, S. E., El-Samad, H., & Walter, P. (2010). BiP binding to the ER-stress sensor Ire1 tunes the homeostatic behavior of the unfolded protein response. *PLoS biology*, *8*(7), e1000415.
- Pinkel, D., & Albertson, D. G. (2005a). Comparative genomic hybridization. *Annual review of genomics and human genetics*, *6*, 331–54.
- Pinkel, D., & Albertson, D. G. (2005b). Array comparative genomic hybridization and its applications in cancer. *Nature genetics*, *37* Suppl, S11–7.
- Pinsky, B. A., Kotwaliwale, C. V., Tatsutani, S. Y., Breed, C. A., & Biggins, S. (2006). Glc7/protein phosphatase 1 regulatory subunits can oppose the Ipl1/aurora protein kinase by redistributing Glc7. *Molecular and cellular biology*, *26*(7), 2648–60.
- Platara, M., Ruiz, A., Serrano, R., Palomino, A., Moreno, F., & Arino, J. (2006). The transcriptional response of the yeast Na(+)-ATPase *ENA1* gene to alkaline stress involves three main signaling pathways. *Journal of Biological Chemistry*, *281*(0021-9258; 48), 36632–36642.
- Polizotto, R. S., & Cyert, M. S. (2001). Calcineurin-dependent nuclear import of the transcription factor Crz1p requires Nmd5p. *J. Cell Biol.*, *154*(0021-9525; 5), 951–960.
- Posas, F., Chambers, J. R., Heyman, J. A., Hoeffler, J. P., de Nadal, E., & Arino, J. (2000). The transcriptional response of yeast to saline stress. *Journal of Biological Chemistry*, *275*(0021-9258; 23), 17249–17255.
- Proudfoot, N. J., Furger, A., & Dye, M. J. (2002). Integrating mRNA processing with transcription. *Cell*, *108*(4), 501–12.
- Ptacek, J., Devgan, G., Michaud, G., Zhu, H., Zhu, X., Fasolo, J., Snyder, M. (2005). Global analysis of protein phosphorylation in yeast. *Nature*, *438*(1476-4687; 7068), 679–684.
- Ragni, E., Piberger, H., Neupert, C., García-Cantalejo, J., Popolo, L., Arroyo, J., Strahl, S. (2011). The genetic interaction network of *CCW12*, a *Saccharomyces cerevisiae* gene required for cell wall integrity during budding and formation of mating projections. *BMC genomics*, *12*, 107.
- Ramaswamy, N. T., Li, L., Khalil, M., & Cannon, J. F. (1998). Regulation of yeast glycogen metabolism and sporulation by Glc7p protein phosphatase. *Genetics*, *149*(1), 57–72.
- Randez-Gil, F., Bojunga, N., Proft, M., & Entian, K. D. (1997). Glucose derepression of gluconeogenic enzymes in *Saccharomyces cerevisiae* correlates with phosphorylation of the gene activator Cat8p. *Molecular and cellular biology*, *17*(5), 2502–10.

- Randez-Gil, Francisca, Córcoles-Sáez, I., & Prieto, J. A. (2013). Genetic and phenotypic characteristics of baker's yeast: relevance to baking. *Annual review of food science and technology*, 4, 191–214.
- Raymond, C. K., Howald-Stevenson, I., Vater, C. A., & Stevens, T. H. (1992). Morphological classification of the yeast vacuolar protein sorting mutants: evidence for a prevacuolar compartment in class E vps mutants. *Molecular biology of the cell*, 3(12), 1389–1402.
- Reinke, A., Chen, J. C., Aronova, S., & Powers, T. (2006). Caffeine targets TOR complex I and provides evidence for a regulatory link between the FRB and kinase domains of Tor1p. *Journal of Biological Chemistry*, (0021-9258).
- Reynolds, A., Lundblad, V., Dorris, D., & Keaveney, M. (1997). *Current Protocols in Molecular Biology* 121. (F. M. Ausubel, R. Brent, R. E. Kingston, D. D. Moore, J. G. Seidman, J. A. Smith, & K. Struhl, Eds.) (pp. 13.6.1–13.6.6). John Wiley & Sons.
- Robbins, P. W. (1991). Genetic regulation of asparagine-linked oligosaccharide synthesis. *Biochemical Society transactions*, 19(3), 642–5.
- Rodriguez-Navarro, A. (2000). Potassium transport in fungi and plants. *Biochim.Biophys.Acta*, 1469(0006-3002; 1), 1–30.
- Roemer, T., Delaney, S., & Bussey, H. (1993). SKN1 and KRE6 define a pair of functional homologs encoding putative membrane proteins involved in beta-glucan synthesis. *Molecular and cellular biology*, 13(7), 4039–48.
- Ronne, H. (1995). Glucose repression in fungi. *Trends in genetics : TIG*, 11(1), 12–7.
- Rothstein, R. J. (1983). One-step gene disruption in yeast. *Methods in enzymology*, 101, 202–11.
- Rubio, C., Pincus, D., Korennykh, A., Schuck, S., El-Samad, H., & Walter, P. (2011). Homeostatic adaptation to endoplasmic reticulum stress depends on Ire1 kinase activity. *The Journal of cell biology*, 193(1), 171–84.
- Rudolph, H. K., Antebi, A., Fink, G. R., Buckley, C. M., Dorman, T. E., LeVitre, J., ... Moir, D. T. (1989). The yeast secretory pathway is perturbed by mutations in PMR1, a member of a Ca²⁺ ATPase family 1. *Cell*, 58(0092-8674; 1), 133–145.
- Rüeggsegger, U., Leber, J. H., & Walter, P. (2001). Block of HAC1 mRNA translation by long-range base pairing is released by cytoplasmic splicing upon induction of the unfolded protein response. *Cell*, 107(1), 103–14.
- Ruepp, A., Zollner, A., Maier, D., Albermann, K., Hani, J., Mokrejs, M., ... Mewes, H. W. (2004). The FunCat, a functional annotation scheme for systematic classification of proteins from whole genomes. *Nucleic acids research*, 32(18), 5539–5545.
- Ruiz, A, Gonzalez, A., Garcia-Salcedo, R., Ramos, J., & Arino, J. (2006). Role of protein phosphatases 2C on tolerance to lithium toxicity in the yeast *Saccharomyces cerevisiae*. *Molecular microbiology*, 62(0950-382; 1), 263–277.
- Ruiz, Amparo, & Ariño, J. (2007). Function and regulation of the *Saccharomyces cerevisiae* ENA sodium ATPase system. *Eukaryotic cell*, 6(12), 2175–83.
- Russell, P., & Nurse, P. (1986). *Schizosaccharomyces pombe* and *Saccharomyces cerevisiae*: a look at yeasts divided. *Cell*, 45(6), 781–2.
- Russnak, R., Nehrke, K. W., & Platt, T. (1995). REF2 encodes an RNA-binding protein directly involved in yeast mRNA 3'-end formation. *Molecular and cellular biology*, 15(3), 1689–97.
- Sambrook, J., E.F., F., & Maniatis, T. (1989). *Molecular Cloning: A Laboratory Manual*. Cold Spring Harbor, NY: Cold Spring Harbor Laboratory Press.
- Sanz, P., Alms, G. R., Haystead, T. A., & Carlson, M. (2000). Regulatory interactions between the Reg1-Glc7 protein phosphatase and the Snf1 protein kinase. *Molecular and cellular biology*, 20(4), 1321–8.

- Sanz, P., Ludin, K., & Carlson, M. (2000). Sip5 interacts with both the Reg1/Glc7 protein phosphatase and the Snf1 protein kinase of *Saccharomyces cerevisiae*. *Genetics*, *154*(1), 99–107.
- Schröder, M., Clark, R., & Kaufman, R. J. (2003). IRE1- and HAC1-independent transcriptional regulation in the unfolded protein response of yeast. *Molecular microbiology*, *49*(3), 591–606.
- Schubert, U., Antón, L. C., Gibbs, J., Norbury, C. C., Yewdell, J. W., & Bennink, J. R. (2000). Rapid degradation of a large fraction of newly synthesized proteins by proteasomes. *Nature*, *404*(6779), 770–4.
- Schuberth, C., Richly, H., Rumpf, S., & Buchberger, A. (2004). Shp1 and Ubx2 are adaptors of Cdc48 involved in ubiquitin-dependent protein degradation. *EMBO reports*, *5*(8), 818–24.
- Scrimale, T., Didone, L., de Mesy Bentley, K. L., & Krysan, D. J. (2009). The unfolded protein response is induced by the cell wall integrity mitogen-activated protein kinase signaling cascade and is required for cell wall integrity in *Saccharomyces cerevisiae*. *Molecular biology of the cell*, *20*(1), 164–75.
- Serrano, R. (1996). Salt tolerance in plants and microorganisms: toxicity targets and defense responses. *Int.Rev.Cytol.*, *165*(0074-7696), 1–52.
- Serrano, R., Ruiz, A., Bernal, D., Chambers, J. R., & Arino, J. (2002). The transcriptional response to alkaline pH in *Saccharomyces cerevisiae*: evidence for calcium-mediated signalling. *Molecular microbiology*, *46*(0950-382; 5), 1319–1333.
- Serrano, Raquel, Ruiz, A., Bernal, D., Chambers, J. R., & Ariño, J. (2002). The transcriptional response to alkaline pH in *Saccharomyces cerevisiae*: evidence for calcium-mediated signalling. *Molecular microbiology*, *46*(5), 1319–33.
- Shamu, C. E., & Walter, P. (1996). Oligomerization and phosphorylation of the Ire1p kinase during intracellular signaling from the endoplasmic reticulum to the nucleus. *The EMBO journal*, *15*(12), 3028–39.
- Sheltzer, J. M., Blank, H. M., Pfau, S. J., Tange, Y., George, B. M., Humpton, T. J., ... Amon, A. (2011). Aneuploidy drives genomic instability in yeast. *Science (New York, N.Y.)*, *333*(6045), 1026–30.
- Shi, Y. (2009). Serine/threonine phosphatases: mechanism through structure. *Cell*, *139*(1097-4172; 3), 468–484.
- Shilatifard, A. (2008). Molecular implementation and physiological roles for histone H3 lysine 4 (H3K4) methylation. *Current opinion in cell biology*, *20*(3), 341–8.
- Sidrauski, C., Cox, J. S., & Walter, P. (1996). tRNA ligase is required for regulated mRNA splicing in the unfolded protein response. *Cell*, *87*(3), 405–13.
- Sikorski, R. S., & Hieter, P. (1989). A system of shuttle vectors and yeast host strains designed for efficient manipulation of DNA in *Saccharomyces cerevisiae*. *Genetics*, *122*(1), 19–27.
- Smets, B., Ghillebert, R., De Snijder, P., Binda, M., Swinnen, E., De Virgilio, C., & Winderickx, J. (2010). Life in the midst of scarcity: adaptations to nutrient availability in *Saccharomyces cerevisiae*. *Current genetics*, *56*(1), 1–32.
- Smriti, Krishnamurthy, S., Dixit, B. L., Gupta, C. M., Milewski, S., & Prasad, R. (2002). ABC transporters Cdr1p, Cdr2p and Cdr3p of a human pathogen *Candida albicans* are general phospholipid translocators. *Yeast (Chichester, England)*, *19*(4), 303–18.
- Solomon, F. (1991). Analyses of the cytoskeleton in *Saccharomyces cerevisiae*. *Annual review of cell biology*, *7*, 633–62.
- Song, W., & Carlson, M. (1998). Srb/mediator proteins interact functionally and physically with transcriptional repressor Sfl1. *The EMBO journal*, *17*(19), 5757–65.
- Sopko, R., Huang, D., Preston, N., Chua, G., Papp, B., Kafadar, K., ... Andrews, B. (2006). Mapping pathways and phenotypes by systematic gene overexpression. *Molecular cell*, *21*(3), 319–30.

- Stark, M. J. (1996). Yeast protein serine/threonine phosphatases: multiple roles and diverse regulation. *Yeast (Chichester, England)*, *12*(16), 1647–1675.
- Stathopoulos, A. M., & Cyert, M. S. (1997a). Calcineurin acts through the CRZ1/TCN1-encoded transcription factor to regulate gene expression in yeast. *Genes Dev.*, *11*(0890-9369; 24), 3432–3444.
- Stathopoulos, A. M., & Cyert, M. S. (1997b). Calcineurin acts through the CRZ1/TCN1-encoded transcription factor to regulate gene expression in yeast. *Genes & development*, *11*(24), 3432–44.
- Steffen, K. K., McCormick, M. A., Pham, K. M., MacKay, V. L., Delaney, J. R., Murakami, C. J., ... Kennedy, B. K. (2012). Ribosome deficiency protects against ER stress in *Saccharomyces cerevisiae*. *Genetics*, *191*(1), 107–18. 9
- Steinmetz, E. J., Conrad, N. K., Brow, D. A., & Corden, J. L. (2001). RNA-binding protein Nrd1 directs poly(A)-independent 3'-end formation of RNA polymerase II transcripts. *Nature*, *413*(6853), 327–31.
- Strayle, J., Pozzan, T., & Rudolph, H. K. (1999). Steady-state free Ca(2+) in the yeast endoplasmic reticulum reaches only 10 microM and is mainly controlled by the secretory pathway pump pmr1. *The EMBO journal*, *18*(0261-4189; 17), 4733–4743.
- Stuart, J. S., Frederick, D. L., Varner, C. M., & Tatchell, K. (1994). The mutant type 1 protein phosphatase encoded by *glc7-1* from *Saccharomyces cerevisiae* fails to interact productively with the GAC1-encoded regulatory subunit. *Molecular and cellular biology*, *14*(2), 896–905.
- Sutherland, C. M., Hawley, S. A., McCartney, R. R., Leech, A., Stark, M. J. R., Schmidt, M. C., & Hardie, D. G. (2003). Elm1p is one of three upstream kinases for the *Saccharomyces cerevisiae* SNF1 complex. *Current biology : CB*, *13*(15), 1299–305.
- Tabba, S., Mangat, S., McCartney, R., & Schmidt, M. C. (2010). PP1 phosphatase-binding motif in Reg1 protein of *Saccharomyces cerevisiae* is required for interaction with both the PP1 phosphatase Glc7 and the Snf1 protein kinase. *Cellular signalling*, *22*(7), 1013–21.
- Tachikawa, H., Bloecher, A., Tatchell, K., & Neiman, A. M. (2001). A Gip1p-Glc7p phosphatase complex regulates septin organization and spore wall formation. *The Journal of cell biology*, *155*(5), 797–808.
- Tan, S.-X., Teo, M., Lam, Y. T., Dawes, I. W., & Perrone, G. G. (2009a). Cu, Zn superoxide dismutase and NADP(H) homeostasis are required for tolerance of endoplasmic reticulum stress in *Saccharomyces cerevisiae*. *Molecular biology of the cell*, *20*(5), 1493–508. d
- Tan, S.-X., Teo, M., Lam, Y. T., Dawes, I. W., & Perrone, G. G. (2009b). Cu, Zn superoxide dismutase and NADP(H) homeostasis are required for tolerance of endoplasmic reticulum stress in *Saccharomyces cerevisiae*. *Molecular biology of the cell*, *20*(5), 1493–508.
- Tan, Y. S. H. (2002). Pho85 Phosphorylates the Glc7 Protein Phosphatase Regulator Glc8 in Vivo. *Journal of Biological Chemistry*, *278*(1), 147–153.
- Tang, Y.-C., & Amon, A. (2013). Gene copy-number alterations: a cost-benefit analysis. *Cell*, *152*(3), 394–405.
- Taylor, I. A., McIntosh, P. B., Pala, P., Treiber, M. K., Howell, S., Lane, A. N., & Smerdon, S. J. (2000). Characterization of the DNA-binding domains from the yeast cell-cycle transcription factors Mbp1 and Swi4. *Biochemistry*, *39*(14), 3943–54.
- Thomas, B. J., & Rothstein, R. (1989). Elevated recombination rates in transcriptionally active DNA. *Cell*, *56*(4), 619–30.
- Thompson, S. L., Bakhoun, S. F., & Compton, D. A. (2010). Mechanisms of chromosomal instability. *Current biology : CB*, *20*(6), R285–95.
- Thorburn, R. R., Gonzalez, C., Brar, G. A., Christen, S., Carlile, T. M., Ingolia, N. T., ... Amon, A. (2013). Aneuploid yeast strains exhibit defects in cell growth and passage through START. *Molecular biology of the cell*, *24*(9), 1274–89.

- Timmers, H. T. M., & Tora, L. (2005). SAGA unveiled. *Trends in biochemical sciences*, *30*(1), 7–10. doi:10.1016/j.tibs.2004.11.007
- Tong, A. H., Lesage, G., Bader, G. D., Ding, H., Xu, H., Xin, X., ... Boone, C. (2004). Global mapping of the yeast genetic interaction network. *Science*, *303*(1095-9203; 5659), 808–813.
- Torre-Ruiz, A. de la, Torres, J., Arino, J., & Herrero, E. (2002). Sit4 is required for proper modulation of the biological functions mediated by Pkc1 and the cell integrity pathway in *Saccharomyces cerevisiae*. *Journal of Biological Chemistry*, *277*(0021-9258; 36), 33468–33476.
- Torres, E M, Williams, B. R., Tang, Y.-C., & Amon, A. (2010). Thoughts on aneuploidy. *Cold Spring Harbor symposia on quantitative biology*, *75*, 445–51.
- Torres, Eduardo M, Dephoure, N., Panneerselvam, A., Tucker, C. M., Whittaker, C. A., Gygi, S. P., ... Amon, A. (2010). Identification of aneuploidy-tolerating mutations. *Cell*, *143*(1), 71–83.
- Torres, Eduardo M, Sokolsky, T., Tucker, C. M., Chan, L. Y., Boselli, M., Dunham, M. J., & Amon, A. (2007). Effects of aneuploidy on cellular physiology and cell division in haploid yeast. *Science (New York, N.Y.)*, *317*(5840), 916–24.
- Torres, Eduardo M, Williams, B. R., & Amon, A. (2008). Aneuploidy: cells losing their balance. *Genetics*, *179*(2), 737–46.
- Torres, J., Di Como, C. J., Herrero, E., & De la Torre, M. A. (2002). Regulation of the cell integrity pathway by rapamycin-sensitive TOR function in budding yeast. *Journal of Biological Chemistry*, *277*(0021-9258; 45), 43495–43504.
- Torres-Quiroz, FranciscoTorres-Quiroz, F., García-Marqués, S., Coria, R., Randez-Gil, F., & Prieto, J. A. (2010). The activity of yeast Hog1 MAPK is required during endoplasmic reticulum stress induced by tunicamycin exposure. *The Journal of biological chemistry*, *285*(26), 20088–96.
- Travers, K. J., Patil, C. K., Wodicka, L., Lockhart, D. J., Weissman, J. S., & Walter, P. (2000). Functional and genomic analyses reveal an essential coordination between the unfolded protein response and ER-associated degradation. *Cell*, *101*(3), 249–58.
- Trinder, P. (1969). Determination of blood glucose using 4-amino phenazone as oxygen acceptor. *Journal of clinical pathology*, *22*(2), 246.
- Truman, A. W., Kim, K. Y., & Levin, D. E. (2009). Mechanism of Mpk1 mitogen-activated protein kinase binding to the Swi4 transcription factor and its regulation by a novel caffeine-induced phosphorylation. *Molecular and cellular biology*, *29*(24), 6449–6461.
- Tu, J., & Carlson, M. (1995a). REG1 binds to protein phosphatase type 1 and regulates glucose repression in *Saccharomyces cerevisiae* 1. *The EMBO journal*, *14*(0261-4189; 23), 5939–5946.
- Tu, J., Song, W., & Carlson, M. (1996). Protein phosphatase type 1 interacts with proteins required for meiosis and other cellular processes in *Saccharomyces cerevisiae*. *Molecular and cellular biology*, *16*(8), 4199–206.
- Tung, H. Y., Wang, W., & Chan, C. S. (1995). Regulation of chromosome segregation by Glc8p, a structural homolog of mammalian inhibitor 2 that functions as both an activator and an inhibitor of yeast protein phosphatase 1. *Molecular and cellular biology*, *15*(11), 6064–74.
- Van Drogen, F., & Peter, M. (2002). Spa2p functions as a scaffold-like protein to recruit the Mpk1p MAP kinase module to sites of polarized growth. *Current biology : CB*, *12*(0960-9822; 19), 1698–1703.
- Van Oevelen, C. J. C., van Teeffelen, H. A. A. M., van Werven, F. J., & Timmers, H. T. M. (2006). Snf1p-dependent Spt-Ada-Gcn5-acetyltransferase (SAGA) recruitment and chromatin remodeling activities on the *HXT2* and *HXT4* promoters. *The Journal of biological chemistry*, *281*(7), 4523–31.
- Van Werven, F. J., Neuert, G., Hendrick, N., Lardenois, A., Buratowski, S., van Oudenaarden, A., Amon, A. (2012). Transcription of two long noncoding RNAs mediates mating-type control of gametogenesis in budding yeast. *Cell*, *150*(6), 1170–81.

- Varadarajan, S., Tanaka, K., Smalley, J. L., Bampton, E. T. W., Pellicchia, M., Dinsdale, D., ... Cohen, G. M. (2013). Endoplasmic reticulum membrane reorganization is regulated by ionic homeostasis. *PLoS one*, *8*(2), e56603.
- Venema, J., & Tollervey, D. (1999). Ribosome synthesis in *Saccharomyces cerevisiae*. *Annual review of genetics*, *33*, 261–311. 1
- Venkatasubrahmanyam, S., Hwang, W. W., Meneghini, M. D., Tong, A. H. Y., & Madhani, H. D. (2007). Genome-wide, as opposed to local, antisilencing is mediated redundantly by the euchromatic factors Set1 and H2A.Z. *Proceedings of the National Academy of Sciences of the United States of America*, *104*(42), 16609–14.
- Vida, T. A., & Emr, S. D. (1995). A new vital stain for visualizing vacuolar membrane dynamics and endocytosis in yeast. *The Journal of cell biology*, *128*(5), 779–92.
- Viladevall, L., Serrano, R., Ruiz, A., Domenech, G., Giraldo, J., Barcelo, A., & Arino, J. (2004). Characterization of the calcium-mediated response to alkaline stress in *Saccharomyces cerevisiae*. *Journal of Biological Chemistry*, *279*(0021-9258; 42), 43614–43624.
- Vincent, O., Townley, R., Kuchin, S., & Carlson, M. (2001). Subcellular localization of the Snf1 kinase is regulated by specific beta subunits and a novel glucose signaling mechanism. *Genes & development*, *15*(9), 1104–14.
- Wakula, P., Beullens, M., Ceulemans, H., Stalmans, W., & Bollen, M. (2003). Degeneracy and function of the ubiquitous RVXF motif that mediates binding to protein phosphatase-1. *Journal of Biological Chemistry*, *278*(0021-9258; 21), 18817–18823.
- Walsh, E. P., Lamont, D. J., Beattie, K. A., & Stark, M. J. R. (2002). Novel interactions of *Saccharomyces cerevisiae* type 1 protein phosphatase identified by single-step affinity purification and mass spectrometry. *Biochemistry*, *41*(7), 2409–20.
- Walter, P., & Ron, D. (2011). The unfolded protein response: from stress pathway to homeostatic regulation. *Science (New York, N.Y.)*, *334*(6059), 1081–6.
- Wanke, V., Cameroni, E., Uotila, A., Piccolis, M., Urban, J., Loewith, R., & De Virgilio, C. (2008). Caffeine extends yeast lifespan by targeting TORC1. *Molecular microbiology*, *69*(1), 277–85.
- Wapinski, I., Pfeffer, A., Friedman, N., & Regev, A. (2007). Natural history and evolutionary principles of gene duplication in fungi. *Nature*, *449*(7158), 54–61.
- Weerapana, E., & Imperiali, B. (2006). Asparagine-linked protein glycosylation: from eukaryotic to prokaryotic systems. *Glycobiology*, *16*(6), 91R–101R.
- Welihinda, A. A., Tirasophon, W., Green, S. R., & Kaufman, R. J. (1998). Protein serine/threonine phosphatase Ptc2p negatively regulates the unfolded-protein response by dephosphorylating Ire1p kinase. *Molecular and cellular biology*, *18*(0270-7306; 4), 1967–1977.
- Welihinda, A. A., Tirasophon, W., & Kaufman, R. J. (n.d.). The transcriptional co-activator ADA5 is required for HAC1 mRNA processing in vivo. *The Journal of biological chemistry*, *275*(5), 3377–81.
- White, R. J. (2005). RNA polymerases I and III, growth control and cancer. *Nature reviews. Molecular cell biology*, *6*(1), 69–78.
- Wickner, W., & Schekman, R. (2005). Protein translocation across biological membranes. *Science (New York, N.Y.)*, *310*(5753), 1452–6.
- Wieland, J., Nitsche, A. M., Strayle, J., Steiner, H., & Rudolph, H. K. (1995). The *PMR2* gene cluster encodes functionally distinct isoforms of a putative Na⁺ pump in the yeast plasma membrane. *The EMBO journal*, *14*(0261-4189; 16), 3870–3882.
- Williams-Hart, T, Wu, X., & Tatchell, K. (2002). Protein phosphatase type 1 regulates ion homeostasis in *Saccharomyces cerevisiae*. *Genetics*, *160*(0016-6731; 4), 1423–1437.

- Wilson, W. A., Hawley, S. A., & Hardie, D. G. (1996). Glucose repression/derepression in budding yeast: *SNF1* protein kinase is activated by phosphorylation under derepressing conditions, and this correlates with a high AMP:ATP ratio. *Current biology : CB*, *6*(11), 1426–34. R
- Winey, M., & Culbertson, M. R. (1988). Mutations affecting the tRNA-splicing endonuclease activity of *Saccharomyces cerevisiae*. *Genetics*, *118*(4), 609–17.
- Winzeler, E. A., Shoemaker, D. D., Astromoff, A., Liang, H., Anderson, K., Andre, B., ... Bussey, H. (1999). Functional characterization of the *S. cerevisiae* genome by gene deletion and parallel analysis. *Science (New York, N.Y.)*, *285*(5429), 901–6.
- Withee, J. L., Sen, R., & Cyert, M. S. (1998). Ion tolerance of *Saccharomyces cerevisiae* lacking the Ca²⁺/CaM-dependent phosphatase (calcineurin) is improved by mutations in *URE2* or *PMA1*. *Genetics*, *149*(0016-6731; 2), 865–878.
- Woodbury, E. L., & Morgan, D. O. (2007). The role of self-association in Fin1 function on the mitotic spindle. *The Journal of biological chemistry*, *282*(44), 32138–43.
- Woods, A., Munday, M. R., Scott, J., Yang, X., Carlson, M., & Carling, D. (1994). Yeast *SNF1* is functionally related to mammalian AMP-activated protein kinase and regulates acetyl-CoA carboxylase in vivo. *The Journal of biological chemistry*, *269*(30), 19509–15.
- Wu, J., & Trumbly, R. J. (1998). Multiple regulatory proteins mediate repression and activation by interaction with the yeast Mig1 binding site. *Yeast (Chichester, England)*, *14*(11), 985–1000.
- Wu, X., Hart, H., Cheng, C., Roach, P. J., & Tatchell, K. (2001). Characterization of Gac1p, a regulatory subunit of protein phosphatase type I involved in glycogen accumulation in *Saccharomyces cerevisiae*. *Mol. Genet. Genomics*, *265*(1617-4615; 4), 622–635.
- Wu, X., & Tatchell, K. (2001). Mutations in yeast protein phosphatase type 1 that affect targeting subunit binding. *Biochemistry*, *40*(25), 7410–20.
- Xu, H., & Boeke, J. D. (1987). High-frequency deletion between homologous sequences during retrotransposition of Ty elements in *Saccharomyces cerevisiae*. *Proceedings of the National Academy of Sciences of the United States of America*, *84*(23), 8553–7.
- Yadav, J., Muend, S., Zhang, Y., & Rao, R. (2007). A phenomics approach in yeast links proton and calcium pump function in the Golgi. *Molecular biology of the cell*, *18*(4), 1480–9.
- Yen, K., Gitsham, P., Wishart, J., Oliver, S. G., & Zhang, N. (2003). An improved tetO promoter replacement system for regulating the expression of yeast genes. *Yeast (Chichester, England)*, *20*(15), 1255–62.
- Yenush, L., Mulet, J. M., Arino, J., & Serrano, R. (2002). The Ppz protein phosphatases are key regulators of K⁺ and pH homeostasis: implications for salt tolerance, cell wall integrity and cell cycle progression. *The EMBO journal*, *21*(0261-4189; 5), 920–929.
- Yona, A. H., Manor, Y. S., Herbst, R. H., Romano, G. H., Mitchell, A., Kupiec, M., ... Dahan, O. (2012). Chromosomal duplication is a transient evolutionary solution to stress. *Proceedings of the National Academy of Sciences of the United States of America*, *109*(51), 21010–5.
- Yoshimoto, H., Saltsman, K., Gasch, A. P., Li, H. X., Ogawa, N., Botstein, D., ... Cyert, M. S. (2002). Genome-wide analysis of gene expression regulated by the calcineurin/Crz1p signaling pathway in *Saccharomyces cerevisiae*. *Journal of Biological Chemistry*, *277*(0021-9258; 34), 31079–31088.
- Young, C., Mapes, J., Hanneman, J., Al Zarban, S., & Ota, I. (2002). Role of Ptc2 type 2C Ser/Thr phosphatase in yeast high-osmolarity glycerol pathway inactivation. *Eukaryot. Cell*, *1*(1535-9778; 6), 1032–1040.
- Zeng, G., Huang, B., Neo, S. P., Wang, J., & Cai, M. (2007). Scd5p mediates phosphoregulation of actin and endocytosis by the type 1 phosphatase Glc7p in yeast. *Molecular biology of the cell*, *18*(12), 4885–98.
- Zhang, S., Guha, S., & Volkert, F. C. (1995). The *Saccharomyces* SHP1 gene, which encodes a regulator of phosphoprotein phosphatase 1 with differential effects on glycogen metabolism, meiotic

- differentiation, and mitotic cell cycle progression. *Molecular and cellular biology*, 15(0270-7306; 4), 2037–2050.
- Zhao, C., Jung, U. S., Garrett-Engle, P., Roe, T., Cyert, M. S., & Levin, D. E. (1998a). Temperature-induced expression of yeast FKS2 is under the dual control of protein kinase C and calcineurin. *Molecular and cellular biology*, 18(0270-7306; 2), 1013–1022.
- Zhao, S., & Lee, E. Y. (1997a). Targeting of the catalytic subunit of protein phosphatase-1 to the glycolytic enzyme phosphofructokinase. *Biochemistry*, 36(27), 8318–24.
- Zhao, S., & Lee, E. Y. (1997b). A protein phosphatase-1-binding motif identified by the panning of a random peptide display library. *Journal of Biological Chemistry*, 272(0021-9258; 45), 28368–28372.
- Zhao, Y., Du, J., Xiong, B., Xu, H., & Jiang, L. (2013). ESCRT components regulate the expression of the ER/Golgi calcium pump gene PMR1 through the Rim101/Nrg1 pathway in budding yeast. *Journal of molecular cell biology*.
- Zhou, H., & Winston, F. (2001). *NRG1* is required for glucose repression of the *SUC2* and *GAL* genes of *Saccharomyces cerevisiae* 3. *BMC.Genet.*, 2(1471-2156; 1), 5.
- Zimmer, C., & Fabre, E. (2011). Principles of chromosomal organization: lessons from yeast. *The Journal of cell biology*, 192(5), 723–33.
- Zou, J., Friesen, H., Larson, J., Huang, D., Cox, M., Tatchell, K., & Andrews, B. (2009). Regulation of cell polarity through phosphorylation of Bni4 by Pho85 G1 cyclin-dependent kinases in *Saccharomyces cerevisiae*. *Molecular biology of the cell*, 20(14), 3239–50.

Publications



Ref2, a regulatory subunit of the yeast protein phosphatase 1, is a novel component of cation homeostasis

Jofre FERRER-DALMAU*, Asier GONZÁLEZ*, Maria PLATARA*, Clara NAVARRETE†, José L. MARTÍNEZ†, Lina BARRETO*, José RAMOS†, Joaquín ARIÑO* and Antonio CASAMAYOR*¹

*Departament de Bioquímica i Biologia Molecular and Institut de Biotecnologia i Biomedicina, Universitat Autònoma de Barcelona, Barcelona 08193, Spain, and †Departamento de Microbiología, Universidad de Córdoba, Córdoba 14071, Spain

Maintenance of cation homeostasis is a key process for any living organism. Specific mutations in Glc7, the essential catalytic subunit of yeast protein phosphatase 1, result in salt and alkaline pH sensitivity, suggesting a role for this protein in cation homeostasis. We screened a collection of Glc7 regulatory subunit mutants for altered tolerance to diverse cations (sodium, lithium and calcium) and alkaline pH. Among 18 candidates, only deletion of *REF2* (RNA end formation 2) yielded increased sensitivity to these conditions, as well as to diverse organic toxic cations. The Ref2^{F374A} mutation, which renders it unable to bind Glc7, did not rescue the salt-related phenotypes of the *ref2* strain, suggesting that Ref2 function in cation homeostasis is mediated by Glc7. The *ref2* deletion mutant displays a marked decrease in lithium efflux, which can be explained by the inability of these cells to

fully induce the Na⁺-ATPase *ENA1* gene. The effect of lack of Ref2 is additive to that of blockage of the calcineurin pathway and might disrupt multiple mechanisms controlling *ENA1* expression. *ref2* cells display a striking defect in vacuolar morphogenesis, which probably accounts for the increased calcium levels observed under standard growth conditions and the strong calcium sensitivity of this mutant. Remarkably, the evidence collected indicates that the role of Ref2 in cation homeostasis may be unrelated to its previously identified function in the formation of mRNA via the APT (for associated with Pta1) complex.

Key words: associated with Pta1 (APT) complex, calcineurin, cation tolerance, *ENA1*, type 1 protein phosphatase, vacuolar defect.

INTRODUCTION

An elevated intracellular concentration of sodium ions is harmful for most eukaryotic cells, probably because it interferes with the correct functioning of certain cellular targets [1]. Yeasts, as well as other single-cell eukaryotic organisms, have developed mechanisms to maintain a safe cytosolic concentration of sodium even when the external concentration of sodium ions in their natural environments is high. To this end, these organisms employ three distinct strategies: (i) discrimination among different alkali metal cations at the level of uptake (favouring transport of potassium compared with sodium); (ii) triggering the efficient efflux of toxic cations; and (iii) sequestering the excess of cations in organelles, such as the vacuole.

The budding yeast *Saccharomyces cerevisiae* is a model organism very often used for cation tolerance studies. In this organism, the capacity to extrude sodium (or other toxic cations, such as lithium) represents a major mechanism to maintain low intracellular levels. This is achieved in two different and complementary ways. First, via the function of an H⁺/Na⁺-antiporter, encoded by the *NHA1* gene, which is able to extrude sodium, lithium and even potassium cations by exchange with protons and therefore with biological relevance at rather acidic external pHs [2,3]. The second mechanism is based on a P-type ATPase pump encoded by the *ENA* system (see [4] for a review). In *S. cerevisiae* the *ENA* genes are disposed in tandem repeats with a variable number of copies (*ENA1–ENA5*) encoding identical or very similar proteins [5–7]. Deletion of the entire *ENA* cluster in *S. cerevisiae* results in a dramatic phenotype of sensitivity to

sodium and lithium cations or alkaline pHs [5,6,8,9]. It is widely accepted that *ENA1* is the functionally relevant component of the cluster on the basis that (i) cation sensitivity is largely restored by expression of *ENA1* [6,10] and (ii) whereas under standard growth conditions expression from the *ENA* genes is almost undetectable, *ENA1* expression dramatically increases in response to osmotic, saline or alkaline pH stress [6,8,9,11].

Regulation of *ENA1* expression in response to saline or alkaline stress is under the control of different pathways [12]. These include the osmoreponsive MAPK (mitogen-activated protein kinase) Hog1, the calcium-activated protein phosphatase calcineurin, the Rim101/Nrg1, the Snf1 and the Hal3/Ppz1 pathways, among others (see [4] and references therein). Activation of calcineurin upon saline or alkaline pH stress results in dephosphorylation and nuclear entry of the Crz1 (calcineurin-responsive zinc finger) transcription factor [13–15], which binds to specific sequences, known as CDREs (calcineurin-dependent response elements), in calcineurin-responsive promoters. Two CDREs have been defined in the *ENA1* promoter (at –821/–813 and –727/–719 relative to the translation start site), with the downstream element being the most relevant for induction of the gene in cells exposed to saline or high pH stress [16–19].

Protein phosphatase 1 is a conserved serine/threonine protein phosphatase whose catalytic subunit is encoded in *S. cerevisiae* by a single, essential gene, named *GLC7* [20,21]. The Glc7 protein is required for a myriad of cellular functions and specific regulation of these functions is achieved by interaction of the catalytic subunit with a variety of regulatory protein that influence Glc7 intracellular localization and/or substrate

Abbreviations used: APT, associated with Pta1; CDRE, calcineurin-dependent response element; CPF, cleavage and polyadenylation factor; ORF, open reading frame; Ref2, RNA end formation 2; RLU, relative luminescence unit; snoRNA, small nucleolar RNA; TMA, tetramethylammonium; YNB, yeast nitrogen base.

¹ To whom correspondence should be addressed (email antonio.casamayor@uab.es).

recognition. Many of these regulatory proteins have a conserved binding site, with a consensus sequence of (R/K)(V/I)X(F/W), that is necessary for the interaction with Glc7 [22,23]. Databases searches (at the *Saccharomyces* Genome Database, <http://www.yeastgenome.org/>) reveal at least 119 proteins that are annotated as Glc7-interacting proteins. However, most of these relationships are based on recent high-throughput analysis, whereas compelling regulatory evidence has been only collected for a limited subset of these proteins.

Among the cellular functions attributed to the Glc7 phosphatase, a role in ion homeostasis was postulated some years ago as a result of the characterization of the *glc7-109* allele [24], which carried a mutation at Arg-260 found to be responsible for the mutant phenotypes. *glc7-109* mutants displayed, among other phenotypes, a marked sensitivity to sodium cations and alkaline pH, which was remedied by inclusion of potassium ions in the medium. Interestingly, Arg-260 lies in the vicinity of Phe-256, a residue in the Glc7 hydrophobic channel that makes contact with the aromatic residue of the (R/K)(V/I)X(F/W) binding-partner motif. Therefore we hypothesized that the defect in ion homeostasis in the *glc7-109* mutant could be due to a deficient interaction of the mutated protein with a regulatory subunit relevant for ion tolerance. To this end, we have analysed the tolerance to diverse cations of 18 known or putative Glc7 regulatory subunits and found that deletion of *REF2* (RNA end formation 2) yields a rather severe and unique phenotype of sensitivity to sodium and lithium cations and alkaline pH. *REF2* was initially described as a gene encoding a protein required for mRNA 3'-end maturation prior to the final polyadenylation step [25]. Evidence for interaction between Ref2 and Glc7 was obtained by both two-hybrid and affinity purification techniques [26–28]. Subsequently, it has been found that Ref2 is a component of the APT (for associated with Pta1) subcomplex of the large CPF (cleavage and polyadenylation factor)-containing complex (holo-CPF), which is required for formation of mRNA and snoRNA (small nucleolar RNA) 3'-ends and also contains Glc7 [29]. It has been shown that Ref2 is required for the permanence of Glc7 within the complex [30]. The Ref2 protein contains a R³⁶⁸ISSIKFLD³⁷⁶ sequence that resembles the Glc7-binding motif (the bold residues are a perfect match with the consensus sequence) and recent evidence indicates that mutation of Ref2 Phe-374 to an alanine residue disrupts the interaction between the protein and Glc7, thus preventing incorporation of Glc7 to the APT subcomplex [30].

In the present study, we highlight the cation-sensitivity phenotype of the *ref2* mutant and investigate the molecular basis of this defect. Our results indicate that mutation of *REF2* results in a deficient efflux of toxic cations that can, at least in part, be attributed to impaired expression of the *ENA1* ATPase gene. Remarkably, this role in salt tolerance seems unrelated to the function of Ref2 in the APT complex.

EXPERIMENTAL

Growth of *Escherichia coli* and yeast strains

E. coli DH5 α cells were used as plasmid DNA hosts and were grown at 37 °C in LB (Luria–Bertani) medium, supplemented with 50 μ g/ml ampicillin when plasmid selection was required. Yeast cells were cultivated at 28 °C in YPD medium [1 % (w/v) yeast extract/2 % (w/v) peptone/2 % (w/v) glucose], or in synthetic complete drop-out medium when carrying plasmids. Restriction reactions, DNA ligations and other standard recombinant DNA techniques were performed as described in [31]. Yeast cells were transformed using the lithium acetate method [32]. Sensitivity of

yeast cells to lithium, sodium or calcium chloride and alkaline pH was evaluated by growth on YPD or YP-based [1 % (w/v) yeast extract/2 % (w/v) peptone] plates (drop tests) or in liquid cultures as described previously [8,33]. Growth under limiting potassium concentration was carried out using an YNB (yeast nitrogen base)-based medium (Translucent K-free medium; Formedium) formulated so that potassium content in the final medium is negligible (approx. 15 μ M).

Gene disruption and plasmid construction

Single *KanMX* deletion mutants in the BY4741 background (*MATa his3 Δ 1 leu2 Δ met15 Δ ura3 Δ*) were generated in the context of the *Saccharomyces* Genome Deletion Project [34]. Replacement of the *REF2* coding region by the *nat1* marker from *Streptomyces noursei* was accomplished as follows: the 1.40 kbp DNA fragment containing the *nat1* gene, flanked by genomic sequences corresponding to –40/–1 and +1603/+1643, relative to the *REF2* ATG codon, was amplified from the plasmid pAG25 [35] with the oligonucleotides OJFD021 and OJFD022 (see Supplementary Table S1 available at <http://www.BiochemJ.org/bj/426/bj4260355add.htm>) and transformed in the wild-type strains BY4741 and its *cnb1::KanMX* derivative to yield strains YJFD1 and YJFD7 respectively. The *ref2::nat1* mutation was also introduced into the wild-type DBY746 background (*MATa, ura3-52 leu2-3,112 his3 Δ 1 trp1 Δ 239*) to yield strain YJFD5, which was used for measurement of intracellular calcium levels. Positive clones were selected in the presence of 100 μ g/ml nourseothricin (Werner BioAgents) and the presence of the deletions was verified by PCR. Strains YJFD17 and YJFD18 were made by co-transformation of wild-type BY4741 and its *ref2::KanMX* derivative respectively with plasmid pJFD10 (containing the *glc7-109* allele, see below) and a disruption cassette containing the *nat1* gene flanked by genomic sequences corresponding to –41/–1 and +1465/+1509, relative to the *GLC7* ATG codon (amplified from plasmid pAG25 with the oligonucleotides OJFD81 and OJFD82). Diverse tests were carried out to ensure that the only Glc7-encoding gene copy corresponded to the plasmid-borne *glc7-109* allele. Strains KT1112 (*GLC7*), KT1935 (*glc7-109*) and KT2210 (*glc7-F256A*) were a gift from Professor K. Tatchell (Department of Biochemistry and Molecular Biology, Louisiana State University Health Sciences Center, Shreveport, LA, U.S.A.) and have been reported previously [24]. Strains SB6 (*YTH1*) and SB7 (*yth1-1*) [36], YWK168 (*SWD2*) and YWK172 (*swd2-3*) [37], as well as W303 (*SSU72*) and YWK186 (*ssu72-2*) [38], were a gift from Dr B. Ditchl (Institute of Molecular Biology, University of Zurich, Zurich, Switzerland). Strains PTA1 (*PTA1*) and *pta1* (*pta1 Δ 1–75*) [39] were a gift from Professor C. Moore (Department of Microbiology, Tufts University, Boston, MA, U.S.A.).

To clone the *glc7-109* allele in the YCplac33 plasmid (centromeric with a *URA3* marker) the Glc7-encoding ORF (open reading frame), flanked by 2068 bp upstream and 148 bp downstream, was amplified by PCR using genomic DNA from strain KT1935 and oligonucleotides Glc7-BamHI.Up and Glc7-PstI.Do, which contain artificial BamHI and PstI restriction sites respectively (see Supplementary Table S1). The amplified DNA fragment was digested by BamHI and PstI and cloned in the same restriction sites of YCplac33 to yield plasmid pJFD10 (YCplac33-*glc7-109*). Plasmid YEp195-GLC7 was constructed using the same strategy except that genomic wild-type DNA was used for the PCR. These plasmids were then isolated and sequenced.

For low-copy, centromeric expression of *REF2*, a 2.28 kbp fragment containing the *REF2* ORF, flanked by 500 bp and 200 bp from its promoter and terminator regions respectively,

was amplified using a specific pair of oligonucleotides containing artificially added BamHI (OJFD027) and SacI (OJFD026) restriction sites (see Supplementary Table S1). The resulting DNA fragment was digested with BamHI and SacI and cloned in the same restriction sites of the pRS415 plasmid (centromeric with a *LEU2* marker) to yield pRS415-*REF2* (pJFD1).

To generate the F374A allele of *REF2* (pJFD2), the pRS415-*REF2* construct was used as a PCR template to change the TTT codon, encoding a phenylalanine residue at position 374, to a GCT codon, encoding an alanine residue. Two overlapping DNA fragments (a and b) were generated. The 1.75 bp fragment (a), spanning from -501 to +1140 (relative to the initiating methionine residue), was obtained using oligonucleotides OJFD029 and M13-20 reverse. The 0.7 bp length fragment (b) comprises from +1101 to +1785 and was amplified with oligonucleotides OJFD063 and M13-20 (see Supplementary Table S1). To allow *in vivo* DNA-recombination, these two fragments were co-transformed in yeast cells together with the linearized pRS415 plasmid digested with BamHI and SacI. Cells carrying the pRS415^{F374A} construct were selected in a medium lacking leucine and the plasmid was recovered and sequenced to ensure the absence of unexpected mutations.

LacZ reporter plasmids used in the present study have been reported previously: *ENAI* reporters were pKC201, containing the entire *ENAI* promoter [40] and pMRK212 and pMRK213, containing the ARR1 and ARR2 regions of this same promoter [17]. pMRK-based constructs were derived from plasmid pSLFΔ-178K [41], which contains a *CYCI* minimal promoter and displays virtually no reporter activity in the absence of a transcriptionally active DNA insert. Plasmid pAMS366 [14] contains four copies of a CDRE from the *FKS2* promoter.

Lithium content and lithium efflux measurements

Lithium content and efflux were measured as reported previously, with minor modifications [42]. For determination of the intracellular lithium cation concentration, cells were grown overnight in liquid YPD medium. When cultures reached an attenuation of 0.5–0.6, cells were collected (centrifugation at 1620 g for 5 min) and diluted (to a D_{600} of 0.2–0.3), in fresh YPD medium containing the appropriate concentration of LiCl. Cells were loaded with lithium for 8 h and then samples were filtered, washed with 20 mM MgCl₂, and treated with acid overnight (0.2 M HCl and 10 mM MgCl₂). Lithium was analysed by atomic absorption spectrophotometry as described previously [43]. Lithium efflux was studied in cells grown overnight as described above. Cells were suspended in fresh medium and loaded with 75 mM LiCl for 2 h. Yeast cells were separated from the culture medium by centrifugation (1620 g for 5 min), washed, and suspended in fresh lithium-free medium. At various time intervals, samples were taken and treated as above for lithium determination.

β-Galactosidase assays

The different strains were transformed with the reporter plasmids pKC201, pMRK212, pMRK213 or pAMS366. Cultures were grown up to saturation in the appropriate drop-out medium, then they were inoculated on YPD (at pH 5.5) until the D_{600} reached 0.6–0.7 and collected by centrifugation (5 min at 750 g). Then cells were resuspended in fresh YPD (pH 5.5) containing the indicated concentrations of LiCl, NaCl or CaCl₂, or in medium adjusted to pH 8.2 in the presence of 50 mM Taps buffer, and incubated for a further 60 min, unless otherwise stated, at the specified temperatures. β-Galactosidase activity was measured

as described previously [17] and results are expressed as Miller Units [44a].

Intracellular calcium monitoring

The determination of intracellular calcium was based on the use of pEV11/AEQ [44] which carries the apoaequorin gene under the control of the *ADHI* promoter. Evaluation of cytoplasmic calcium was carried out essentially as described previously [18,44]. Briefly, DBY746 wild-type and *ref2*-mutant cells (YJFD5) were transformed with plasmid pEVP11/AEQ and grown to a D_{600} of 1.0. Aliquots of 30 μl were incubated in luminometer tubes for 20 min at room temperature (22°C), a one-tenth volume of 592 μM coelenterazine (Sigma–Aldrich) in methanol was then added to each sample and the mixture was incubated further at room temperature for 20 min. Basal luminescence was recorded every 0.1 s for 5 s using a Berthold LB9507 luminometer. The RLU (relative luminescence units) were normalized to the number of cells in each sample.

Vacuolar staining and visualization

Vacuole morphology was assessed basically as described previously [45]. Yeast cultures (5 ml at a D_{600} of 0.8–1.0) were harvested (1620 g for 5 min), washed with YPD, and resuspended in 0.1 ml of fresh YPD. The lipophilic fluorescent dye FM4-64 (Invitrogen) was added at a final concentration of 20 μM and cells were incubated for 15 min at 30°C. The cells were then washed, resuspended in 3 ml of YPD, and incubated for 15–45 min to allow the internalization, by endocytosis, and accumulation of the dye within the vacuole. Cells were visualized with a FITC filter using a Nikon Eclipse E800 fluorescence microscope (at 400×). Digital images were captured with an ORCA-ER 4742-80 camera (Hamamatsu) using the Wasabi software.

RESULTS

Lack of Ref2 causes defects in cation tolerance

The observation that Glc7 point mutations lying in the vicinity of residues relevant for binding diverse regulatory subunits may cause alterations in ion homeostasis [24] prompted us to examine tolerance to NaCl, LiCl, alkaline pH and CaCl₂ in 18 strains carrying a deletion of functionally well-documented regulatory subunits of Glc7. Figure 1 shows a selected panel of conditions. As shown, mutation of most regulatory subunits did not result in significantly altered tolerance to the indicated treatments, with the exception of the *ref2* and *shp1* mutants. However, deletion of *shp1* caused a rather severe growth defect even in the absence of stress, as previously described [46], making it difficult to assess the actual effect of the mutation under the conditions tested. In contrast, lack of Ref2, which only caused a slight growth defect under standard culture conditions, prevented growth in the presence of lithium, sodium and calcium cations, as well as under alkaline conditions. *ref2* cells were also markedly sensitive to caesium ions (results not shown). The intensity of the phenotype for sodium and lithium stress was comparable with that of a *trk1 trk2* strain, which has defective potassium uptake (results not shown). The phenotype was not caused by the inability to adapt to hyperosmotic stress, as (i) growth was not affected by inclusion of 1 M sorbitol or KCl in the medium and (ii) an obvious growth defect was already observed at a lithium concentration as low as 30 mM, which does not represent an osmotic stress condition (results not shown). Increased sensitivity to sodium and lithium cations is often observed in strains with defective potassium uptake (i.e. in *trk1* mutants) [46a]. This prompted us to test the requirements

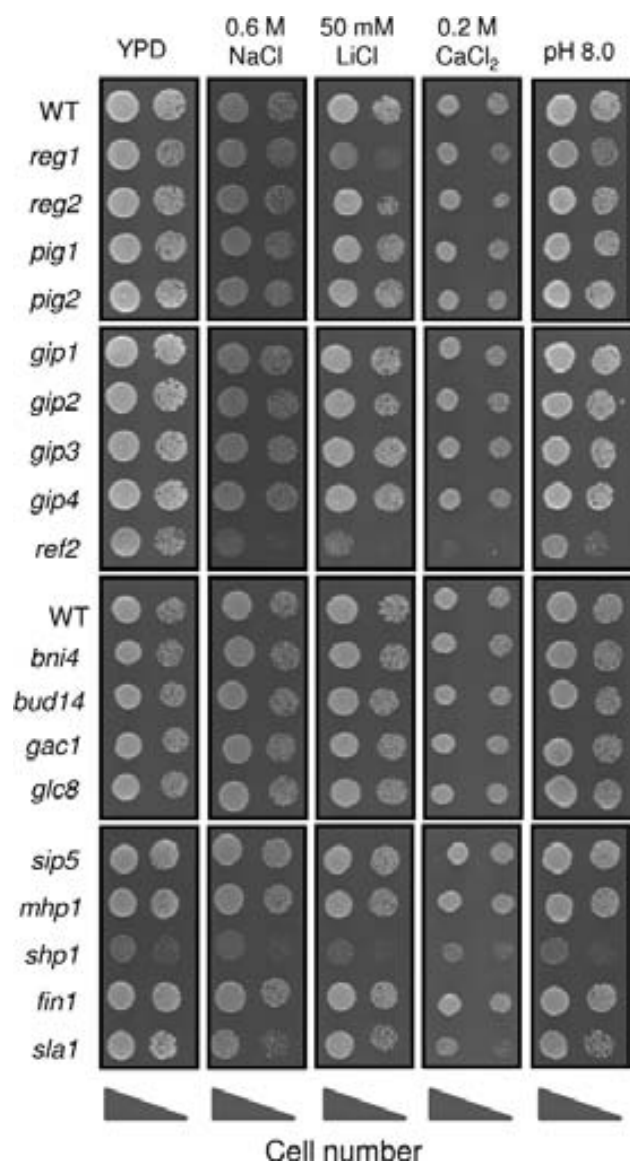


Figure 1 Effect of the mutation of several Glc7-interacting proteins on cation-related phenotypes

Two dilutions (of approx. 3×10^3 and 3×10^2 cells) from cultures of wild-type strain BY4741 (WT) and the indicated isogenic derivatives were grown on YPD plates in the presence of 0.6 M NaCl, 50 mM LiCl, 0.2 M CaCl₂ or at alkaline pH (pH 8.0) for 2 days.

for potassium in the *ref2* mutant, by using a recently developed YNB-based potassium-free medium. As shown in Figure 2, *ref2* cells display a slow-growth phenotype at limiting potassium concentrations (0.5–1.5 mM) that was alleviated by increasing the amount of potassium in the medium. This suggests that *ref2* cells might have a decreased high-affinity potassium uptake, although direct measurement of rubidium influx (an analogue commonly used to assess for potassium uptake capacity [46b]) failed to reveal a significant decrease in rubidium ion uptake (results not shown). In any case, the *ref2* strain showed increased sensitivity to several organic toxic cations, such as hygromycin B, spermine and TMA (tetramethylammonium) (Figure 3A), a phenotype which is commonly observed in strains with altered cation homeostasis [46c].

Ref2 contains a RISSIKFLD sequence (residues 368–376) that closely matches the (R/K)(V/I)X(F/W) Glc7-binding consensus

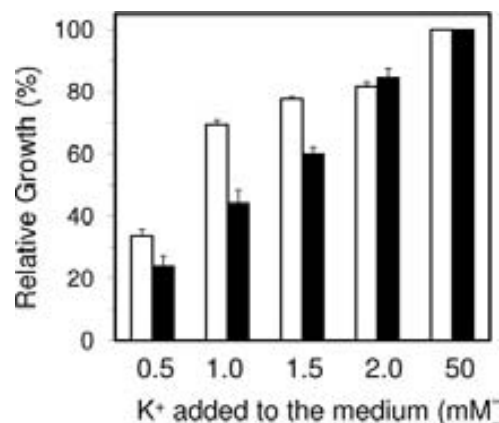


Figure 2 Mutation of *REF2* increases potassium requirements for growth

Cultures of wild-type strain BY4741 (white bars) and its *ref2* derivative (black bars) were inoculated at a D_{600} of 0.004 in Translucent K-free medium, supplemented with the indicated amounts of KCl, and grown for 16 h. Results are represented as a percentage of growth compared with cells incubated with 50 mM KCl and are means \pm S.E.M. for three independent cultures.

sequence. We considered it necessary to test whether or not the salt-related phenotypes, derived from the absence of Ref2, could be explained by its role as a putative Glc7-regulatory subunit. To this end, Phe-374 was replaced with an alanine residue and the mutated version of the gene (including its own promoter) was cloned into a centromeric plasmid. As shown in Figure 3(A), introduction of the wild-type version of *REF2* (pJFD1) in a *ref2* mutant was able to increase tolerance to sodium, lithium and alkaline pH, as well as to diverse toxic organic cations. In contrast, mutation of Phe-374 (pJFD2) resulted in a complete inability to do so. It must be noted that this mutation does not affect Ref2 cellular levels, but it is known to disrupt the interaction with Glc7 [30]. Expression of the mutated form of Ref2 from a high-copy number plasmid, which should lead to overexpression of the protein, was also unable to rescue the *ref2* defects (results not shown). These evidences suggest that blocking the interaction between Ref2 and Glc7 results in loss of the Ref2 function in salt tolerance. A similar effect was observed when the growth deficiency of the *ref2* mutant was tested (Figure 3B). In this case, expression of the F374A-mutated version of *REF2* (pJFD2) even aggravated the growth defect of the strain lacking the chromosomal copy of the gene. We then considered the possibility that the cation-related defects of the *ref2* strain could be attenuated or even suppressed by a surplus of Glc7. However, expression of Glc7 on a multicopy plasmid did not increase the tolerance of a *ref2* strain to LiCl or NaCl (see Supplementary Figure S1A available at <http://www.BiochemJ.org/bj/426/bj4260355add.htm>). In contrast, the same plasmid was able to abolish the salt-sensitive phenotype of specific Glc7 mutants (Supplementary Figure S1B), indicating proper expression of Glc7.

Increased sensitivity to sodium and lithium cations can be the result of increased uptake, decreased efflux, or inability to sequester these toxic cations into intracellular compartments, such as the vacuole. To get an insight into a possible cause for sensitivity in the *ref2* mutant, the intracellular concentration of lithium in cells grown in the presence of 25 or 50 mM LiCl was tested. As shown in Figure 4(A), *ref2* mutants accumulate 60–70% more lithium than the wild-type strain. This suggested that lack of Ref2 might favour lithium entry or make detoxification of the cation more difficult by interfering with the efflux systems. To this end, we tested the ability of *ref2* cells to extrude lithium. As shown in

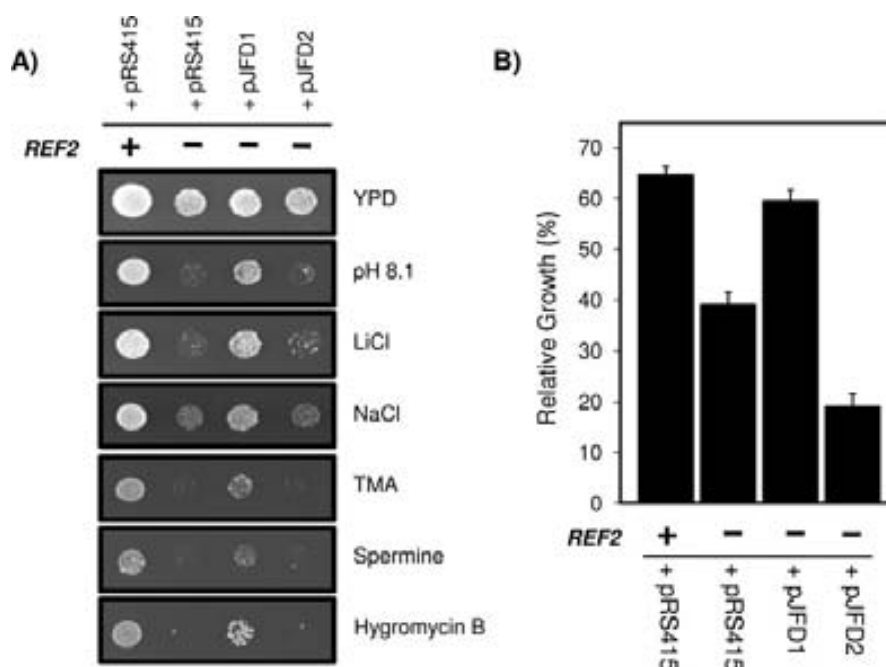


Figure 3 Mutation of Phe-374 within the Glc7-binding consensus sequence abolishes the function of Ref2 in cation tolerance

(A) Wild-type BY4741 (+) and *ref2* strains (-) were transformed with the empty plasmid pRS415 or the same plasmid expressing the wild-type Ref2 protein (pJFD1) or the Ref2^{F374A}-mutated version (pJFD2). Transformants were spotted on to YPD plates, which were adjusted to pH 8.1 or contained LiCl (150 mM), NaCl (1 M), TMA (0.3 M), spermine (0.6 mM) or hygromycin B (20 μ g/ml) as indicated. Growth was monitored after 3 days, except for the LiCl and NaCl conditions when growth was monitored after 6 days. (B) Wild-type (+) and *ref2* (-) strains were transformed with the indicated plasmids and growth was tested at a limiting concentration of external potassium (1 mM). Experimental conditions were as described in Figure 2.

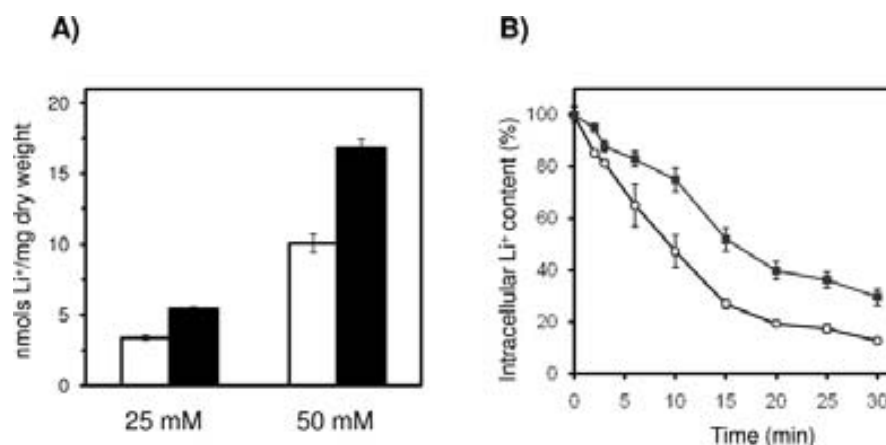


Figure 4 Effects of the *ref2* mutation on intracellular lithium accumulation and efflux

(A) Wild-type BY4741 cells (white bars) and the *ref2* derivative (black bars) were incubated with 25 or 50 mM LiCl as described in the Experimental section and the intracellular content of lithium ions measured. Results are means \pm S.D. for at least six independent determinations. (B) Strains BY4741 (○) and *ref2* (■) were loaded with 75 mM LiCl, samples taken at different times and the efflux of the cation determined as described in the Experimental section. Results are expressed as a percentage of the intracellular lithium content for each strain at the start of the experiment and are means \pm S.D. for at least six independent assays.

Figure 4(B), lithium efflux was markedly impaired in cells lacking Ref2, suggesting that the absence of this Glc7 regulatory subunit interferes with the normal efflux mechanisms.

Mutation of Ref2 affects expression of the *ENA1* ATPase gene under saline and alkaline pH stresses

The Na⁺-ATPase *Ena1* is a major determinant of sodium and lithium tolerance. The expression of the gene is dramatically increased by exposure to high concentrations of sodium or lithium cations or by alkalization of the medium, and many mutations

impairing *ENA1* induction upon stress have been shown to lead to hypersensitivity to these cations. Therefore we considered it necessary to monitor the expression of *ENA1* in *ref2* cells under cation stress conditions. To this end, cells were transformed with plasmid pKC201, which carries the entire *ENA1* promoter fused to the *lacZ* reporter gene. As shown in Figure 5(A), expression driven from the *ENA1* promoter in cells exposed to sodium or lithium cations, as well as to alkaline pH, is drastically reduced in *ref2* cells. Therefore the increased sensitivity of the *ref2* mutant to these stresses could be attributable, at least in part, to a defect in *ENA1* induction.

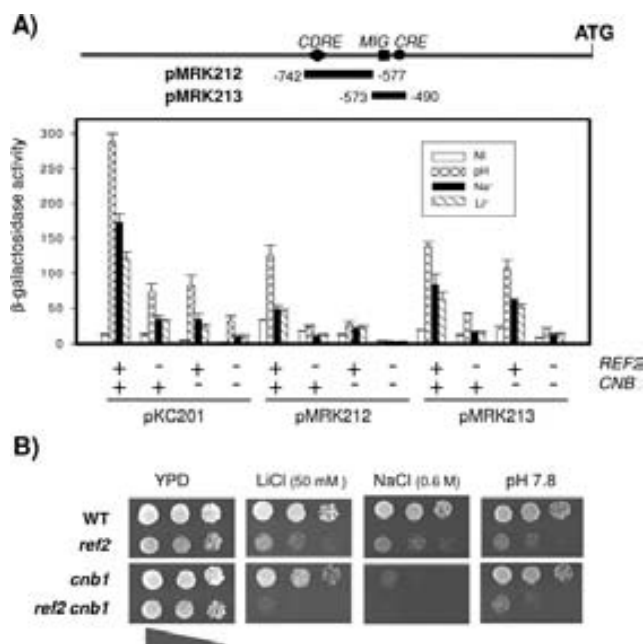


Figure 5 Effects of the *ref2* mutation in wild-type and *cnb1* strains on the *ENA1* promoter activity

(A) The indicated strains were transformed with plasmids pKC201, carrying the entire *ENA1* ATPase gene promoter, or plasmids pMRK212 or pMRK213, which contain specific regions of the *ENA1* promoter, as indicated in the diagram at the top of the panel. MIG, Mig1/2 binding sequence; CRE, cAMP regulatory element. Cells received no treatment (NI), were shifted to pH 8.2 (pH) or were exposed to 0.4 M NaCl (Na) or 0.2 M LiCl (Li) for 1 h. β -Galactosidase activity was measured in permeabilized cells as described in the Experimental section. Results are means \pm S.E.M. for eight or nine independent transformants. (B) Three dilutions of the indicated cultures were spotted on to plates at the conditions shown and growth recorded after 72 h (LiCl and NaCl) or 48 h (alkaline pH).

The expression of *ENA1* under saline or alkaline stress is controlled by a variety of signalling pathways, including activation of calcineurin, which is triggered by a burst of cytosolic calcium. As observed in Figure 5(A), the effect of the *ref2* mutation on *ENA1* expression can be even more severe than that caused by mutation of *CNBI*, encoding the regulatory subunit of calcineurin. Furthermore, the *cnb1* mutation seems additive to *ref2* both with respect to *ENA1* expression (Figure 5A) and to lithium, sodium and alkaline pH tolerances (Figure 5B). Therefore *ref2* phenotypes cannot be exclusively explained by a hypothetical impairment of calcineurin signalling under stress. Most regulatory inputs acting on the *ENA1* promoter target two relatively small regions named ARR1 and ARR2 (see [4] for a review). To gain insight into the effect of the *ref2* mutation, cells were transformed with plasmids pMRK212 and pMRK213. The former contains a region that mostly integrates calcium/calcineurin inputs, whereas the latter is regulated by calcineurin-independent stimuli. As shown in Figure 5(A), deletion of *REF2* decreases expression driven from both promoter regions, suggesting that the mutation has a complex and diverse effect. Analysis of the expression from these constructs further supports an additive effect of the *cnb1* and *ref2* mutations on cation homeostasis.

***ref2* cells display a hyperactivated calcium/calcineurin pathway in the absence of stress and show altered vacuole morphology**

A striking phenotype that can be observed in Figure 1 is that lack of Ref2 results in a substantial sensitivity to calcium cations. It has been reported that hyperactivation of calcineurin results in a calcium-sensitive phenotype, whereas deletion of calcineurin-

encoding genes yields calcium hypertolerance [46d,46e]. We therefore hypothesized that the calcium-sensitive phenotype of *ref2* mutants could be attributed to an unusually high basal calcineurin activity (i.e. in the absence of saline or alkaline pH stress). To test this possibility, we evaluated calcium tolerance in cells lacking both Ref2 and Cnb1, and compared them with the single *ref2* and *cnb1* mutants. As shown in Figure 6(A), the calcium sensitivity conferred by the *ref2* mutation is largely abolished in the absence of Cnb1. This suggests that the *ref2* growth defect in the presence of calcium is caused by hyperactivation of calcineurin and leads to the possibility that calcium levels might be higher than normal in *ref2* cells. This was directly tested by introducing the calcium-reporter plasmid pEV11/AEQ in wild-type and *ref2*-mutant cells. Our measurements indicated that the luminescence observed in *ref2* cells was 141.9 ± 3.7 RLU per 10^6 cells, whereas this parameter was 64.8 ± 3.5 in the wild-type strain, thus confirming the existence of higher free cytosolic calcium levels in the mutant. On the basis of this result, one would expect that expression from a specific calcium/calcineurin-sensitive promoter would be increased in *ref2* cells grown under basal (non-stressing) conditions. To test this conjecture, wild-type and *ref2* strains (as well as their *cnb1* derivatives) were transformed with plasmid pAMS366, which carries a tandem-repeat of four copies of the CDRE from the promoter of the *FKS2* gene. As shown in Figure 6(B), under basal growth conditions, expression from this synthetic promoter is 4–5-fold higher in *ref2* cells than in the wild-type strain. As expected, this effect is abolished in the absence of calcineurin activity (*ref2 cnb1* strain). Remarkably, whereas in the wild-type strain addition of calcium ions to the medium triggers a dramatic, calcineurin-mediated increase in expression, this effect is much less prominent in cells lacking Ref2. This could be explained if the *ref2* mutation somehow interferes with stress-triggered effects mediated by activation of calcineurin. Increased sensitivity to alkaline pH and calcium is a characteristic phenotype of yeast strains with deficient vacuolar function [46f]. Therefore the possibility that *ref2* mutants may display some alteration in this subcellular compartment was considered. As shown in Figure 6(C), incubation of wild-type and *ref2* cells with the lipophilic fluorescent dye FM4-64, which stains the vacuole membrane, reveals that vacuolar structure is dramatically altered in the *ref2* mutant, with a punctuated fluorescent pattern and lack of discernible vacuolar structure. Because of the similarity between the saline phenotypes of the *ref2* deletion and the *glc7-109* allele, we considered it interesting to evaluate vacuolar morphology in the latter. As shown in Figure 6(C), FM4-64 staining of strain YJFD17, which carries a centromeric plasmid-borne *glc7-109* allele as the only source of *GLC7* function, reveals that this strain has vacuoles with essentially wild-type morphology (in a similar manner to the original cation-sensitive strain KT1935; results not shown). Interestingly, combination of the *ref2* deletion and the *glc7-109* mutation results in cells with a *ref2*-type phenotype, i.e. altered vacuoles. The disruption of *REF2* in the KT1935 background was repeatedly attempted without success. This is probably due to the close genetic relationship of this strain with the W303 genetic background (K. Tatchell, personal communication), in which the *REF2* deletion was reported to be lethal [47].

Mutants in components of the APT complex do not share the cation-related phenotypes of the *ref2* strain

Given the Ref2 function described previously, as a component of the APT complex, it was reasonable to consider whether the striking cation-related phenotypes of the *ref2* strain could be

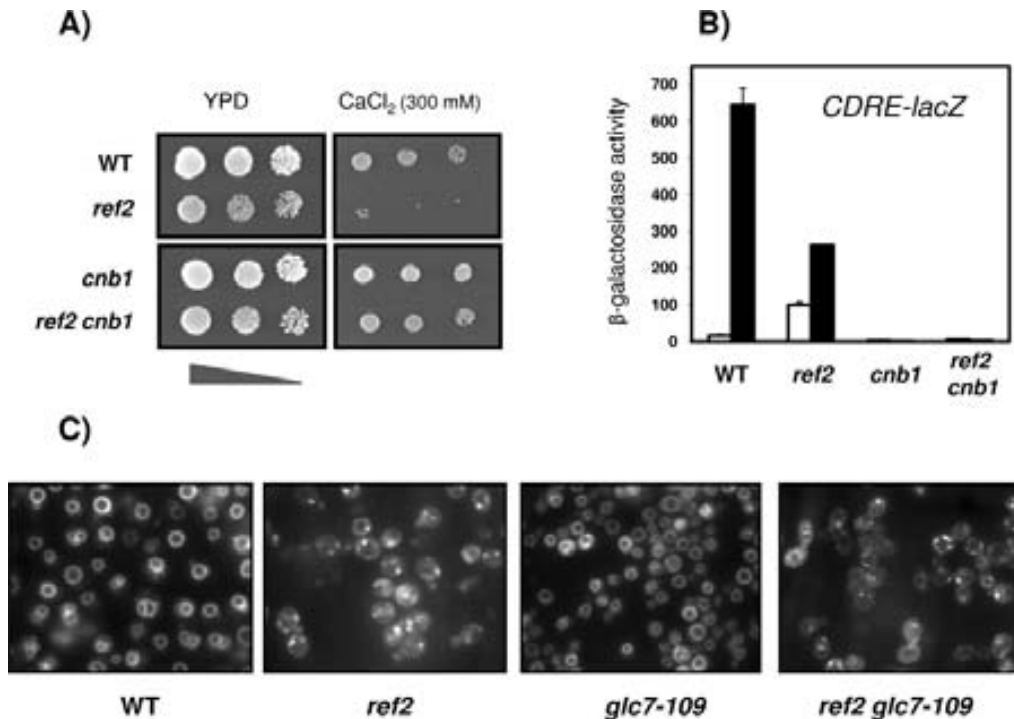


Figure 6 Lack of *REF2* results in altered calcium homeostasis and vacuolar morphology

(A) The indicated strains were grown in the presence or absence of calcium cations (300 mM CaCl_2) and growth was monitored after 72 h. (B) Yeast strains were transformed with plasmid pAMS366, which contains a tandem-repeat of four CDREs fused to a *lacZ* reporter (*CDRE-lacZ*), and incubated for 1 h in the absence (white bars) or presence (black bars) of 0.2 M CaCl_2 . β -Galactosidase activity was measured as described in the Experimental section. Results are means \pm S.E.M. for six independent transformants. (C) Vacuolar staining of wild-type BY4741 (WT), *ref2::kanMX* (*ref2*), YJFD17 (*glc7-109*) and YJFD18 (*ref2 glc7-109*) strains with the fluorescent dye FM4-64 was performed as described in the Experimental section for 30 min and monitored by fluorescence microscopy.

attributed to the role of the protein in this complex. We reasoned that, if this was the case, mutations in other components of the complex would yield phenotypes reminiscent of those of the *ref2* strain. As many members of the APT complex are essential (including Pta1), we had to resort in most cases to temperature-sensitive mutants cultured at sublethal temperatures. Figure 7(A) shows that deletion of *SYC1*, encoding a non-essential member of the complex, does not alter cell growth under conditions that clearly affect proliferation of *ref2* mutants. The *yth1-1* mutant displayed a slight sensitivity to LiCl, but was indistinguishable from the wild-type in its sensitivity to NaCl and alkaline pH. The *swd2-3* and *ssu72-2* strains did not show any sensitivity to LiCl or NaCl and only a marginal sensitivity to high pH. None of these strains displayed sensitivity to high calcium levels in the medium. Similarly, a temperature-sensitive strain lacking the N-terminal region of Pta1 (strain *pta1* $\Delta 1-75$) exhibited a near wild-type tolerance to cations or alkaline pH even at 37 °C. None of the tested APT complex mutants were sensitive to low glucose or non-fermentable carbon sources (Supplementary Figure S2 available at <http://www.BiochemJ.org/bj/426/bj4260355add.htm>). We also observed sensitivity to formamide in the *yth1-1* strain when grown at 30 °C as reported previously [36]. Interestingly, we observed a similar phenotype in the *swd2-3* mutant at 30 °C and the *ref2* or *pta1* $\Delta 1-75$ strains at 37 °C, clearly showing that under these conditions the function of the APT complex is compromised. The almost complete lack of overlap between specific *ref2* phenotypes and those of the other mutants in components of the APT complex is exemplified in the phenotypic array shown in Figure 7(B).

We also examined the basal expression level of *ENA1* in these strains and the ability of the *ENA1* promoter to be activated by salt

stress. As shown in Figure 8, changes in expression levels induced by exposure to LiCl or NaCl were smaller in the *swd2-3* strain. However, the expression observed in the *sys1*, *ssu72-2* or *pta1-1-75* derivatives was virtually identical with that of their respective wild-type strains. Taken together, these results demonstrate that the mutation of diverse components of the APT complex does not mimic the cation-related phenotypes of the *ref2* strain.

DISCUSSION

In the present study we have screened for defects in cation tolerance of 18 strains lacking specific regulatory subunits of the yeast type 1 protein phosphatase Glc7. Among them, only the *ref2* mutant presented phenotypes which were undoubtedly associated with altered cation homeostasis, such as decreased tolerance to lithium and sodium, sensitivity to alkaline pH and decreased growth at limiting external potassium concentrations. We also observed that *ref2* cells were sensitive to diverse toxic organic cations that interfere with very different cellular functions. It is generally accepted that these compounds are 'driven' to enter the cell by the electrochemical gradient generated by the Pma1 plasma membrane proton ATPase and it has been observed that many mutations that affect sodium and/or potassium homeostasis result in an altered electrochemical gradient (e.g. *trk1*, *ppz1*, *hal4,5*) [47a]. Therefore the observation that *ref2* cells are sensitive to hygromycin B, spermine and TMA is consistent with the notion that Ref2 is a relevant component of cation homeostasis. Our results suggest that the decreased tolerance to alkaline cations in the *ref2* mutant could be due, at least in part, to the inability to fully induce expression of the *ENA1* Na^+ -ATPase gene, which is a major determinant in saline tolerance. As lack

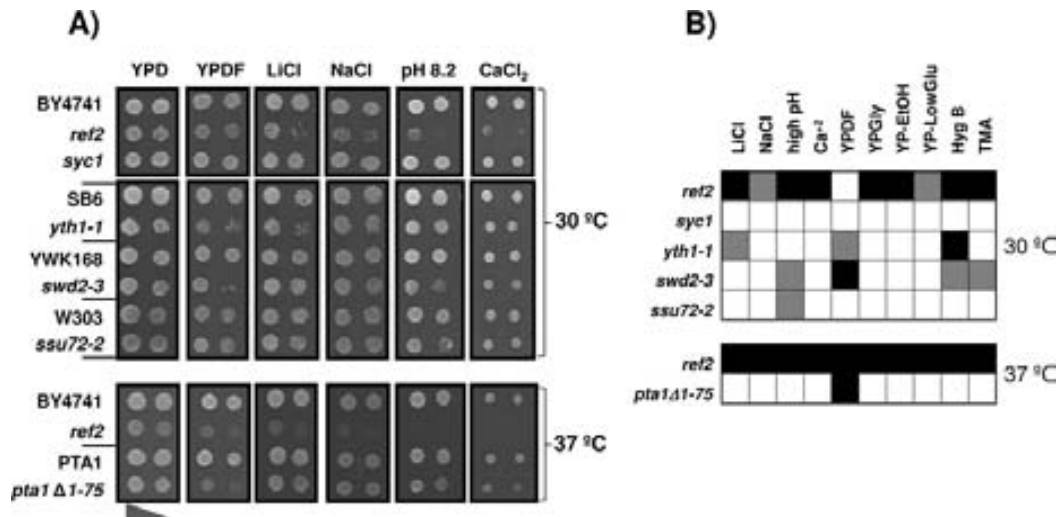


Figure 7 Comparison of *ref2* phenotypes with those of diverse APT-related mutants

(A) Cultures (approx. 3×10^3 and 3×10^2 cells) of the strains indicated to the left of the panel were spotted on to plates and grown at the temperatures indicated to the right of the panel for 3 days. Conditions used were: YPDF, YPD plus 3% formamide; LiCl, 100 mM LiCl (30°C) or 150 mM LiCl (37°C); NaCl, 800 mM NaCl; pH 8.2; CaCl_2 , 200 mM CaCl_2 . (B) Phenotypic array comparing multiple *ref2* phenotypes with those of other APT-related mutants. Growth of each mutant was compared with that of the corresponding wild-type strain grown under the same set of conditions. Black squares denote strong sensitivity, grey squares indicate a mild phenotype and white squares correspond with wild-type behaviour. Conditions tested to construct the array were: LiCl, 50–200 mM LiCl; NaCl, 0.4–1.2 M NaCl; high pH, pH 8.0–8.3; Ca^{2+} , 100–300 mM CaCl_2 ; YPDF, YPD plus 3% formamide; YPGly, YP plus 2% glycerol; YP-EtOH, YP plus 2% ethanol; YP-LowGlu, YP plus 0.05% glucose; Hyg B, 20–60 $\mu\text{g/ml}$ hygromycin B; TMA, 0.2–0.6 M TMA.

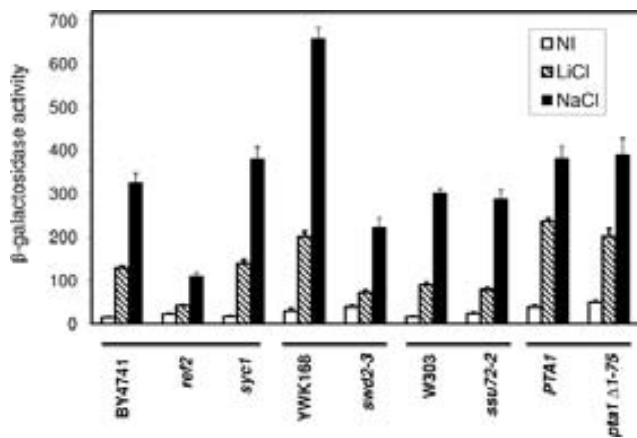


Figure 8 Expression of *ENA1* under saline stress in diverse APT-related mutants

The indicated mutants and their corresponding wild-type strains (the bars show isogenic strains) were transformed with plasmid pKC201, carrying the entire *ENA1* ATPase gene promoter. Stress conditions were as in described in Figure 5, except that the growth temperature was 30°C for all strains but *PTA1* and *pta1Δ1-75*, which were grown at 37°C. Results are means \pm S.E.M. for 12 independent transformants.

of Ref2 blocked the response of *ENA1* to diverse stresses, which are mediated through a variety of signalling pathways [12,48], the effect of Ref2 on *ENA1* expression is possibly pleiotropic and may involve multiple targets.

Ref2 and Glc7 are components of the APT complex and they are required for efficient 3' processing of mRNAs and transcription termination of certain snoRNA genes [25,29,30,47]. Therefore it would be reasonable to speculate that the cation-related phenotypes of the *ref2* mutant could be caused by malfunction of this complex, which is itself a component of the holo-CPF. However, our results show that deletion or temperature-sensitive mutations of diverse components of the APT complex, tested

under conditions that impair their function in the complex [37–39], do not consistently mimic the growth defects or impaired *ENA1* expression of the *ref2* strain (Figures 7B and 8). The same situation is observed for the conditional mutation of *YTH1*, whose product participates in polyadenylation factor I, a different subcomplex of the CPF [36]. Furthermore, we also observe that, whereas the *ref2* strain fails to grow on non-fermentable carbon sources and grows poorly on low-glucose medium, none of the APT-related mutations tested display such phenotypes (Figure 7B and Supplementary Figure S2), thus providing an additional example of disparate phenotypes. On the other hand, Ref2 function has been implicated in COMPASS/Set1 complex function via the Swd2 protein [29]. The function of Swd2 in this complex has been shown to be independent from its role in the APT complex [37]. The COMPASS/Set1 complex is required for histone H3 methylation at Lys-4, which is a fingerprint of actively transcribed genes [49]. Therefore defective COMPASS function could be invoked to explain the effect of the *ref2* mutation on *ENA1* expression. However, this seems to be unlikely as (i) a survey of the literature [49a] (and our own results, not shown) indicate that mutants in the non-essential components of the complex do not display salt-related phenotypes nor are they sensitive to organic toxic cations; (ii) no evidence for a role of Glc7 on COMPASS function has been reported so far; and (iii) deletion of *REF2* does not perturb histone H3 methylation at Lys-4 [50].

Our observation that *ref2* cells are calcium-sensitive is consistent with the identification of *REF2* in a screen for mutations sharing multiple *pmr1* phenotypes [51]. *PMR1* encodes an ATPase that sequesters calcium and manganese ions in the Golgi/secretory pathway, which is pivotal to maintaining proper cytosolic concentrations of these ions. In addition, in a similar manner to *vma* and *pmr1* mutants [51], the *ref2* mutant displays strong sensitivity to the cell-wall perturbing agent Calcofluor White (results not shown). Remarkably, we observe that in *ref2* cells grown in the absence of any source of stress there is an increased cytosolic calcium level and higher than normal expression from

a synthetic calcium/calcineurin-regulated promoter (Figure 6B). This suggests that basal calcineurin activity is abnormally high in *ref2* mutants. Further activation of calcineurin, by exposure to high concentrations of extracellular calcium, would therefore explain the hypersensitive phenotype of *ref2* cells to this cation, as it is known that excessive calcineurin activity is detrimental to the cell [52,53]. The observation that deletion of *CNBI*, which blocks calcineurin signalling, relieves calcium toxicity provides further support to this hypothesis. We also show in the present study that *ref2* cells displayed altered vacuolar morphology, which is reminiscent of the class B/C *vps* mutants [45,54,55]. As the vacuole is the most important calcium store in yeast [56], it is reasonable to assume that the calcium-related phenotypes displayed by *ref2* cells could be derived from their incapacity for normal vacuole assembly. It must be noted, however, that whereas lack of Ref2 increases basal calcineurin activity, the mutation also interferes with stress signals that transiently activate the phosphatase, as deduced from the lower short-term response of the calcineurin-regulatable promoter (Figure 6B).

We show in the present study that a version of Ref2 that cannot interact with Glc7 [30] is unable to rescue the saline phenotypes of the *ref2* strain. Therefore it is reasonable to consider that the perturbed cation homeostasis observed in a *ref2* strain is due to a deregulation of Glc7 activity. Altered cation homeostasis has been described in the past for specific mutations of Glc7, such as the *glc7-109* allele, which carries an R260A mutation near the hydrophobic channel that is likely to be responsible for the interaction with the binding motif present in Ref2 [24]. Remarkably, the *glc7-109* mutant displays a subset of phenotypes that closely resembles those reported in the present study for the *ref2* disruption, such as enhanced sensitivity to sodium, lithium, alkaline pH and organic toxic cations [24]. We have also observed that deletion of *REF2* in a strain carrying the *glc7-109* allele (YJFD18) does not result in enhanced sensitivity to NaCl or alkaline pH (results not shown). In addition, the saline-stress-related phenotypes of the *glc7-109* allele are additive with those caused by disruption of calcineurin activity, a circumstance also observed for the *ref2* strain (Figure 5B). All this evidence suggests that the cation-related phenotypes of the *glc7-109* allele could be caused, at least in part, by its incapacity to interact with Ref2. It must be stressed, however, that the *ref2* and *glc7-109* phenotypes are not identical. For instance, the *glc7-109* strain hyperaccumulates glycogen [24], whereas the *ref2* mutant does not (results not shown). More importantly, the *glc7-109* strain does not display altered calcium levels and increased calcium sensitivity [24], or altered vacuolar morphology (Figure 6C). Therefore it could be that the R260A mutation in *glc7-109* may affect the interaction of the phosphatase catalytic subunit with diverse regulatory subunits, one of these being Ref2. The relevance of the role of Ref2 is highlighted by the observation that the salt-related defects of *ref2* cells cannot be overridden by simply overexpressing Glc7.

In conclusion, the results of the present study demonstrate that the role of Ref2 on cation tolerance is not attributable to its function in regulating Glc7 in the CPF complex but, instead, it suggests that Ref2 must direct Glc7 to alternative target(s). This implies that Ref2 may have multiple cellular functions. Although remarkable, this is not fully surprising; a similar scenario has been reported for the Gac1 regulatory subunit, which functions as a molecular scaffold to tether Glc7 to Gsy2 (encoding glycogen synthase), thus controlling glycogen accumulation [24] but also binds the transcription factor Hsf1, and thus controls the transcription of certain heat-shock responsive genes, such as *CUP1* [57]. Therefore Ref2 would represent a novel example of multifunctional Glc7 regulatory subunit.

AUTHOR CONTRIBUTION

Jofre Ferrer-Dalmau performed the majority of the experiments. Asier González and Maria Platara performed the *lacZ*-measurements. Lina Barreto measured the growth of diverse strains at limiting external potassium. Clara Navarrete, José Martínez and José Ramos measured lithium content and efflux. Joaquín Ariño and Antonio Casamayor designed the experiments and wrote the paper.

ACKNOWLEDGEMENTS

We thank H. Sychrovà and G. Wiesenberger for help in developing and testing the YNB-based, K-free medium. We also thank C. Moore, B. Dichtl, K. Tatchell and M. Marquina for provision of strains and plasmids. The excellent technical assistance of our colleagues Anna Vilalta and Montserrat Robledo at the Universitat Autònoma de Barcelona is acknowledged.

FUNDING

This work was supported by the Ministry of Science and Innovation, Spain [grant numbers BFU2008-04188-C03-01, GEN2006-27748-C2-1-E/SYS (to J.A.), BFU2007-60342 (to A.C.), BFU2008-04188-C03-03, GEN2006-27748-C2-2-E/SYS (to J.R.)]. J.A. is the recipient of a Generalitat de Catalunya "Ajut de Suport a les Activitats dels Grups de Recerca" award [grant number 2009SGR-10911].

REFERENCES

- Serrano, R. (1996) Salt tolerance in plants and microorganisms: toxicity targets and defense responses. *Int. Rev. Cytol.* **165**, 1–52
- Prior, C., Potier, S., Souciet, J. L. and Sychrova, H. (1996) Characterization of the NHA1 gene encoding a Na⁺/H⁺-antiporter of the yeast *Saccharomyces cerevisiae*. *FEBS Lett.* **387**, 89–93
- Banuelos, M. A., Sychrova, H., Bleykasten-Grosshans, C., Souciet, J. L. and Potier, S. (1998) The Nha1 antiporter of *Saccharomyces cerevisiae* mediates sodium and potassium efflux. *Microbiology* **144**, 2749–2758
- Ruiz, A. and Arino, J. (2007) Function and regulation of the *Saccharomyces cerevisiae* ENA sodium ATPase system. *Eukaryotic Cell* **6**, 2175–2183
- Haro, R., Garcíadeblas, B. and Rodríguez-Navarro, A. (1991) A novel P-type ATPase from yeast involved in sodium transport. *FEBS Lett.* **291**, 189–191
- Garcíadeblas, B., Rubio, F., Quintero, F. J., Banuelos, M. A., Haro, R. and Rodríguez-Navarro, A. (1993) Differential expression of two genes encoding isoforms of the ATPase involved in sodium efflux in *Saccharomyces cerevisiae*. *Mol. Gen. Genet.* **236**, 363–368
- Martínez, R., Latreille, M. T. and Mirande, M. (1991) A PMR2 tandem repeat with a modified C-terminus is located downstream from the KRS1 gene encoding lysyl-tRNA synthetase in *Saccharomyces cerevisiae*. *Mol. Gen. Genet.* **227**, 149–154
- Posas, F., Camps, M. and Arino, J. (1995) The PPZ protein phosphatases are important determinants of salt tolerance in yeast cells. *J. Biol. Chem.* **270**, 13036–13041
- Wieland, J., Nitsche, A. M., Strayle, J., Steiner, H. and Rudolph, H. K. (1995) The PMR2 gene cluster encodes functionally distinct isoforms of a putative Na⁺ pump in the yeast plasma membrane. *EMBO J.* **14**, 3870–3882
- Rodríguez-Navarro, A., Quintero, F. J. and Garcíadeblas, B. (1994) Na⁺-ATPases and Na⁺/H⁺ antiporters in fungi. *Biochim. Biophys. Acta* **1187**, 203–205
- Mendoza, I., Rubio, F., Rodríguez-Navarro, A. and Pardo, J. M. (1994) The protein phosphatase calcineurin is essential for NaCl tolerance of *Saccharomyces cerevisiae*. *J. Biol. Chem.* **269**, 8792–8796
- Marquez, J. A. and Serrano, R. (1996) Multiple transduction pathways regulate the sodium-extrusion gene PMR2/ENA1 during salt stress in yeast. *FEBS Lett.* **382**, 89–92
- Matheos, D. P., Kingsbury, T. J., Ahsan, U. S. and Cunningham, K. W. (1997) Tcn1p/Crz1p, a calcineurin-dependent transcription factor that differentially regulates gene expression in *Saccharomyces cerevisiae*. *Genes Dev.* **11**, 3445–3458
- Stathopoulos, A. M. and Cyert, M. S. (1997) Calcineurin acts through the CRZ1/TCN1-encoded transcription factor to regulate gene expression in yeast. *Genes Dev.* **11**, 3432–3444
- Mendizabal, I., Rios, G., Mulet, J. M., Serrano, R. and de Larrinoa, I. F. (1998) Yeast putative transcription factors involved in salt tolerance. *FEBS Lett.* **425**, 323–328
- Mendizabal, I., Pascual-Ahuir, A., Serrano, R. and de Larrinoa, I. F. (2001) Promoter sequences regulated by the calcineurin-activated transcription factor Crz1 in the yeast ENA1 gene. *Mol. Genet. Genomics* **265**, 801–811
- Serrano, R., Ruiz, A., Bernal, D., Chambers, J. R. and Arino, J. (2002) The transcriptional response to alkaline pH in *Saccharomyces cerevisiae*: evidence for calcium-mediated signalling. *Mol. Microbiol.* **46**, 1319–1333

- 18 Viladevall, L., Serrano, R., Ruiz, A., Domenech, G., Giraldo, J., Barcelo, A. and Arino, J. (2004) Characterization of the calcium-mediated response to alkaline stress in *Saccharomyces cerevisiae*. *J. Biol. Chem.* **279**, 43614–43624
- 19 Ruiz, A., Serrano, R. and Arino, J. (2008) Direct regulation of genes involved in glucose utilization by the calcium/calcieneurin pathway. *J. Biol. Chem.* **283**, 13923–13933
- 20 Feng, Z. H., Wilson, S. E., Peng, Z. Y., Schlender, K. K., Reimann, E. M. and Trumbly, R. J. (1991) The yeast GLC7 gene required for glycogen accumulation encodes a type 1 protein phosphatase. *J. Biol. Chem.* **266**, 23796–23801
- 21 Clotet, J., Posas, F., Casamayor, A., Schaaff-Gerstenschlager, I. and Arino, J. (1991) The gene DIS2S1 is essential in *Saccharomyces cerevisiae* and is involved in glycogen phosphorylase activation. *Curr. Genet.* **19**, 339–342
- 22 Zhao, S. and Lee, E. Y. (1997) A protein phosphatase-1-binding motif identified by the panning of a random peptide display library. *J. Biol. Chem.* **272**, 28368–28372
- 23 Egluff, M. P., Johnson, D. F., Moorhead, G., Cohen, P. T., Cohen, P. and Barford, D. (1997) Structural basis for the recognition of regulatory subunits by the catalytic subunit of protein phosphatase 1. *EMBO J.* **16**, 1876–1887
- 24 Williams-Hart, T., Wu, X. and Tatchell, K. (2002) Protein phosphatase type 1 regulates ion homeostasis in *Saccharomyces cerevisiae*. *Genetics* **160**, 1423–1437
- 25 Rusznak, R., Nehrke, K. W. and Platt, T. (1995) REF2 encodes an RNA-binding protein directly involved in yeast mRNA 3'-end formation. *Mol. Cell. Biol.* **15**, 1689–1697
- 26 Uetz, P., Giot, L., Cagney, G., Mansfield, T. A., Judson, R. S., Knight, J. R., Lockshon, D., Narayan, V., Srinivasan, M., Pochart, P. et al. (2000) A comprehensive analysis of protein-protein interactions in *Saccharomyces cerevisiae*. *Nature* **403**, 623–627
- 27 Walsh, E. P., Lamont, D. J., Beattie, K. A. and Stark, M. J. (2002) Novel interactions of *Saccharomyces cerevisiae* type 1 protein phosphatase identified by single-step affinity purification and mass spectrometry. *Biochemistry* **41**, 2409–2420
- 28 Gavin, A. C., Bosche, M., Krause, R., Grandi, P., Marzioch, M., Bauer, A., Schultz, J., Rick, J. M., Michon, A. M., Cruciat, C. M. et al. (2002) Functional organization of the yeast proteome by systematic analysis of protein complexes. *Nature* **415**, 141–147
- 29 Nedea, E., He, X., Kim, M., Pootoolal, J., Zhong, G., Canadien, V., Hughes, T., Buratowski, S., Moore, C. L. and Greenblatt, J. (2003) Organization and function of APT, a subcomplex of the yeast cleavage and polyadenylation factor involved in the formation of mRNA and small nucleolar RNA 3'-ends. *J. Biol. Chem.* **278**, 33000–33010
- 30 Nedea, E., Nalbant, D., Xia, D., Theoharis, N. T., Suter, B., Richardson, C. J., Tatchell, K., Kislinger, T., Greenblatt, J. F. and Nagy, P. L. (2008) The Glc7 phosphatase subunit of the cleavage and polyadenylation factor is essential for transcription termination on snoRNA genes. *Mol. Cell* **29**, 577–587
- 31 Sambrook, J. and Russell, D. W. (2001) *Molecular Cloning: A Laboratory Manual*, Cold Spring Harbor Laboratory Press, Cold Spring Harbor, NY
- 32 Gietz, R. D. and Woods, R. A. (2002) Transformation of yeast by lithium acetate/single-stranded carrier DNA/polyethylene glycol method. *Methods Enzymol.* **350**, 87–96
- 33 Calero, F., Gomez, N., Arino, J. and Ramos, J. (2000) Trk1 and Trk2 define the major K⁺ transport system in fission yeast. *J. Bacteriol.* **182**, 394–399
- 34 Winzler, E. A., Shoemaker, D. D., Astromoff, A., Liang, H., Anderson, K., Andre, B., Bangham, R., Benito, R., Boeke, J. D., Bussey, H. et al. (1999) Functional characterization of the *S. cerevisiae* genome by gene deletion and parallel analysis. *Science* **285**, 901–906
- 35 Goldstein, A. L. and McCusker, J. H. (1999) Three new dominant drug resistance cassettes for gene disruption in *Saccharomyces cerevisiae*. *Yeast* **15**, 1541–1553
- 36 Barabino, S. M., Hubner, W., Jenny, A., Minvielle-Sebastia, L. and Keller, W. (1997) The 30-kD subunit of mammalian cleavage and polyadenylation specificity factor and its yeast homolog are RNA-binding zinc finger proteins. *Genes Dev.* **11**, 1703–1716
- 37 Dichtl, B., Aasland, R. and Keller, W. (2004) Functions for *S. cerevisiae* Swd2p in 3' end formation of specific mRNAs and snoRNAs and global histone 3 lysine 4 methylation. *RNA* **10**, 965–977
- 38 Dichtl, B., Blank, D., Ohnacker, M., Friedlein, A., Roeder, D., Langen, H. and Keller, W. (2002) A role for SSU72 in balancing RNA polymerase II transcription elongation and termination. *Mol. Cell* **10**, 1139–1150
- 39 Ghazy, M. A., He, X., Singh, B. N., Hampsey, M. and Moore, C. (2009) The essential N terminus of the Pta1 scaffold protein is required for snoRNA transcription termination and Ssu72 function but is dispensable for pre-mRNA 3'-end processing. *Mol. Cell. Biol.* **29**, 2296–2307
- 40 Cunningham, K. W. and Fink, G. R. (1996) Calcineurin inhibits VCX1-dependent H⁺/Ca²⁺ exchange and induces Ca²⁺ ATPases in *Saccharomyces cerevisiae*. *Mol. Cell. Biol.* **16**, 2226–2237
- 41 Idrissi, F. Z., Fernandez-Larrea, J. B. and Pina, B. (1998) Structural and functional heterogeneity of Rap1p complexes with telomeric and UASprg-like DNA sequences. *J. Mol. Biol.* **284**, 925–935
- 42 Ruiz, A., González, A., García-Salcedo, R., Ramos, J. and Arino, J. (2006) Role of protein phosphatases 2C on tolerance to lithium toxicity in the yeast *Saccharomyces cerevisiae*. *Mol. Microbiol.* **62**, 263–277
- 43 Gomez, M. J., Luyten, K. and Ramos, J. (1996) The capacity to transport potassium influences sodium tolerance in *Saccharomyces cerevisiae*. *FEMS Microbiol. Lett.* **135**, 157–160
- 44 Batiza, A. F., Schulz, T. and Masson, P. H. (1996) Yeast respond to hypotonic shock with a calcium pulse. *J. Biol. Chem.* **271**, 23357–23362
- 44a Miller, J. H. (1972) *Experiments in Molecular Genetics*, pp. 352–355, Cold Spring Harbor Laboratory Press, Cold Spring Harbor
- 45 Vida, T. A. and Emr, S. D. (1995) A new vital stain for visualizing vacuolar membrane dynamics and endocytosis in yeast. *J. Cell Biol.* **128**, 779–792
- 46 Zhang, S., Guha, S. and Volkert, F. C. (1995) The *Saccharomyces* SHP1 gene, which encodes a regulator of phosphoprotein phosphatase 1 with differential effects on glycogen metabolism, meiotic differentiation, and mitotic cell cycle progression. *Mol. Cell. Biol.* **15**, 2037–2050
- 46a Gómez, M. J., Luyten, K. and Ramos, J. (1996) The capacity to transport potassium influences sodium tolerance in *Saccharomyces cerevisiae*. *FEMS Microbiol. Lett.* **135**, 157–160
- 46b Rodríguez-Navarro, A. (2000) Potassium transport in fungi and plants, *Biochim Biophys Acta.* 1469:1–30.
- 46c Yenush, L., Mulet, J. M., Ariño, J. and Serrano, R. (2002) The Ppz protein phosphatases are key regulators of K⁺ and pH homeostasis: implications for salt tolerance, cell wall integrity and cell cycle progression. *EMBO J.* **21**, 920–929
- 46d Cunningham, K. W. and Fink, G. R. (1994) Calcineurin-dependent growth control in *Saccharomyces cerevisiae* mutants lacking PMC1, a homolog of plasma membrane Ca²⁺ ATPases. *J. Cell Biol.* **124**, 351–363
- 46e González, A., Ruiz, A., Serrano, R., Ariño, J. and Casamayor, A. (2006) Transcriptional profiling of the protein phosphatase 2C family in yeast provides insights into the unique functional roles of Ptc1. *J. Biol. Chem.* **281**, 35057–35069
- 46f Kane, P. M. (2006) The where, when, and how of organelle acidification by the yeast vacuolar H⁺-ATPase. *Microbiol. Mol. Biol. Rev.* **70**, 177–191
- 47 Dheur, S., Voile, T. A., Voisin-Hakil, F., Minet, M., Schmitter, J. M., Lacroute, F., Wyers, F. and Minvielle-Sebastia, L. (2003) Pti1p and Ref2p found in association with the mRNA 3' end formation complex direct snoRNA maturation. *EMBO J.* **22**, 2831–2840
- 47a Arino, J., Ramos, J. and Sychrova, H. (2010) Alkali-metal-cation transport and homeostasis in yeasts. *Microbiol. Mol. Biol. Rev.*, in the press
- 48 Platara, M., Ruiz, A., Serrano, R., Palomino, A., Moreno, F. and Arino, J. (2006) The transcriptional response of the yeast Na⁺-ATPase ENA1 gene to alkaline stress involves three main signaling pathways. *J. Biol. Chem.* **281**, 36632–36642
- 49 Shilatifard, A. (2008) Molecular implementation and physiological roles for histone H3 lysine 4 (H3K4) methylation. *Curr. Opin. Cell Biol.* **20**, 341–348
- 49a Giaefer, G., Chu, A. M., Ni, L., Connelly, C., Riles, L., Véronneau, S., Dow, S., Lucau-Danila, A., Anderson, K., André, B. et al. (2002) Functional profiling of the *Saccharomyces cerevisiae* genome. *Nature* **418**, 387–391
- 50 Cheng, H., He, X. and Moore, C. (2004) The essential WD repeat protein Swd2 has dual functions in RNA polymerase II transcription termination and lysine 4 methylation of histone H3. *Mol. Cell. Biol.* **24**, 2932–2943
- 51 Yadav, J., Muend, S., Zhang, Y. and Rao, R. (2007) A phenomics approach in yeast links proton and calcium pump function in the Golgi. *Mol. Biol. Cell* **18**, 1480–1489
- 52 Cunningham, K. W. and Fink, G. R. (1994) Calcineurin-dependent growth control in *Saccharomyces cerevisiae* mutants lacking PMC1, a homolog of plasma membrane Ca²⁺ ATPases. *J. Cell Biol.* **124**, 351–363
- 53 Mendoza, I., Quintero, F. J., Bressan, R. A., Hasegawa, P. M. and Pardo, J. M. (1996) Activated calcineurin confers high tolerance to ion stress and alters the budding pattern and cell morphology of yeast cells. *J. Biol. Chem.* **271**, 23061–23067
- 54 Banta, L. M., Robinson, J. S., Klionsky, D. J. and Emr, S. D. (1988) Organelle assembly in yeast: characterization of yeast mutants defective in vacuolar biogenesis and protein sorting. *J. Cell Biol.* **107**, 1369–1383
- 55 Bonangelino, C. J., Chavez, E. M. and Bonifacio, J. S. (2002) Genomic screen for vacuolar protein sorting genes in *Saccharomyces cerevisiae*. *Mol. Biol. Cell* **13**, 2486–2501
- 56 Halachmi, D. and Eilam, Y. (1989) Cytosolic and vacuolar Ca²⁺ concentrations in yeast cells measured with the Ca²⁺-sensitive fluorescence dye indo-1. *FEBS Lett.* **256**, 55–61
- 57 Lin, J. T. and Lis, J. T. (1999) Glycogen synthase phosphatase interacts with heat shock factor to activate CUP1 gene transcription in *Saccharomyces cerevisiae*. *Mol. Cell. Biol.* **19**, 3237–3245

SUPPLEMENTARY ONLINE DATA

Ref2, a regulatory subunit of the yeast protein phosphatase 1, is a novel component of cation homoeostasis

Jofre FERRER-DALMAU*, Asier GONZÁLEZ*, Maria PLATARA*, Clara NAVARRETE†, José L. MARTÍNEZ†, Lina BARRETO*, José RAMOS†, Joaquín ARIÑO* and Antonio CASAMAYOR*¹

*Departament de Bioquímica i Biologia Molecular and Institut de Biotecnologia i Biomedicina, Universitat Autònoma de Barcelona, Barcelona 08193, Spain, and †Departamento de Microbiología, Universidad de Córdoba, Córdoba 14071, Spain

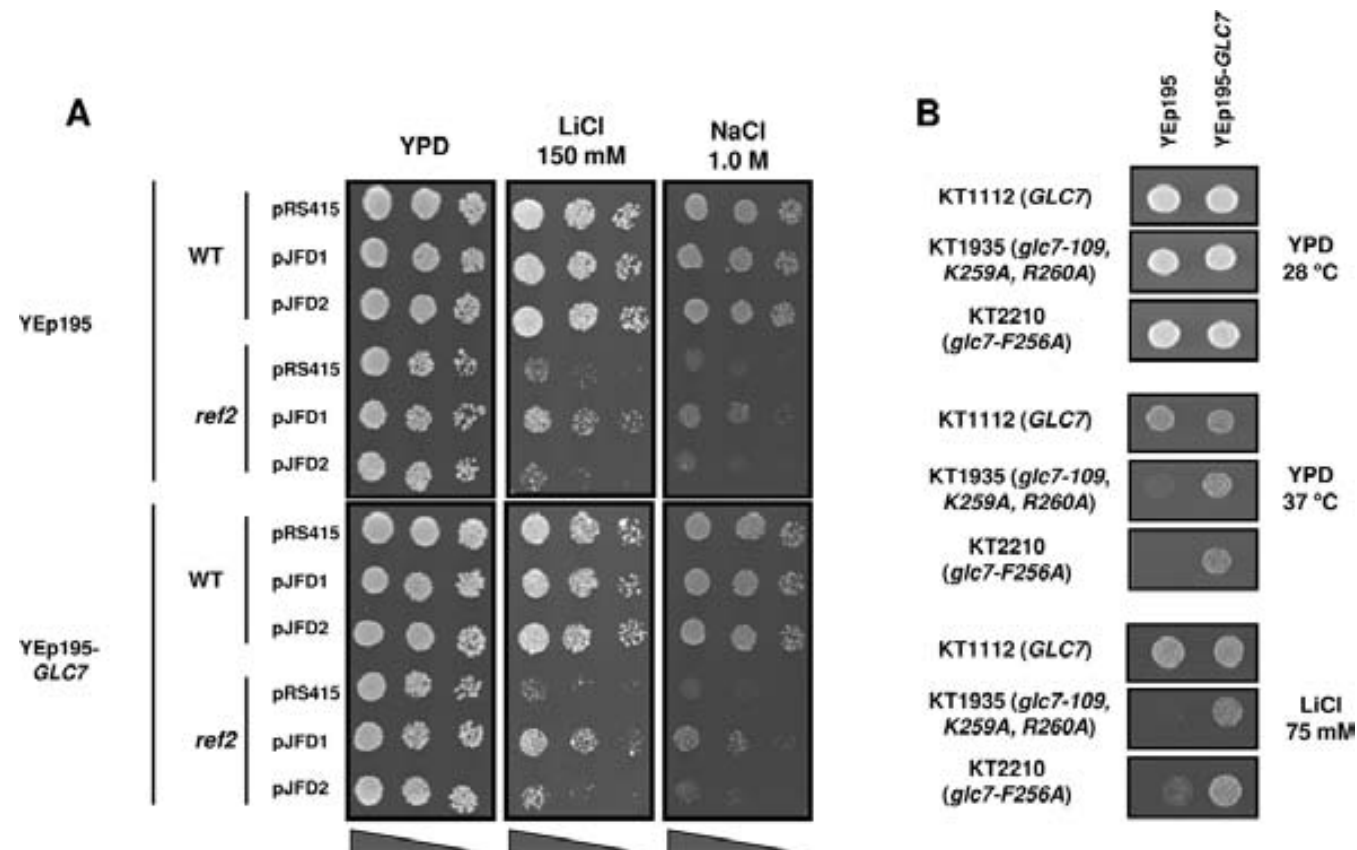


Figure S1 Effects of overexpression of Glc7 on Ref2-deficient *S. cerevisiae* strains

(A) Wild-type strain BY4741 (WT) and its *ref2* derivative were co-transformed with the indicated plasmids. Dilutions of the cultures (approx. 3000 to 120 cells) were plated in the conditions indicated. Growth was recorded after 4 days. (B) Strains carrying wild-type (KT1112) and mutated forms of Glc7 (KT1935 or KT2210) were transformed with the indicated plasmid and approx. 3000 cells were spotted. Growth was recorded after 3 days.

¹ To whom correspondence should be addressed (email antonio.casamayor@uab.es).

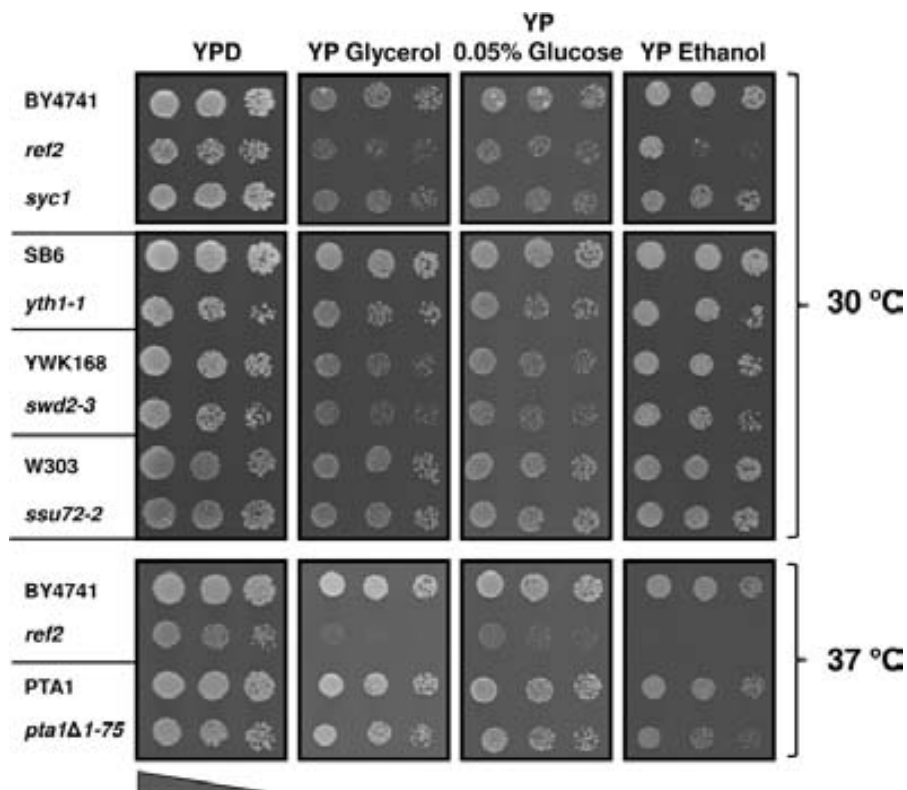


Figure S2 Growth of mutants of several APT components on different carbon sources

Dilutions (approx. 3000 to 120 cells) of the indicated strains were grown for 3 days on the different carbon sources [at 2% (w/v), except glucose which was used at 0.05%]. The growth temperature is shown to the right of the panels.

Table S1 Oligonucleotides used in the present study

Nucleotides modified to introduce the F374A mutation are denoted in a bold and italic font.

Code	Sequence	Utilization
OJFD021	AACGATACGATAAGTAAAGACACTGTGGAAGAATTGAACACGTACGCTGCAGGTCGAC	<i>ref2::nat1</i> cassette amplification
OJFD022	TGTATATACTACATGTTTATGTATCAGCATGTCATAGCTCGATGAATTCGAGCTCG	<i>ref2::nat1</i> cassette amplification
OJFD026	CGGCCAGTGAATTGTAATACGACTCACTATAGGGCGAATGGAGCTCCATAAGTAAAGACACTTTGAG	Amplification of <i>REF2</i> gene for cloning in pRS415
OJFD027	GTATCGATAAGCTTGATATCGAATTCCTGCAGCCCGGGGGATCCTGGAGTATTTCCACCTTTTG	Amplification of <i>REF2</i> gene for cloning in pRS415
OJFD029	ATTAGTTGGGAATCATCCAAA GCTTTT GATGCTACTTATGCG	Generation of F374A mutation in <i>REF2</i>
OJFD063	ACGCATAAGTAGCATCAAAA GCTTTT GGATGATTCCCAAC TAATAAAAG	Generation of F374A mutation in <i>REF2</i>
OJFD081	TATACATTCAAATTAAGAAATGGACTCACAACCAGTTGACGTACGCTGCAGGTCGAC	<i>glc7::nat1</i> cassette amplification
OJFD082	GTATTTGGTTTTTAAACTTTGATTTAGGACGTGAATCTATCGATGAATTCGAGCTCG	<i>glc7::nat1</i> cassette amplification
Glc7-BamHI.Up	CGGGATCCGATGGTGGTTGTAATACGGTC	Amplification of <i>glc7-109</i> allele for cloning in YCplac33
Glc7-PstI.Do	AAAACCTGCAGACGAGTGATGATTGCATCTTCC	Amplification of <i>glc7-109</i> allele for cloning in YCplac33
M13-20 reverse	GGAAACAGCTATGACCATG	General purpose
M13-20	GTAAAACGACGGCCAGTG	General purpose

Received 16 December 2009; accepted 22 December 2009

Published as BJ Immediate Publication 22 December 2009, doi:10.1042/BJ20091909